Universidade de Aveiro Secção Autónoma de Ciências da Saúde
2014

Mariana Santos Moreda Graça

Caracterização de novos complexos da LAP1 e a sua relevância na distonia DYT1

Characterization of novel LAP1 complexes and their relevance in DYT1 dystonia

Universidade de Aveiro Secção Autónoma de Ciências da Saúde
2014

Mariana Santos Moreda Graça

Caracterização de novos complexos da LAP1 e a sua relevância na distonia DYT1

Characterization of novel LAP1 complexes and their relevance in DYT1 dystonia

Tese apresentada à Universidade de Aveiro para cumprimento dos requisitos necessários à obtenção do grau de Doutor em Ciências Biomédicas, realizada sob a orientação científica da Professora Doutora Odete Abreu Beirão da Cruz e Silva, Professora Auxiliar com Agregação da Secção Autónoma de Ciências da Saúde da Universidade de Aveiro, e coorientação científica da Professora Doutora Sandra Maria Tavares da Costa Rebelo, Professora Auxiliar Convidada da Secção Autónoma de Ciências da Saúde da Universidade de Aveiro.

Apoio financeiro da FCT e do FSE no âmbito do III Quadro Comunitário de Apoio (Bolsa de Doutoramento SFRH/ BD/65353/2009).

o júri

presidente

Professor Doutor António Carlos Mendes de Sousa
Professor Catedrático do Departamento de Engenharia Mecânica da Universidade de Aveiro

Professora Doutora Maria João Gameiro de Mascarenhas Saraiva
Professora Catedrática do Instituto de Ciências Biomédicas Abel Salazar da Universidade do Porto

Professor Doutor Carlos Jorge Alves Miranda Bandeira Duarte
Professor Associado com Agregação da Faculdade de Ciências e Tecnologia da Universidade de Coimbra

Professor Doutor João Carlos Cruz de Sousa
Professor Auxiliar da Escola de Ciências da Saúde da Universidade do Minho

Doutora Sónia Cristina das Neves Ferreira
Investigadora de Pós-Doutoramento da Universidade de Coimbra

Professora Doutora Ana Gabriela Henriques
Professora Auxiliar Convidada da Secção Autónoma de Ciências da Saúde da Universidade de Aveiro

Professora Doutora Odete Abreu Beirão da Cruz e Silva
Professora Auxiliar com Agregação da Secção Autónoma de Ciências da Saúde da Universidade de Aveiro

Professora Doutora Sandra Maria Tavares da Costa Rebelo
Professora Auxiliar Convidada da Secção Autónoma de Ciências da Saúde da Universidade de Aveiro

agradecimentos

Ao Prof. Edgar da Cruz e Silva pela orientação na fase inicial do meu doutoramento, por todo o conhecimento partilhado e pela oportunidade de trabalhar neste projeto.

À Prof. Odete pela orientação e oportunidade de trabalhar no Laboratório de Neurociências. À Sandra Rebelo pela orientação, e por me encorajar e acompanhar durante este trabalho.

A todos os colegas do CBC pela ajuda e apoio. Em particular, às minhas "companheiras de bancada" Filipa e Pati, e à Joana Rocha, à Joana Oliveira, à Lili, à Regina, ao Roberto e à Sara Soares por todo o apoio, companheirismo e por animarem os meus dias no laboratório. À Patrícia Costa por me ter acompanhado neste trabalho. Ao Luís Godinho pela ajuda e conhecimentos partilhados. À Sara Domingues, à Sara Esteves, ao Korrodi, à Sandra Vieira, à Margarida Fardilha, à Fátima e ao Miguel por estarem sempre disponíveis a ajudar.
À Mónica Ferreira, que me acompanha desde que cheguei ao CBC, e à Mónica Almeida. Obrigado pelos bons momentos partilhados ao longo destes anos e pela vossa amizade.
E ainda aos nossos colaboradores Dr. William Dauer e Dr. Thorsten Muller por terem contribuído para a realização de alguns objetivos deste trabalho.

Aos amigos de sempre pela vossa amizade. À Tatiana, ao Daniel, ao Avelino, ao Pedro, ao Álvaro, à Ângela, à Inês e ao Chico.
Ao Eurico por todo o apoio, carinho e paciência.

Aos meus pais e à minha irmã por me terem sempre apoiado.

palavras-chave

Proteína 1B associada com a lâmina (LAP1B), invólucro nuclear, fosforilação de proteínas, proteína fosfatase 1 (PP1), torsinaA, distonia.

resumo

A distonia é a terceira doença de movimento mais comum depois do tremor essencial e da doença de Parkinson e abrange um variado número de síndromes clínicos. A distonia DYT1 é a forma mais comum de distonia isolada de início precoce e é causada por uma mutação no gene *DYT1,* a qual resulta na perda de um ácido glutâmico na proteína torsinaA (ΔE-torsinaA). A torsinaA localiza-se no retículo endoplasmático e no invólucro nuclear (IN), enquanto que a ΔE-torsinaA é anormalmente distribuída para o IN. No IN, a torsinaA interage com a proteína 1 associada com a lâmina (LAP1), cuja função ainda não é totalmente conhecida. A LAP1 é uma proteína da membrana interna do núcleo e três isoformas (LAP1A, B e C) desta proteína já foram descritas na literatura.

As interações proteína-proteína têm vindo a ser determinantes no estudo de doenças humanas e de sinalização celular. Neste trabalho, foi identificada uma nova interação entre a LAP1B humana e a proteína fosfatase 1 (PP1). A PP1 é uma fosfatase serina/treonina que é responsável pela desfosforilação de cerca de um terço de todas as proteínas em células eucarióticas. A versatilidade da PP1 é possível através da sua ligação a diferentes proteínas reguladoras responsáveis pela sua especificidade e atividade. A LAP1B é desfosforilada pela PP1 e liga-se a esta através de um motivo semelhante ao RVxF que se encontra no seu domínio nucleoplasmático. No decorrer deste trabalho, identificamos também uma nova isoforma da LAP1 humana – LAP1C, que nunca tinha sido descrita em células humanas. A expressão da LAP1B e LAP1C humanas parece ser regulada durante a diferenciação celular e neuronal e são ambas desfosforiladas pela PP1. Além disso, estas proteínas são provavelmente crucias para a manutenção do IN e regulação da mitose. Dado que a PP1 interage com a LAP1 no nucleoplasma e esta interage com a torsinaA no espaço perinuclear, a existência do tricomplexo PP1/LAP1/torsinaA foi validada em cérebro de rato e linhas celulares. A torsinA é desfosforilada pela PP1 mas liga-se a esta, provavelmente, através da LAP1. Dada a localização aberrante da ΔE-torsinaA no IN, é possível que o papel dos complexos formados pela LAP1 no IN e a sua regulação por fosforilação esteja na base da patologia da distonia DYT1. Além disso, a distonia DYT1 tem sido relacionada com uma disfunção nos circuitos dos gânglios de base e da sinalização dopaminérgica. Curiosamente as proteínas PP1 e DARPP-32 desempenham um papel fundamental na sinalização dopaminérgica. Assim, os nossos resultados podem ajudar a compreender os mecanismos moleculares e celulares inerentes à distonia DYT1, onde a fosforilação de proteínas pode desempenhar um papel crucial.

keywords

Lamina associated polypeptide 1 (LAP1), nuclear envelope, protein phosphorylation, protein phosphatase 1 (PP1), torsinA, dystonia.

abstract

Dystonia is the third most common movement disorder, following essential tremor and Parkinson's disease, and comprises a large number of clinical syndromes. DYT1 dystonia is recognized as the most common form of early onset isolated dystonia and is caused by a mutation in the *DYT1* gene, resulting in the loss of a single glutamic acid within the torsinA protein (ΔE-torsinA). TorsinA resides in the endoplasmic reticulum and nuclear envelope (NE), but the mutant form is abnormally relocated to the NE. At the NE, torsinA interacts with lamina associated polypeptide 1 (LAP1), whose function is poorly understood. LAP1 is a transmembrane protein of the inner nuclear membrane that was described to exist as three alternatively spliced isoforms (LAP1A, B and C) in rat.

Protein-protein interactions are becoming increasingly important in the study of human diseases and signaling pathways. In this work, human LAP1B was identified as a novel protein phosphatase 1 (PP1) binding protein. PP1 is a major Ser/Thr phosphatase that is estimated to dephosphorylate about one third of all proteins in eukaryotic cells. The versatility of PP1 is only possible by complexing with different binding proteins that play regulatory and targeting roles. We found that LAP1B is a substrate of PP1 and binds to the latter through an RVxF-like motif located in the nucleoplasmic domain. In the course of this work, we also identified a novel human LAP1 isoform - LAP1C that is N-terminally truncated. Human LAP1B and LAP1C isoforms seem to be developmentally regulated and are both dephosphorylated by PP1. Moreover, LAP1 proteins seem to be important for NE integrity and mitosis regulation. Given that PP1 interacts with LAP1 in the nucleoplasm, which in turn interacts with torsinA in the perinuclear space, the existence of the tricomplex PP1/LAP1/torsinA was validated in rat brain and cultured cells. Moreover, torsinA was dephosphorylated by PP1 but probably binds to the latter via LAP1. The aberrant behavior of ΔE-torsinA in the NE implicates nuclear dysfunction in DYT1 dystonia pathogenesis. Thereby, the role of LAP1 complexes in the NE and its regulation by protein phosphorylation may underlie the pathology of DYT1 dystonia and other NE-related diseases. Moreover, DYT1 dystonia has been related with a dysfunction in the basal ganglia circuit, including dopamine signaling disturbance. Interestingly, PP1/DARPP-32 cascade plays a key role in mediating the actions of dopamine and modulating the phosphorylation and activity of effectors in dopaminoceptors neurons. Thus, our results may lead to novel insights into the molecular and cellular mechanisms of DYT1 dystonia, where protein phosphorylation cascades represent a regulatory mechanism.

CONTENTS

ABBREVIATIONS

AAA^+	ATPases associated with a variety of cellular activities
ADLD	Autosomal dominant leukodystrophy
AKAP	A-kinase anchoring protein
AMPA	α-amino-3-hydroxy-5-methyl-4-isoxazolepropionic acid
ATM	Ataxia-telangiectasia mutated
ATR	Ataxia-telangiectasia and Rad 3-related
BAF	Barrier autointegration factor
BM	Binding motif
CaMKII	Ca2+/calmodulin-dependent kinase II
CDK	Cyclin-dependent kinase
cDNA	Complementary deoxyribonucleic acid
CENP-E	Centromere-associated protein E
CMS	Control missense
CNS	Central nervous system
Co-IP	Co-immunoprecipitation
CREB	cAMP-responsive element-binding protein
DARPP-32	Dopamine and cAMP-regulated phosphoprotein, Mr 32 kDa
DIV	Days *in vitro*
DNA	Deoxyribonucleic acid
DOPAC	3-,4-dihydroxyphenylacetic acid
ECL	Enhanced chemiluminescence
EDMD	Emery-Dreifuss muscular dystrophy
ER	Endoplasmic reticulum
EST	Expressed sequence tag
FI	Fluorescence intensity
FITC	Fluorescein isothiocyanate
GABA	γ-aminobutyric acid
GFP	Green fluorescente protein
GSK3β	Glycogen synthase kinase 3β
HP1	Heterochromatin protein 1
HSP	Heat shock protein

HVA	Homovanilic acid
INM	Inner nuclear membrane
IP	Immunoprecipitation
IVT	*In vitro* translation
KASH	Klarsicht/ANC-1/Syne-1 homology
KLC	Kinesin light chain
LAP	Lamina associated polypeptide
LBR	Lamin B receptor
LINC	Linker of nucleoskeleton and cytoskeleton
LTD	Long-term depression
LTP	Long-term potentiation
LULL1	Lumenal domain- like LAP1
MAD2	Mitotic arrest deficient 2
MEF2	Myocyte enhancer factor-2
mRNA	Messenger ribonucleic acid
MS	Mass spectrometry
Mypt1	Myosin phosphatase targeting subunit 1
NE	Nuclear envelope
NIPP1	Nuclear inhibitor of PP1
NLS	Nuclear localization signal
NMDA	N-methyl-D-aspartate
NPC	Nuclear pore complex
OA	Okadaic acid
ONM	Outer nuclear membrane
ORF	Open reading frame
PK	Protein kinase
PLK1	Polo-like kinase 1
PNUTS	Phosphatase 1 nuclear targeting subunit
PP	Protein phosphatase
PP1c	Protein phosphatase 1 catalytic subunit
PPPs	Phosphoproteins phosphatases
PPMs	Metal-dependent protein phosphatases
QDO	Quadruple dropout medium
Repo-man	Recruits PP1 onto mitotic chromatin at anaphase

RNA	Ribonucleic acid
RNAi	RNA interference
RT-PCR	Reverse transcriptase- polymerase chain reaction
SAC	Spindle assembly checkpoint
SAP155	Spliceosome-associated protein 155
SD	Synthetic dropout medium
Ser	Serine
shRNA	Short/Small hairpin RNA
SUN	Sad1-UNC84 homology
Thr	Threonine
TM	Transmembrane
TRF2	Telomeric repeat binding factor 2
Tyr	Tyrosine
UTR	Untranslated region
VAMP	Vesicle-associated membrane protein
VMAT2	Vesicular monoamine transporter 2
Wt	Wild-type
YTH	Yeast two-hybrid

CHAPTER I - INTRODUCTION

I.1. PROTEIN PHOSPHORYLATION

Reversible protein phosphorylation is the most common type of pos-translational modification in eukaryotic organisms. It involves either the addition of phosphate groups via the transference of the terminal phosphate from ATP to an amino acid residue by protein kinases or its removal by protein phosphatases (Fig. I.1). Protein phosphorylation is a crucial mechanism for signal transduction that regulates the biological activity of diverse proteins. For example, protein phosphorylation allows for the regulation of enzymatic activities and is important for modulation of protein-protein interactions (Barford et al., 1998). About one third of all eukaryotic proteins can be phosphorylated, mainly at serine (Ser), threonine (Thr) and tyrosine (Tyr) amino acids. Proteomic analysis of more than 2000 human proteins revealed that phosphorylation at Ser, Thr and Tyr accounts for 86.4%, 11.8% and 1.8%, respectively, of the phosphorylated amino acids (Olsen et al., 2006). Analysis of the human genome revealed that it contains about 518 kinases that are classified as Tyr kinases or Ser/thr kinases (Johnson and Hunter, 2005). Whereas the number of Tyr kinases is approximately the same as that for Tyr phosphatases, the number of Ser/Thr kinases is much higher when compared to Ser/Thr phosphatases. The discrepancy of this number can be explained by the unique manner by which Ser/Thr phosphatases are regulated. These enzymes have additional interacting and regulatory proteins that bind to the phosphatase catalytic subunits and control their activity and/or subcellular location (Bollen et al., 2010; Cohen, 2002b; Moorhead et al., 2007).

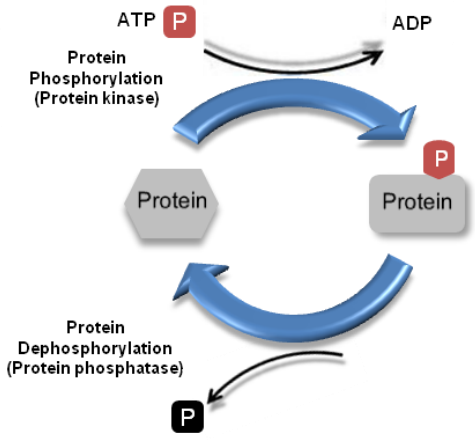

Figure I.1. Schematic representation of reversible protein phosphorylation. Protein kinases transfer a phosphate group from ATP to the target protein (protein phosphorylation), while protein phosphatases catalyze the hydrolysis of the phosphate group from the target protein (protein dephosphorylation).

Protein phosphorylation is a major mechanism for controlling several intracellular events in eukaryotic cells, such as, metabolism, contractility, membrane transport and secretion, transcription and translation, cell division, fertilization and memory (reviewed in Cohen, 1989). Additionally, aberrant protein phosphorylation of key proteins has been linked to many diseases and dysfunctional states, such as, cancer, metabolic disorders and inflammatory and neurological diseases. In neurodegenerative diseases, such as Alzheimer's disease, there is evidence for abnormal regulation of protein phosphorylation. Alzheimer's disease is primarily characterized by the presence of neuritic plaques and neurofibrillary tangles in the brains of affected individuals. Neurofibrillary tangles result from the aggregation of hyperphosphorylated tau protein into paired helical filaments. Glycogen synthase kinase 3β (GSK3β) and protein kinase A (PKA) may be key kinases involved in tau phosphorylation (Delobel et al., 2002a), while inhibition of protein phosphatase 2A (PP2A) and protein phosphatase 1 (PP1) lead to tau hyperphosphorylation (Bennecib et al., 2000; Planel et al., 2001). Moreover, the inactivation of PP1 leads to a relative increase in Alzheimer's amyloid precursor protein processing by the non-amyloidogenic pathway (da Cruz e Silva et al., 1995a). Other neurodegenerative diseases associated with abnormal protein phosphorylation are Parkinson's disease and Huntington's disease. Parkinson's disease is characterized by the presence of Lewy bodies (proteinaceous inclusions) that contain phosphorylated and aggregated α-synuclein. It was demonstrated that α-synuclein is constitutively phosphorylated, predominantly on serine residues (Okochi et al., 2000), and the levels of phosphorylated α-synuclein were found to be higher in Parkinson's disease patients compared to the control cases (Foulds et al., 2011). Synapsin I, a major phosphoprotein important in regulating neurotransmitter release, is abnormally phosphorylated in mice expressing the Huntington's disease mutation. It has been suggested that an imbalance between kinase and phosphatase activities also occurs in Huntington's disease (Lievens et al., 2002). Therefore, protein phosphorylation systems represent attractive targets for diagnostics and therapeutics in several diseases. Indeed, kinases are the second most important group of drug targets in the pharmaceutical industry's (Cohen, 2002a). In contrast, protein phosphatases were recognized later as potential therapeutic targets. Further, the therapeutic value of protein phosphatases interacting proteins as targets is only currently being addressed (da Cruz e Silva et al., 2004; Fardilha et al., 2010).

I.1.1. Protein phosphatases

Based on substrate specificity, eukaryotic protein phosphatases can be classified into two families: ser/thr protein phosphatases, that catalyze the dephosphorylation of ser and thr amino acids, and tyr phosphatases, which catalyze the dephosphorylation of tyr amino acids. Ser/thr protein phosphatases can be categorized into three families: phosphoproteins phosphatases (PPPs), metal-dependent protein phosphatases (PPMs) and the aspartate-based phosphatases represented by FCP/SCP (TFIIF-associating component of RNA polymerase II CTD phosphatase/small CTD phosphatase). Members of the PPPs family include: PP1, PP2A, PP2B (also known as calcineurin), PP4, PP5, PP6 and PP7. PP1 and PP2A are some of the most well conserved enzymes with a variety of cellular functions attributed to the interaction with a large number of regulatory subunits (reviewed in Honkanen and Golden, 2002; Moorhead et al., 2009; Shi, 2009). PP2B alone is inactive, acquiring phosphatase activity after binding with Ca^{2+}-calmodulin. In contrast, PP1 and PP2A are mainly active in the absence of divalent cations, despite dephosphorylation of some substrates being strongly stimulated by Mn^{2+} (Cohen, 1989; Wang et al., 2008a). PP4, PP5 and PP6, like PP1, PP2A and PP2B, were identified in all mammalian tissues examined. At the structural level, PP4 and PP6 are closely related to the catalytic subunit of PP2A. PP5 contains an N-terminus tetratricopeptide repeat domain that is a protein-protein interaction motif (Cohen, 1997; Shi, 2009). In contrast with other PPPs, human PP7 is not ubiquitous and was primarily found in retina. PP7 contains multiple Ca^{2+} binding sites and its activity is dependent of Mg^{2+} (Kutuzov et al., 2002). These PPPs contain a common catalytic core domain that is conserved among species. The remarkable degree of evolutionary conservation of these enzymes (Fig. I.2) is related to their essential role in the regulation of fundamental cellular processes (Honkanen and Golden, 2002). PP1, PP2A, and PP2B together with PP2C of the PPM family, account for the majority of the protein ser/thr phosphatase activity *in vivo* (Barford et al., 1998). The PPM family includes PP2C and pyruvate dehydrogenase phosphatase, which are Mn^{2+}/Mg^{2+} dependent enzymes. Unlike most PPP family members, PPMs do not have additional regulatory subunits but contain additional domains and conserved motifs that may determine substrate specify. Members of the FCP/SCP family use an aspartate-based catalysis mechanism (reviewed in Moorhead et al., 2009; Shi, 2009).

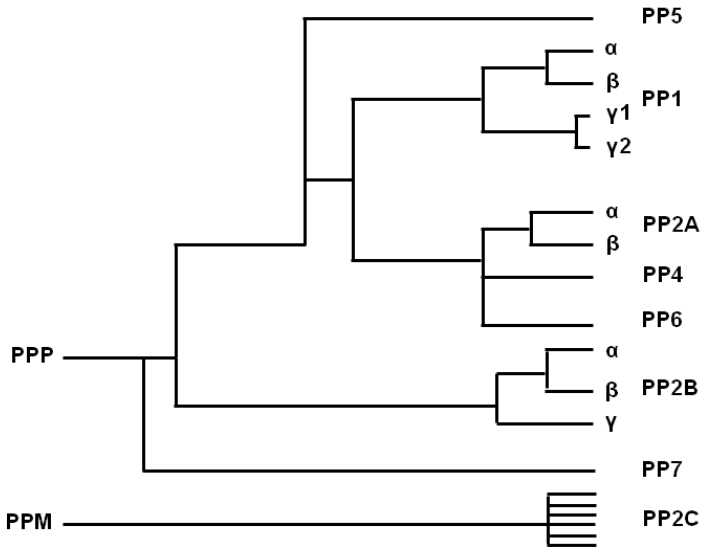

Figure I.2. Phylogenic tree representing the homology between members of the phosphoprotein phosphatase (PPP) family based on their primary amino acid sequence. PP1-PP7 belongs to the PPP family that is structurally different from PP2C (metal-dependent protein phosphatase family, PPM) (adapted from Honkanen and Golden, 2002).

I.1.2. Protein phosphatase 1

PP1 and PP2A together are responsible for more than 90% of the protein phosphatase activity in eukaryotic cells. However, in terms of substrate diversity, PP1 is predicted to catalyze the majority of protein dephosphorylation events (Bollen et al., 2010; Heroes et al., 2013). As a major phosphatase, PP1 is present in various eukaryotic organisms. Eukaryotic genomes contain multiple genes encoding PP1 isoforms with the exception of yeast *Saccharomyces cerevisiae* which only contains one PP1 gene. PP1 isoforms are about 70% identical in the central region and mainly differ at the N- and C-terminal sequences. Moreover, PP1 was shown to be one of the most conserved eukaryotic proteins. PP1 sequences are highly conserved between different species, as is the case for *Giardia lamblia* which expresses a PP1 isoform very similar to the mammalian form. This suggests that PP1 may have similar functions in different organisms (reviewed in Ceulemans and Bollen, 2004; Lin et al., 1999). In mammals, PP1 isoforms are encoded by three genes: *PPP1CA*, *PPP1CB* and *PPP1CC* that encode for PP1alpha (PP1α), PP1beta/delta (PP1β/δ) and PP1gamma (PP1γ), respectively (Barker et al., 1994; Barker et al., 1993; Sasaki et al., 1990). These isoforms are about

90% identical in amino acid sequence; most of the differences are located at the N- and C-terminals (Fig. I.3). The gene encoding PP1γ undergoes alternative splicing to originate an ubiquitous PP1gamma1 (PP1γ1) variant and a PP1gamma2 (PP1γ2) variant enriched in testis (da Cruz e Silva et al., 1995b).

```
PP1gamma1       MADLDKLNIDSIIQRLLEVRGSKPGKNVQLQENEIRGLCLKSREIFLSQPILLELEAPLK 60
PP1gamma2       MADLDKLNIDSIIQRLLEVRGSKPGKNVQLQENEIRGLCLKSREIFLSQPILLELEAPLK 60
PP1alpha        MSDSEKLNLDSIIGRLLEVQGSRPGKNVQLTENEIRGLCLKSREIFLSQPILLELEAPLK 60
PP1beta         MADG-ELNVDSLITRLLEVRGCRPGKIVQMTEAEVRGLCIKSREIFLSQPILLELEAPLK 59
                *:*  :**:**:* *****:*.:*** **: * *:****:********************

PP1gamma1       ICGDIHGQYYDLLRLFEYGGFPPESNYLFLGDYVDRGKQSLETICLLLAYKIKYPENFFL 120
PP1gamma2       ICGDIHGQYYDLLRLFEYGGFPPESNYLFLGDYVDRGKQSLETICLLLAYKIKYPENFFL 120
PP1alpha        ICGDIHGQYYDLLRLFEYGGFPPESNYLFLGDYVDRGKQSLETICLLLAYKIKYPENFFL 120
PP1beta         ICGDIHGQYTDLLRLFEYGGFPPEANYLFLGDYVDRGKQSLETICLLLAYKIKYPENFFL 119
                ********* **************:**********************************

PP1gamma1       LRGNHECASINRIYGFYDECKRRYNIKLWKTFTDCFNCLPIAAIVDEKIFCCHGGLSPDL 180
PP1gamma2       LRGNHECASINRIYGFYDECKRRYNIKLWKTFTDCFNCLPIAAIVDEKIFCCHGGLSPDL 180
PP1alpha        LRGNHECASINRIYGFYDECKRRYNIKLWKTFTDCFNCLPIAAIVDEKIFCCHGGLSPDL 180
PP1beta         LRGNHECASINRIYGFYDECKRRFNIKLWKTFTDCFNCLPIAAIVDEKIFCCHGGLSPDL 179
                **********************:**********************************

PP1gamma1       QSMEQIRRIMRPTDVPDQGLLCDLLWSDPDKDVLGWGENDRGVSFTFGAEVVAKFLHKHD 240
PP1gamma2       QSMEQIRRIMRPTDVPDQGLLCDLLWSDPDKDVLGWGENDRGVSFTFGAEVVAKFLHKHD 240
PP1alpha        QSMEQIRRIMRPTDVPDQGLLCDLLWSDPDKDVQGWGENDRGVSFTFGAEVVAKFLHKHD 240
PP1beta         QSMEQIRRIMRPTDVPDTGLLCDLLWSDPDKDVQGWGENDRGVSFTFGADVVSKFLNRHD 239
                ***************** *************** ***************:**:***::**

PP1gamma1       LDLICRAHQVVEDGYEFFAKRQLVTLFSAPNYCGEFDNAGAMMSVDETLMCSFQILKPAE 300
PP1gamma2       LDLICRAHQVVEDGYEFFAKRQLVTLFSAPNYCGEFDNAGAMMSVDETLMCSFQILKPAE 300
PP1alpha        LDLICRAHQVVEDGYEFFAKRQLVTLFSAPNYCGEFDNAGAMMSVDETLMCSFQILKPAD 300
PP1beta         LDLICRAHQVVEDGYEFFAKRQLVTLFSAPNYCGEFDNAGGMMSVDETLMCSFQILKPSE 299
                ************************************.*****************::

PP1gamma1       KKK---------PNATRPVTPPRG------MITKQAKK-------- 323
PP1gamma2       KKK---------PNATRPVTPPRVGSGLNPSIQKASNYRNNTVLYE 337
PP1alpha        KNKGKYGQFSGLNPGGRPITPPRN-------SAKAKK--------- 330
PP1beta         KKAKYQYG---GLNSGRPVTPPRT--------ANPPKKR------- 327
                *:            . **:****          :  :
```

Figure I.3. Analysis of homology of PP1 isoforms using CLUSTALW algorithm. Identical (*); conservative (:); similar (.).

PP1 holoenzymes are composed by a highly conserved catalytic subunit called protein phosphatase 1 catalytic subunit (PP1c) complexed with one or two variable regulatory subunits. The crystal structure of mammalian PP1c revealed that PP1 is a metalloenzyme with two divalent metal ions (Mn^{2+} and Fe^{2+}) at the center of the catalytic site (Egloff et al., 1995; Goldberg et al., 1995). The catalytic site of PP1 is located at the intersection of three potential substrate-binding grooves (Fig. I.4): the hydrophobic, the acidic and the C-terminal grooves (Peti et al., 2013). Most PP1 regulatory subunits interact with the PP1 catalytic subunit through a conserved PP1 binding motif termed the RVxF motif. The RVxF motif binds to a hydrophobic groove of PP1c that is distant from the catalytic site (Egloff et al., 1997). The residues of PP1c

responsible for binding of the RVxF motif are conserved in all isoforms of different species (Barford et al., 1998; Egloff et al., 1997). Initially, the RVxF motif was defined as a five-residue motif with the consensus sequence [R/K] $X_{A(0-1)}$ [V/I] X_B [F/W], where X_A is any amino acid and X_B is any amino acid except proline (Wakula et al., 2003). Later on, a more specific consensus sequence for the RVxF motif was proposed: [HKR]-[ACHKMNQRSTV]-V-[CHKNQRST]-[FW] (Meiselbach et al., 2006). The latter definition has only 40% of sensitivity but is more specific compared to the first one (Ceulemans and Bollen, 2006; Meiselbach et al., 2006). A remarkable aspect is that the RVxF motif is often N-terminally flanked by basic residues and C-terminal flanked by acidic residues and this affects the binding affinity for the RVxF motif (Meiselbach et al., 2006; Wakula et al., 2003). Based on the two proposed definitions for the RVxF motif, Hendrickx and colleagues (Hendrickx et al., 2009) performed an *in silico* screening for novel PP1 interactors in combination with biochemical validation, and proposed a novel consensus sequence: [KRL][KRSTAMVHNQ][VI]{FIMYDP}[FW]. The binding of PP1 to regulatory proteins through the RVxF motif does not cause major effects on the conformation and activity of PP1 (Egloff et al., 1997; Meiselbach et al., 2006; Wakula et al., 2003). However, the RVxF motif mediates the initial anchoring of regulatory subunits to PP1 and thereby promotes the occupation of secondary binding sites, and this often does affect the activity and/or substrate specificity of PP1 (Bollen, 2001). Additional PP1 binding motifs were identified, the SILK and MyPhone motifs. The SILK motif has the consensus sequence [GS]IL[RK] (Hendrickx et al., 2009) and it was first described for inhibitor-2. The SILK motif was shown to be essential for PP1 inhibiton by inhibitor-2 (Huang et al., 1999) and can functionally replace the RVxF motif in nuclear inhibitor of PP1 (NIPP1) (Wakula et al., 2003). The SILK motif is always positioned N-terminal to the RVxF sequence and binds in a hydrophobic groove on the opposite face of the PP1 active site (Bollen et al., 2010). The myosin phosphatase targeting subunit 1 (Mypt1) has a N-terminal PP1 binding motif (MyPhone motif) with the consensus sequence RxxQ[VIL][KR]x[YW], where x can be any residue (Terrak et al., 2004). The MyPhone motif is present in other PP1 regulatory proteins and is also N-terminal to the RVxF sequence (Bollen et al., 2010). Some members of the anti-apoptotic Bcl-2 family have, in addition to the RVxF motif, another PP1 binding motif with the consensus sequence F-X-X-[KR]-X-[KR] (Ayllon et al., 2001; Godet et al., 2010). This motif, termed apoptotic signature, was also found in other PP1 binding proteins (Esteves et al., 2012b).

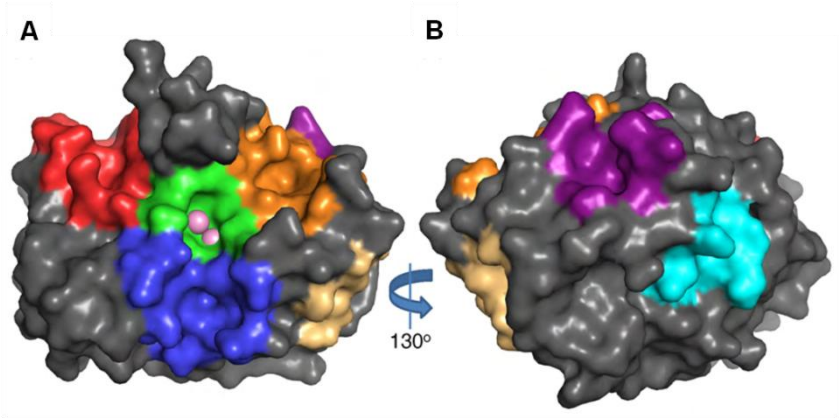

Figure I.4. Representation of the PP1α structure. **A-** PP1α contains two divalent metal ions (pink spheres) at the center of the catalytic site (green), which is located at the intersection of three potential substrate-binding grooves: the hydrophobic (blue), the acidic (orange) and the C-terminal (red). **B-** 130º rotation of A to show the binding sites for the RVxF (purple), SILK (cyan) and MyPhone (wheat) motifs (Bollen et al., 2010).

Close to 200 PP1 interacting proteins have been identified and many more are expected to be found (Esteves et al., 2012a; Esteves et al., 2012b; Fardilha et al., 2010; Fardilha et al., 2011; Hendrickx et al., 2009; Heroes et al., 2013). As explained, the versatility of PP1 is largely determined by the binding of its catalytic subunit to different specific regulatory subunits. These PP1 binding proteins can function as inhibitors of the catalytic activity, substrate-specifying subunits, targeting subunits or substrates (Fig. I.5) (Bollen et al., 2009; Bollen et al., 2010). Many substrates that directly associate with PP1c are enzymes that are activated by dephosphorylation, as is the case for focal adhesion kinase, E3 ubiquitin ligase and caspase 2 (Bollen et al., 2010). In contrast, PP1α dephosphorylates NEK2, Aurora-A and C-Nap1 and keeps these proteins in an inactive state (Mi et al., 2007). Some substrates are dephosphorylated specifically on a single residue, whereas others are dephosphorylated on multiple residues (Bollen et al., 2010). Many PP1 binding proteins mediate the targeting of PP1 to specific subcellular compartments or protein complexes. This brings PP1 in close proximity to specific substrates (Bollen et al., 2010; Ceulemans et al., 2002a). For example, spinophilin directs PP1 to dendritic spines in brain, near to potential substrates, which mediate the regulation of PP1 synaptic function (Allen et al., 1997). NIPP1 was initially identified as a nuclear inhibitor of PP1c but it also targets PP1 to dephosphorylate spliceosome-associated protein 155 (SAP155), not as an inhibitor of PP1 (Tanuma et al., 2008). Some PP1 binding proteins selectively inhibit

PP1 dephosphorylation of only a subset of substrates such as glycogen phosphorylase. Thus, these proteins are defined as substrate specifiers rather than as inhibitors. In addition, some substrate specifiers enhance PP1 activity toward PP1 substrates, as is the case of the MYPT1. Interaction of MYPT1 with PP1 not only promotes the dephosphorylation of the myosin regulatory light chain but also decreases PP1 activity towards other substrates. PP1 true inhibitors are capable of blocking the PP1 active site and inhibit the dephosphorylation of all substrates. Innibitor-1 and DARPP-32 (dopamine and cAMP-regulated phosphoprotein, Mr 32 kDa) potently inhibit PP1c when phosphorylated on a thr residue, while inhibitor-2 and -3 activity does not require prior phosphorylation (Bollen, 2001; Bollen et al., 2010; Ceulemans and Bollen, 2004). Targeting and inhibitor proteins were also found to associate simultaneously with PP1 forming a trimeric complex (Lesage et al., 2007; Terry-Lorenzo et al., 2002).

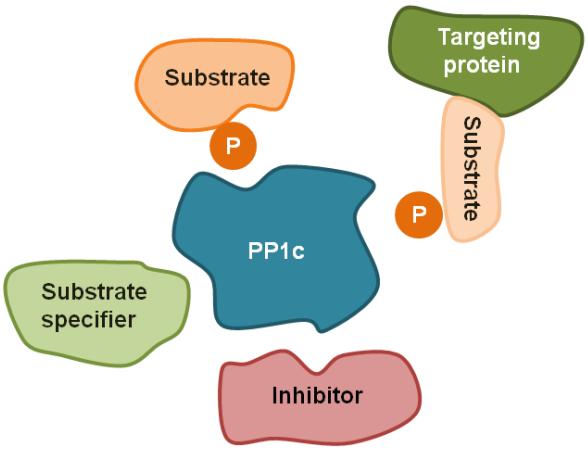

Figure I.5. Schematic representation of the PP1 holoenzyme structure. The protein phosphatase 1 catalytic subunit (PP1c) interacts with regulatory subunits that can be substrates, targeting proteins, inhibitors of the catalytic activity or substrate-specifiers.

PP1 is the most widely expressed ser/thr phosphatase and regulates a variety of cellular functions. It is involved in glycogen metabolism, transcription, protein synthesis, cellular division and meiosis, and apoptosis. When nutrients are abundant PP1 stimulates the synthesis of glycogen and also enables the return to the basal state of protein synthesis and the recycling of transcription and splicing factors. PP1 is required for anaphase progression, exit from mitosis and is also responsible for maintenance of the cells in G_1 or G_2 cell cycle phases. In addition, PP1 can also promote apoptosis when cells are damaged. PP1 in combination with its regulatory proteins is also

involved in neurotransmission, neurite outgrowth and synapse formation (reviewed in Ceulemans and Bollen, 2004; Cohen, 2002b). Most PP1 binding proteins identified so far have an annotated function. In accordance with the broad action of PP1, its binding proteins are also linked to diverse cellular functions. However, they function predominantly in signal transduction events, including regulation of nucleic acid, cell cycle, protein synthesis, stress response, metabolism and transport (Esteves et al., 2012b; Heroes et al., 2013). Some PP1 binding proteins do not show cell or tissue-specific expression, while others are selectively expressed in brain, testis or white blood cells (Heroes et al., 2013), accordingly with the high expression levels of PP1 in those tissues (da Cruz e Silva et al., 1995b; Fardilha et al., 2011; Heroes et al., 2013). Regarding the subcellular localization, PP1 binding proteins are mainly found in the nucleus, cytoplasm and plasma membrane (Esteves et al., 2012b; Heroes et al., 2013). This is consistent with the fact that all PP1 isoforms can be found in the nucleus and cytoplasm (Andreassen et al., 1998).

I.1.2.1. PP1 functions in the nucleus

The nucleus is a highly dynamic subcellular compartment where reversible protein phosphorylation is a crucial regulatory mechanism (Moorhead et al., 2007; Olsen et al., 2006). The activity of protein phosphatases that regulate nuclear events are often enriched in the nucleus, as is the case for PP1 (Kuret et al., 1986). All PP1 isoforms can be found in the nucleus and cytoplasm with PP1γ and PP1β/δ showing additional accumulation in the nucleoli. The localization of PP1 isoforms is dynamic and changes throughout mitosis. Moreover, each PP1 isoform shows different localization patterns during cell cycle, suggesting isoform-specific roles. During mitosis PP1α was found in centrosomes, PP1β/δ was located in chromosomes, and PP1γ was differentially found at kinetochores, chromosomes, cleavage furrow and midbody throughout mitosis progression (Andreassen et al., 1998; Trinkle-Mulcahy et al., 2003; Trinkle-Mulcahy et al., 2001). The specific locations of PP1 isoforms can be due to different affinities for regulatory subunits which have distinct subcellular distribution themselves (Moorhead et al., 2007; Trinkle-Mulcahy and Lamond, 2006).

I.1.2.1.1. mRNA processing and transcription

The two most abundant nuclear PP1 binding proteins are phosphatase 1 nuclear targeting subunit (PNUTS) and NIPP1 (Tran et al., 2004), both bind to RNA and are thought to play a role in pre-mRNA splicing. PNUTS may anchor PP1 to specific RNA complexes in the nucleus (Kim et al., 2003). Moreover PNUTS can inhibit the phosphatase activity of PP1γ and PP1α towards exogenous substrates *in vitro* (Allen et al., 1998; Kreivi et al., 1997). NIPP1 is a potent inhibitor of PP1 that has a nucleoplasmic distribution, but also accumulates in nuclear speckles where it binds to pre-mRNA splicing factors (Trinkle-Mulcahy et al., 1999). When overexpressed in cells, NIPP1 is capable of redirecting PP1γ and PP1α to nuclear speckles (Trinkle-Mulcahy et al., 2001). NIPP1 was also found to mediate the interaction of PP1 with a regulator of pre-mRNA splicing (CDC5L). It was suggested that CDC5L and PP1-NIPP1 complex may be involved in the splicing reaction and in the spliceosome disassembly (Boudrez et al., 2000). NIPP1 also associates with the spliceosomal component SAP155 and recruits PP1 to dephosphorylate the latter (Tanuma et al., 2008). Indeed, previous reports showed that activity of ser/thr phosphatases, including PP1, is required for pre-mRNA splicing (Mermoud et al., 1992; Mermoud et al., 1994). PP1 may also be involved in alternative 5' splice site selection, possibly by dephosphorylating splicing factors of the SR family (Cardinali et al., 1994). Furthermore, PP1 was found to associate with splicing factors regulating its activity, including PTB-associated RNA splicing factor and non-POU-domain-containing, octamer binding protein (Liu et al., 2011) and transformer2-beta1 (Novoyatleva et al., 2008).

In the nucleus, PP1 has been linked to other processes, such as, regulation of transcription. The transcription by RNA polymerase II relies on the reversible phosphorylation of the C-terminal domain of the largest subunit of the polymerase. PP1 was found to associate with RNA polymerase II in nuclear extracts and to dephosphorylate, the C-terminal domain of the polymerase, at least *in vitro* (Ceulemans and Bollen, 2004; Washington et al., 2002). The transcription factor cAMP-responsive element-binding protein (CREB) was initially identified as a mediator of cAMP-induced gene expression. CREB has several phosphorylation sites that differentially regulate its activity (reviewed in Carlezon et al., 2005). PP1 dephosphorylates CREB

and inhibits c-AMP dependent transcription, thus regulating CREB activity (Hagiwara et al., 1992). It was also reported that histone deacetylase associates with CREB and PP1, and promotes CREB Ser133 dephosphorylation via interaction with PP1 (Canettieri et al., 2003). Furthermore, PP1 was found in association with several transcription factors in the nucleus, namely Hox11 (Kawabe et al., 1997; Riz and Hawley, 2005), human factor C1 (Ajuh et al., 2000) and myocyte enhancer factor-2 (MEF2) (Perry et al., 2009). Hox11 is a homeobox proto-oncogene that may function as a transcription factor for G_1/S cell cycle progression. The interaction with PP1 and PP2A are important effectors of Hox11 transcriptional activity (Riz and Hawley, 2005). Human factor C1 is involved in regulation of G0/G1 phase of the cell cycle and can inhibit the phosphatase activity of PP1 toward phosphorylase a (Ajuh et al., 2000). MEF2 interaction with PP1α blocks MEF2-dependent transcription and MEF2 mediated neuronal survival (Perry et al., 2009).

I.1.2.1.2. Cell Cycle

PP1 has different localization patterns during the cell cycle suggesting an association with different regulatory subunits. The PP1 complexes are capable of controlling cell cycle progression in diverse aspects (Fig. I.6). Protein phosphatases are important regulators of G1/S transition by maintaining retinoblastoma proteins dephosphorylated, which enables the latter proteins to recruit stimulators of G1/S transition (e.g. E2F transcription factor) (Bollen and Beullens, 2002). The retinoblastoma protein pRB is dephosphorylated at the end of mitosis by PP1, but at the G1/S transition PP1 is inactivated by a cyclin-dependent kinase (CDK) phosphorylation, allowing S phase entry (Liu et al., 1999; Rubin et al., 2001). PP1, like other protein phosphatases, controls the entry into mitosis by regulating the activity of mitotic kinases. Activation of CDK1 in association with cyclins is crucial for entry into mitosis and requires dephosphorylation by Cdc25B and Cdc25C phosphatases at the centrosomes and nucleus. Dephosphorylation of Cdc25C on Ser287 partially activates Cdc25C and it is mediated by PP1, resulting in the activation of a pool of CDK1 at the G2/M transition (reviewed in Bollen et al., 2009).

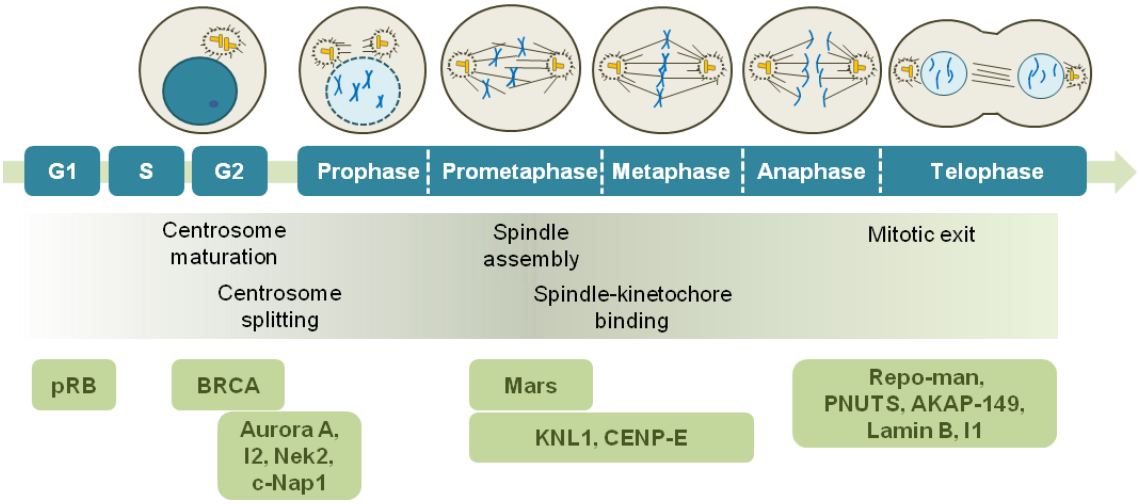

Figure I.6. Activity of PP1 and its regulatory proteins during cell cycle progression. The upper panel shows a timeline of cell cycle stages, the middle panel underlines the major events known to be regulated by PP1 and the lower panel shows the activity stage of PP1 regulatory proteins. PP1 regulates G1/S transition by dephosphorylation of the retinoblastoma protein pRB. BRCA prevents centrosome maturation in a PP1-dependent manner. PP1 keeps Aurora A, Nek2 and c-Nap1 dephosphorylated to prevent centrosome splitting. The inhibitor-2 (I2) restrain PP1 activity and promotes Nek2 activation and centrosome splitting. PP1-Mars complex stabilize microtubules. PP1 dehosphorylates KNL1 and CENP-E and stabilizes microtubule-kinetochore attachments. PP1 and its binding proteins Repo-man and PNUTS are required for chromatin decondensation at the end of mitosis. AKAP-149 recruits PP1 to the nuclear envelope to dephosphorylate lamin B, promoting nuclear envelope reassembly. Inhibitor 1 (I1) is inactivated by PP1 allowing PP1 to dephosphorylate proteins required for mitotic exit.

When cells enter mitosis, one of the first steps for mitotic spindle formation is the separation of duplicated centrosomes (duplication occurs at S phase), the main microtubule organizing centers that form the two spindle poles. Formation of a stable mitotic spindle is crucial for accurate separation of chromosomes during mitosis. PP1 may prevent the premature splitting of the duplicated centrosomes at the beginning of mitosis by inactivating the kinases involved in this process (Fig. I.6). One of these kinases is Aurora A, which is required for centrosome separation. Aurora A and PP1 antagonize each other and inhibitor-2 additionally regulates this complex by inhibiting PP1 and activating Aurora A. Centrosome separation also depends on Nek2a activity and its substrates C-Nap1 and Rootletin. PP1, Nek2 and C-Nap1 form a trimeric complex. During interphase, PP1 dephosphorylates Nek2 leading to its inhibition and also dephosphorylates c-Nap1 maintaining centrosome cohesion. Additionally, inhibitor-2 associates with the Nek2/PP1 complex, where it inhibits PP1, and thereby promotes Nek2 activation and centrosome splitting. In turns, Nek2 phosphorylates PP1, reducing its phosphatase activity (Bollen et al., 2009; Ceulemans and Bollen, 2004).

Recently, it was reported that a leucine rich repeat protein that binds to PP1 termed PPP1R42 also regulates centrosome separation. PPP1R42 is a positive regulator of PP1 and its depletion reduces PP1 activity and consequently leads to Nek2 activation (Devaul et al., 2013). It seems that separation of centrosomes at early mitosis requires inactivation of PP1 and that PP1 maintains centrosomes together during interphase (reviewed in Bollen et al., 2009; Ceulemans and Bollen, 2004). Indeed, PP1 was shown to be involved in centrosome maturation (G2 phase), a process characterized by the accumulation of γ-tubulin and other proteins. The BRCA protein promotes ubiquitination and further degradation of γ-tubulin, and thus inhibits centrosome maturation. During interphase PP1α activates BRCA by dephosphorylation, suggesting an additional role for PP1 in centrosome maturation (reviewed in Bollen et al., 2009). Furthermore, PP1 also binds to the centrosomal proteins SFI1, CEP192, CEP170 and inhibitor-3 (Esteves et al., 2012a; Hendrickx et al., 2009; Huang et al., 2005).

Furthermore, mitotic spindle assembly that begins with microtubule outgrowth at the centrosomes, is regulated by different phosphatases, including PP1 (Fig. I.6) (Bollen et al., 2009). It was proposed that the PP1 binding protein Mars targets the centrosomal microtubule stabilizer dTACC to be dephosphorylated by PP1, thus contributing to mitotic spindle stability (Tan et al., 2008). Others functions that have been attributed to PP1 are the maintenance of microtubules-kinetochores attachment and spindle assembly checkpoint (SAC) silencing. Stable attachment of kinetochores to spindle microtubules is crucial for accurate chromosome separation. Aurora B phosphorylates diverse proteins to destabilize the binding of microtubules to kinetochores, thus preventing erroneous attachments. Conversely, PP1 stabilizes correct microtubule-kinetochore attachments during metaphase by opposing Aurora B-mediated phosphorylation (reviewed in Bollen et al., 2009; Funabiki and Wynne, 2013). It was demonstrated that the kinetochore protein KNL1 targets PP1γ to kinetochores and this recruitment is required for PP1γ dephosphorylation of other Aurora B substrates at kinetochores (Liu et al., 2010). PP1γ is also directed to kinetochores through binding to the centromere-associated protein E (CENP-E). Binding and dephosphorylation of CENP-E by PP1 is required for stable attachment of kinetochores to microtubules (Kim et al., 2010b). On the other hand, Aurora B inhibits targeting of PP1 to kinetochores by phosphorylation of the PP1 binding motif in KNL1 and CENP-E (Kim et al., 2010b; Liu

et al., 2010). In addition, polo-like kinase 1 (PLK1) was reported to promote kinetochore-microtubule attachment and SAC silecing. The SAC signaling pathway is activated on unattached kinetochores to block the metaphase-anaphase transition, until chromosomes are properly attached to the mitotic spindle. When the chromosomes align at methaphase, the levels of the PLK1 at kinetochore decrease and this seems to be dependent on PP1 recruitment. Like Aurora B, PLK1 substrates are likely to be dephosphorylated in a PP1-dependent manner (Liu et al., 2012). Moreover, PLK1 directly binds to the PP1 interactor MYPT1. Depletion of MYPT1 increases PLK1 phosphorylation on Thr210 and thus increases its kinase activity, suggesting that MYPT1/PP1 antagonizes PLK1 activity (Yamashiro et al., 2008). It was also shown that, in yeast, PP1 localization at the kinetochores is necessary for SAC silencing, indicating that dephosphorylation of kinetochore-associated proteins is required for SAC silencing. In yeast the association of PP1 with Spc7 (KLN1 in human) and kinesins Klp5/6 is needed for SAC silencing and kinetochore-microtubule attachment. IF18A, the vertebrate orthologue of Klp5/6, also interacts with PP1 (Meadows et al., 2011).

Protein phosphatases, including PP1, are required for mitotic exit (Bollen et al., 2009). Mitotic exit is characterized by mitotic spindle breakdown, chromosome decondensation and reassembly of interphase structures, particularly the NE. PP1 was shown to be required for kinetochore disassembly, possibly by dephosphorylation of a chromatin or kinetochore-bound substrate (Emanuele et al., 2008). Moreover, it was demonstrated that inhibitor-2 is required for accurate chromosome segregation and cytokinesis by regulating the Aurora B and PP1 activity (Wang et al., 2008b). PP1 and its regulatory subunits Repo-man (recruits PP1 onto mitotic chromatin at anaphase) and PNUTS are required for chromatin decondensation. Repo-man was initially found to recruit PP1γ to chromatin at anaphase and when overexpressed also recruits PP1α to chromatin (Trinkle-Mulcahy et al., 2006). The PP1γ/Repo-man complex, in particular, mediates the dephosphorylation of histone H3 at the end of mitosis and regulates chromosomal targeting of Aurora B (Qian et al., 2011). Dephosphorylation of histone H3 by PP1 seems to be correlated with chromosome decondensation in budding yeast and nematodes (Hsu et al., 2000). PNUTS is targeted to the reforming nucleus in telophase concomitantly with chromatin decondensation and promotes chromatin decondensation in a PP1-dependent manner (Landsverk et al., 2005). Furthermore, it

was reported that PP1 is involved in the first step of nuclear envelope (NE) reassembly by stimulating the targeting of membrane vesicles to chromatin in *Xenopus* egg extracts (Ito et al., 2007). Moreover, the reassembly of the nuclear lamina is mediated in part by dephosphorylation of lamin B (Thompson et al., 1997). The PP1 regulatory subunit A-kinase anchoring protein (AKAP)-149 recruits PP1 to the NE upon NE assembly *in vitro* and promotes lamin B dephosphorylation and polymerization (Steen et al., 2000). Mitotic exit also requires CDK1 inactivation by cyclin B degradation and dephosphorylation of CDK1 and other kinases substrates. PP1 activity is repressed at early-mid mitosis by CDK1 phosphorylation on PP1 residue Thr320 (Kwon et al., 1997) and by binding to inhibitor-1. CDK1 inactivation at the end of mitosis allows PP1 auto-dephosphorylation promoting partial PP1 activation. PP1 is then able to dephosphorylate and inactivate inhibitor-1, allowing for the complete activation of PP1. Active PP1 dephosphorylates mitotic phosphoproteins required for mitotic exit (Wu et al., 2009).

A role for PP1 in the regulation of cytokinesis has also been suggested (Cheng et al., 2000; Fernandez et al., 1992), consistent with the co-localization of PP1γ and F-actin at the cleavage furrow and spindle midzone (Trinkle-Mulcahy et al., 2003). PP1γ was also found in the center of the midbody during cytokinesis (Zeitlin et al., 2001).

I.1.2.2. PP1 signaling in the brain

PP1 isoforms α, β/δ and γ1 are ubiquitously expressed in mammalian tissues but have higher abundance in brain. Within the brain, the mRNAs for these isoforms were widely distributed with particular incidence in the hippocampus and the cerebellum (da Cruz e Silva et al., 1995b). At the protein level PP1α and PP1γ1 have highest levels of expression in the striatum, where they are relatively enriched in the medium-sized spiny neurons (da Cruz e Silva et al., 1995b; Ouimet et al., 1995). At the ultrastructural level, PP1α and PP1γ1 are highly and specifically concentrated in dendritic spines in the striatum. At spines, PP1α and γ1 are concentrated at the postsynaptic density. The localization of PP1α and PP1γ1 at dendritic spines, the principal sites for excitatory synapses in the central nervous system, suggests that these isoforms are involved more extensively in postsynaptic mechanisms of neurotransmission rather than PP1β/δ. In

addition, PP1α, γ1 and β/δ are also located at the cell body, dendritic shafts and axons (Bordelon et al., 2005; Ouimet et al., 1995). Additionally, PP1β/δ and PP1γ1 were detected in all cytoskeletal fractions (neurofilaments, microtubules and actin cytoskeleton) from hindbrain proteins. However, PP1β/δ was found enriched in the microtubules whereas PP1γ1 was found mostly in the actin cytoskeleton fraction (Strack et al., 1999). Indeed, PP1, alongside with PP2A, were reported to have a role in the neurite structure. Inhibition of PP1 and PP2A in cultured hippocampal neurons leads to decrease number and length of neurites, synapse loss and also hyperphosphorylation of the microtubule-stabilizing protein tau (Malchiodi-Albedi et al., 1997). Hyperphosphorylation of tau leads to tau aggregation and formation of neurofibrillary tangles, a feature of Alzheimer's disease.

I.1.2.2.1. PP1/DARPP-32 signaling pathway

Medium-sized spiny neurons are highly enriched for DARPP-32 (Ouimet et al., 1984), which has a crucial role in the biology of dopamineceptive neurons. Dopamine and others neurotransmitters in the striatum alter the (de)phosphorylation state of DARPP-32 (Greengard et al., 1999). When phosphorylated by PKA on Thr34, DARPP-32 is a potent inhibitor of PP1 (Hemmings et al., 1984). Conversely, phosphorylation of DARPP-32 on Thr75 by CDK5 turns DARPP-32 into an inhibitor of PKA and blocks phosphorylation on Thr34 (Bibb et al., 1999). Thus, DARPP-32 modulates PP1 and PKA activities in the striatum, which in turn regulate the expression of neuropeptides and ion channels and pumps (Fig. I.7). Dopamine has opposite effects on PKA signalling when bound to D1 or D2 dopamine receptors of medium-sized spiny neurons. These neurons contain both D1 class (D1, D5) and D2 class (D2, D3, D4) dopamine receptors. However, D1 receptors are predominantly expressed in striatonigral neurons, while D2 receptors are mainly found in striatopallidal neurons. Dopamine has an excitatory effect on striatonigral neurons expressing D1 receptors and causes increased activity of adenylyl cyclase and cAMP-mediated activation of PKA, which phosphorylates DARPP-32 on Thr34 converting DARPP-32 into a PP1 inhibitor. Ligands that stimulate PKA also promote the dephosphorylation of Thr75 by PP2A. In contrast, striatopallidal neurons expressing D2 receptors are inhibited by dopamine by two mechanisms: inhibition of adenylyl cyclase and thus PKA; and Ca^{2+} and PP2B-

mediated dephosphorylation of DARPP-32 and restore of PP1 activity (reviewed in Greengard et al., 1999).

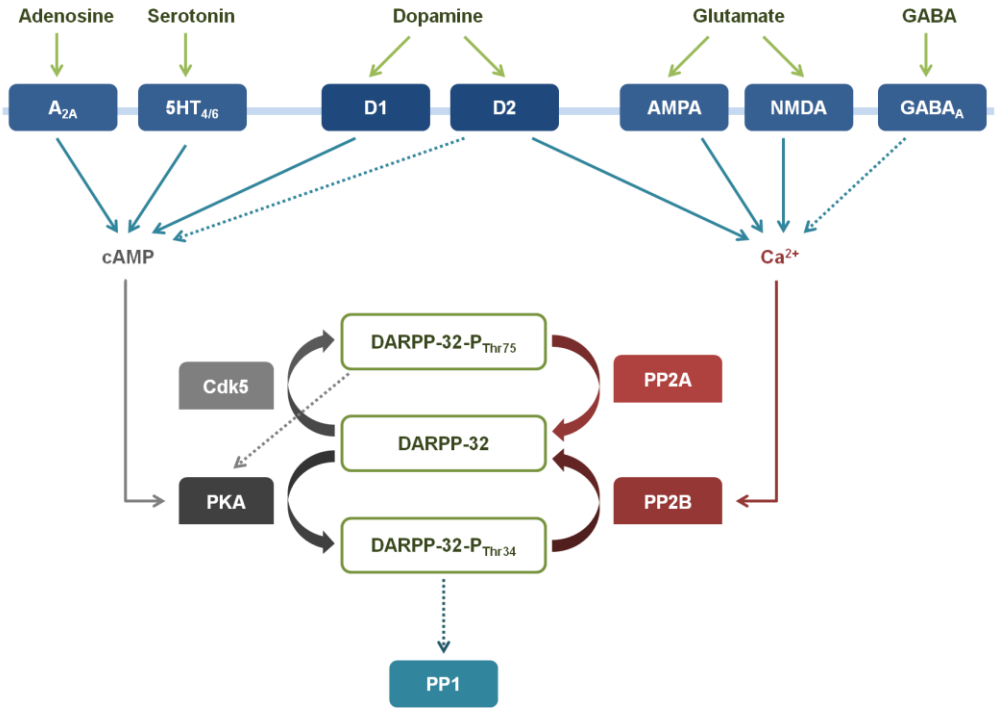

Figure I.7. Regulation of DARPP-32/PP1 signaling pathway. Dopamine acts on D1 receptors to increase cAMP formation and activation of PKA, which phosphorylates DARPP-32 on Thr34 leading to PP1 inhibition. Conversely, activation of D2 receptors leads to an increase in $Ca2^{+}$ levels and activity of PP2B, which dephosphorylates DARPP-32. D2 receptors can also act to decrease cAMP formation. Cdk5 phosphorylates DARPP-32 on Thr75 converting DARPP-32 into a PKA inhibitor. Further, PP2A dephosphorylates DARPP-32 on Thr75. Both adenosin and serotonin act on A_{2A} and 5-$HT_{4/6}$, respectively, and promote cAMP formation, PKA activation and thus DARPP-32 Thr34 phosphorylation. Glutamate act on NMDA and AMPA receptors leading to increase Ca^{2+} levels and PP2B activity, whereas GABA action on $GABA_A$ receptors has an opposite effect. Stimulatory effects are represented as solid arrows and inhibitory effects as dashed arrows.

DARPP-32/PP1 pathway in medium-sized spiny neurons is also affected by other neurotransmitters (Fig, I.7). Adenosine via A_{2A} adenosine receptor stimulates adenylyl cyclase and activates PKA, leading to the phosphorylation of DARPP-32 at Thr34 (Svenningsson et al., 1998). Serotonin binding to 5-$HT_{4/6}$ receptor also promotes the activity of adenylyl cyclase and PKA and thus phosphorylation of DARPP-32 at Thr34 (Svenningsson et al., 2002). Glutamate acting on N-methyl-D-aspartate (NMDA) and α-amino-3-hydroxy-5-methyl-4-isoxazolepropionic acid (AMPA) receptors stimulates DARPP-32 dephosphorylation by PP2B by influx of Ca^{2+}. In contrast, γ-aminobutyric

acid (GABA) acting on $GABA_A$ receptors stimulates DARPP-32 phosphorylation by hyperpolarization of the neuron and decreases influx of Ca^{2+}, resulting in the inactivation of PP2B. Inhibition of PP1 by phospho-DARPP-32, in concert with PKA and other kinase activities, results in an increased phosphorylation of various downstream effector proteins. Higher levels of phosphorylation are associated with decreased activity of $GABA_A$ receptors, Na^+ channels, and the Na^+/K+-ATPase and increased activity of NMDA and AMPA glutamate receptors, L-, N-, and P-type Ca^{2+} channels and CREB (Greengard et al., 1999).

I.1.2.2.2. PP1 regulation of synaptic plasticity

PP1 has been associated with changes in glutamatergic transmission. Glutamate is the major excitatory neurotransmitter in the mammalian nervous system and its effects are mediated in part by NMDA and AMPA receptors. NMDA and AMPA glutamate receptor subunits are pivotal in synaptic plasticity and its activity is regulated by protein phosphorylation (Munton et al., 2004; Soderling and Derkach, 2000). The efficiency of transmission at glutamatergic synapses can be strengthened (long-term potentiation, LTP) by brief, high-frequency stimulation or weakened (long-term depression, LTD) by prolonged, low-frequency stimulation (Malenka, 1994). It was reported that inhibition of PP1 is required for LTP induction in hippocampal neurons. Stimulation that induces LTP leads to cAMP-dependent phosphorylation of inhibitor-1 resulting in decreased PP1 activity. Moreover, this also results in increased phosphorylation of Ca^{2+}/calmodulin-dependent kinase II (CaMKII) at Thr286 and thus increased activity of CaMKII (Blitzer et al., 1998), which phosphorylates the AMPA receptor subunits and potentiates synaptic current (Soderling and Derkach, 2000). Moreover, at the postsynaptic density, PP1 dephosphorylates CaMKII on Thr286 and inactivates it (Strack et al., 1997).

Conversely, LTD was associated with activation of PP1 after dephosphorylation and inactivation of inhibitor-1 by PP2B in hippocampus (Mulkey et al., 1994). Dephosphorylation of AMPA receptors is correlated with LTD. Introduction of peptides that disrupt the binding of PP1 to its regulatory subunits inhibited NMDA receptor-dependent LTD and addition of active PP1 enhanced LTD. It was also reported that synaptic activation of NMDA receptor in cultured hippocampal neurons caused a

redistribution of PP1 to synapses (Morishita et al., 2001). Recently, it was reported that PP1α regulates the NR2B subunit of the NMDA receptor by dephosphorylating a specific residue on N2RB (Farinelli et al., 2012).

I.1.2.2.3. Localization of PP1 to dendritic spines

Regulation of dendritic spine motility is mediated by signaling pathways that involve PP1 and some of its regulatory subunits. PP1α and PP1γ are specifically concentrated at the postsynaptic density of dendritic spines (Bordelon et al., 2005; Ouimet et al., 1995). Among the known neuronal PP1 regulators that are also postsynaptically localized are spinophilin (Allen et al., 1997), neurabin I (McAvoy et al., 1999), yotiao (Westphal et al., 1999), neurofilament light chain (Terry-Lorenzo et al., 2000) and AKAP79 (Le et al., 2011).

Spinophilin (also named neurabin II) and neurabin I can both target PP1 to dendritic spines. Spinophilin was identified as a PP1 binding protein enriched in spines heads (Allen et al., 1997). Spinophilin binds to F-actin and it was demonstrated that the F-actin binding domain is necessary and sufficient for targeting PP1 to dendritic spines (Grossman et al., 2002). Spinophilin can also target PP1 to the postsynaptic density in close proximity with the AMPA receptors (Yan et al., 1999). Thus, PP1 is important for AMPA receptor activity and synaptic plasticity not only through DARPP-32/PP1 pathway, but also by association with spinophilin. Spinophilin is also important for PP1-mediated regulation of NMDA receptors. Consistent with altered glutamatergic transmission, spinophilin-knockout mice showed reduced LTD and altered spine density and filopodia formation (Feng et al., 2000). Recently, it was reported that spinophilin can target CaMKII to F-actin as well as targets PP1 to CaMKII (Baucum et al., 2012).

Neurabin I is a F-actin binding protein mainly expressed in neural tissues, that binds to PP1α and PP1γ. Neurabin I is phosphorylated on Ser461 by PKA disrupting the interaction with PP1 (McAvoy et al., 1999). PP1 also binds yotiao, a protein member of the AKAP family. It seems that yotiao attaches PP1 and PKA to NMDA receptors regulating synaptic transmission mediated by the NMDA receptor (Westphal et al., 1999). At the postsynaptic density PP1 also binds to neurofilament light chain, a component of the intermediate filament network in neurons, which can be

phosphorylated by PKA and by protein kinase N (PKN) (Terry-Lorenzo et al., 2000). AKAP79 was recently identified as a PP1 regulatory protein (Le et al., 2011) but it was previously described to anchor PKA, protein kinase C (PKC) and PP2B at the postsynaptic density regulating AMPA receptors phosphorylation in these pathways (Bauman et al., 2004).

I.2. THE NUCLEAR ENVELOPE

The eukaryotic nucleus is a complex organelle enclosed by a double membrane, the NE. The NE separates the cytoplasm from de the nucleus in eukaryotic cells and is structurally composed by the inner nuclear membrane (INM), the outer nuclear membrane (ONM), the nuclear lamina and the nuclear pore complexes (NPCs) (Fig. I.8) (reviewed in Gerace and Burke, 1988; Worman and Courvalin, 2005). The INM and the ONM are separated by a perinuclear space (Stewart et al., 2007) that is 40-50 nm wide in mammalian cells. However these membranes are joined in some regions at the NPCs, structures that regulate molecular transport between the cytoplasm and the nucleoplasm. NPCs are large macromolecular complexes composed of 30 different proteins, termed nucleoporins (reviewed in Fahrenkrog and Aebi, 2003). The ONM is continuous with the endoplasmic reticulum (ER) and contains various proteins found in the ER and associated ribosomes (Pathak et al., 1986). Nonetheless, the ONM also contains specific proteins that are involved in nuclear positioning by linking the nucleus to the cytoskeleton (Crisp et al., 2006; Starr and Han, 2002; Wilhelmsen et al., 2005). In contrast, the INM contains a set of distinctive integral membrane proteins. Using proteomic approaches nearly 70 transmembrane proteins were found to associate with the INM (Malik et al., 2010; Schirmer et al., 2003) but, so far, few have been characterized in detail. The major components of the nuclear lamina are A-type and B-type lamins (Aebi et al., 1986), which are found in association with proteins of the INM and also in the nucleoplasm.

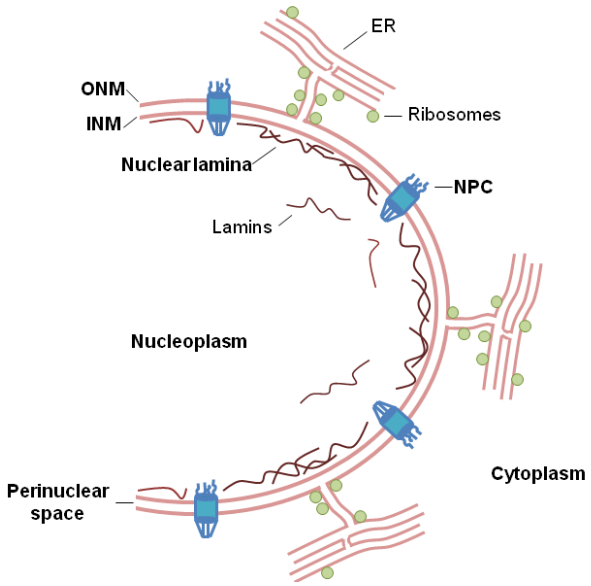

Figure I.8. Schematic illustration of the nuclear envelope. The nuclear envelope surrounds the nucleus and is composed by the inner nuclear membrane (INM) and outer nuclear membrane (ONM) that are separated by the perinuclear space, the nuclear pore complexes (NPCs) and the nuclear lamina. The endoplasmic reticulum (ER) is contiguous with the ONM. The nuclear lamina lines the INM and is mainly composed by lamins that are also found within the nucleus.

I.2.1. Lamins, the main components of the nuclear lamina

The nuclear lamina is located in the inner surface of the INM (Dwyer and Blobel, 1976) and is mainly composed by lamins, members of the type V intermediate filament family (Aebi et al., 1986). Nuclear lamina was originally proposed to be important for nuclear structure and anchorage of chromatin and nuclear envelope proteins. In addition, nuclear lamins are involved in DNA replication, gene expression, mitosis, regulation of chromatin, cell proliferation and differentiation and connection to the cytoskeleton (reviewed in Dechat et al., 2010).

In mammals, three genes encode lamins: *LMNA*, *LMNB1* and *LMNB2*. *LMNA* encodes lamins A and C and two less abundant isoforms C2 and AΔ10 (A-type lamins), which arise from alternative splicing (Furukawa et al., 1994; Lin and Worman, 1993; Machiels et al., 1996). Lamin A, C and probably lamin AΔ10 are expressed only in differentiated cells, while lamin C2 is uniquely expressed in germ cells (Furukawa et al., 1994; Rober et al., 1989). Early studies in mouse revealed that A-type lamins are not expressed in early embryonic cells (Stewart and Burke, 1987) and some cells (e.g. cells

of the central nervous system) express A-type lamins only after mouse birth (Rober et al., 1989). However, recent studies reported the presence of low levels of lamin A/C in mouse embryonic stem cells (Eckersley-Maslin et al., 2013). *LMNB1* and *LMNB2* encode B-type lamins (lamin B1, B2 and B3). Lamin B1 is encoded by *LMNB1* gene and lamin B2 by *LMNB2* gene, and both are expressed in most somatic cells (Hoger et al., 1990; Lin and Worman, 1995), while lamin B3 derives from *LMNB2* by alternative splicing and is germ cell-specific (Furukawa and Hotta, 1993).

In terms of structure, lamins have conserved α-helical central rod domains and head and tail domains that vary in sequence among intermediate filament proteins. Unlike cytoplasmic intermediate filaments, lamins also possess a nuclear localization signal (NLS) and an immunoglobulin-like β-fold within the tail domain (Fig. I.9). Moreover, lamin A and lamins B1 and B2 contain CAAX motifs at their C-terminus, which are a signal for farnesylation and carboxy methylation. These modifications at the C-terminal of lamins begin immediately after their synthesis. However, lamin A is synthesized as a precursor termed pre-lamin A that, after being incorporated in the nuclear lamina, is proteolytically cleaved to originate mature lamin A. This process abolishes the site for farnesylation and carboxy methylation of lamin A. In contrast, B-type lamins do not undergo this processing, thereby it remain farnesylated and carboxy methylated (reviewed in Burke and Stewart, 2013; Dauer and Worman, 2009). Farnesylation is an important modification for membrane association of lamins and may also mediate protein-protein interactions (Maske et al., 2003). In addition, lamins are post translationally modified by phosphorylation (Gerace and Blobel, 1980; Glass and Gerace, 1990), sumoylation (Zhang and Sarge, 2008) or ADP-rybosilation (Adolph, 1987). Phosphorylation is an important mechanism in the regulation of lamins properties. Thus, hiperphosphorylation of lamins was found to lead to disassembly of lamins polymers and consequently nuclear envelope disassembly. On the other hand, dephosphorylation at the end of mitosis promotes lamina assembly (Gerace and Blobel, 1980; Glass and Gerace, 1990).

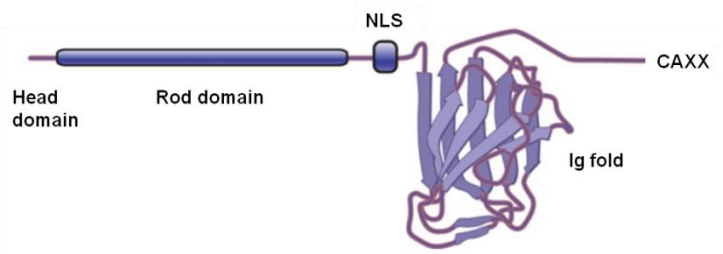

Figure I.9. Schematic illustration of lamins structure. Lamins have a head domain followed by a α-helical central rod domain and a tail domain that includes a nuclear localization signal (NLS) and an immunoglobulin (Ig)-like β-fold. Lamin A and lamins B1 and B2 also contain CAAX motifs at their C-terminus (adapted from Dauer and Worman, 2009).

Most proteins of the INM interact directly or indirectly with lamins at the nuclear periphery and are sometimes considered a part of the nuclear lamina. The first lamin associated proteins to be identified were the lamina associated polypeptide (LAP) 1 and 2 (Foisner and Gerace, 1993) and the lamin B receptor (LBR) (Worman et al., 1988). Many other lamin binding proteins were identified over the years, such as, emerin (Clements et al., 2000), MAN1 (Mansharamani and Wilson, 2005), SUN1 and SUN2 proteins (Crisp et al., 2006; Haque et al., 2006) and nesprin-1 and -2 (Libotte et al., 2005; Mislow et al., 2002). Besides being part of the nuclear lamina lining the NE, lamins are also found within the nucleoplasm. Originally, lamin A/C was observed in the nucleus of cells through mitosis and predominantly during early G1 phase. These internal lamins seemed to associate with chromatin (Bridger et al., 1993). Lamin B1 was also found within the nucleus during S-phase coincident with sites of DNA replication (Moir et al., 1994). Later, lamin A/C and lamin B1 were found to co-localize with RNA splicing factors SC-35 and U5-116 kDa in nuclear speckles (Jagatheesan et al., 1999) and lamin A/C was found to associate *in vitro* and *in vivo* with the transcription factor MOK2 (Dreuillet et al., 2002). Furthermore, lamin A/C was found in a complex with the nucleoplasmic LAP2α, which is the only LAP2 isoform not integrated in the INM (Dechat et al., 2000).

I.2.2. Properties and targeting of INM proteins

The INM contains specific integral membrane proteins and most interact with lamins and/or chromatin, thereby contributing to the NE structure. The majority of the INM proteins have the N-terminal domain located in the nucleoplasm and may have one or multiple transmembrane domains. According to the "diffusion-retention" model, after synthesis in the rough ER, INM proteins with nucleoplasmic domains smaller than 60 kDa, can diffuse laterally and reach the INM passing through the NPCs. When retained at the INM, integral membrane proteins do not diffuse back to the ER. Instead, proteins are retained in the membrane by interaction with chromatin and/or nuclear lamina (Ellenberg et al., 1997; Soullam and Worman, 1995; Wu et al., 2002). Subsequent studies suggested that transport of some proteins to the INM requires energy (ATP and/or Ran GTPase). Moreover, the putative NLS present in most mammalian INM proteins can also be responsible for targeting integral proteins to the INM in a Ran- and karyopherin- dependent manner (King et al., 2006; Zuleger et al., 2011).

The number of INM proteins identified has grown in the past years and many others are likely to be discovered in the future. Most INM proteins (Fig. I.10) have been characterized in terms of their interacting partners. Specifically, LBR contains eight putative transmembrane domains and was identified by its binding to lamin B1. LBR was also found to associate with heterochromatin protein 1 (HP1), histones H3/H4 and DNA (reviewed in Mattout-Drubezki and Gruenbaum, 2003). LAP1 was firstly identified by a monoclonal antibody (RL13) generated against lamina-enriched fractions of rat liver nuclei (Senior and Gerace, 1988). Later on, LAP2 was also identified by a monoclonal antibody against rat liver NE (RL29) (Foisner and Gerace, 1993). LAP1 will be described in detail in the following section. In human, three isoforms of LAP2 were identified: α, β and γ (Harris et al., 1994). In mouse, six LAP2 isoforms were identified: α, β, γ, ε, δ and ζ (Berger et al., 1996). While LAP2β, γ, ε and δ contain a transmembrane (TM) domain, LAP2α and ζ are not bounded to the membrane. LAP2β binds to B-type lamins and chromatin (Foisner and Gerace, 1993), and to the chromatin protein barrier autointegration factor (BAF) (Shumaker et al., 2001). LAP2α binds to both lamins A/C and chromatin (Dechat et al., 2000). All LAP2 isoforms have a LEM domain near the C-terminus as well as emerin, MAN1 and otefin (Lin et al., 2000). This LEM domain mediates binding to the chromatin associated protein BAF (Brachner and

Foisner, 2011). Emerin was firstly discovered as the gene responsible for Emery-Dreifuss muscular dystrophy (Bione et al., 1994) and later found to be located in the INM where it interacts with A-type lamins (Lee et al., 2001). Interestingly, a fraction of emerin was also detected in the ONM where it can interact directly with microtubules and contribute to the positioning of the centrosome near the ONM (Salpingidou et al., 2007). MAN1 has two putative transmembrane domains and has been linked to three related bone disorders: osteopoikilosis, Buschke-Ollendorff syndrome and melorheostosis (Hellemans et al., 2004). In contrast with others INM proteins, nurin is neither associated with NPCs nor with lamins, and contains 6 putative TM domains (Hofemeister and O'Hare, 2005). LUMA contains 4 putative TM domains and associates with SUN2, emerin and lamins (Bengtsson and Otto, 2008). Nesprins (nuclear envelope spectrin repeat domains) localizes to both NE membranes. Nesprin-1 and nesprin-2 exist in a variety of isoforms, the largest are ~1 MDa (known as giant isoforms) and contain an actin-binding domain, several spectrin repeats, a Klarsicht/ANC-1/Syne-1 homology (KASH) domain and a single TM domain (Zhang et al., 2001; Zhen et al., 2002). Nesprin-1 co-localizes with LAP1, emerin and lamins at the NE and with heterochromatin in the nucleus (Zhang et al., 2001). Nesprin-2 also localizes in the INM and ONM and binds to lamins A/C and emerin (Libotte et al., 2005). Nesprin-3 and nesprin-4 are both located at the ONM (Roux et al., 2009; Wilhelmsen et al., 2005). SUN1 and SUN2 proteins are characterized by a Sad1-UNC84 homology (SUN) domain and interact with the nuclear lamina and also with nesprins in the ONM. SUN proteins bind the KASH domain of nesprins in the perinuclear space and nesprins form a functional link with the networks of intermediate filaments, microtubules and actin filaments (Fig. I.10), thus resulting in a complex that links the nucleoskeleton and the cytoskeleton (the LINC complex) (Crisp et al., 2006; Haque et al., 2006).

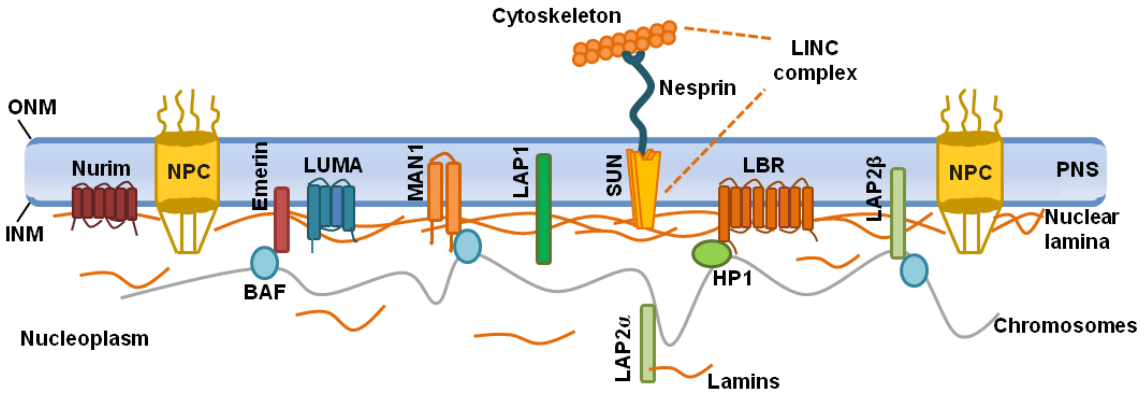

Figure I.10. Schematic view of the proteins at the inner nuclear membrane. Most proteins of the inner nuclear membrane (INM) have one or multiple transmembrane domains and bind to the nuclear lamina. Lamin B receptor (LBR) and the LEM domain-containing proteins [lamina associated polypeptide 2β (LAP2β), emerin and MAN1] bind to chromatin associated proteins, like heterochromatin protein 1 (HP1) for LBR and barrier autointegration factor (BAF) for LEM-proteins. Nurim does not seem to interact with lamins or chromatin. Lamina associated polypeptide 1 (LAP1) may bind indirectly to chromatin. SUN proteins interact in the perinuclear space with nesprin-1 and -2 of the outer nuclear membrane (ONM) and the last bind to cytoskeleton elements forming the LINC complex (links the nucleoskeleton and cytoskeleton). LAP2α is not bound to membrane and interacts with soluble lamins A/C. PNS, perinuclear space; NPC, nuclear pore complex.

Using proteomic approaches many other proteins were found to be associated with the INM (Malik et al., 2010; Schirmer et al., 2003) but are not well characterized. Some of these INM proteins are found in vertebrates and *Drosophila* but are absent in *C. elegans* and yeast, including LBR and nurin. Emerin and MAN1 were found in vertebrates, *Drosophila* and *C. elegans* but not in yeast. Other proteins might be only present in vertebrates, such as LAP1 and LAP2 (reviewed in Cohen et al., 2001). Moreover expression of INM proteins may also vary between different tissues or analyzed cell lines (Malik et al., 2010; Schirmer et al., 2005; Schirmer and Gerace, 2005).

I.2.3. NE disassembly and reassembly during mitosis

Most eukaryotic cells undergo an "open mitosis" where the NE is disassembled at the onset of mitosis (prophase) and reassembled at the end of mitosis (late anaphase/telophase). NE breakdown involves the disassembly of the NPCs, depolymerization of lamins, and spreading of most NE soluble components in the cytoplasm and INM proteins through the tubular mitotic ER (reviewed in Guttinger et al., 2009).

One of the first steps of NE breakdown is the NPC disassembly and release of nucleoporins. After this, NPCs are no longer able to regulate the transport between the cytoplasm and the nucleus. Most nucleoporins disassemble at the same time, with the exception of NUP98 that seems to be the first one to set off NPC breakdown. In early prophase the nuclear lamina is depolymerized and lamins are released into the nucleoplasm. At the same time, INM proteins are disconnected from lamins and chromatin and are dispersed through the ER (reviewed in Guttinger et al., 2009). However, while B-type lamins remain attached to the nuclear membranes during mitosis, lamin A/C are solubilized throughout the nucleoplasm (Gerace and Blobel, 1980; Stick et al., 1988). Interestingly, it was described that microtubules are important elements for NE breakdown. Microtubules that are connected to the ONM apply pulling forces that cause NE invaginations around centrosomes and this seems to open holes in the membranes. This mechanical force is provided by the microtubule minus-end directed motor protein dynein and its associated protein dynactin. NPCs disassembly, lamina depolymerization and the dissociation of proteins from nuclear membranes are mediated by phosphorylation (reviewed in Foisner, 2003; Guttinger et al., 2009). Among the different kinases involved in this process are CDK1, PKC, Aurora A and PLK1. CDK1 is a major kinase that is activated to promote mitosis and inactivated to allow mitotic exit. CDK1 phosphorylates lamins leading to lamin depolymerization and may also be involved in NPCs disassembly since many nucleoporins are phosphorylated in CDK1 sites during mitosis. CDK1 phosphorylation might also cause the dissociation of INM proteins from lamins and chromatin (reviewed in Guttinger et al., 2009). LAP2β and LAP2α are CDK1 targets (Blethrow et al., 2008) and phosphorylation of LAP2β was described to inhibit its binding to chromatin and to lamin B1 (Foisner and Gerace, 1993). Furthermore, phosphorylation of LBR by CDK1 negatively regulates the binding

of LBR to chromatin and is an important mechanism for controlling the NE assembly at the end of mitosis (Tseng and Chen, 2011).

The NE begins to reform in late anaphase and is completely reassembled at telophase. The NE reassembly involves the recruitment of membranes, NPCs insertion, polymerization of lamins and targeting of INM proteins to chromatin. NPCs assembly starts at late anaphase when chromatin recruits the NUP107-160 complex. This step is mediated by RanGTP that induces the dissociation of the NUP107-160 complex from importin-β and allow the complex to bind to chromatin. Numerous studies showed that NE reassembly requires the targeting of lamins and INM proteins to chromosomes in a synchronized way. LAP2α appears to be the first lamin binding protein to associate with chromosomes in anaphase. Transmembrane proteins LAP2β, LBR and emerin assembled around chromosomes approximately at the same time (reviewed in Foisner, 2003; Guttinger et al., 2009). Lamin B1 associates with chromosomes during late anaphase/telophase when the NE begins to reform, while lamin A can not be detected until chromosome decondensation and assembly of the major components in daughter cells. Thus, it seems that chromosome association of these proteins is regulated by different mechanisms (Moir et al., 2000). Nuclear envelope reassembly also requires inhibition of mitotic kinases and the action of phosphatases. PP1 and PP2A are important regulators of mitosis (as previously described) and its activity is required for NE assembly.

I.2.4. Lamina associated polypeptide 1 (LAP1)

Members of the LAP1 family were initially identified using monoclonal antibodies generated against lamina-enriched fractions of rat liver nuclei (Senior and Gerace, 1988). This antibody recognized a major peptide of 75 kDa and two minor peptides of 68 and 55 kDa, which were later termed LAP1A, LAP1B and LAP1C, respectively. Further, the three peptides were found to be specifically located at the INM (Senior and Gerace, 1988). Evidence of lamina association with LAP1, was provided by chemical extraction of NEs. For example, after treatment of NEs with nonionic detergent and low salt concentration, all LAP1A and LAP1B and most LAP1C remain associated with the lamina fraction (insoluble fraction). However, when NEs

were incubated with nonionic detergent and high salt concentration most LAP1A and LAP1B remain associated with the insoluble lamina fraction while LAP1C was solubilized. These results lead to the assumption that LAP1C has a weaker interaction with the nuclear lamina than the two other proteins (Foisner and Gerace, 1993; Senior and Gerace, 1988). Specifically, LAP1A and LAP1B were found to bind directly to lamins A, C and B1 *in vitro* and probably indirectly to chromosomes (Foisner and Gerace, 1993) and LAP1A/C co-immunoprecipitated with B-type lamins (Maison et al., 1997)

In 1995 (Martin et al., 1995) the cDNA for LAP1C was completely sequenced in rat. Partial characterization of other cDNAs suggested that the three LAP1 family members arise from alternative splicing, given that LAP1A and LAP1B partial cDNAs were identical to the LAP1C sequence with the addition of two insertions. Moreover, it was demonstrated that LAP1C is a type II transmembrane protein, containing a nucleoplasmic N-terminal domain, a single TM domain and a lumenal C-terminal domain located in the perinuclear space (Martin et al., 1995). The full-length cDNA of human LAP1B was only reported in 2002. LAP1B was isolated from an expression library of HeLa cells and showed 73.6% amino acid identity with the predicted rat LAP1B (Kondo et al., 2002). Human LAP1B has a single TM domain and the lumenal domain and the nucleoplasmic domain have 89% and 65.8% amino acid identity with the predicted rat LAP1B (Fig. I.11), respectively (Kondo et al., 2002). Additionally, another splice variant of LAP1 was identified, but has only one more amino acid (alanine) than the previously reported LAP1B. This LAP1B splice variant results from the exclusion of three nucleotides (CAG) from exon 3 but did not alter the translational frame. Indeed, it was reported that alternative splicing involving a 3' tandem splice site NAGNAG sequence, which results in one amino acid insertion or deletion, is very common among other proteins (Tadokoro et al., 2005; Tsai et al., 2007). Analysis of the subcellular localization of different LAP1B deletion mutants demonstrated that the latter half of the nucleoplasmic domain and the TM domain are responsible for the localization of LAP1B at the NE. In contrast, only constructs with the whole nucleoplasmic domain were fully resistant to extraction with Triton X-100. Deletion mutants containing only a part of the nucleoplasmic domain were extractable using this detergent. These data suggested that full retention of LAP1B at the NE requires the complete nucleoplasmic domain. Furthermore, interaction with other nuclear

components, like lamins or chromatin, may also be important for the proper localization of LAP1B (Kondo et al., 2002).

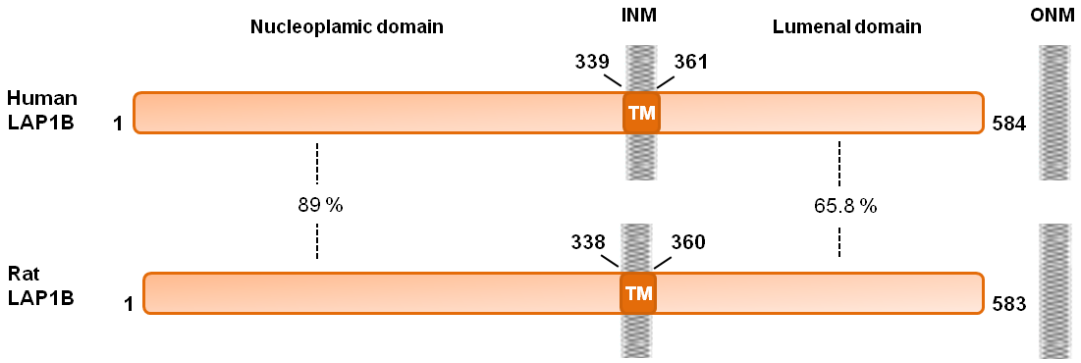

Figure I.11. Schematic representation of homology between human LAP1B and rat LAP1B. Both human and rat LAP1B have a long N-terminal nucleoplasmic domain with 89% of homology and a shorter C-terminal lumenal domain with 65.8% of homology, and one transmembrane domain (TM) (Kondo et al., 2002). INM, inner nuclear membrane; ONM, outer nuclear membrane.

The expression of the three LAP1 isoforms seems to be developmentally regulated. Immunoblot analysis of rat tissues and cells, demonstrated that rat LAP1A, B and C are present in similar amounts in liver, spleen, brain and kidney tissues, while LAP1C is the major peptide identified in cultured cells (Senior and Gerace, 1988). By comparing the mouse P19 teratocarcinoma cell line and the differentiated P19MES line, LAP1C was found to be similarly expressed in both cells, while LAP1A and LAP1B were expressed at higher levels in the differentiated cells (Martin et al., 1995). LAP1 is ubiquitously expressed in neuronal and non-neuronal tissues and also during embryogenesis (Goodchild and Dauer, 2005; Goodchild et al., 2005). However, during mouse spinal cord development, the expression of each mouse LAP1 isoform is different. LAP1A is upregulated approximately at the same time as the NE vesicles begin to form (Goodchild et al., 2005)

As referred above, phosphorylation is an important regulatory mechanism for the assembly/disassembly of lamins polymers. Like lamins, LAP1 is also phosphorylated. Rat LAP1 isoforms were found to be phosphorylated *in vitro* and at least LAP1C was also phosphorylated *in vivo*. However, the (de)phosphorylated state of LAP1A and B did not influence the binding to lamins *in vitro* (Foisner and Gerace, 1993). More recently, diverse phosphorylated sites of LAP1B (Fig. I.12) were identified by high-

throughput studies (Chi et al., 2008; Dephoure et al., 2008; Han et al., 2010; Olsen et al., 2006; Olsen et al., 2010; Wang et al., 2010; Weber et al., 2012). Moreover, it seems that LAP1 is highly phosphorylated during mitosis, as is the case for other nuclear proteins (Dephoure et al., 2008; Olsen et al., 2010). Indeed, kinases that regulate cell cycle, such as, CDKs, ataxia-telangiectasia mutated (ATM) and ataxia-telangiectasia and Rad 3-related (ATR) might be involved in LAP1 phosphorylation. Human LAP1B was found to be phosphorylated on Ser143, in a proline-directed manner similar to CDKs substrates (Chi et al., 2008), and on Ser164 within the ATM/ATR recognition sequence motifs (Olsen et al., 2010). Rat LAP1B Ser142 (homologous to human LAP1B Ser143) was found to be phosphorylated by CDK1-cyclin B (Blethrow et al., 2008). In addition, LAP1 was also found to be post-translationally modified by ubiquitination (Fig. I.12) (Kim et al., 2011; Wagner et al., 2011). Ubiquitination is a crucial regulatory mechanism for various cellular processes, including protein degradation, cell division and DNA repair as well as for controlling stability and localization of proteins (Ciechanover, 1994).

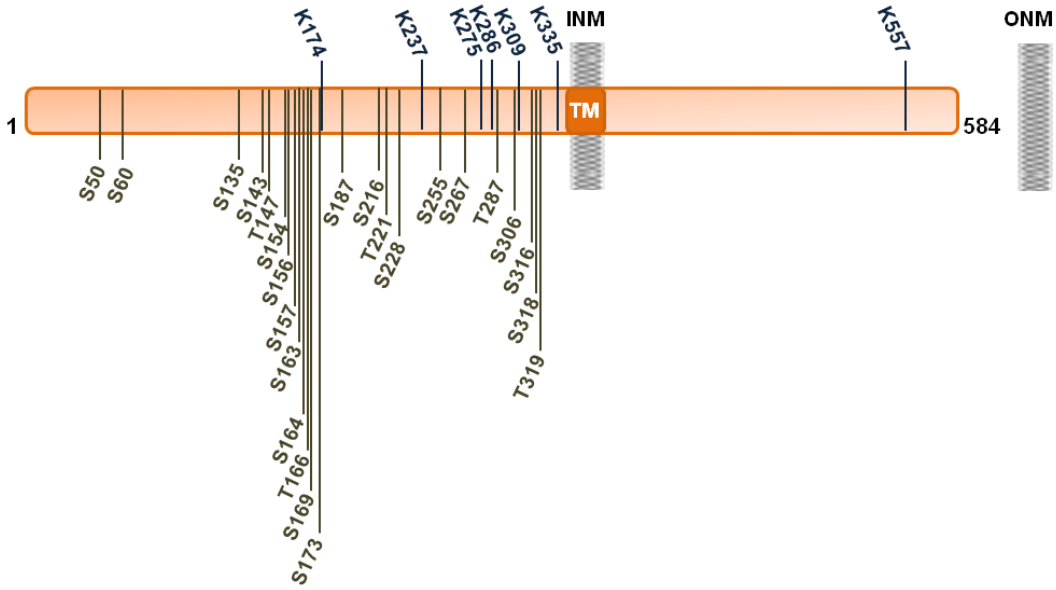

Figure I.12. LAP1B post-translational modifications. LAP1B can be phosphorylated in the nucleoplasmic domain at numerous serine (S) and threonine (T) residues. Each residue phosphorylated is indicated. Ser143 and Ser164 are probably phosphorylated by CDK2 and ATM/ATR kinases, respectively. LAP1B can also be modified by ubiquitination at the sites indicated (K). INM, inner nuclear membrane; ONM, outer nuclear membrane; TM, transmembrane domain. The sites indicated at relative to the GenBank sequence NM_001267578 (Human LAP1B).

I.2.4.1. LAP1 distribution during the cell cycle

In interphase cells LAP1 is well described to be located at the INM in association with lamins and chromosomes. However, when the NE is completely disassembled at prometaphase, LAP1 seems to be redistributed through the ER (Fig. I.13). At this point LAP1 is no longer associated with chromosomes or lamins. At late anaphase LAP1 reappeares at the chromosomes' surface and by telophase LAP1 acquires again a perinuclear location (Foisner and Gerace, 1993; Senior and Gerace, 1988; Yang et al., 1997). However, it seems that LAP1 reappears in the reforming NE prior to lamins (Foisner and Gerace, 1993). Another study (Maison et al., 1997) reported that during mitosis LAP1C and lamin B colocalize in mitotic vesicles which associate transiently with the mitotic spindle. Moreover, during anaphase, LAP1C was located at the surfaces of chromosomes, particularly on the sides facing the mitotic spindle poles. At telophase/cytokinesis LAP1C has reassembled at the NE but LAP1C was also detected in the mid-body (Fig. I.13).

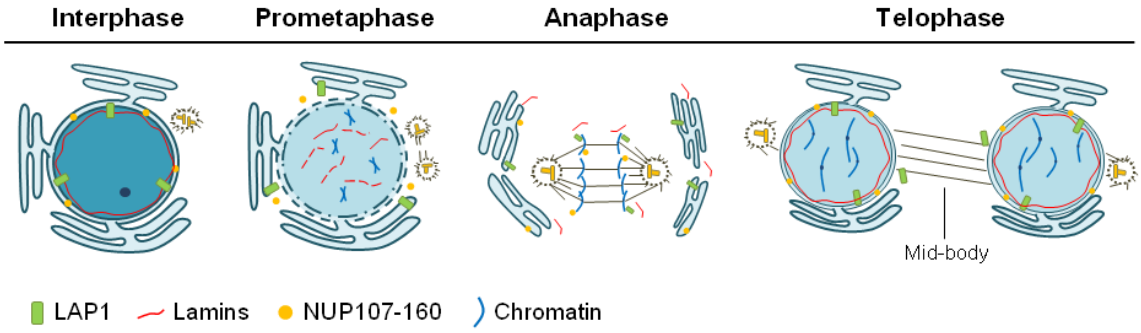

Figure I.13. LAP1 localization during the cell cycle. In interphase cells LAP1 is located in the inner nuclear membrane but at prometaphase LAP1 is distributed through the endoplasmic reticulum. At anaphase LAP1 localizes at chromosomes surface and at telophase LAP1 is redistributed again to the inner nuclear membrane, but is also detected in the mid-body. Nuclear pore complex and nuclear lamina are also disassembled at prometaphase and NUP107-160 are the first nucleoporins recruited by chromatin at anaphase.

I.2.4.2. LAP1 physiological function and associated proteins

The function of LAP1 remains poorly understood. The interaction with nuclear lamins suggests that LAP1 may be important for attaching the nuclear lamina to the INM and thereby contribute to the NE architecture (Foisner and Gerace, 1993; Martin et al., 1995). Kim and colleagues (Kim et al., 2010a) assessed the LAP1 function *in vivo* using a mouse model in which the *TOR1AIP1* locus (encoding LAP1) was disrupted with a gene trap cassette. The nuclear membranes of various tissues and cultured neurons of TOR1AIP1$^{-/-}$ mice embryos showed abnormalities. These defects included "blebs – vesicle-appearing structures" in the perinuclear space. Moreover, TOR1AIP1$^{-/-}$ mice usually die on the last prenatal day or first postnatal day, while TOR1AIP$^{+/-}$ mice were identical to wild-type mice (Kim et al., 2010a). Other authors (Neumann et al., 2010) also proposed a function for LAP1 in the assembly of the mitotic spindle. Knockdown of LAP1 in HeLa cells using RNAi cause mitotic spindle formation to fail in prometaphase, probably because centrosomes could not form a bipolar mitotic spindle or align chromosomes. This lead to anomalous mitosis resulting in cell death. Thus, it seems that LAP1 is a crucial protein in the NE and its absence leads to cell death.

LAP1 has been implicated in the pathogenesis of a neurological disorder termed DYT1 dystonia. DYT1 dystonia is caused by a mutation in the *DYT1* gene that encodes the torsinA protein, a member of the AAA^{+} superfamily of ATPases associated with several subcellular activities (Ozelius et al., 1997) (described in the following sections). LAP1 was found to relocate the torsinA to the NE, although the latter is normally found in ER (Goodchild and Dauer, 2005). The torsinA mutant form, which is present in DYT1 dystonia patients, is also primarily relocated to the NE (Goodchild and Dauer, 2004; Naismith et al., 2004). In addition, LAP1 co-immunoprecipitated with all four members of the human torsin family: torsinA, torsinB, torsin2 and torsin3 (Kim et al., 2010a). Introducing a key mutation in the AAA+ domain stabilizes torsin proteins in an ATP-bound, substrate-trapped state and causes its redistribution from the ER to the NE. However, LAP1 depletion in NIH-3T3 cells and mouse embryonic fibroblasts led to a shift of the NE-located torsinA and torsinB to the ER. In contrast the localization of torsin2 and torsin3 is not affected by LAP1 depletion. Thus, LAP1 is required for the NE localization of torsinA and torsinB (Jungwirth et al., 2010; Kim et al., 2010a). Recently, it was described that torsinA alone is catalytically inactive. However, its

ATPase activity is induced by the lumenal domains of LAP1 and a protein with a lumenal domain- like LAP1 (LULL1) (Zhao et al., 2013a).

Recently, it was reported that LAP1 binds to emerin and the interaction occurs through their nucleoplasmic domains. Moreover, LAP1 was found to be required for the normal localization of emerin. Conditional deletion of LAP1 from mouse striated muscle caused muscular dystrophy leading to early lethality, thus arguing that LAP1 plays a crucial role in skeletal muscle maintenance (Shin et al., 2013).

Other proteins were found to interact with LAP1 (described in table I.1) and may uncover potentially nuclear functions for LAP1, such as, the mitotic arrest deficient 2 (MAD2)-like 1 (MAD2L1) (Hutchins et al., 2010). MAD2 is an element of the mitotic spindle checkpoint that prevents the onset of anaphase until chromosomes are aligned at the metaphase plate (Luo et al., 2000). In a large-scale screen for telomere interacting proteins, human LAP1B was identified as novel putative regulator of telomeres. LAP1B was found to associate with the human Rap1, a TRF2 (telomeric repeat binding factor 2) binding protein (Lee et al., 2011). Rap1 regulates the telomere length and may modulate the recruitment of potential regulators of telomere length (O'Connor et al., 2004). Havugimana and colleagues (Havugimana et al., 2012) performed large screens of stably associated human protein complexes present in cytoplasmic and nuclear extracts. In these screens various proteins were found in association with LAP1B (Table I.1) but some are located at subcellular compartments not previously described for LAP1B (e. g. mitochondria). Therefore, these interactions should be validated by additional methodologies.

Table I.1. List of the identified LAP1 interacting proteins.

Interactor	Description	Experimental evidence	References
LMNB1	Lamin B1 Nuclear lamina protein	*In vitro* binding assay	(Foisner and Gerace, 1993)
		Co-IP	(Maison et al., 1997)
LMNA	Lamin A/C Nuclear lamina protein	*In vitro* binding assay	(Foisner and Gerace, 1993)
TOR1A	TorsinA AAA+ ATPase	FRAP	(Goodchild and Dauer, 2005)
		Co-IP and MS	(Naismith et al., 2009a)
		Co-IP	(Kim et al., 2010a)
TOR1B	TorsinB AAA+ ATPase	Co-IP	(Kim et al., 2010a)
		In-cell competition assay	(Jungwirth et al., 2010)
TOR2	Torsin2 AAA+ ATPase	Co-IP	(Kim et al., 2010a)
TOR3	Torsin3 AAA+ ATPase		
ATP1B4	Na, K-ATPase βm-subunit Transcriptional regulator in placental mammals	Yeast two-bybrid Co-IP	(Pestov et al., 2007)
HUR	Hu antigen R, RNA binding protein	Affinity capture - RNA	(Abdelmohsen et al., 2009)
Tat	Tat , transcriptional activator of human immunodeficiency virus type 1	Affinity chromatography - MS	(Gautier et al., 2009)
PPP1CA	Protein Phosphatase 1 alpha Major Ser/Thr phosphatase	Yeast two-hybrid	(Esteves et al., 2012a; Santos, 2009)
PPP1CC	Protein Phosphatase 1 gamma Major Ser/Thr phosphatase	Yeast two-hybrid	(Esteves et al., 2013b; Santos, 2009)
MAD2L1	Mitotic arrest deficient-like 1 Mitotic spindle checkpoint protein	Affinity capture - MS	(Hutchins et al., 2010)
TERF2	Telomeric repeat binding factor 2 Telomere nucleoprotein	Protein complementation array screen	(Lee et al., 2011)
Rap1	TRF2 binding protein	Protein complementation array screen GST pull-down	

Interactor	Description	Experimental evidence	References
RIF1	RAP1 interacting factor 1 homologue	Complex fractioning - MS	(Havugimana et al., 2012)
SEPT9	Septin 9 Involved in cytokinesis		
NUP50	Nucleoporin 50kDa Nuclear pore complex protein		
HNRNPM	Heterogeneous nuclear ribonucleoprotein M RNA binding protein		
HPDL	4-hydroxyphenylpyruvate dioxygenase-like protein		
S100A16	S100 calcium binding protein A16		
NIT2	Nitrilase family, member 2 Omega-amidase activity		
NDUFV1	NADH dehydrogenase [ubiquinone] flavoprotein 1, mitochondrial		
OXCT1	Succinyl-CoA: 3-ketoacid-coenzyme A transferase 1, mitochondrial		
ACA11	Orphan small nucleolar RNA, encoded within an intron of the histone methyltransferase WHSC1	RNA affinity purification - MS	(Chu et al., 2012)
EMD	Emerin INM protein	Co-IP, Pull down, MS	(Shin et al., 2013)
RFX7	DNA-binding protein RFX7 Transcription factor	MS	
PRKDC	Protein kinase, DNA-activated, catalytic subunit		
E4F1	E4F transcription factor 1		
MATR3	Matrin 3 Nuclear matrix protein		
HNRNPUL1	Heterogeneous nuclear ribonucleoprotein U-like 1 Nuclear RNA-binding protein		
AIFM1	Apoptosis-inducing factor 1, mitochondrial Regulator of apoptosis		
SF3B3	Splicing factor 3B subunit 3		
IMMT	Mitofilin Mitochondrial inner membrane protein		
SMARCC2	SWI/SNF related, matrix associated, actin dependent regulator of chromatin, subfamily c, member 2		

Co-IP, co-immunoprecipitation; FRAP, fluorescence recovery after photobleaching; INM, inner nuclear membrane; MS, mass spectrometry.

I.2.5. Relevance of nuclear envelope proteins in disease

About 20 different inherited diseases have been linked to NE proteins. The diversity of functions of these proteins as well as the range of NE-associated diseases suggests that NE proteins have essential regulatory functions. Maintenance of nuclear structure and regulation of transcription and cell cycle could explain how NE proteins cause these diseases. Moreover mutations in NE proteins may also cause disruption of functional protein complexes (Kavanagh et al., 2007).

Diverse conditions termed laminophaties have been linked to mutations in the *LMNA* gene. *LMNA* mutations cause tissue-specific phenotypes involving striated muscle, adipose tissue, peripheral nerve or multiple systems. Most inherited *LMNA* mutations lead to disorders that affect striated muscles with or without tendon involvement and also affect the heart (cardiomyopathy). Mutations that cause muscle syndromes mostly result in decreased levels of A-type lamins (reviewed in Dauer and Worman, 2009). Although no loss-of-function mutations have been found in B-type lamins, two rare diseases affecting the central nervous system (CNS) have been associated with high levels of lamin B1. Duplication of the *LMNB1* gene has been linked to autosomal dominant leukodystrophy (ADLD), a demyelinating disorder, (Padiath et al., 2006) and increased levels of lamin B1 were also identified in lymphoblast and fibroblasts from patients with ataxia telangiectasia, a neurodegenerative disease (Barascu et al., 2012). In contrast, reduced levels of lamin B1 were observed in fibroblasts from patients with Hutchinson-Gilford progeria syndrome (Scaffidi and Misteli, 2005), an accelerated aging condition, and senescent human fibroblasts (Dreesen et al., 2013). A recent study identified two missense *LMNB1* mutations in neural tube defects patients that were predicted to compromise the interaction of lamin B1 with the nuclear lamina. These mutation may contribute to susceptibility to neural tube defects (Robinson et al., 2013). Emerin was firstly discovered as the gene responsible for the X-linked form of Emery-Dreifuss muscular dystrophy (EDMD), characterized by progressive skeletal muscle wasting, contractures and cardiomyopathy (Bione et al., 1994). Diverse disease-causing mutations in the emerin gene have been found and most result in reduced levels of emerin and mistargeting to the cytoplasm (Manilal et al., 1998). Interestingly, mutations in *LMNA* cause the autosomal type of EDMD (Bonne et al., 1999). Studies using mouse models for autosomal dominant EDMD and Hutchinson-Gilford progeria laminophaties showed

that accumulation of SUN1 is pathogenic in those conditions (Chen et al., 2012). LAP2α gene mutations are associated with dilated cardiomyopathy and the mutated LAP2α does not bind to lamin A in *vitro* (Taylor et al., 2005). As described above, the mutant torsinA (in DYT1 dystonia) is relocated to the perinuclear space where it interacts with LAP1 (Goodchild and Dauer, 2004, 2005). Rodent models of DYT1 dystonia present abnormal nuclear membranes in neurons (Goodchild et al., 2005; Grundmann et al., 2012). Moreover, similar NE defects were observed for LAP1 null mice (Kim et al., 2010a). LBR mutations are associated with Pelget-Huet anomaly, an autosomal dominant syndrome characterized by abnormal nuclear shape and chromatin organization in blood granulocytes. Mutations in LBR mostly result in reduced protein levels (Hoffmann et al., 2002). LBR has also been linked to Greenberg's skeletal dysplasia characterized by lethal skeletal and visceral anomalies (Waterham et al., 2003). Loss-of-function mutations in MAN1 gene cause osteopoikilosis, Buschke-Ollendorff syndrome, and melorheostosis. These diseases are characterized by increased bone density and may be caused by impairment of MAN1 function in Smad signaling, which is important for bone development (Hellemans et al., 2004). Mutations in nesprin-1 gene lead to autosomal recessive cerebellar ataxia characterized by lack of coordination and impaired walking (Gros-Louis et al., 2007). In mice, deletion of the KASH domain of nesprin-1 causes an EDMD-like phenotype (Puckelwartz et al., 2009). Mutations in NPC proteins were also found to cause different disorders, such as, atrial fibrillation (heart disorder) or infantile striatal necrosis and acute necrotizing encephalopathy (CNS disorders) (reviewed in Dauer and Worman, 2009).

I.3. TORSINA

TorsinA and its related family members belong to the ATPases associated with a variety of cellular activities (AAA^+) superfamily (Ozelius et al., 1997). AAA^+ proteins are chaperone proteins that mediate conformational changes in target proteins. These proteins are involved in several functions, including protein folding and degradation, membrane trafficking, DNA replication and repair, mitosis and cytoskeletal regulation (reviewed in Ogura and Wilkinson, 2001; Vale, 2000).

TorsinA is encoded by the *TOR1A* (or *DYT1*) gene and has three homologous proteins in mammals: torsinB, which is about 70% identical to torsinA; torsin2 and torsin3. *TOR1A* and *TOR1B* (encodes torsinB) genes are adjacent to each other in opposite directions on chromosome 9q. The torsin2 gene (*TOR2*) is also located on chromosome 9, while the torsin3 gene (*TOR3*) is located on chromosome 1q. Related sequences have been found in Drosophila (torp4a), nematodes (OOC-5, tor2 and tor3), zebrafish (torsinC), but not in yeast or prokaryotic genomes (Ozelius et al., 1999). TorsinA has been the most studied torsin family member due to its relation with DYT1 dystonia. A mutation of a single glutamic acid within the C-terminal of torsinA (ΔE302/303, also referred just as ΔE) was found in most cases of DTY1 dystonia (Ozelius et al., 1997). DYT1 dystonia or early-onset torsion dystonia is a movement disorder characterized by sustained or intermittent muscle contractions causing twisting and repetitive movements, abnormal postures or both (Fahn et al., 1998), as described in detail in the following sections.

The predicted structure of torsinA contains a single AAA^+ domain, which includes Walker A and Walker B nucleotide binding motifs, and the α-helical domains sensor-1 and sensor-2 (Fig. I.12), which are are thought to be important for the ATPase activity of AAA^+ proteins. Walker A and Walker B motifs are important for ATP binding and hydrolysis, respectively. The sensor-1 and -2 domains have been shown to mediate substrate interactions and to be critical for ATP hydrolysis (Iyer et al., 2004; Neuwald et al., 1999; Ogura and Wilkinson, 2001). The sequence similarity between torsinA and other AAA^+ proteins is poor within the C-terminal, where the sensor-2 motif is located (Neuwald et al., 1999). Interestingly, torsinA was the first AAA^+ protein found to reside inside the ER lumen of eukaryotic cells. Indeed, torsinA is targeted to the ER by an N-terminal signal peptide (Figure I.14) that it is cleaved and the mature torsinA resides in the lumen of the ER (Hewett et al., 2003; Kustedjo et al., 2000).

Some reports indicated that an N-terminal hydrophobic domain anchors torsinA to the ER membrane with a type II orientation (Kustedjo et al., 2000; Liu et al., 2003). However, recent reports showed that torsinA is not an integral membrane protein. The N-terminal domain does not transverse the membrane, defining torsinA as a lumenal monotopic membrane protein (Callan et al., 2007; Vander Heyden et al., 2011). Additionally, the torsinA sequence revealed the presence of a bipartite nuclear localization sequence (aa 76-94) (Shashidharan et al., 2000b). Indeed, torsinA was found to also be located in the NE in addition to the ER, when overexpressed. Furthermore, a mutation in the Walker B domain (E171Q-torsinA) inhibits ATP hydrolysis and results in an ATP-bound state, causing high affinity substrate interactions. This mutation causes a redistribution of torsinA from the ER to the NE (Goodchild and Dauer, 2004; Naismith et al., 2004). The ΔE-torsinA mutation, located within sensor-2 (Figure I.14), also causes a relocalization of torsinA from the ER to the NE (Goodchild and Dauer, 2004; Naismith et al., 2009a).

Figure I.14. Representation of torsinA protein and its characteristic domains. The structure of torsinA is predicted to contain an N-terminal signal peptide (SP) sequence which is removed from the mature protein, a putative transmembrane domain (TM) and a putative bipartite nuclear localization signal (NLS). The site of SP cleavage is indicated, which results in translocation of torsinA into the lumen of the endoplasmatic reticulum. Walker A (WA) and Walker B (WB) are nucleotide binding sites and sensor 1 (S1) and sensor 2 (S2) are configurational domains of AAA^+ proteins. The ΔE302/303 mutation is located within sensor 2 domain.

TorsinA is ubiquitously expressed but shows higher levels in liver, muscle, pancreas and brain (Ozelius et al., 1997). In brain, torsinA is expressed in all brain regions with higher levels in cerebral cortex, thalamus, hippocampus, striatum, substantia nigra pars compacta and cerebellum (Augood et al., 1999; Augood et al., 1998; Konakova et al., 2001; Rostasy et al., 2003). The expression of torsinA seems to be developmentally regulated, with higher expression during prenatal and early postnatal periods in mouse brain. Thus it was suggested that torsinA may play a role in the developing brain (Vasudevan et al., 2006; Xiao et al., 2004). Neurons showed

torsinA immunoreactivity in neuronal bodies, axons, dendrites and synaptic terminals (Augood et al., 2003; Rostasy et al., 2003).

I.3.1. TorsinA interactors and related functions

TorsinA has been shown to be involved in several cellular processes by interacting with different binding proteins (Fig. I.15). Thus, torsinA is thought to play a role in the organization of the NE and ER, cytoskeletal network, protein processing in the secretory pathway, synaptic vesicle recycling and response to stress (reviewed in Granata et al., 2009).

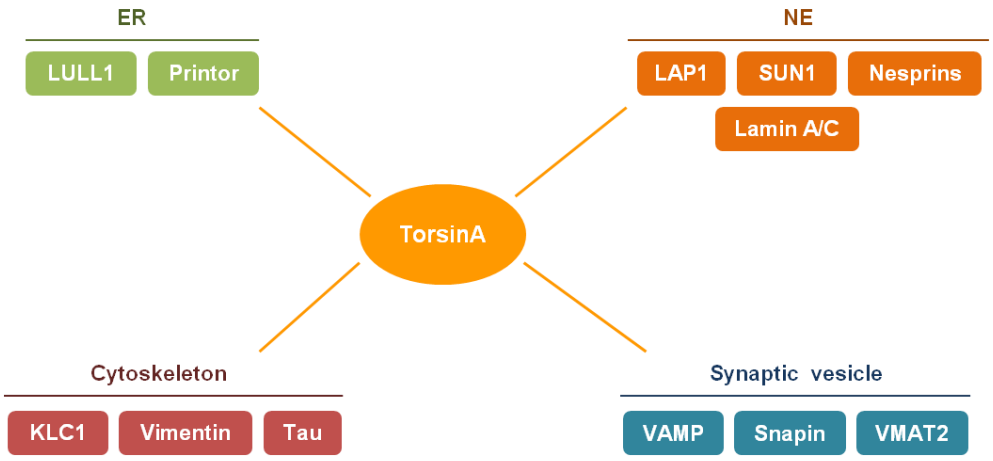

Figure I.15. TorsinA interactors and potential functions. TorsinA is located in the endoplasmic reticulum (ER), where it interacts with LULL1, and in the nuclear envelope (NE), where it binds to LAP1, SUN1 and nesprins-1, -2 and -3. Therefore it could be involved in either the organization of the ER and NE. TorsinA may be involved in cytoskeleton dynamics through interaction with kinesin light chain 1 (KLC1), vimentin or tau. TorsinA also appears to be involved in synaptic vesicle dynamics through association with vesicle-associated membrane protein (VAMP) or snapin and ΔE-torsinA causes the entrapment of snapin and vesicular monoamine transporter 2 (VMAT2) in inclusions.

I.3.1.1. TorsinA in the endoplasmic reticulum

As previously described, several studies confirmed that torsinA resides inside the ER lumen using different techniques, including subcellular fractionation, protease resistance in the presence/absence of detergent and co-localization with ER markers (Hewett et al., 2000; Hewett et al., 2003; Kustedjo et al., 2000). Recent work has shown that torsinA is not an integral membrane protein but it is instead peripherally associated with the ER membrane (Callan et al., 2007; Vander Heyden et al., 2011). Moreover, it was demonstrated that torsinA is glycosylated *in vivo* on Asn143 and Asn158, and exists as a high mannose, glycosylated state consistent with the primary localization in the ER (Hewett et al., 2003; Kustedjo et al., 2000). In the ER, torsinA was found to interact with a protein with a lumenal domain like LAP1, termed LULL1. The LULL1 gene is located adjacent to the LAP1 gene on human chromosome 1q24. Overexpression of LULL1 caused the redistribution of the E171Q-torsinA (ATP hydrolysis mutant) from the NE to the ER (Goodchild and Dauer, 2005; Naismith et al., 2009a). Furthermore, a new torsinA interactor termed printor was found in a yeast two-hybrid screen and both proteins co-localize in the ER. However, ΔE-torsinA abolishes the interaction between torsinA and printor (Giles et al., 2009).

I.3.1.2. Cytoskeleton and cell polarity

TorsinA has been implicated in cytoskeleton dynamics through interaction with kinesin light chain (KLC) 1 (Kamm et al., 2004), vimentin (Hewett et al., 2006; Nery et al., 2008), nesprins (Canettieri et al., 2003) and tau (Ferrari-Toninelli et al., 2004). KLC1 is a subunit of kinesin-I protein, a plus-end-directed motor protein involved in the transport of membranous organelles along microtubules (Goldstein and Philp, 1999). TorsinA was found to interact directly with the tetratricopeptide repeat domain of KLC1, which is a cargo binding site of kinesin-I. Co-localization studies showed that wt-torsinA and KLC1 were distributed throughout the cytoplasm and processes of neuronal cells, with enrichment at the distal ends, while ΔE-torsinA forms cell body inclusions positive for KLC1. Thus, it was suggested that torsinA may participate in intracellular trafficking mediated by kinesin (Kamm et al., 2004). TorsinA also binds to

the intermediate filament vimentin in cultured fibroblasts. Vimentin is involved in cell attachment and changes in neuronal shape associated with initial neurite outgrowth. Immunoprecipitation of vimentin not only brings down torsinA, but also other cytoskeleton components as α-tubulin, kinesin and actin and the NE protein LAP1. Expression of ΔE-torsinA altered the localization of vimentin, induced a delay in fibroblast adhesion to a substrate and inhibited neurite extension of SH-SY5Y cells (Hewett et al., 2006).

Furthermore, torsinA was found to associate with the KASH domain of nesprin-1, 2 and 3 (Nery et al., 2008) and also with SUN1 protein (Jungwirth et al., 2011). Nesprin-3 is located in the ONM, binds to SUN proteins of the INM and to vimentin through plectin (Wilhelmsen et al., 2005). When torsinA is depleted, nesprin-3 is redistributed to the ER, indicating that torsinA is important for the proper localization of nesprin-3 at the ONM and participates in the linkage between the NE and the cytoskeleton (LINC complex) (Nery et al., 2008). Nesprin-3, plectin and vimentin co-immunoprecipitated with torsinA. Given the role of vimentin on nuclear shape and the involvement of vimentin and plectin in cell migration, it was suggested that torsinA affects the positioning of the nuclei and cell migration through its association with nesprin-3 (Nery et al., 2008). Further, the torsinA homologue OOC-5 in *C. elegans* was found to be necessary for spindle orientation and cell polarity (Basham and Rose, 2001). TorsinA also immunoprecipitates with tau and may be able to modulate the association of tau with microtubules, thus influencing microtubules stabilization, neurite outgrowth and cell polarity (Ferrari-Toninelli et al., 2004).

I.3.1.3. TorsinA in the nuclear envelope

The discovery that torsinA not only resides in the ER but also in the NE, suggested that torsinA plays a role in the NE. Wt-torsinA was found in both the ER and NE, while E171Q-torsinA (ATP-bound trapped) and ΔE-torsinA were found to specifically accumulate in the NE (Goodchild et al., 2005; Naismith et al., 2004). Likewise, torsinA abnormally accumulates in the NE in DYT1 patient fibroblasts and ΔE-torsinA knock-in mice (Goodchild and Dauer, 2004). Accumulation of ΔE-torsinA in the NE causes abnormal morphology of the NE, including formation of blebs and herniations in the perinuclear space in cultured neurons from ΔE-torsinA knock-in mice.

This was also seen for torsinA null mice (Goodchild et al., 2005; Kim et al., 2010a). In cultured cells, overexpression of ΔE-torsinA leads to protein accumulation in membranous inclusions around the nucleus. These inclusions may be originated from the NE, since they stained for lamin A/C, B1 and emerin (Gonzalez-Alegre and Paulson, 2004; Hewett et al., 2000). Moreover, perinuclear inclusions were also identified in DYT1 patients' cholinergic neurons and others neurons, which positively stained for torsinA, ubiquitin and nuclear lamin A/C (McNaught et al., 2004). However, the accumulation of ΔE-torsinA in the NE and the related abnormalities, seem to be specific for neuronal cells and tissues (Giles et al., 2008; Goodchild et al., 2005). A study which provides a quantitative analysis of the relative NE/ER distribution, reported that accumulation of ΔE-torsinA in the NE is specific of neuronal cells by comparing the localization of torsinA in HeLa and SH-SY5Y cells (Giles et al., 2008).

Abnormal accumulation of ΔE-torsinA in the NE suggests that a NE dysfunction may contribute to DYT1 dystonia pathogenesis. The accumulation of torsinA in the NE leads to the discovery of LAP1 as a binding partner of torsinA in the perinuclear space (Fig. I.16). LAP1 was found to relocate wt-torsinA to the NE in a perinuclear distribution (Goodchild and Dauer, 2005). More recently, torsinA was found to interact with SUN1, another INM protein. It seems that the presence of SUN1 is required for the NE localization of the ΔE-torsinA (Jungwirth et al., 2011). At the NE, torsinA also binds to the ONM protein nesprin-1, -2 and -3 (Fig. I.16) and it was shown that torsinA is crucial for the correct localization of nesprin-3 (Nery et al., 2008). Further, overerexpression of ΔE-torsinA alters the localization of vimentin to the NE and KLC to inclusions (Hewett et al., 2006; Kamm et al., 2004).

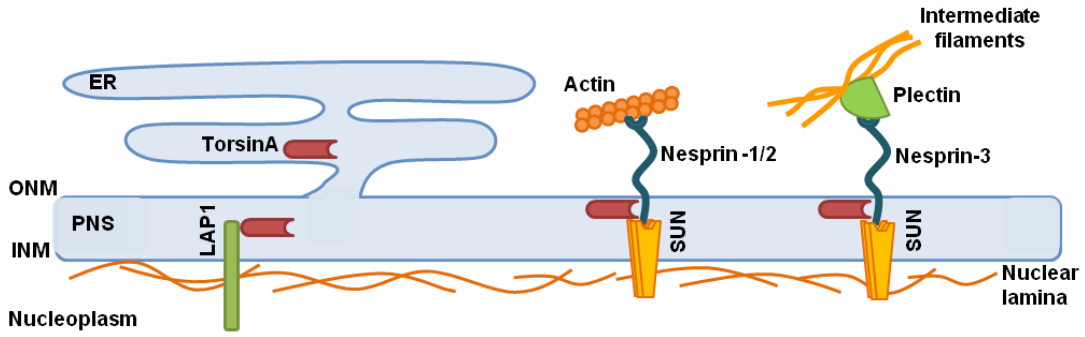

Figure I.16. Representation of torsinA interactions between the nuclear envelope and the cytoskeleton. TorsinA is primarily found in the endoplasmic reticulum (ER) but it is also located in the nuclear envelope. In the perinuclear space (PNS), torsinA interacts with LAP1, SUN1 and nesprin-1, -2 and -3. Nesprin-1 and -2 bind directly to actin, while nesprin-3 associates indirectly with intermediate filaments through plectin. Thus, torsinA plays a role in the connection between the nuclear envelope and the cytoskeleton. INM, inner nuclear membrane; ONM, outer nuclear membrane.

I.3.1.4. Chaperone function

The homology between torsinA and heat shock proteins (HSPs), including the HSP100/Clp family of proteins (Ozelius et al., 1997; Zhu et al., 2008), suggested a role for torsinA as a chaperone. HSPs are critical for the stress response and are involved in folding of proteins, prevention of protein aggregation, ubiquitination and degradation of misfolded proteins (Vale, 2000). TorsinA was found to co-localize with HSPs, α-synuclein and ubiquitin in Lewy bodies (Caldwell et al., 2003; McLean et al., 2002). In addition, a study of *post-mortem* brains of Parkinson's disease patients showed that torsinA accumulates in Lewy bodies (Shashidharan et al., 2000a). Moreover overexpresssion of torsinA has the ability to prevent the formation of α-synuclein aggregates in cultured cells (McLean et al., 2002), as well as polyglutamine repeat-induced protein aggregation in *C. Elegans* (Caldwell et al., 2003). More recently, it was reported that torsinA can recognize and bind directly to misfolded proteins and also prevent aggregation with specificity for misfolded proteins, thus acting as a chaperone (Burdette et al., 2010).

However, torsinA does not behave as a typical HSP, since its expression is not affected by some ER stress agents (Bragg et al., 2004). Nevertheless, torsinA is sensitive to some types of oxidative stress (Hewett et al., 2003; Kuner et al., 2003) and nerve injury (Zhao et al., 2008b). Additionally, overexpression of torsinA protects against oxidative stress induced cell death in cultured cells (Kuner et al., 2003) and

reduce ER stress caused by mutant proteins in *C. elegans* (Nery et al., 2011). Overexpression of torsinA and tor2 (torsinA *C. elegans* homolog) in *C. elegans* dopaminergic neurons can lead to the suppression of neurodegeneration induced by 6-OHDA treatment or overexpression of α-synuclein (Cao et al., 2005).

I.3.1.5. Neurotransmission and synaptic vesicle dynamics

TorsinA is ubiquitously expressed, but the mutant protein for DYT1 dystonia (ΔE-torsinA) has a specific neurological phenotype (Giles et al., 2008; Goodchild et al., 2005), suggesting that torsinA plays a specific role in neuronal cells. In neurons, torsinA localization seems to be different from non-neuronal cells. Neurons showed torsinA immunoreactivity in neuronal bodies, axons and dendrites (Augood et al., 2003; Rostasy et al., 2003). Moreover, torsinA was detected in small vesicles within axons and pre-synaptic terminals and it was also enriched in a fraction of synaptosomal membranes (Augood et al., 2003). In the neuroblastoma SH-SY5Y cell line, torsinA was localized in the cytoplasm, around the NE and in neurites. TorsinA was distributed in a punctuate pattern and an intense staining was observed in the synaptic varicosities of differentiated SH-SY5Y cells (Ferrari-Toninelli et al., 2004). In addition, co-localization between torsinA and vesicle-associated membrane protein (VAMP)/synaptobrevin was oberved, the latter is a synaptic vesicle marker (Ferrari-Toninelli et al., 2004; Hewett et al., 2000). TorsinA has also been implicated in vesicle transport and consequently neurotransmitter turnover. In differentiated PC12 cells (cell line derived from a pheochromocytoma of the rat adrenal medulla) and hippocampal neurons, torsinA was found to interact with snapin, a SNAP25 (synaptosomal associated protein of 25 kDa) binding protein, on secretory granules at neurite tips (Granata et al., 2008). Snapin is involved in vesicle exocytosis by enhancing the association between the SNARE complex and synaptotagmin I, a synaptic vesicle marker (Ilardi et al., 1999). Based on the torsinA/snapin interaction, a role for torsinA in synaptic vesicle dynamics has been proposed. It was found that overexpression of wt-torsinA negatively affects synaptic vesicle endocytosis. Conversely, overexpression of ΔE-torsinA increases uptake of a lipophilic dye and causes the persistence of synaptotagmin I on the plasma membrane. Knockdown of torsinA causes similar effects. This in turn may

disrupt the neuronal pathways involved in the control of movement. (Granata et al., 2008). In *Drosophila*, torp4 (torsinA homologous) interacts with the adaptor protein 3, which is involved in the transport from the Golgi to the lysosome, synaptic vesicle formation and sorting of proteins into synaptic vesicles. A study in *Drosophila* proposed that ΔE-torsinA disrupts the trafficking of transforming growth factor beta (TGF-β) receptor and Smads from synapses to cell bodies (reviewed in Granata et al., 2009). Overexpression of ΔE-torsinA causes the entrapment of the vesicular monoamine transporter 2 (VMAT2), a regulator of dopamine levels, in membranous inclusions. This may cause a reduction of monoamine neurotransmitter release (Misbahuddin et al., 2005). TorsinA can protect *C. elegans* dopaminergic neurons from 6-OHDA-induced neurodegeneration, possibly through downregulation of the dopamine transporter DAT-1, which is responsible for 6-OHDA uptake (Cao et al., 2005). This is consistent with the fact that torsinA can regulate cell-surface distribution of DAT-1 (Torres et al., 2004).

I.4. DYSTONIA

The term dystonia was coined by Oppenheim in 1911 describing a condition that he termed *Dystonia Musculorum Deformans*. The definition and classification of dystonia has evolved over time as the condition became better understood (reviewed in Fahn, 2011). Since 1984, dystonia has been defined as a "syndrome of sustained muscle contractions, frequently causing twisting and repetitive movements, or abnormal postures" (Fahn, 1988). However, this definition had some limitations and the *Dystonia Medical Research Foundation* committee proposed in 2013 the following revised definition: "Dystonia is a movement disorder characterized by sustained or intermittent muscle contractions causing abnormal, often repetitive, movements, postures, or both. Dystonic movements are typically patterned, twisting, and may be tremulous. Dystonia is often initiated or worsened by voluntary action and associated with overflow muscle activation". This new definition of dystonia attempts to exclude some conditions that may mimic dystonia, since it is known that several conditions also cause abnormal movements, postures or spasms (Albanese et al., 2013).

Dystonia is the third most common movement disorder, following essential tremor and Parkinson's disease (Butler et al., 2004) and comprises a large number of clinical syndromes. The classification of the diverse dystonia syndromes has been changed over time (reviewed in Fahn, 2011). The main difficulties to correctly classify dystonia are related with the etiology. For example, the term "primary" has been used to describe phenotypes not associated with other neurological features or pathological abnormalities. However, it is known that tremor occurs in patients with primary dystonia and the presence of other neurological features has been recognized, which indicates that the phenomenology may be not purely motor (Albanese et al., 2013; Stamelou et al., 2012). Thus, in 2013, dystonia syndromes were primarily classified into two axes: clinical features and etiology (Table I.2). Five categories were utilized to specify clinical characteristics: age at onset, body distribution, temporal pattern, coexistence of other movement disorders, and other neurological manifestations. The etiology of many dystonia syndromes is still not well understood, but two characteristics were used for classification: identifiable anatomical changes and pattern of inheritance (Table I.2) (Albanese et al., 2013).

Table I.2. Classification of dystonia (adapted from Albanese et al., 2013).

Axis I. Clinical characteristics	**Axis II. Etiology**
▪ Clinical characteristics of dystonia	▪ Nervous system pathology
Age of onset Infancy (birth to 2 years) Childhood (3-12 years) Adolescence (13-20 years) Early adulthood (21-40 years) Late adulthood (>40 years)	Evidence of degeneration Evidence of structural (often static) lesions No evidence of degeneration or structural lesion
	▪ Inherited or acquired
Body distribution Focal Segmental Multifocal Generalized Hemidystonia	Inherited Autosomal dominant Autosomal recessive X-linked recessive Mitochondrial
Temporal pattern • Disease course Static Progressive • Variability Persistent Action-specific Diurnal Paroxysmal	Acquired Perinatal brain injury Infection Drug Toxic Vascular Neoplastic Brain injury Psychogenic
▪ Associated features	Idiopathic Sporadic Familial
Isolated dystonia Combined dystonia with another movement disorder Occurrence of other neurological or systemic manifestations	

Most cases of dystonia have revealed an abnormal simultaneous contraction of agonist and antagonist muscles at rest that is often exacerbated by movement, which is believed to reflect a dysfunction in the central nervous system regions controlling movement (Farmer et al., 1998). It is believed that this dysfunction may result from an imbalance in neurotransmission, particularly in the basal ganglia, sensorimotor cortex,

brainstem and cerebellum. Several studies have linked dystonia to abnormal neurotransmitter communication involving striatal dopaminergic and cholinergic systems and loss of GABA-mediate inhibition. Despite that multiple neurotransmitter systems may contribute to dystonia pathogenesis, the most extensively studied to date is dopamine. Indeed, some types of dystonia have been related to a dysfunction in dopamine signaling. For example, dopa-responsive dystonia (DYT5 dystonia) can be caused by mutations in GTP cyclohydrolase I or tyrosine hydroxylase that result in the impairment of dopamine synthesis. Dystonic symptoms in these patients can be effectively treated with administration of the dopamine precursor L-DOPA. DYT11 myoclonus-dystonia is attributed to deficits in the epsilon-sarcoglycan protein, which is highly expressed in dopamine neurons (reviewed in Breakefield et al., 2008; Tanabe et al., 2009). A mouse model of DYT11 revealed high levels of striatal dopamine and its metabolites (Yokoi et al., 2006). X-linked recessive dystonia-parkinsonism (DYT3 dystonia) seems to be caused by mutations in the transcription factor TATA-box binding protein associated factor 1 (TAF1) that leads to reduced expression of TAF1 and D2 receptor in the caudate nucleus (Makino et al., 2007). DYT1 dystonia has also been related with dopaminergic dysfunction and this will be discussed in detail latter. In addition to these inherited syndromes, dystonia can also occur in the context of other dopamine-related diseases or treatments. Thus, dystonia is frequently a feature of Parkinsonism and can appear after Parkinsonian therapy. Moreover, imaging studies detected dopamine-related abnormalities in patients with different forms of dystonia (reviewed in Wichmann, 2008).

I.4.1. Early-onset generalized isolated dystonia

Early-onset dystonia arising in childhood is a progressive disorder that often begins in a limb and progresses to generalized dystonia, thus involving other limbs and trunk. Generalized dystonia is less common than focal dystonia (normally arising in adulthood) and most cases have a genetic origin (reviewed in Ozelius and Bressman, 2011; Phukan et al., 2011; Standaert, 2011). Several genes have been mapped for dystonia. However dystonia associated with the *DYT1* gene encoding torsinA protein is the best characterized and studied etiology. DYT1 dystonia (also named Opphenheim

dystonia) is an autosomal dominant trait with penetrance of around 30% and it is caused by a 3 bp (GAG) deletion in the coding region of the *DYT1* (*TOR1A*) gene. This deletion results in the loss of a single glutamic acid in the C-terminal of the torsinA protein (Ozelius et al., 1997). This mutation in the *DYT1* gene is the commonest cause of early-onset isolated dystonia and is about five times more frequent in Ashkenazi Jews compared to non-Ashkenazi. This difference in disease frequency is thought to result from a founder mutation in *DYT1* that was introduced into the Ashkenazi population (Valente et al., 1998). Three other variations in torsinA have been found but none has been unequivocally associated with disease: a 18 bp deletion that causes loss of residues 323-328 (Leung et al., 2001), a 4 bp deletion that causes a truncation starting at residue 312 (Kabakci et al., 2004) and a polymorphism that replaces aspartic acid at residue 216 with histidine in 12% of normal alleles (Kock et al., 2006; Ozelius et al., 1997). Typically, DYT1 dystonia appears in childhood or adolescence (onset 9-15 years). Initially, it affects one limb and then spreads to involve other body regions and represents the most severe form of dystonia. Although it is not degenerative, it is chronic and the treatment is purely symptomatic and sometimes not effective. Current treatments for dystonia include anticholinergic drugs, botulinum toxin injections and surgical interventions as pallidal deep brain stimulation (reviewed in Jankovic, 2013).

I.4.1.1. DYT1 dystonia pathology

Early studies on brains from patients with dystonia revealed no consistent neuropathological abnormalities. The lack of neurodegeneration and neuropathological specific features has been used to distinguish isolated dystonia from other etiologies. The identification of dystonia genes (DYT) allowed for the identification of specific genetic cases. After defining torsinA as the *DYT1* protein, localization studies showed that torsinA is highly expressed in dopaminergic neurons of the substantia nigra pars compacta (Augood et al., 1999; Augood et al., 1998). This leads to the assumption that torsinA may be involved in dopaminergic signaling and DYT1 dystonia may be linked with dopaminergic dysfunction. Neurochemical analysis of the few available post-mortem brains of DYT1 dystonia patients did not clearly detect pathological lesions in dopaminergic neurons in the substantia nigra or other brain regions. However, animal and imaging studies identified structural alterations, especially involving the basal

ganglia and cerebello-thalamo-cortical tracts (reviewed in Bragg et al., 2011; Bressman and Saunders-Pullman, 2013).

I.4.1.1.1. Human DYT1 dystonia studies

A study of the brain from a patient with DYT1 dystonia showed that nigral cellularity was normal but in the putamen and caudate nucleus the striatal dopamine and homovanilic acid (HVA) levels was slightly decreased compared to controls (Furukawa et al., 2000). Another post-mortem study involving four DYT1-positive brains reported an increase of the striatal 3-,4-dihydroxyphenylacetic acid (DOPAC)/dopamine ratio in the striatum compared to controls, suggesting an increased dopamine turnover (Augood et al., 2002). Moreover, a reduction in D1 and D2 receptor binding and consequent hyperactivity of striatal cholinergic interneurons was also reported (Asanuma et al., 2005; Augood et al., 2002). Despite the absence of neuronal loss, Rostasy el al found that, in DYT1-postive brains, neurons in the substantia nigra pars compacta appear to be larger and more densely packed when compared to controls (Rostasy et al., 2003). A further study examining four DYT1-postive brains found perinuclear inclusion bodies in the midbrain reticular formation and periaqueductal gray. The inclusions were located within cholinergic and other neurons and stained for ubiquitin, torsinA and lamin A/C. Additionally, it was also reported the presence of ubiquitin immunoreactive aggregates in pigmented neurons of the substantia nigra pars compacta and locus coeruleus in all four DYT1 dystonia cases, but not in controls (McNaught et al., 2004). Further, imaging studies showed a significant reduction in D2 receptor availability (Carbon et al., 2009) in the striatum of DYT1 mutation carriers compared to controls. Of note, dysfunction of $GABA_A$ receptor in the sensorimotor system of DYT1 mutation carriers is evident. Specifically, DYT1 patients showed a reduction of $GABA_A$ receptor expression/affinity (Garibotto et al., 2011). Carriers of the DYT1 mutation also showed abnormal motor learning in testing paradigms, correlated with abnormal brain activity (Ghilardi et al., 2003).

I.4.1.1.2. Rodent models of DYT1 dystonia

Given the few available human postmortem samples, the investigation using animal models could potentially help to elucidate DYT1 dystonia neuropathology and the underlying structural changes. Thus, several genetically-modified mouse models (Table I.3) have been developed for studying DYT1 dystonia pathogenesis. However, none of these models show clear dystonic movements, the different transgenic lines showed some histological abnormalities and behavioral and motor defects. Furthermore, these changes were not consistent among the different studies and DYT1 mouse models used. Histological changes were observed in torsinA knockout and ΔE-torsinA knock-in homozygous mice. These animals showed severe abnormalities of the NE ultrastructure in the CNS, including formation of vesicles and herniations in the perinuclear space (Goodchild et al., 2005; Kim et al., 2010a). Moreover, the mice died within 48 hours of birth. A DYT1 transgenic rat model also demonstrated a severally altered NE ultrastructure with an irregular perinuclear space (Grundmann et al., 2012). Other studies reported the presence of perinuclear inclusions that stained positively for torsinA, lamins and ubiquitin in different brain areas of DYT1 mouse models (Dang et al., 2005; Grundmann et al., 2007; Shashidharan et al., 2005). Recently, some studies have reported structural changes in neurons of ΔE-torsinA knock-in mouse models. These changes include reduction of the length of dendrites and number of spines among cerebellar Purkinje neurons (Zhang et al., 2011) and striatal medium spiny neurons (Song et al., 2013); fewer substantia nigra neurons immunopositive for tyrosine hydroxylase (Song et al., 2012); reduction in the ratio of axo-spinous to axo-dendritic synaptic inputs from glutamatergic and dopaminergic sources and enlarged interneurons immunoreactive for cholineacetyltransferase or parvalbumin (Song et al., 2013). Further, neurochemical abnormalities, particularly regarding dopamine function, have been described. Data from ΔE-torsinA-overexpressing and torsinA knock-down mice, showed altered levels of dopamine or its metabolites, including DOPAC and HVA (Dang et al., 2005; Dang et al., 2006; Shashidharan et al., 2005; Song et al., 2012; Zhao et al., 2008a). It was also reported that dopamine release is impaired in ΔE-torsinA-overexpressing mice (Balcioglu et al., 2007; Bao et al., 2010; Page et al., 2010). Additionally, a study showed that the DAT activity is reduced in the presence of ΔE-torsinA. Further, postsynaptic defects in DYT1 mouse models have been described. Specifically, these animals exhibited decreased D2 receptor activity and lower D2

protein levels compared to the controls (Dang et al., 2012; Giannakopoulou et al., 2010; Napolitano et al., 2010; Yokoi et al., 2011). Moreover, it seems that D2 receptor impairment can lead to abnormal cholinergic (Pisani et al., 2006) and GABAergic signaling (Sciamanna et al., 2009). Furthermore, in ΔE-torsinA knock-in mice, thalamic stimulation caused a shortened pause response and triggered an abnormal activity of cholinergic interneurons. The abnormal cholinergic signaling affects the integration between corticostriatal and thalamostriatal inputs (Sciamanna et al., 2012b). Another study, reported microstructural abnormalities in the cerebellothalamocortical pathway in ΔE-torsinA knock-in mice using imaging techniques (Ulug et al., 2011). Finally, using electrophysiological techniques, deficits in LTD and synaptic depotentiation in DYT1 mouse models were reported (Dang et al., 2012; Martella et al., 2009).

Table I.3. Rodent models of DYT1 dystonia.

Model	Neuronal phenotype	Neurochemistry and electrophysiology	References
TorsinA KO ΔE-torsinA KI	NE abnormalities, inclusions in the PNS		(Goodchild et al., 2005)
ΔE-torsinA overexpression [1]	Perinuclear ubiquitin and torsinA positive inclusions	↓ striatal DA ↓ striatal DOPAC/DA	(Shashidharan et al., 2005)
ΔE-torsinA KI	Perinuclear ubiquitin and torsinA positive inclusions	↓ striatal HVA	(Dang et al., 2005)
TorsinA KD		↓ striatal DOPAC	(Dang et al., 2006)
ΔE-torsinA overexpression [2]		Abnormal cholinergic response to D2 activation	(Pisani et al., 2006)
ΔE-torsinA overexpression[2]		↓ DA (upon amphetamine) Normal DA, DAT, VMAT2, D1 and D2	(Balcioglu et al., 2007)
Wt-torsinA overexpression[3]	Striatum and brainstem NE abnormalities, brainstem Perinuclear inclusions positive for torsinA, ubiquitin and lamin A/C	↓ striatal DA, serotonin, 5-HIAA ↓ brainstem HVA	(Grundmann et al., 2007)
ΔE-torsinA overexpression[3]		↑ brainstem DOPAC, serotonin, 5-HIAA Normal in striatum	
ΔE-torsinA overexpression[2]		↑ striatal DOPAC/DA, HVA/DA	(Zhao et al., 2008a)
ΔE-torsinA overexpression[2]		↑ AChe activity ↓ LTD	(Martella et al., 2009)
ΔE-torsinA overexpression[2]		↑striatal GABA activity (impairment of D2 receptor)	(Sciamanna et al., 2009)
ΔE-torsinA overexpression [4]		↓ striatal DA release (after cocaine)	(Page et al., 2010)
wt-torsinA overexpression[4]		↓ striatal DA, DOPAC	
ΔE-torsinA overexpression[1]		↓ striatal DA release	(Bao et al., 2010)
ΔE-torsinA overexpression[2]		↓ DAT function	(Hewett et al., 2010)
ΔE-torsinA overexpression[1]		↓ SNpc D2 mRNA ↓ striatal D2 density and binding	(Giannakopoulou et al., 2010)
ΔE-torsinA overexpression[2]		↓ striatal D2 protein ↓ Go/i proteins activation by D2	(Napolitano et al., 2010)

Model	Neuronal phenotype	Neurochemistry and electrophysiology	References
ΔE-torsinA KI Purkinje cells-specific torsinA KO	↓ Length and spines number of Purkinje cells dendrites		(Zhang et al., 2011)
Striatum-specific torsinA KO	Normal NE in striatal MSN	↓ striatal D2 binding	(Yokoi et al., 2011)
ΔE-torsinA KI		Microstructural abnormalities in cerebellothalamocortical pathway	(Ulug et al., 2011)
ΔE-torsinA KI		↓ D2 binding and D2 protein levels ↓corticostriatal LTD	(Dang et al., 2012)
Cholinergic-specific torsinA KO		Abnormal D2 response Altered M2/4 function	(Sciamanna et al., 2012a)
ΔE-torsinA KI		↓ pause response by thalamic stimulation in ChIs	(Sciamanna et al., 2012b)
ΔE-torsinA KI	↓ Number and ↑ size of TH positive nigral cells	↓ midbrain DA ↑ striatal HVA (age-dependent)	(Song et al., 2012)
* ΔE-torsinA overexpression[4]	NE abnormalities, irregular PNS		(Grundmann et al., 2012)
ΔE-torsinA KI	↑ Size of interneurons immunoreactive for ChAT and PV ↓ Number of MSN dendrites and spines		(Song et al., 2013)

AChE, acetylcholinesterase; ChAT, choline acetyltransferase; ChIs, cholinergic interneurons; DA, dopamine; DAT, dopamine transporter; DOPAC, 3,4-dihydroxyphenylacetic acid; D1, dopamine D1 receptor; D2, dopamine D2 receptor; 5-HIAA, 5-hydroxyindoleacetic acid; HVA, Homovanillic acid; KD, Knockdown; KI, knock-in; KO, knockout; LTD, long-term depression; MSN, medium spiny neurons; NE, nuclear envelope; PNS, perinuclear space; PV, parvalbumin; SNpc, substantia nigra pars compacta; TH, tyrosine hydroxylase; VMAT2, vesicular monoamine transporter 2. [1]Rat neuron-specific enolase promoter. [2]Human cytomegalovirus promoter. [3]Murine prion protein promoter. [4]Human TH promoter. [4] Human torsinA promoter. *Rat model. All the other are mouse models.

I.5. OBJECTIVES

DYT1 dystonia is caused by a mutation in the *DYT1* gene resulting in the loss of a single glutamic acid within torsinA protein (Ozelius et al., 1997). TorsinA resides in the ER and NE, but ΔE-torsinA is abnormally relocated to the nuclear envelope. LAP1 was found to recruit torsinA to the NE (Goodchild and Dauer, 2005). Previous work from our laboratory, using yeast two-hybrid (YTH) screens, resulted in the identification of several PP1 binding proteins (Esteves et al., 2012a; Esteves et al., 2012b). One of the novel PP1 regulators isolated was LAP1B, whose function is poorly understood. The identification of LAP1B as a novel PP1 binding protein opened new perspectives for the study of DYT1 dystonia, where protein phosphorylation might be a regulatory mechanism. Indeed, aberrant protein phosphorylation of key proteins has been linked to many diseases. Therefore, the aim of this thesis was to characterize the PP1/LAP1B and PP1/LAP1/torsinA complexes and unravel its potential physiological relevance to DYT1 dystonia. Additionally, we identified a novel human LAP1 isoform and provided new insights about the family of LAP1 proteins. Hence, the specific aims of this thesis were to:

1. Characterize the interaction between LAP1B and PP1.
   1.1. Determine the functional relevance of the LAP1B/PP1 complex.

2. Validate the existence of new LAP1 isoforms in human cells.
   2.1. Characterize the human LAP1 isoforms.
   2.2. Analyze the cell and tissue specific expression patterns of human LAP1 isoforms.

3. Determine the potential role of LAP1 in cell cycle-dependent nuclear dynamics.

4. Test cellular models of DYT1 dystonia.

5. Validate the interaction between LAP1, PP1 and torsinA proteins.
   5.1. Determine if LAP1 and PP1 form a complex with both wt- and ΔE-torsinA.
   5.2. Ascertain weither wt- and ΔE-torsinA are regulated by protein phosphorylation.

CHAPTER II - LAP1B IS A NOVEL PP1 BINDING PROTEIN

Previous work from our laboratory identified LAP1B as a putative PP1 interacting protein using yeast two-hybrid assays (Esteves et al., 2012a; Esteves et al., 2012b; Santos, 2009). Therefore the aim of work described in chapter II was to validate and characterize the interaction between LAP1B and PP1 and was included in the following research paper (manuscript 1): "The nuclear envelope protein, LAP1B, is a novel Protein Phosphatase 1 substrate", *PLoS One, 8*(10), e76788. doi: 10.1371/journal.pone.0076788.

"The nuclear envelope protein, LAP1B, is a novel Protein Phosphatase 1 substrate"

Mariana Santos[1], Sandra Rebelo[1], Paula J. M. Van Kleeff[2], Connie E. Kim[3], William T. Dauer[3], Margarida Fardilha[2], Odete A. da Cruz e Silva[1], Edgar F. da Cruz e Silva[2]

[1] Neuroscience Laboratory, Centre for Cell Biology, Health Sciences Department, University of Aveiro, Portugal

[2] Signal Transduction Laboratory, Centre for Cell Biology, Health Sciences Department, University of Aveiro, Portugal

[3] Departments of Neurology and Cell & Developmental Biology, University of Michigan Medical School, Ann Arbor, MI USA

Abstract

Protein phosphatase 1 (PP1) binding proteins are quintessential regulators, determining substrate specificity and defining subcellular localization and activity of the latter. Here, we describe a novel PP1 binding protein, the nuclear membrane protein lamina associated polypeptide 1B (LAP1B), which interacts with the DYT1 dystonia protein torsinA. The PP1 binding domain in LAP1B was here identified as the REVRF motif at amino acids 55-59. The LAP1B:PP1 complex can be immunoprecipitated from cells in culture and rat cortex and the complex was further validated by yeast co-transformations and blot overlay assays. PP1, which is enriched in the nucleus, binds to the N-terminal nuclear domain of LAP1B, as shown by immunocolocalization and domain specific binding studies. PP1 dephosphorylates LAP1B, confirming the physiological relevance of this interaction. These findings place PP1 at a key position to participate in the pathogenesis of DYT1 dystonia and related nuclear envelope-based diseases.

II.1. INTRODUCTION

Reversible protein phosphorylation is a major mechanism controlling key intracellular events that are essential for cell health and viability (Cohen, 1989; da Cruz e Silva et al., 2004; Fardilha et al., 2010). Protein phosphatase 1 (PP1) is a ubiquitous serine/threonine phosphatase that is estimated to dephosphorylate about one third of all proteins in eukaryotic cells (Ceulemans and Bollen, 2004; Cohen, 2002b). PP1 regulates a variety of cellular functions, such as glycogen metabolism, transcription, protein synthesis, cellular division and meiosis (Bollen, 2001; Ceulemans et al., 2002a; Cohen, 2002b). In mammalian cells, three genes encode the three PP1 isoforms: PP1alpha (PP1α), PP1Beta/Delta (PP1β/δ) and PP1gamma (PP1γ). Furthermore, the PP1γ gene undergoes alternative splicing to originate a ubiquitous PP1γ1 variant and a PP1γ2 variant that is enriched in testis (da Cruz e Silva et al., 1995b; Sasaki et al., 1990). PP1 isoforms are expressed in virtually all tissues but exhibit different expression levels depending on the tissue, and different subcellular distribution (Andreassen et al., 1998; Bordelon et al., 2005; da Cruz e Silva et al., 1995b). The versatility of PP1 is largely determined by the binding of its catalytic subunit to different specific regulatory subunits, that are responsible for the directed targeting of PP1 to a particular subcellular compartment and also determine its substrate specificity and activity (Bollen, 2001; Bollen et al., 2010; Ceulemans et al., 2002a; Cohen, 2002b). More than 200 binding/regulatory subunits have been already described, making PP1 an essential protein in many distinct cellular processes (Fardilha et al., 2010; Fardilha et al., 2011). Most PP1 binding proteins interact with the PP1 catalytic subunit through a conserved PP1 binding motif termed the RVxF motif, which has the consensus sequence [R/K] $X_{A(0-1)}$ [V/I] X_B [F/W], where X_A is any amino acid and X_B is any amino acid except proline (Wakula et al., 2003). More recently, other consensus sequence have been proposed for the RVxF motif: [HKR]-[ACHKMNQRSTV]-V-[CHKNQRST]-[FW] (Meiselbach et al., 2006) and [KRL] [KRSTAMVHNQ][VI]{FIMYDP}[FW] (Hendrickx et al., 2009). The binding of PP1 to regulatory proteins through the RVxF motif does not cause major effects on the conformation and activity of PP1, but mediates the initial anchoring of regulatory subunits and thereby promotes the interaction at secondary binding sites (Bollen, 2001; Egloff et al., 1997; Hendrickx et al., 2009). Subsequently other PP1 binding motifs have also been reported, such as the

apoptotic signature F-X-X-[KR]-X-[KR] (Ayllon et al., 2002), the SILK and the MyPhoNE motifs (Hendrickx et al., 2009). The existence of these conserved binding sites within regulatory subunits explains the ability of PP1 catalytic subunit to interact with numerous regulatory proteins and consequently the binding of most regulatory subunits is mutually exclusive (Bollen, 2001). Since the regulatory subunits control the specificity and the diversity of PP1 activity, the key to understanding PP1 function lies in studying these regulatory subunits and their cellular functions. Several yeast two-hybrid (YTH) screens of a human brain cDNA library were performed using the three PP1 isoforms (PP1α, PP1γ1 and PP1γ2) as baits. From each screen many positive clones were identified encoding several different proteins. Among them, were proteins already known as PP1 regulators and also novel putative PP1 regulators (Esteves et al., 2012a; Esteves et al., 2012b). The majority of the novel putative PP1 regulators comprise at least one of the conserved PP1 binding motifs. One of the novel PP1 regulators isolated in the three independent YTH screens was torsinA interacting protein 1 (TOR1AIP1) or lamina associated polypeptide 1B (LAP1B). LAP1B belongs to a family of integral proteins of the inner nuclear membrane, named lamina associated polypeptide 1 (LAP1). Members of the LAP1 family (LAP1A, B and C) were initially identified using monoclonal antibodies generated against lamina-enriched fractions of rat liver nuclei (Senior and Gerace, 1988). The three LAP1 isoforms result from alternative splicing of the *TOR1AIP1* gene (Martin et al., 1995) and have been poorly studied. Moreover, the cDNA for LAP1B isoform was, to date, the only human isoform completely sequenced (Kondo et al., 2002). The function of LAP1B is poorly understood but it is known that it binds to lamins and chromosomes and that it is phosphorylated during interphase and mitosis (Foisner and Gerace, 1993). As indicated by the nomenclature, LAP1 was found to interact with torsinA (Goodchild and Dauer, 2005; Naismith et al., 2009b), the central protein of a neurologic disorder known as DYT1 dystonia (Ozelius et al., 1997). However, the physiological relevance of this novel complex has not yet been determined. In the present study we validated the novel complex LAP1B:PP1 using several *in vitro* and *in vivo* techniques, namely a blot overlay assay, co-immunoprecipitation and yeast co-transformation. Furthermore, the PP1 binding motif responsible for the interaction was mapped. The functional relevance of this complex was pursued and we determined that LAP1B is dephosphorylated by PP1 *in vitro.*

II.2. MATERIALS AND METHODS

II.2.1. Antibodies

The primary antibodies used were rabbit polyclonal LAP1 (Goodchild and Dauer, 2005); rabbit polyclonal CBC2C and CBC3C, that recognizes the C-terminal of PP1α and PP1γ, respectively (da Cruz e Silva et al., 1995b); rabbit polyclonal lamin B1 (Santa Cruz Biotechnology); 6xHis-tag antibody (Novagen), that recognizes 6xHis-tag-proteins; and Myc-tag antibody (Cell Signaling), that recognizes Myc-fusion proteins. The secondary antibodies used were anti-mouse and anti-rabbit horseradish peroxidase-linked antibodies (GE Healthcare) for ECL detection, and FITC-conjugated anti-mouse IgG (Molecular Probes) and Alexa 594-conjugated anti-rabbit IgG (Molecular Probes) for co-localization studies.

II.2.2. Expression vectors and DNA constructs

For yeast co-transformation assays, PP1α, PP1γ1, PP1γ2 and the specific C-terminal of PP1γ2 (PP1γ2End) cDNAs were cloned into the pAS2-1 (Clontech), in frame with the GAL4-binding domain, as described in Esteves *et al*, 2012 (Esteves et al., 2012a; Esteves et al., 2012b). pACT2-LAP1B (in frame with the GAL4 activation domain) was obtained from a human brain cDNA library (Clontech, HL4004AH) (Esteves et al., 2012a; Esteves et al., 2012b). LAP1B binding motif (BM) deletion mutants comprising amino acids 1-209 (LAP1B-BM1), 61-508 (LAP1B-BM2), 1-508 (LAP1B-BM1/2) and 238-584 (LAP1B-BM3) were prepared by PCR amplification with appropriate primers (Table II.1). The amplified fragments were subcloned into the *EcoRI/XhoI* restriction sites of the pACT2 vector (Clontech). The same methodology was used to clone additional LAP1B deletion mutants comprising amino acids 1-338 (LAP1B-BM1/2-TM), 1-369 (LAP1B-BM1/2+TM), 332-584 (LAP1B-BM3-TM) and 365-584 (LAP1B-BM3+TM) into the pET-28c vector (Novagen). Full-length LAP1B and the mutants 1-209 (LAP1B-BM1) and 61-508 (LAP1B-BM2) in the pACT2 vector were subcloned into the pET-28c vector. Full-length LAP1B and LAP1B-BM2 and LAP1B-BM3 in the pACT2 vector were also subcloned into the mammalian expression vector pCMV-Myc (Clontech) to obtain a Myc-fusion protein. Additionally a LAP1B

(ΔA185) mutation was introduced into pET-LAP1B by site-directed mutagenesis using the primers described in Table II.1. The constructs were all verified by DNA sequencing using an ABI PRISM 310 Genetic Analyzer (Applied Biosystems, Porto, Portugal).

Table II.1. Oligonucleotides used to generate LAP1B deletion mutants by PCR.

	Plasmid name	**Oligonucleotide sequence (5' – 3')**	
		FW	**RV**
pACT2 vector constructs	LAP1B-BM1	GGAATTCATATGGCGGGCG ACGGG	CCGCTCGAGTTAGACACTGGTGG CTTC
	LAP1B-BM2	GGAATTCATATGGACGAGCC GCCAGAA	CCGCTCGAGTTAGGCTACATCTT TGAAGGC
	LAP1B-BM1/2	GGAATTCATATGGCGGGCG ACGGG	CCGCTCGAGTTAGACACTGGTGG CTTC
	LAP1B-BM3	GGAATTCATATGGCCAGATC CAGGGAT	CCTCGAGTTATAAGCAGATGCCC CT
pET-28c vector constructs	LAP1B-BM1/2+TM	GGAATTCATATGGCGGGCG ACGGG	CCTCGAGTTAGAACTCTTGAACA G
	LAP1B-BM1/2-TM	GGAATTCATATGGCGGGCG ACGGG	CCTCGAGTTACCGGTTCCTCTTG AC
	LAP1B-BM3+TM	GGAATTCATATGGTCAAGAG GACGG	CCTCGAGTTATAAGCAGATGCCC CT
	LAP1B-BM3-TM	GGAATTCATATGGCTGTTCA AGTTC	CCTCGAGTTATAAGCAGATGCCC CT
	LAP1B (ΔA185)	CATACAAGAGGCTCCAGTG AGTGAAGATCTTG	CAAGATCTTCACTCACTGGAGCC TCTTGTATG

II.2.3. Yeast co-transformation analysis

Each of the bait plasmids (pAS2-1-PP1α, pAS2-1-PP1γ1, pAS2-1-PP1γ2 or pAS2-1-PP1γ2end) was co-transformed with one of the specific target proteins; pACT-LAP1B or its deletions mutants (pACT-BM1, pACT-BM2, pACT-BM1/2 and pACT-BM3), into the yeast strain AH109 by the lithium acetate method (according to the manufacturer's instructions, Clontech). In parallel, co-transformations of the vectors pAS2-1 and pACT2 were performed as a negative control. The association of murine p53 (encoded by plasmid pVA3-1) and SV40 large T antigen (plasmid pTD1) was used as a positive control. The transformants were assayed for *HIS3*, *ADE2* and *MEL1* reporter genes. All positive clones were replated in SD/QDO medium containing X-α-Gal and incubated at 30ºC for 2-4 days.

II.2.4. Expression of recombinant proteins in *Escherichia coli*

Escherichia coli Rosetta cells (DE3) were transformed with one of the pET-LAP1B constructs and grown overnight in 5 mL of Luria-Bertani/Kanamycin medium at 37ºC. Aliquots (500 µL) were transferred to 50 ml of Luria-Bertanini/Kanamycin until the OD_{600} was around 0.5-0.6. Expression was induced by adding 1 mM isopropyl-β-D-thiogalactopyranoside (IPTG) to the culture at 37˚C for different periods of time (1, 3 and 5 hours) with shaking. Cells were recovered by centrifugation (4000 rpm for 10 min), resuspended in 500 µL of 1x PBS and lysed by sonication. Cells were then centrifuged (13200 rpm for 30 min), the supernatant was transferred to a new microtube (soluble fraction) and the pellet resuspended in 500 µL of boiling 1% SDS (insoluble fraction).

II.2.5. Blot overlay assays

II.2.5.1. LAP1B deletion mutants

Bacterial extracts, prepared as described above, were separated on a 10% SDS-PAGE and the proteins were subsequently transferred to a nitrocellulose membrane. The membrane was overlaid with 1 µg/mL of purified recombinant PP1γ1 protein (Watanabe et al., 2003). After washing to remove excess protein, bound PP1γ1 was detected by incubating the membrane with PP1γ antibody and developed by enhanced chemiluminescence (ECL, GE Healthcare).

II.2.5.2. LAP1B isoforms

LAP1B and LAP1B (ΔA185) proteins were generated by *in vitro* transcription/ translation (IVT) from pET-LAP1B and pET-LAP1B(ΔA185) expression vectors, respectively, using the TnT-coupled transcription/translation kit (Promega), according to the manufactures' instructions. For the overlay assays, two samples of 250 ng of purified recombinant PP1γ1 protein (Watanabe et al., 2003) were separated on a 12% SDS-PAGE. Both proteins were transferred to a nitrocellulose membrane but one was overlaid with LAP1B-IVT, while the other was overlaid with LAP1B (ΔA185)-IVT.

The bound proteins were detected by incubating the membrane with LAP1 antibody and developed by ECL.

II.2.6. Cell culture and transfection

COS-7 (ATCC CRL-1651) and HEK293 (ATCC CRL-1573) cells were grown in Dulbecco's modified Eagle's medium (DMEM) supplemented with 10% Fetal Bovine Serum (FBS), 100 U/ml penicillin, 100 mg/ml streptomycin and 3.7 g/l $NaHCO_3$ (Complete DMEM). SH-SY5Y cells (ATCC CRL-2266) were grown in Minimal Essential Medium (MEM) supplemented with F-12 Nutrient Mixture (Gibco, Invitrogen), 10% FBS (Gibco, Invitrogen), 1.5 mM L-glutamine, 100 U/mL penicillin and 100 mg/mL streptomycin (Gibco, Invitrogen). HeLa cells (ATTC CRM-CCL-2) were grown in Minimal Essential Medium (MEM) with Earle's salts and GlutaMAX (MEM), supplemented with 10% fetal bovine serum, 1% MEM Non-Essential amino acids and 100 U/mL penicillin and 100 mg/mL streptomycin. All cultures were maintained at 37ºC and 5% CO_2. Transient transfections of COS-7 and HeLa cells were performed using LipofectAMINE 2000 (Invitrogen Life technologies). After 24 hours of transfection, cells were harvested for subsequent immunoprecipitation (IP) experiments or were fixed, using 4% paraformaldehyde, for immunocytochemical analysis.

II.2.7. Brain dissection

Winstar rats (9-12 weeks) were obtained from Harlan Interfaune Ibérica, SL. All experimental procedures observed the European legislation for animal experimentation (2010/63/EU). No specific ethics approval under EU guidelines was required for this project, since the rats were only euthanized, by cervical stretching followed by decapitation, for brain removal. This is within the European law (Council Directive 86/609/EEC) and during this procedure we took all steps to ameliorate animal suffering and used the minimum number of animals possible. The procedures were approved and supervised by our Institutional Animal Care and Use Committee (IACUC): Comissão Responsável pela Experimentação e Bem-Estar Animal (CREBEA).

Briefly, animals were euthanized by cervical stretching followed by decapitation and the cortex was dissected out on ice. The tissue was then homogenized on ice, in

non-denaturing lysis buffer (50 mM Tris-HCl pH 8.0, 120 mM NaCl, 4% CHAPS) containing protease inhibitors (1 mM PMSF, 10 mM Benzamidine, 2 µM Leupeptin, 1.5 µM Aprotinin, 5 µM Pepstatin A), with a Potter-Elvehjem tissue homogenizer with 10-15 pulses at 650-750 rpm (Rebelo et al., 2013). Resulting tissue extracts were used for IP analysis using Dynabeads Protein G (Dynal, Invitrogen) as described below.

II.2.8. Co-immunoprecipitation

COS-7 cells transfected with Myc-LAP1B were collected in lysis buffer (50 mM Tris-HCl pH 8, 120 mM NaCl, 4% CHAPS) containing protease inhibitors (1 mM PMSF, 10 mM Benzamidine, 2 µM Leupeptin, 1.5 µM Aprotinin, 5 µM Pepstatin A). Dynabeads Protein G (Dynal, Invitrogen) were washed in 3% BSA/1x PBS. Primary antibodies were cross-linked to Dynabeads according to the manufacter's protocol. Cell lysates were precleared with 20 µL (0.6 mg) Dynabeads for 1 hour and then incubated with antibody-dynabeads for 2h at 4ºC. The immunoprecipitates were washed in 1x PBS and proteins eluted by boiling in loading buffer before SDS-PAGE and immunoblotting analysis. For analysis of endogenous proteins, COS-7 cells and SH-SY5Y cells were collected in lysis buffer and immunoprecipitated as described above, but cell lysates were incubated with antibody-dynabeads overnight at 4ºC. HEK293 immunoprecipitation was carried out as previously described (Kim et al., 2010a)

II.2.9. Immunocytochemistry

Once fixed as described above, HeLa cells were permeabilized with methanol for 2 min. Cells were first incubated with one of the primary antibodies (anti-PP1γ or PP1α) for 2 hours, followed by Alexa 594-conjugated secondary antibody. After washing with 1x PBS, cells were subsequently incubated with a second primary antibody (anti-myc) for 2 hours, followed by anti-mouse fluorescein isothiocyanate (FITC) conjugated secondary antibody. Preparations were washed with PBS, mounted using Vectashield mounting media with DAPI (Vector) and visualized using an LSM510-Meta confocal microscope (Zeiss) and a 63x/1.4 oil immersion objective. The argon laser lines of 405 nm, 488 nm, and a 561nm DPSS laser were used. Microphotographs were acquired in a sole section in the Z-axis (xy mode) and represent a mean of 16 scans. Profiles were

acquired using the Zeiss LSM 510 4.0 software as previously described (Rebelo et al., 2013; Vieira et al., 2010).

II.2.10. *In vitro* dephosphorylation of LAP1B

SH-SY5Y cells were treated with 0.25 nM or 500 nM okadaic acid (OA) for 3 hours. Then, cells were collected in lysis buffer (50 mM Tris-HCl pH 8, 120 mM NaCl, 4% CHAPS, 250 mM EDTA, 1 mM sodium orthovanadate, 5 mM sodium fluoride) containing protease inhibitors (1 mM PMSF, 10 mM Benzamidine, 2 µM Leupeptin, 1.5 µM Aprotinin, 5 µM Pepstatin A) and immunoprecipitated with LAP1 antibody, as described above. Immunoprecipitates were incubated at 30ºC for 1 hour with or without 100 ng of purified PP1γ1 protein in PP1 buffer (50 mM Tris-HCl ph 7.5, 0.1 mM EGTA, 1 mM $MnCl_2$, 5 mM DTT). Samples were further analyzed by 7.5 % SDS-PAGE followed by immunoblotting.

II.2.11. SDS-PAGE and Immunobloting

Samples were separated on SDS-PAGE and electrophoretically transferred onto nitrocellulose, followed by immunological detection with specific antibodies as indicated. Membranes were saturated in 5% non-fat dry milk in TBS-T for 3 hours and further incubated with primary antibodies. The incubations with the CBC2C, CBC3C and LAP1 antibodies were performed overnight. The incubations with the His-tag and Myc-tag antibodies were carried out for 2 hours. Detection was achieved using horseradish peroxidase-conjugated anti-rabbit or anti-mouse IgGs as secondary antibodies and proteins visualized by ECL (GE Healthcare).

II.3. RESULTS

II.3.1. Identification of LAP1B as a novel putative PP1 regulatory protein

In order to identify novel potential PP1 regulatory proteins, the three PP1 isoforms (PP1α, PP1γ1 and PP1γ2) were used as baits to screen a human brain cDNA library by the YTH system. From these screens 298, 241 and 228 positive clones were identified using PP1α, PP1γ1 and PP1γ2 as baits, respectively (Esteves et al., 2012a; Esteves et al., 2012b). Detailed analysis revealed 14, 4 and 2 positive clones, encoding a potentially novel PP1 regulatory protein - LAP1B, for the PP1α, PP1γ1 and PP1γ2 screens, respectively (Table II.2) (Santos, 2009). Sequencing of the identified clones determined that all correspond to the LAP1B variant 1, recently reported in the GenBank database (NM_001267578.1). The variant 1 differs from the variant 2 (NM_015602) only by a CAG insertion, which results in an additional alanine in the coding sequence, otherwise the sequence is identical to the first human LAP1B sequence reported in 2002 (Kondo et al., 2002). Moreover, others reports showed that *TOR1AIP1* gene possesses a 3' tandem splice site, TAGCAG, at the exon 3 boundary, which results in an amino acid insertion or deletion in the encoded protein (Tadokoro et al., 2005; Tsai et al., 2007). From all LAP1B clones obtained we selected a full-length clone (clone 135; Table II.2) for further studies. The latter comprises a short 5' untranslated region followed by the ATG start codon, an open reading frame of 2000 nucleotides, that encodes 584 amino acids, followed by a stop codon and a short 3' untranslated region (Fig. II.1.A). LAP1B was previously described as a type 2 integral membrane protein, with an N-terminal nucleoplasmic domain, one predicted transmembrane domain (TM) and a C-terminal lumenal domain (Kondo et al., 2002). Our *in silico* analysis also revealed that LAP1B has three conserved PP1 binding motifs (BM): REVRF (amino acids 55-59), KVNF (amino acids 212-215) and KVKF (amino acids 538-541), that were called BM1, BM2 and BM3, respectively. BM1 and BM2 are localized in the nucleoplasm, while BM3 is localized in the lumen of the perinuclear space. Additionally, a second generic PP1 binding motif termed SILK (amino acids 306-309) was also identified (Fig. II.1A). Further *in silico* characterization of these four potential PP1 binding motifs (BM1, BM2, BM3 and SILK) was achieved using the ClustalW algorithm, which allowed for the determination of the homology between

species (Fig. II.1B). Interestingly, the BM1 and BM3 are totally conserved motifs among the species analyzed (Human, Chimpanzee, Orangutan, Mouse, Rat). The other binding motifs (BM2 and SILK) are also completely conserved between Human, Chimpanzee and Orangutan but do deviate markedly in mouse and rat; with two residues common to all species in the SILK domain and only one residue is common to all species for the BM2 domain (Fig. II.1B). Subsequent to the *in silico* LAP1B characterization, the novel LAP1B:PP1 complex was validated *in vitro* and *in vivo*.

Table II.2. Summary of LAP1B clones isolated from the yeast-two hybrid (YTH) screens.

Bait	Nº of screened clones	Nº of positive clones	Nº of LAP1B clones	YTH clone ID	Insert (Kb)	Start position
PP1α	2×10^7	298	14	12	2.0	384
				31	1.75	382
				36	2.25	268
				45	2.15	382
				50	2.75	274
				61	3.85	265
				76	3.5	262
				96	2.2	383
				184	4.3	265
				192	3.75	274
				261	4.0	265
				262	2.1	382
				271	2.2	382
				273	3.75	365
PP1γ1	1×10^6	241	4	120	2.4	261
				124	1.5	266
				135	2.0	382
				164	1.6	268
PP1γ2	6.6×10^5	228	2	124	1.8	262
				164	0.3	270

Clone 135 (interaction with PP1γ1) was selected for further study. The start position indicated is relative to the GenBank sequence NM_001267578.

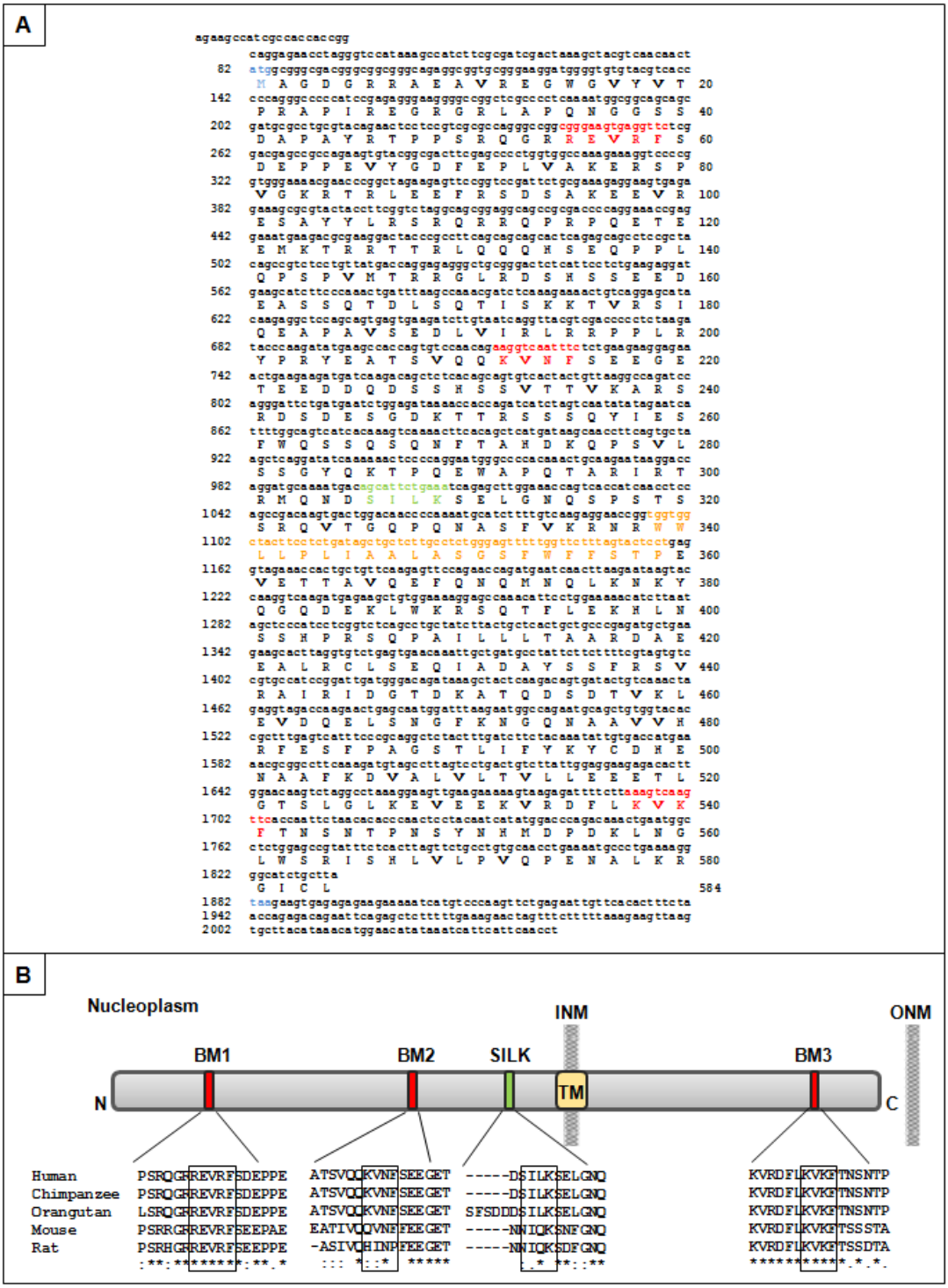

Figure II.1. Human LAP1B sequence and domains. **A-** Nucleotide and corresponding amino acid sequence of human LAP1B encoded by clone 135. Stop and start codons are coloured blue. The three well conserved PP1 binding motifs (RVxF) are highlighted in red (positions 55-59, 212-215 and 538-541 in aa sequence) and a second generic PP1 binding motif (SILK) is coloured green (position 306-309 in aa sequence). The transmembrane domain is highlighted in orange (position 339-361 in aa sequence). **B-** Schematic illustration of LAP1B domains. Sequence of human LAP1B was aligned against others species using ClustalW algorithm. Sequence conservation is indicated by asterisks (identical sequences), colons (conserved substitutions) and periods (semi-conserved substitutions). BM1, BM2 and BM3, RVxF-like PP1 binding motif 1, 2 and 3, respectively; INM, inner nuclear membrane; ONM, Outer nuclear membrane; SILK, a second generic PP1 binding motif; TM, transmembrane domain

II.3.2. LAP1B and PP1 interact *in vitro*

The *in vitro* validation of this novel complex as well as the identification of the binding motif responsible for the interaction was accomplished using a blot overlay assay. Several deletion mutants were prepared as described above, each comprising at least one of the PP1 binding motifs as represented in Fig. II.2A. The importance of the TM was also addressed by evaluating the binding in the presence or absence of the latter (Fig. II.2A). Thus, both full-length LAP1B and the different deletion mutants were expressed in bacteria as 6xHis-tag fusion proteins by adding 1 mM IPTG to the growing cultures at 37ºC. All recombinant proteins (full-length and mutants) were efficiently expressed in bacteria, including the deletion mutants with or without the TM domain (data not shown). The proteins thus expressed were used to carry out the blot overlay assay. Briefly, the different recombinant proteins were separated by SDS-PAGE and electrotransferred onto nitrocellulose membranes. Recombinant protein detection was achieved with the His-tag antibody (Fig. II.2B) and for the overlay assay the purified PP1γ1 protein was applied (Fig. II.2C). The negative controls used included the pET-28c vector without an insert or with a non-induced insert. As a positive control the pET28c-Nek2A was used, given that Nek2A is a well known protein that strongly interacts with PP1 (Fardilha et al., 2004). The immunoblotting using His-tag antibody (Fig. II.2B) of both full-length and deletion mutants revealed that all the expressed proteins have the expected molecular weight as indicated in Figure 2A. Additional bands were sometimes detected for LAP1B, LAP1B-BM1 and LAP1B-BM2, these could possibly correspond to proteolytic fragments (Fig. II.2B). The overlay assays revealed increased PP1γ1 binding concomitant with increasing amounts of recombinant full-length LAP1B (Fig. II.2C). Additionally, we also demonstrated that PP1γ1 binds to the deletion mutant that comprises the residues 1-209 encompassing the BM1, and also to the construct that comprises both BM1 and BM2 with or without the TM (Fig. II.2C). However, PP1γ1 does not bind to the recombinant protein comprising only the BM2 or the BM3 (Figure II.2C). Thus, using *in vitro* techniques we established that LAP1B binds to PP1γ1 through the BM1 (REVRF).

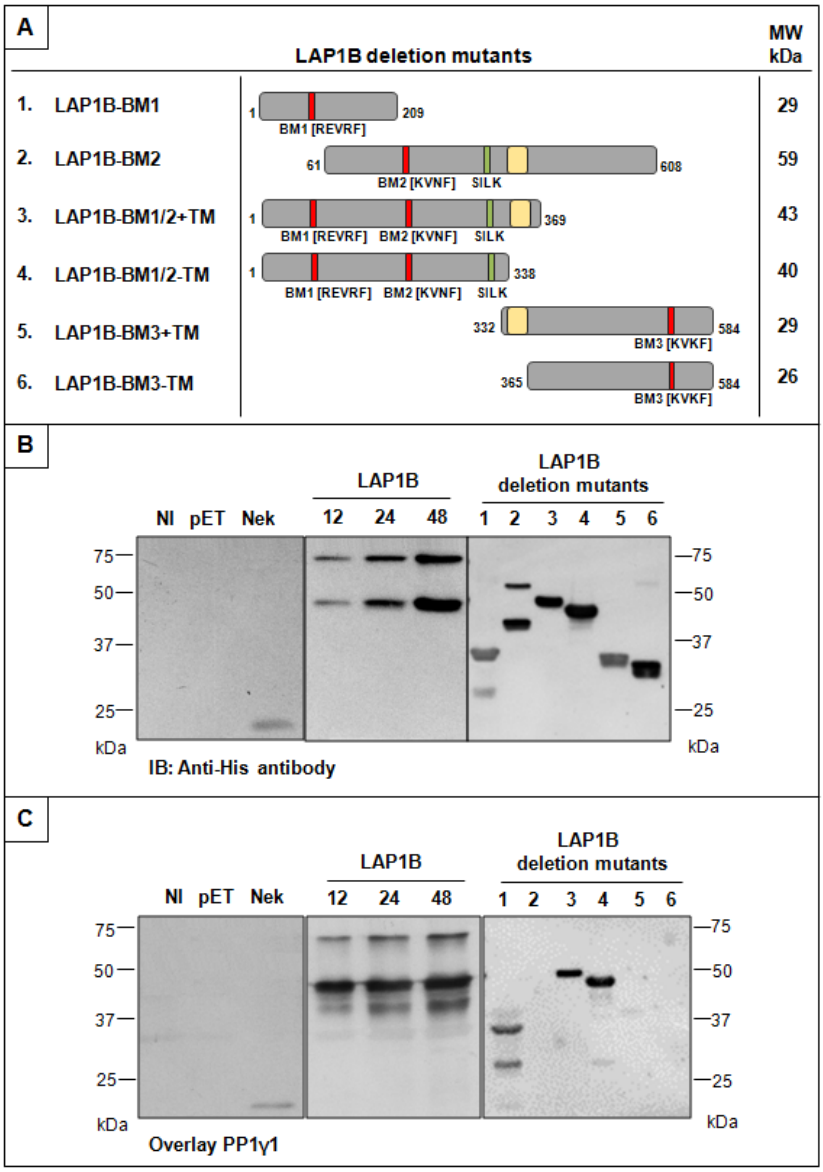

Figure II.2 . Blot overlay assay with PP1γ1. Immunoblotting analysis using a His-tag antibody is also shown. **A-**Schematic representation of LAP1B deletion mutants cloned into the pET-28c vector. The expected molecular weight (MW) of each construct is indicated. The red boxes represent the RVxF motifs, the green boxes correspond to the SILK motif, and the yellow boxes represent the transmembrane domain. **B-** Blot overlay assay of full-length LAP1B. Increasing amounts of recombinant full-length LAP1B (12, 24 and 48 µL) were loaded on each well as indicated. **C-** Blot overlay assay of LAP1B deletion mutants. Deletion mutants: 1, LAP1B–BM1; 2, LAP1B–BM2; 3, LAP1B–BM1/2+TM; 4, LAP1B–BM1/2-TM; 5, LAP1B-BM3+TM; 6, LAP1B-BM3-TM. Non-induced (NI) and pET-28c vector without an insert (pET) were used as negative controls and Nek2A (Nek) as positive control. Bacterial cultures were collected 3 hours after IPTG (1mM) induction at 37ºC.

II.3.3. The novel complex LAP1B:PP1 is also formed *in vivo*

Having shown that the LAP1B:PP1 complex is formed *in vitro* the ability of the same to be formed *in vivo* was addressed. Yeast co-transformations were carried out in order to validate the novel complex formation and to simultaneously confirm relevant domains in LAP1B for the interaction, as well as to test different PP1 isoforms. Firstly, co-transformations were carried out with full-length LAP1B and different PP1 isoforms (α, γ1 or γ2), the assay took advantage of α-Galactosidase activity in the presence of the blue chromogenic substrate X-α-gal, producing a blue colour in the event of an interaction. The results (Fig. II.3) clearly show that LAP1B interacts with all PP1 isoforms tested (PP1α, PP1γ1 and PP1γ2; Fig. II.3A) but does not interact with the C-terminal portion of PP1γ2 isoform (PP1γ2end; Fig. II3A). Subsequently, the relevant domain in LAP1B for the interaction was again tested using the *in vivo* conditions. These LAP1B deletion mutants, previously produced, were co-transformed in yeast with the PP1γ1 isoform and the results are presented in Fig. II.3B. Unequivocally, the results were positive for the deletion mutant that comprises the residues 1-209 including the BM1 (Fig. II.3B) and also with the construct that comprises both BM1 and BM2 (BM1/2). In sharp contrast the results were negative with the LAP1B-BM2 and LAP1B-BM3 (Fig. II.3B). The positive and negative controls are presented in Fig. II.3C. These results show that it is the BM1 (REVRF) that mediates the interaction between LAP1B and PP1.

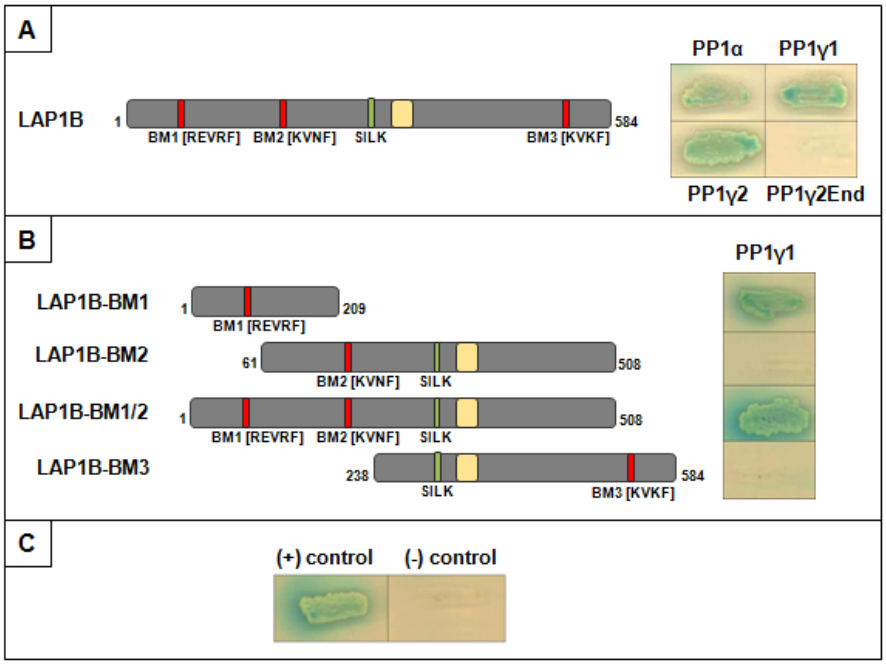

Figure II.3. Yeast co-transformation assay in SD/QDO/X-α-gal medium. Full-length LAP1B and its deletion mutants cloned in the pACT2 vector are represented. The red boxes represent the RVxF motifs present in the constructs, the green boxes correspond to the SILK motif, and the yellow boxes represent the transmembrane domain. **A-** Positive interactions were observed between LAP1B and PP1α, PP1γ1 and PP1γ2, but not with the C-terminus of PP1γ2 (PP1γ2End). **B-** PP1γ1 interacted with LAP1B-BM1 and BM1/2 but not with LAP1B-BM2 and BM3. **C-** Association of murine p53 and SV40 large T antigen was used as positive control (+) and co-transformation of pAS2-1 and pACT2 vectors as negative control (-).

Additionally, the *in vivo* occurrence of the complex was further investigated and distinct models were used, namely a non-neuronal cell line (COS-7), a neuronal-like cell line (SH-SY5Y) and rat brain. Thus, co-IPs using the specific antibodies against PP1α, PP1γ and LAP1B were carried out. Firstly, COS-7 cells were transfected with Myc-LAP1B and Myc-LAP1B deletion mutants (LAP1B-BM2 and LAP1B-BM3) and further immunoprecipitated using the PP1γ antibody (Fig. II.4A). The Myc-LAP1B deletion mutants are similar to those tested in yeast co-transformation assays. Our results showed that PP1γ binds only to the full-length LAP1B but not to LAP1B deletion mutants (LAP1B-BM2 and LAP1B-BM3). Once more our results clearly showed that PP1γ only binds LAP1B when the BM1 is present. Non-transfected COS-7 (Fig. II.4B) and SH-SY5Y (Fig. II.4C) cellular extracts were also immunoprecipitated with PP1α and PP1γ antibodies. Rat cortical extracts were also immunoprecipitated with the same antibodies as well as with the LAP1 antibody and the results are presented in Fig. II.4D. Endogenous LAP1B was also detected after IP with PP1α and PP1γ in COS-

7 cells (Fig. II.4B) and SH-SY5Y cells (Fig. II.4C). Finally, using rat cortical brain extracts we confirmed that the LAP1B:PP1 complex is also formed in brain, since we detected LAP1B after IP with PP1α or γ antibodies. Further, when we immunoprecipitated with LAP1 antibody we could also detect both PP1 isoforms (Fig. II.4D). The complex was also detected in other brain regions, namely rat striatum and cerebellum (data not shown) were PP1 is highly abundant.

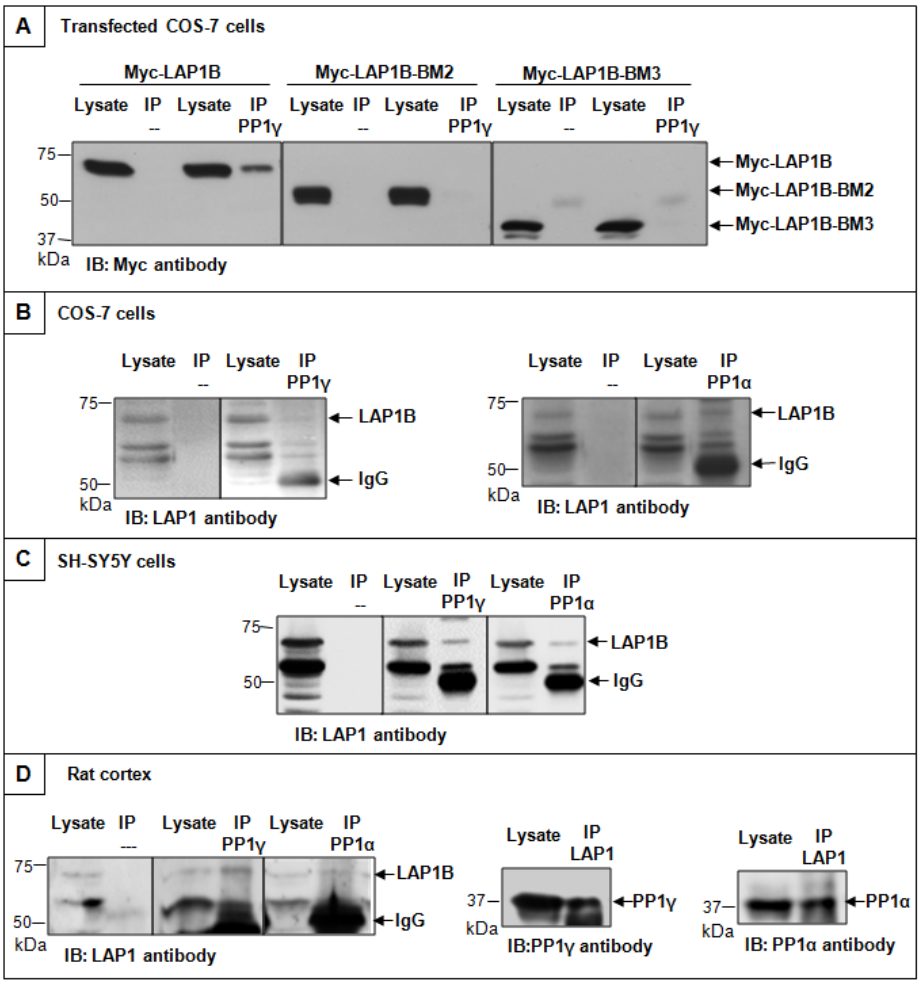

Figure II.4. Co-immunoprecipitation of the PP1:LAP1B complex in COS-7 cells, SH-SY5Y cells and rat cortex. A- COS-7 cells were transfected with Myc-LAP1B, Myc-LAP1B-BM2 or Myc-LAP1B-BM3 and immunoprecipitated with PP1γ bound to protein G- DynaBeads. **B-** Non-transfected COS-7 cells were immunoprecipitated with PP1γ or PP1α antibodies bound to protein G- Dynabeads. **C-** SH-SY5Y cells were immunoprecipitated with PP1γ or PP1α antibodies bound to protein G- Dynabeads. **D-** Rat cortex extracts were immunoprecipitated with PP1γ, PP1α or LAP1 antibodies bound to protein G- Dynabeads. The negative controls were performed by incubating cell extracts with beads. IP, immunoprecipitation. IB, immunoblotting.

II.3.4. Both LAP1B isoforms bind to PP1

Thus far we have unequivocally shown that LAP1B is a novel PP1 regulatory protein and that the complex formed by the two proteins can occur both i*n vitro* and *in vivo*. Given the high degree of similarity between both LAP1B variants and the fact that both comprise the BM1 (REVRF) responsible for the interaction, it is reasonable to deduce that both variants interact with PP1. In order to confirm this hypothesis we generated, by site directed mutagenesis, the LAP1B (ΔA185) construct that corresponds to LAP1B variant 2 reported in GenBank. The interaction of both LAP1B isoforms with PP1 was indeed confirmed by *in vitro* overlay assay. Briefly, 250 ng of recombinant purified PP1γ1 protein were separated by SDS-PAGE and electrotransferred to a nitrocelulose membrane that was subsequently overlaid with each of the LAP1B variants. As expected both LAP1B variants are able to interact with PP1γ1 since we can detect a band of approximately 37 kDa (Fig. II.5) that corresponds to the molecular weight of PP1γ1.

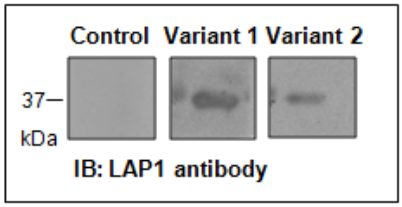

Figure II.5. Blot overlay assay of LAP1B variants. Two samples of purified recombinant PP1γ protein were separated by SDS-PAGE and the resulting blot was overlaid with LAP1B-IVT (1) or LAP1B (ΔA185)-IVT (2). IB, immunoblotting.

II.3.5. Localization of the LAP1B:PP1 complex

Given the confirmation that this novel complex is formed *in vivo*, it is evident that these two proteins are functionally related and therefore it becomes important to describe their localization. Co-localization of both proteins indicated that the complex exists *in vivo* and has physiological relevance. HeLa cells were transiently transfected with Myc-LAP1B and subjected to immunocytochemistry using a Myc-tag antibody. The Myc-LAP1B was mainly found in the nuclear envelope and also in the nucleus where it co-localizes with lamin B1 (Fig. II.6A). Endogenous PP1γ and PP1α were

detected using specific antibodies. All proteins have the expected subcellular distribution; each has been previously described individually (Andreassen et al., 1998; Kondo et al., 2002; Senior and Gerace, 1988). The PP1γ was found predominantly in the nucleus, including the nucleolus, and throughout the cytoplasm (Fig. II.6B). The PP1α was also found predominantly in nucleus, excluding the nucleolus, and throughout the cytoplasm (Fig. II.6B). Despite the quite different subcellular distribution of LAP1B and PP1 isoforms it is evident that they co-localize at specific points within the nucleus and very near to the nuclear envelope, as observed by the yellow color indicated in the ROIs (Fig. II.6B). The co-localizing points were confirmed by confocal profiling (denoted with *), where we demonstrated that the fluorescence intensity of the two channels correlated, particularly in those points, through the white line represented in the image (Fig. II.6C and D). The co-localization quantitative analysis was performed (Fig. II.6E) using a specific co-localization software (Zeiss LSM 510 4.0 software) as previously described (Rebelo et al., 2013; Vieira et al., 2010). Essentially, LAP1B co-localizes similarly with both PP1 isoforms (27.6 ± 0.65% and 27.1 ± 0.8% with PP1γ and PP1α, respectively). The percentage of PP1γ and PP1α that co-localize with LAP1B is lower (13.5 ± 0.48 and 13.8 ± 0.8, respectively).

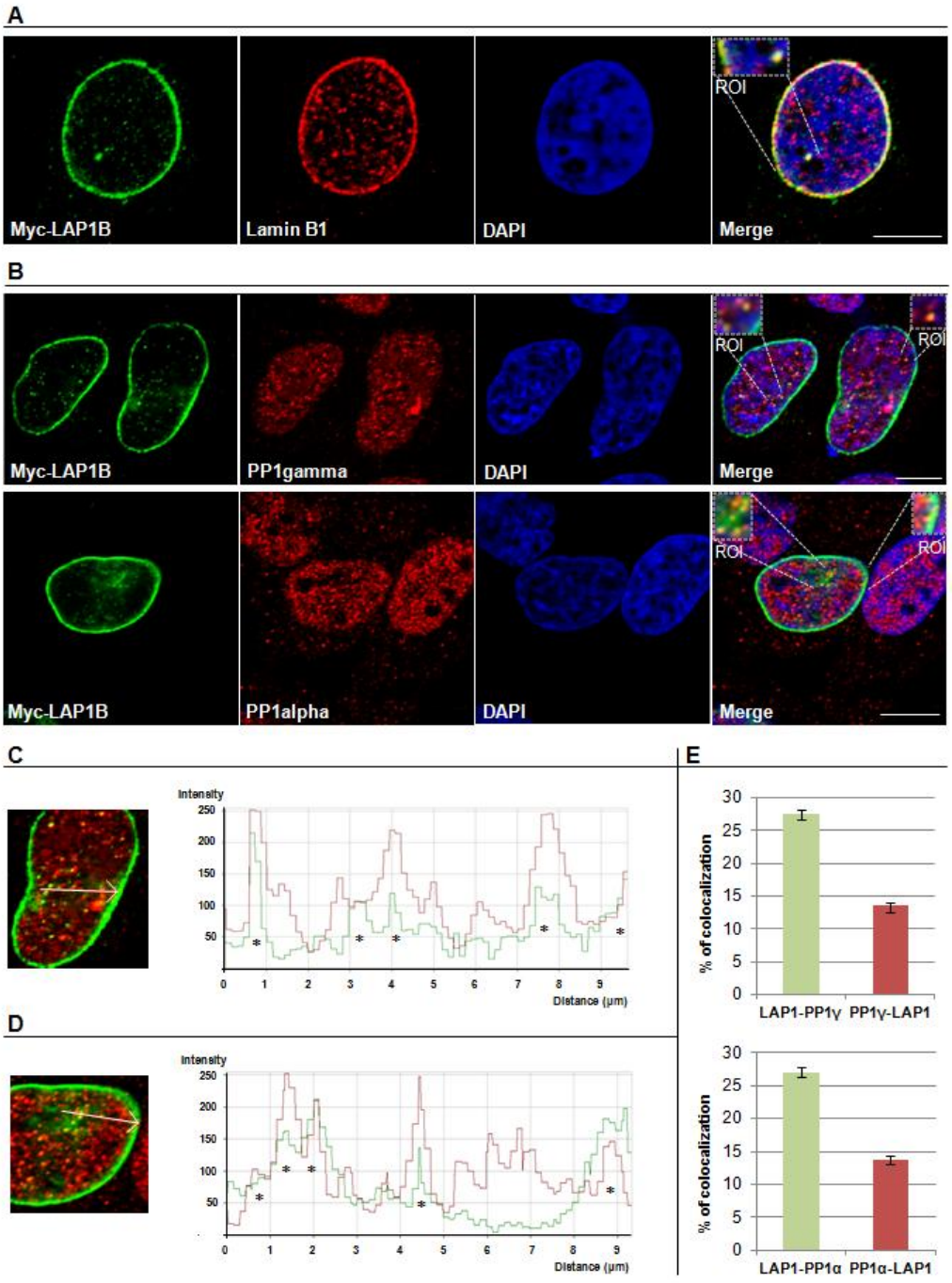

Figure II.6. Subcellular distribution of the LAP1B:PP1 complex in HeLa cells. HeLa cells were transfected with Myc-LAP1B and then processed for immunocytochemistry using specific antibodies to Myc-tag and endogenous lamin B1 and PP1γ and α isoforms. **A-** Immunolocalization of both myc-LAP1B and lamin B1. **B-** Immunolocalization of myc-LAP1B and PP1γ and α isoforms. The presence of the complexes is evidenced by the ROI (region of interest). **C, D-** Confocal profiles representing the green fluorescence intensity (FITC-conjugated secondary antibody labelling Myc-LAP1B) and the red fluorescence intensity (Alexa Fluor 594- conjugated secondary antibody labelling PP1γ [C] or PP1α [D]) in a specific distance (arrow); asterisks denote co-localizing points. **E-** Quantification of % of co-localization between LAP1B and PP1 isoforms. Values are mean ± SEM, n= 75 cells (for PP1γ) and 55 cells (for PP1α). Photographs were acquired using a LSM 510-Meta confocal microscope. Bars, 10 µm.

II.3.6. PP1 specifically binds to LAP1B

Many nuclear membrane proteins are primarily or ultimately linked to each other via direct or indirect interactions involving the nuclear lamina. To test the specificity of the LAP1B:PP1 complex we tested whether other inner nuclear membrane proteins (NPC62, emerin and LAP2β) also bound to PP1. Co-IPs were performed using PP1 antibody and the potential binding partners were further screened using specific antibodies (Fig. II.7). The results presented, clearly show that PP1 only binds to LAP1 and not to the other proteins tested (NPC62, emerin and LAP2β). These results strengthen our hypothesis that LAP1 and PP1 are functionally associated, since they bind specifically in regions near the nuclear envelope (Fig. II.6).

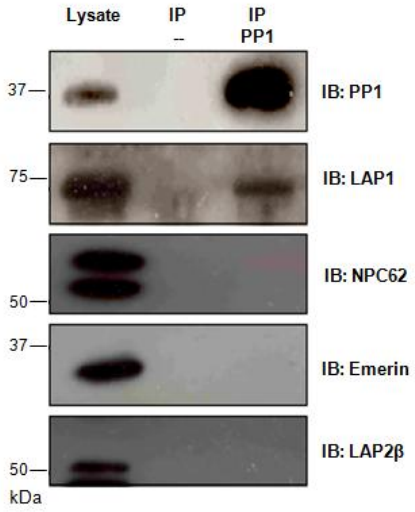

Figure II.7. Co-immunoprecipitation of PP1 binding proteins at the nuclear envelope. HEK293 cells were immunoprecipitated with PP1 antibody bound to protein A- sepharose beads. The negative controls were performed by incubating cell extracts with beads. IP, immunoprecipitation. IB, immunobloting.

II.3.7. LAP1B is a novel substrate for PP1

It is well established that PP1 versatility is largely determined by its regulatory proteins. The latter define subcellular targeting, substrate specificity and even the activity PP1. Having determined that LAP1B is a novel PP1 regulatory protein, since the complex is formed both *in vitro* and *in vivo* and the two proteins co-localize in human cell lines, it is reasonable to deduce that the two proteins are functionally associated. We went on to test if LAP1B is a substrate for PP1, given that LAP1B can

be phosphorylated at several residues (Dephoure et al., 2008; Olsen et al., 2010; Wang et al., 2010). SH-SY5Y cells were incubated with two different concentrations of OA (a protein phosphatase inhibitor), followed by IP with LAP1 antibody and further incubation with recombinant purified PP1γ1 protein (Fig. II.8). Analysis of figure 8 showed that when we inhibit PP2A and PP1 (500 nM OA) a slight decrease in the migration of LAP1B is detected, consistent with an increase in its protein phosphorylation level, this is not evident when only PP2A is inhibited (0.25 nM OA) (Fig. II.8, lysates). In contrast, when we immunoprecipitate LAP1B from cells treated with 500 nM OA and incubated the resulting immunoprecipitates with 100 ng of purified PP1γ1 protein (Fig. II.8, IP) a clear shift in the opposite direction is observed, indicating an *in vitro* dephosphorylation by PP1γ1.

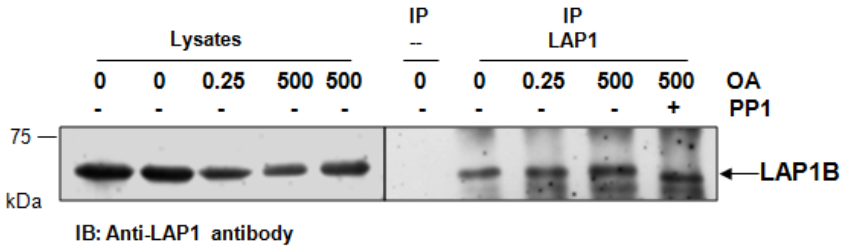

Figure II.8. *In vitro* dephosphorylation of LAP1B. SH-SY5Y cells were incubated with 0, 0.25 or 500 nM okadaic acid (OA) for 3 hours and immunoprecipitated with LAP1 antibody. Immunoprecipitates were incubated at 30ºC for 1 hour with or without 100 ng of PP1γ1 protein. The negative controls were performed by incubation of cells extracts with beads. In the left panel are presented the cell lysates correspondent of each condition immunoprecipitated (right panel). IP, immunoprecipitation. IB, immunobloting.

II.4. DISCUSSION

PP1 regulates numerous cellular functions by binding to different regulatory subunits, which are, in turn, responsible for the targeting of PP1 to a particular subcellular compartment, but also determine substrate specificity and activity (Bollen, 2001; Bollen et al., 2010; Ceulemans et al., 2002a; Cohen, 2002b). In this study we show that LAP1B is a novel PP1 regulatory protein. This LAP1B interaction was originally identified in YTH screens of a human brain cDNA library using three PP1 isoforms (α, γ1 and γ2) as baits (Esteves et al., 2012a; Esteves et al., 2012b). Moreover, LAP1B variant 1, from all these screens, was isolated and fully sequenced (Santos, 2009). In each case the variant obtained was the one recently reported in the GenBank database (NM_001267578) and differs from the LAP1B variant 2 (NM_015602) by only a 3 nucleotide (CAG) insertion, which results in the introduction of a single alanine residue at position 185 of the coding sequence. Typically such variants are generated by alternative splicing (Tadokoro et al., 2005; Watanabe et al., 2003) and this has been shown to be so for the *TOR1AIP1* gene. Despite this subtle difference, both LAP1B variants have the same conserved PP1 binding domains and bind to PP1 (Fig. II.5). Consistent with the YTH results the data here presented, for the yeast co-transformation assays, confirmed that LAP1B is able to bind to all the PP1 isoforms tested (α, γ1 and γ2), but not to the C-terminus of PP1γ2 isoform (Fig. II.3). Thus, this novel LAP1B:PP1 complex was validated not only *in vivo* but also *in vitro* by a blot overlay assay (Figure 2). LAP1 is expressed in both non-neuronal and neuronal tissues (Kim et al., 2010a), as are PP1α and PP1γ1; even though the latter has higher expression levels in brain (da Cruz e Silva et al., 1995b). Thus, we performed co-IP assays in COS-7 cells (non-neuronal cell line), SH-SY5Y cells (neuronal-like cell line) and rat cortex (Fig. II.4). Moreover, the complex LAP1B:PP1 was also found in rat hippocampus and striatum, regions where PP1α and PP1γ are particularly enriched (data not shown)

LAP1B is not a well characterized protein and its main cellular function remains to be defined. However, it is an integral membrane protein of the inner nuclear membrane that interacts with lamins and chromosomes and this is functionally relevant for the maintenance of the nuclear architecture during interphase and mitosis (Foisner and Gerace, 1993). Recently, it was demonstrated that LAP1 recruits torsinA to the nuclear envelope (Goodchild and Dauer, 2005), although the latter is normally located at the endoplasmic reticulum. In contrast, a torsinA mutant form (ΔE302/303-torsinA),

which is present in DYT1 dystonia patients, is primarily relocated to the nuclear envelope (Goodchild and Dauer, 2004; Naismith et al., 2004). Protein:protein interactions can be regulated by protein phosphorylation and consequently by protein kinases and phosphatases. It is therefore highly relevant that LAP1B should bind to PP1. Thus, several LAP1B deletion mutants were generated to determine the binding region responsible for the binding to PP1. *In silico* analysis revealed that LAP1B has three potential PP1 binding RVxF motifs: REVRF (amino acids 55-59) and KVNF (amino acids 212-215) located in the nucleoplasm and KVKF (amino acids 538-541) located in the lumen of the perinuclear space. An additional generic PP1 binding motif termed SILK (Fig. II.1) is also present in the nucleoplasmic domain. We defined that LAP1B:PP1 interaction occurs primarily through a region that comprises the REVRF domains (BM1). These results (Fig. II.2C, 3B, 4A) support an interaction, which in topological terms provides physiological relevance, given that the BM1 is located in the nucleoplasmic portion of LAP1B and PP1 is particularly abundant in the nucleus. The BM2 and the SILK motif are also located in the nucleoplasm but our results clearly showed that these motifs do not mediate the interaction between LAP1B and PP1. BM3 is located in the perinuclear space making this an unlikely domain for the association of both proteins. Moreover, BM1 is conserved among different species (Fig. II.1B) while BM2 and SILK are not. Another remarkable aspect is that RVxF motif is often N-terminal flanked by basic residues and C-terminal flanked by acidic residues and this affects the binding affinity for the RVxF motif (Wakula et al., 2003). Concordantly, BM1 is preceded by basic residues (arginine) and followed by acidic residues (aspartic and glutamic acid) (Fig. II.1B). Further, the SILK motif is always N-terminal to the RVxF motif (Hendrickx et al., 2009), but this is not the case with LAP1B where in fact it is C-terminal to the BM1, reinforcing that the SILK motif is not important for the interaction.

PP1 regulatory proteins can be substrates that directly associate with the PP1 catalytic subunit, but can also be substrate specifiers and/or targeting proteins. Having established that LAP1B is a novel PP1 regulatory protein and that the BM1 is responsible for the interaction, the physiological significance of this complex was addressed. Immunolocatization of LAP1B and PP1 (for both PP1α and PP1γ isoforms) showed that they co-localize near the nuclear envelope (Fig. II.6). These results are in agreement with PP1 interacting with LAP1B through its nucleoplasmic domain, as

discussed above. Furthermore, LAP1B is well described to interact with lamin A/C and B1 (Foisner and Gerace, 1993; Senior and Gerace, 1988). Lamins are not only located at the nuclear membrane periphery but are also found within the nucleus (Bridger et al., 1993; Moir et al., 1994). Indeed, we showed that LAP1B co-localizes with lamin B1 at the nuclear envelope and also in specific intranuclear areas (Fig. II.6). Originally, nuclear lamins were proposed to have a role in supporting the nuclear envelope and binding to chromatin. However, recent reports suggest many other roles for nuclear lamins, namely in DNA replication, transcription, mitosis, apoptosis and cell differentiation (Dechat et al., 2010). Potentially, and in a similar fashion, LAP1B may be involved in other nuclear functions. LAP1B is known to be phosphorylated during both interphase and mitosis and several phosphorylated residues have been identified (Dephoure et al., 2008; Olsen et al., 2010; Wang et al., 2010). However, the involvement of specific kinases and/or phosphatases had not hitherto been documented. Since we validated the interaction between LAP1B and PP1 it is reasonable to deduce that LAP1B may indeed be a substrate for PP1. When PP1 is inhibited with OA a slight shift in the LAP1B migration is observed, consistent with an increase in its protein phosphorylation state (Fig. II.8). Additionally, upon adding purified PP1γ1 protein to LAP1B immunoprecipitates, from cells previously incubated with 500 nM OA, an increase in the migration of LAP1B was detected, indicating that *in vitro* PP1 dephosphorylates LAP1B.

Many PP1 regulators identified thus far are located in the nucleus and are involved in diverse cellular functions, such as, cell cycle regulation, splicing and transcription (Ceulemans and Bollen, 2004; Cohen, 2002b; Esteves et al., 2012b). However, the only known PP1 regulator located specifically at the nuclear membrane is AKAP-149. AKAP149 is a component of the endoplasmic reticulum/nuclear system but the discovery that it interacts with lamins A/C and B (Steen and Collas, 2001), suggests that AKAP149 is associated with both the outer and inner nuclear membranes. AKAP-149 recruits PP1 to the nuclear envelope upon nuclear envelope assembly *in vitro* and promotes lamin B dephosphorylation and polymerization (Steen et al., 2003; Steen et al., 2000). Indeed, PP1 may mediate nuclear lamina reassembly, in part by dephosphorylation of lamin B at the end of mitosis (Thompson et al., 1997). Following nuclear envelope disassembly at mitosis, LAP1B and lamin B have similar localization and both reassemble around the nuclear envelope during telophase (Maison et al., 1997).

In conclusion, we have identified a novel PP1 regulatory protein, LAP1B. Both proteins co-localize in the close proximity of the nuclear envelope. LAP1B is mainly localized to the nuclear envelope whereas PP1 is rich in the nucleus. Co-localization of the LAP1B:PP1 to the nuclear envelope is indicative of specific protein recruitment for signaling events, and this will be addressed in the future. This interaction occurs through the REVRF motif, located in the nucleoplasmic domain of LAP1B. Further we also determined that LAP1B is a substrate for PP1 and PP1 in turn will dephosphorylate LAP1B.

CHAPTER III - CHARACTERIZATION OF HUMAN LAP1 ISOFORMS

LAP1 exist, at least, as three alternatively spliced isoforms in rat (Martin et al., 1995; Senior and Gerace, 1988). However, it remains unclear if the same occurs with the human LAP1, since only the LAP1B isoform had thus far been identified in human cells (Kondo et al., 2002). Therefore, the work described in the chapter III addresses the novel human LAP1 isoforms and characterizes them. This work was included in the manuscript (manuscript 2) entitled: "Identification of a novel human LAP1 isoform that is regulated by protein phosphorylation", submitted for publication in the *Plos One* journal.

"Identification of a novel human LAP1 isoform that is regulated by protein phosphorylation"

Mariana Santos[1], Sara Domingues[1], Patrícia Costa[1], Thorsten Muller[2], Sara Galozzi[2], Katrin Marcus Edgar F. da Cruz e Silva[1], Odete A. da Cruz e Silva[1], Sandra Rebelo[1]

[1] Health Sciences, Centre for Cell Biology, Neuroscience Laboratory, University of Aveiro, Aveiro, Portugal

[2] Department of Functional Proteomics, Medical Proteome Center, Ruhr University Bochum, Bochum, Germany

Abstract

Lamina associated polypeptide 1 (LAP1) is an integral protein of the inner nuclear membrane that is ubiquitously expressed. LAP1 binds to lamins and chromatin, probably contributing to the maintenance of the nuclear envelope architecture. Moreover, LAP1 also interacts with torsinA and emerin, proteins involved in DYT1 dystonia and X-linked Emery-Dreifuss muscular dystrophy disorder, respectively. Given its relevance to human pathological conditions, it is important to better understand the functional diversity of LAP1 proteins. In rat, the LAP1 gene (*TOR1AIP1*) undergoes alternative splicing to originate three LAP1 isoforms (LAP1A, B and C). However, it remains unclear if the same occurs with the human *TOR1AIP1* gene, since only the LAP1B isoform had thus far been identified in human cells.

Our *in silico* analysis suggested that, across different species, potential new LAP1 isoforms could be generated by alternative splicing. Using shRNA to induce LAP1 knockdown and HPLC-mass spectrometry analysis we described and validated the presence of two isoforms in human cells: LAP1B and LAP1C; the latter is N-terminally truncated. LAP1B and LAP1C expression profiles appear to be dependent on the specific tissues analyzed and in cultured cells LAP1C was the major isoform detected. Moreover, LAP1B and LAP1C expression increased during neuronal maturation, suggesting that LAP1 is relevant in this process. Both isoforms were found to be post-translationally modified by phosphorylation and methionine oxidation and two LAP1B/LAP1C residues were shown to be dephosphorylated by PP1. This study permitted the identification of the novel human LAP1C isoform and partially unraveled the molecular basis of LAP1 regulation.

III.1. INTRODUCTION

The eukaryotic nucleus is a complex organelle enclosed by a double membrane, the nuclear envelope (NE). The NE separates the cytoplasm from de the nucleus in eukaryotic cells and is structurally composed by the inner nuclear membrane (INM), the outer nuclear membrane (ONM), the nuclear lamina and the nuclear pore complexes. The perinuclear space is located between the INM and the ONM, however these membranes are joined in some regions at the nuclear pore complexes (reviewed in Gerace and Burke, 1988). The INM contains specific integral membrane proteins (Malik et al., 2010; Schirmer et al., 2003) and most of them interact with lamins (the main components of the nuclear lamina) and/or chromatin.

One of the first lamin associated proteins identified was the lamina associated polypeptide 1 (LAP1) (Senior and Gerace, 1988). LAP1 was initially identified using a monoclonal antibody generated against lamina-enriched fractions of rat liver nuclei. This antibody recognized three rat proteins corresponding to LAP1A, B and C with molecular weights of 75, 68 and 55 kDa, respectively (Senior and Gerace, 1988). These proteins are type 2 transmembrane (TM) proteins, comprising a nucleoplasmic N-terminal domain, a single TM domain and a lumenal C-terminal domain, located in the perinuclear space (Martin et al., 1995). Moreover, rat LAP1 family members are generated by alternative splicing and differ only in their nucleoplasmic domain. The full-length cDNA of rat LAP1C was isolated from a cDNA expression library prepared from rat liver polyA$^+$ mRNA. Additionally, partial clones of LAP1B and LAP1C were also isolated. These clones were identical to some sequences of LAP1C cDNA but have two additional insertions (Martin et al., 1995). To date, only one isoform had been identified and characterized in human cells and it corresponded to LAP1B. Kondo *et al*, isolated a clone from HeLa cells that was similar to the rat LAP1C cDNA, and encoded a protein with a molecular weight (66.3 kDa) very close to the expected size for rat LAP1B. Therefore, it was concluded that this clone should correspond to the human LAP1B isoform (Kondo et al., 2002). Additionally, another human variant of LAP1B was identified, but it has only one amino acid (alanine) less (Tadokoro et al., 2005; Tsai et al., 2007) than the previously reported LAP1B. Of note, and up to the date of this publication, it remains unclear whether LAP1 is also alternatively spliced in human cells, giving rise to human LAP1A and C isoforms.

Moreover, the function of LAP1 remains poorly understood. However, it was described that LAP1 binds directly to lamins and indirectly to chromosomes (Foisner and Gerace, 1993). Thus, LAP1 may be involved in the positioning of lamins and chromatin in close proximity with the NE, thereby contributing to the maintenance of the NE structure (Gerace and Huber, 2012; Martin et al., 1995). LAP1 gained more attention when it was reported to interact with torsinA in the NE (Goodchild and Dauer, 2005). A mutation of a glutamic acid within torsinA is responsible for most cases of DYT1 dystonia, a neurological and movement disorder (Ozelius et al., 1997). Thus, LAP1 is also known as torsinA interacting protein 1 (TOR1AIP1) and the gene encoding LAP1 is termed *TOR1AIP1*. More recently, LAP1 was found to interact with the INM protein emerin (Shin et al., 2013), which is associated with the X-linked Emery-Dreifuss muscular dystrophy disorder (Bione et al., 1994). Furthermore, it was reported that conditional deletion of LAP1 from mouse striated muscle causes muscular dystrophy leading to early lethality (Shin et al., 2013). We have recently reported that human LAP1B binds to protein phosphatase 1 (PP1) in the nucleoplasm and also that it is dephosphorylated *in vitro* by this phosphatase (Santos et al., 2013). In agreement, previous studies showed that rat LAP1 isoforms were phosphorylated *in vitro* and at least LAP1C was also phosphorylated *in vivo* (Foisner and Gerace, 1993).

In the present study, we took advantage of the shRNA technology to knockdown LAP1 in human cells, so as to determine whether other human LAP1 isoform exist. Subsequently two isoforms, LAP1B and LAP1C, were identified. Using HPLC-mass spectrometry (MS) analysis, we showed that human LAP1C is N-terminally truncated. LAP1C was never identified in human cells, thus this is the first time that two human LAP1 isoforms have been described in human cells. Furthermore, the relative abundance of LAP1 isoforms in human cell lines was also estimated. Finally, our data provided evidences that PP1 is responsible for dephosphorylating both Ser306 and Ser310 residues of LAP1B/LAP1C.

III.2. MATERIALS AND METHODS

III.2.1. Antibodies

The primary antibodies used were rabbit polyclonal LAP1 (Goodchild and Dauer, 2005); rabbit polyclonal lamin B1 (Santa Cruz Biotechnology); mouse monoclonal β-tubulin (Invitrogen); mouse monoclonal synaptophysin (Synaptic Systems); rabbit polyclonal CBC3C that recognizes the C-terminal of PP1γ (da Cruz e Silva et al., 1995b); and Myc-tag antibody (Cell Signaling), that recognizes Myc-fusion proteins. The secondary antibodies used were anti-mouse and anti-rabbit horseradish peroxidase-linked antibodies (GE Healthcare) for ECL detection.

III.2.2. Expression vectors and DNA constructs

Myc-LAP1B and pET-LAP1B constructs have been previously described (Santos et al., 2013). The pSIREN-RetroQ vector (Clontech) was kindly provided by Dr. Celso Cunha from the *Instituto de Higiene e Medicina Tropical* , Lisbon (Casaca et al., 2011).

III.2.3. Brain dissection

Winstar rats (9-12 weeks) were obtained from Harlan Interfaune Ibérica, SL. All experimental procedures observed the European legislation for animal experimentation (2010/63/EU). No specific ethics approval under EU guidelines was required for this project, since the rats were only euthanized, by cervical stretching followed by decapitation, for brain removal. This is within the European law (Council Directive 86/609/EEC) and during this procedure we took all steps to ameliorate animal suffering and used the minimum number of animals possible. The procedures were approved and supervised by our Institutional Animal Care and Use Committee (IACUC): Comissão Responsável pela Experimentação e Bem-Estar Animal (CREBEA). Animals were sacrificed by cervical stretching followed by decapitation, and the cortex was dissected out on ice. The tissue was then homogenized on ice, lysis buffer (50 mM Tris-HCl pH 8.0, 120 mM NaCl, 4% CHAPS) containing protease inhibitors (1 mM PMSF, 10 mM

Benzamidine, 2 µM Leupeptin, 1.5 µM Aprotinin, 5 µM Pepstatin A), with a Potter-Elvehjem tissue homogenizer with 10-15 pulses at 650-750 rpm (S. Rebelo., 2013).

III.2.4. Cell culture and transfection

SH-SY5Y cells (ATCC CRL-2266) were grown in Minimal Essential Medium (MEM) supplemented with F-12 Nutrient Mixture (Gibco, Invitrogen), 10% fetal bovine serum (FBS, Gibco, Invitrogen), 1.5 mM L-glutamine and 100 U/mL penicillin, 100 µg/mL streptomycin and 0.25 µg/mL amphotericin B (Gibco, Invitrogen). In order to promote SH-SY5Y cells differentiation, cells were plated at a density of 1 x 10^5 and grown for 10 days in MEM/F12 medium with 10% FBS in the presence of 10 µM retinoic acid (Rocha et al., 2012). HeLa cells (ATTC CRM-CCL-2) were grown in MEM with Earle's salts and GlutaMAX (Gibco, Invitrogen), supplemented with 10% FBS, 1% Non-Essential amino acids (Gibco, Invitrogen) and 100 U/mL penicillin, 100 µg/mL streptomycin and 0.25 µg/mL amphotericin B (Gibco, Invitrogen). SKMEL-28 cells were handled as previously described (Espona-Fiedler et al., 2012). PC12 cells (ATCC CRL-1721) were cultured in RPMI1640 medium (Alfagene) supplemented with 5% FBS, 10% horse serum (Gibco, Invitrogen) and 100 U/mL penicillin, 100 µg/mL streptomycin and 0.25 µg/mL amphotericin B (Gibco, Invitrogen). These cells were plated onto poly-L-ornithine coated dishes (Rebelo et al., 2004). All cultures were maintained at 37ºC and 5% CO_2.

Rat cortical primary cultures were established from embryonic day 18 embryos as previously described (Henriques et al., 2007). Briefly, after dissociation with 0.45 mg/ml trypsin, cells were plated onto poly-D-lysine-coated dishes at a density of $1.0x10^5$ cells/cm^2 in B27-supplemented Neurobasal medium (Gibco, Invitrogen), a serum-free medium combination (Brewer et al., 1993). The medium was supplemented with glutamine (0.5 mM) and gentamicin (60 µg/ml). Cultures were maintained in an atmosphere of 5% CO_2 at 37ºC until 14 days *in vitro* (DIV) before being used for experimental procedures.

Transient transfections of SH-SY5Y cells were performed using TurboFect (Thermo Scientific) according to the manufacturer's protocols. After 24 hours of transfection, cells were harvested for experimental procedures.

III.2.5. LAP1B knockdown

The knockdown of endogenous LAP1 in SH-SY5Y cells was achieved using a short hairpin RNA (shRNA) strategy. To construct shRNA-expressing vectors, oligonucleotides targeting the human LAP1B mRNA and the corresponding complementary sequences, were inserted into the pSIREN-RetroQ vector. The oligonucleotide sequences were designed using the online designer tool of *Clontech*, available at http://bioinfo.clontech.com/rnaidesigner. Two pairs of oligonucleotides were chosen: one aligning between exon 7 and 8 (5'-gatccGTGCTAAGCTCAGGATATCTTCAAGAGAGATATCCTGAGCTTAGCACTTTTTTACGCGTg-3') and other in exon 10 (5´- gatccGGAAGAGACACTTGGAACATTCAAGAGATGTTCCAAGTGTCTCTTCCTTTTTTACGCGTg-3') of the LAP1 mRNA (NM_001267578). The underlined sequences denote the LAP1 shRNA sequence targeting in the LAP1 mRNA. A control shRNA was also generated, by using a negative control oligonucleotide that does not target any human transcript (5´-gatccGCTTCATAAGGCGCATAGCTATTCAAGAGATAGCTATGCGCCTTATGCTTTTTTg-3'). The oligonucleotides were annealed and subcloned into the *BamH*I and *EcoR*I sites of the pSIREN-RetroQ vector. The generated constructs pSIREN-LAP1-C1 (targeted to exon 7/8), pSIREN-LAP1-C2 (targeted to exon 10) and pSIREN-CMS (control) were verified by restriction analysis and DNA sequencing using an ABI PRISM 310 Genetic Analyzer (Applied Biosystems, Porto, Portugal). Constructs were then transfected using the TurboFect reagent (Thermo Scientific) according to the manufacturer's protocols.

III.2.6. RT-PCR and sequencing

Adult brain poly A+ RNA (Clontech) was reverse transcribed using the SuperScript™ First Strand Synthesis System (Invitrogen) and the *TOR1AIP1* gene specific primer E10RV (5'-CTTGGCCTGACCTACTCTTAAGAC-3') or the oligo$(dT)_{20}$ primer. The synthetized cDNA was amplified using the following primer pairs: forward primer E1FW (5'-CAGGAGAACCTAGGGTCCATAAAG-3') and reverse primer E10BRV (5´- GTGAACAATTCTCAGAACTTGGGAC-3'); forward primer E2FW (5'-CATTCC TCTGAAGAGGATG-3') and reverse primer E10BRV;

forward primer E5FW (5'CTGAAGAAGATGATCAAGACAGCTC-3') and reverse primer E10CRV (5'-GTGAGCAGTAAGATAGCAGGCTG-3'). The PCR products were excised from agarose gel and purified using QIAquick Gel Extraction Kit (Promega). The purified fragments were cloned into the Nzy-blunt PCR cloning kit (Nzytech). One clone from each reaction was selected and the inserts sequenced using an ABI PRISM 310 Genetic Analyzer (Applied Biosystems, Porto, Portugal).

III.2.7. RNA isolation

Total RNA was isolated from SH-SY5Y cells using Trifast^{TM} reagent (Peqlab Biotechnologie GmbH) following the supplier's protocols. Briefly, cells were homogenised in 500 µl of Trifast^{TM} reagent with a 20 G needle. Then, cell lysates were incubated at room temperature for 5 min before 100 µL of chloroform were added. Samples were shaken vigorously for 15 seconds and kept at room temperature for 5 min before centrifugation at 12000 g for 15 min. The upper aqueous phase, containing RNA, was transferred into a new tube and the RNA precipitated by adding 250 µl of isopropanol followed by incubation at 4ºC for 10 minutes. The RNA was spun down for 10 min at 12000 g and the pellet washed twice with 500 µl of ice cold 75% ethanol and subsequently centrifuged for 10 min at 12000 g. The RNA was air-dried at room temperature and dissolved in RNAse free water.

III.2.8. Northern blot analysis

Northern blot analysis was performed following the protocol provided with the Odyssey Infrared Imaging System (LI-COR Biosciences) with some alterations. Briefly, 20 µg of total RNA from SH-SY5Y cell were mixed with formaldehyde/formamide RNA loading buffer. The samples were incubated at 65ºC for 15 minutes, chilled on ice followed by the addition of loading buffer (50% glycerol, 1 mM EDTA pH 8.0, 0.25% bromophenol blue and 0.25% xylene cyanol FF). Then, the samples were loaded on 1% agarose gel in formaldehyde gel running buffer (0.02 M MOPS pH 7.0, 8 mM sodium acetate, 1 mM EDTA pH 8.0 and 2.2 M formaldehyde). Samples were transferred onto nitrocellulose membranes by capillary elution in 20x SSC buffer overnight. RNA was cross-linked to the membrane using a UV cross-linker. Membranes were hybridized with a LAP1 biotinylated probe. To generate the biotinylated probe, clone 1A (from the

RT-PCR reaction E1FW+E10BRV) was used as a template for PCR amplification in the presence of biotin-16-dUTP (Roche) and the primers E10FW (5´-CAAGGTCAAGATGAGAAGCTG-3)' and E10BRV (5´-GTGAACAATTCTCAGAACTTGGGAC-3'), both targeting exon 10 of LAP1. A probe directed to human β-actin was also generated using cDNA obtained by RT-PCR from human brain poly A+ RNA, and the primers AFW (5'-GCTCGTCGTCGACAACGGCT C-3') and ARV (5'-CAAACATGAT CTGGGTCATCTTCTC-3'). The membrane was pre-hybridized at 42ºC with ULTRAhyp-Oligo Buffer (Ambion) and hybridized overnight at 42ºC with biotinylated probes (diluted in ULTRAhyp-Oligo Buffer) and then washed with Low and High Stringency Washes (Ambion). Membranes were blocked for 1 hour with Odyssey Blocking Buffer plus 1% SDS (LI-COR Biosciences) and then incubated for 1 hour with Streptavidin IRDye800 CW conjugate (1:10000) in blocking buffer plus 1% SDS (LI-COR Biosciences). Blots were washed three times with PBS-T 1x and one with PBS 1x before scanning on an Odyssey IR Imaging System (LI-COR Biosciences).

III.2.9. Co-immunoprecipitation

SH-SY5Y cells were collected in lysis buffer (50 mM Tris-HCl pH 8, 120 mM NaCl, 4% CHAPS) containing protease inhibitors (1 mM PMSF, 10 mM Benzamidine, 2 µM Leupeptin, 1.5 µM Aprotinin, 5 µM Pepstatin A). Dynabeads Protein G (Dynal, Invitrogen) were washed in 3% BSA/1x PBS. LAP1 antibody was cross-linked to Dynabeads according to the manufacter's protocol. Cell lysates were precleared with 20 µL (0.6 mg) Dynabeads for 1 hour and then incubated with antibody-dynabeads overnight at 4ºC. The immunoprecipitates were washed in 1x PBS and proteins eluted by boiling in loading buffer before SDS-PAGE.

III.2.10. LAP1 solubilization assay

For the LAP1 solubilization we performed a procedure adapted from Goodchild, 2005 (Goodchild and Dauer, 2005). SH-SY5Y cells were collected in the following buffers supplemented with protease inhibitors (1 mM PMSF, 2 µM Leupeptin, 1.5 µM Aprotinin): 50 mM Tris-HCl pH 7.5; 50 mM Tris-HCl pH 7.5 and 1% triton X-100; 50

mM Tris-HCl pH 7.5, 1% triton X-100 and 50 mM NaCl or 500 mM NaCl. Homogenates were incubated on ice for 20 minutes and centrifuged at 20000 g for 15 min to separate supernatant (soluble) and pellet (insoluble) fractions. Pellet fractions were solubilized in 150 µl of 1x loading buffer at 90ºC and supernatants were brought to a 150 µl volume and 1x concentration by adding 4x loading buffer. Equal volumes of pellet and supernatant were loaded on SDS-PAGE.

III.2.11. Nano-HPLC and Mass spectrometry

For nano-HPLC-MS analysis, SH-SY5Y total cell lysates, SH-SY5Y cells membrane-containing fraction (pellet collected by centrifugation in 50 mM Tris-HCl pH 7.5, as previously described) and LAP1 immunoprecipitates (obtained as previously described) were resolved by 10% SDS-PAGE. Gels were stained with Coomassie blue colloidal (Sigma-Aldrich) using standard procedures (Korrodi-Gregorio et al., 2013). Two bands were excised from the gel: one below 75 kDa and other above 50 kDa, corresponding to the molecular weights of LAP1B (68 kDa) and the putative LAP1C (56 kDa) protein, respectively. Bands were then excised from the gel and destained. The measurements were performed on a nano-HPLC system Ultimate 3000 (Dionex, Germany), coupled on-line to a quadrupole-orbitrap mass spectrometer (Q Exactive; Thermo Fischer Scientific, Germany). Samples were loaded on a C18 trap column (Thermo, 100 µm x 2 cm, particle size 5 µm, pore size 100 Å, C18) with 1.1% TFA and 30 µl/min flow rate. Then the trap column was online switched with an analytical C18 column (Thermo, 75µm x 50 cm, particle size 2 µm, pore size 100 Å). The separation was performed with a flow rate of 400 nl/min using the following solvent system: (A) 0.1% FA; (B) 84% ACN, 0.1% FA. The separation gradient was from 4-40% B in 95 min, followed by a washing step at 95% B (5min) and an equilibration step at 4% B (5min). After nano-HPLC separation the eluent was ionized by a nano electrospray ionization source (ESI) and analyzed in data dependent scan mode in a Q Exactive. In the ESI/MS-MS analysis full MS spectra were scanned between 350 – 1400 m/z with a resolution of 70,000 at 200 m/z (AGC target 3e6, 80 ms maximum injection time). The capillary temperature was set at 250°C and the spray voltage at 1600 V (+). Lock mass polydimethylcyclosiloxane (m/z 445.120) was used for internal recalibration. The m/z values initiating MS/MS were set on a dynamic exclusion list for 30 s and the 10 most intensive ions (charge +2, +3, +4) were selected for fragmentation. MS/MS fragments

were generated by higher energy collision induced dissociation (HCD) and the fragmentation was performed with 27% normalized collision energy (NCE). The first MS/MS mass was fixed at 130.0 m/z and isolation window 2.2 m/z. The fragment analysis was performed in an orbitrap analyzer with 35,000 resolution at 200 m/z (AGC 1e6, maximum injection time 120 ms).

III.2.12. *In vitro* translation (IVT)

LAP1B was generated by *in vitro* translation (IVT) from pET-LAP1B expression vector using the TnT-coupled transcription/translation kit (Promega), according to the manufacturer's instructions**.**

III.2.13. SDS-PAGE and immunoblotting

Samples were separated on SDS-PAGE and electrophoretically transferred onto nitrocellulose. Nitrocellulose membranes were incubated in Ponceau S solution for 5 minutes and then scanned in a GS-800 calibrated imaging densitometer (Bio-Rad), in order to assess equal gel loading. Membranes were washed in TBST 1x to remove Ponceau S staining, followed by immunological detection with specific antibodies as indicated. Membranes were saturated in 5% non-fat dry milk and further incubated with primary antibodies. Detection was achieved using horseradish peroxidase-conjugated anti-rabbit or anti-mouse IgGs as secondary antibodies and proteins visualized by ECL (GE Healthcare).

III.2.14. Bioinformatics analysis

Database searches to find homologies between sequences were performed using BLAST algorithm (http://blast.ncbi.nlm.nih.gov/Blast.cgi) (Altschul et al., 1990). Multiple sequence alignments were performed using the CLUSTAL OMEGA alignment tool (http://www.ebi.ac.uk/Tools/msa/clustalo/) (Sievers and Higgins, 2014). The splice prediction was achieved by using the programs NNSPLICE (http://www.fruitfly.org/seq_tools/splice.html) and GENSCAN (http://genes.mit.edu/GENSCAN.html) (Burge and Karlin, 1997; Reese et al., 1997).

The prediction of promoter and transcription factor binding sites was performed using the NNPP program (http://www.fruitfly.org/seq_tools/promoter.html) (Reese, 2001) and the TSSG (http://linux1.softberry.com/berry.phtml) (Solovyev and Salamov, 1997).

III.2.15. Quantification and Statistical Analysis

Autoradiograms were scanned in a GS-800 calibrated imaging densitometer (Bio-Rad) and protein bands quantified using the Quantity One densitometry software (Bio-Rad). Data were expressed as mean ± SEM of at least three independent experiments. Statistical significance analysis was conducted by Student's test, with the level of statistical significance being considered $P < 0.05$.

III.3. RESULTS

III.3.1. Knockdown of human LAP1

To date little information is available regarding the human LAP1 family of proteins and their physiological functions. Recently, we described that one of the family members, LAP1B, is a novel PP1 binding protein (Santos et al., 2013). To clarify the existence of additional human LAP1 family members and their physiological impact, we generated LAP1 specific shRNAs to reduce the cellular levels of LAP1 protein. For this purpose, we designed a pSIREN-RetroQ vector coding for LAP1-specific shRNAs: pSIREN-LAP1-C1 and pSIREN-LAP1-C2 were designed to align between exons 7/8 and in exon 10 of LAP1, respectively. SH-SY5Y cells were transfected with one of the pSIREN-LAP1 plasmids or with both for 24 hours. In parallel, SH-SY5Y cells were also transfected with the negative control, the pSIREN-CMS construct. The efficiency of LAP1 knockdown was monitored by immunoblotting with a LAP1 specific antibody (Goodchild and Dauer, 2005). LAP1 antibody was raised against residues 463-478 (exon 10) of mouse LAP1 and is able to detect the three LAP1 splice variants in mouse cells (Goodchild and Dauer, 2005). Given that the amino acid identity between mouse and human LAP1 is very high in the region recognized by this antibody, the same antibody was used to detect human LAP1. Two major peptides, with reduced endogenous levels in cell lysates, were detected upon transfecting with the pSIREN-LAP1-C1, pSIREN-LAP1-C2 or both constructs simultaneously (Fig. III.1A). The higher migrating band (approximately 68 kDa) corresponds to the molecular weight of the known LAP1B isoform, while the lower band (approximately 56 kDa) has not been previously reported in human cells, but has the same molecular weight of rat LAP1C, described in the literature. Therefore we hypothesized that this novel immunoreactive band is likely to correspond to the human LAP1C isoform. The intracellular levels of LAP1B were reduced by 34%, 45% and 47% upon transfection with pSIREN-LAP1-C1, pSIREN-LAP1-C2 or both constructs, respectively (Fig. III.1A). In a similar fashion the intracellular levels of the putative LAP1C were also reduced by 31%, 41% and 51%, upon transfection with pSIREN-LAP1-C1, pSIREN-LAP1-C2 or both constructs together, respectively. Ponceau S staining was used as loading control (data not shown). The response obtained also permits to conclude that both LAP1B and the

putative LAP1C have in common the regions of exon 7, 8 and 10 targeted by the shRNAs used, which corroborates the fact that all LAP1 isoforms have a conserved C-terminal.

In order to clarify that the new putative human LAP1C isoform is not a product of cleavage or post-translational proteolytic processing of LAP1B, we transfected SH-SY5Y cells with two different amounts of Myc-LAP1B (0.5 µg and 1µg). After immunoblotting with Myc antibody, only one band was detected corresponding to the transfected Myc-LAP1B (Fig. III.1B). Moreover, we performed immunoblotting with LAP1 antibody and did not detect an increase in the expression of the putative LAP1C immunoreactive band upon transfection (Fig. III.1B). These results support the fact that the putative LAP1C is not a product of LAP1B cleavage or proteolytic processing, but in fact a distinct isoform.

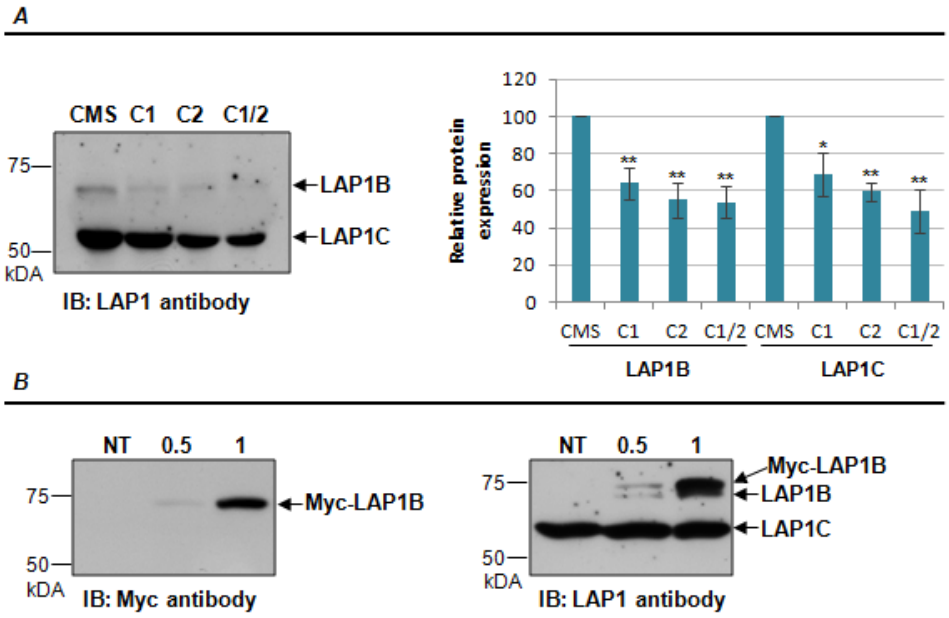

Figure III.1. Identification of a new putative human LAP1 isoform. A- Transfection of SH-SY5Y cells with pSIREN-RetroQ vector coding for LAP1-specific shRNAs resulted in the knockdown of two LAP1 isoforms: LAP1B and putative LAP1C. Data are presented as mean ± SEM of at least three independent experiments. Statistically different from CMS transfected cells, *****$p < 0.05$, ******$p < 0.01$. C1, pSIREN-C1 (directed against exon 7/8 of LAP1), C2, pSIREN-C2 (directed against exon 10 of LAP1); CMS, pSIREN-CMS (control missense). **B-** Transfection of SH-SY5Y cells with Myc-LAP1B (0.5 or 1µg). NT, non-transfected; IB, immunoblotting

III.3.2. *In silico* analysis of the *TOR1AIP1* gene

In silico analysis of the *TOR1AIP1* gene was performed to predict the potential diversity of human LAP1 proteins. Two human LAP1 transcripts have in fact been reported (Tadokoro et al., 2005; Tsai et al., 2007). Bioinformatic analysis of those transcripts and the alignment with the genomic sequence, revealed the presence of 10 exons (Fig. III.2A). Transcript variant 1 [GenBank: NM_001267578] represents the longest transcript and is identical to the first human LAP1B sequence reported in 2002 (Kondo et al., 2002). This transcript differs from variant 2 [GenBank: NM_015602], only by a CAG insertion, which results in an additional alanine in the coding sequence (Figure III.2B). Some reports showed that *TOR1AIP1* gene possesses a 3' tandem splice site, TAGCAG, at the exon 3 boundary, which results in one amino acid insertion or deletion in the encoded protein (Tadokoro et al., 2005; Tsai et al., 2007).

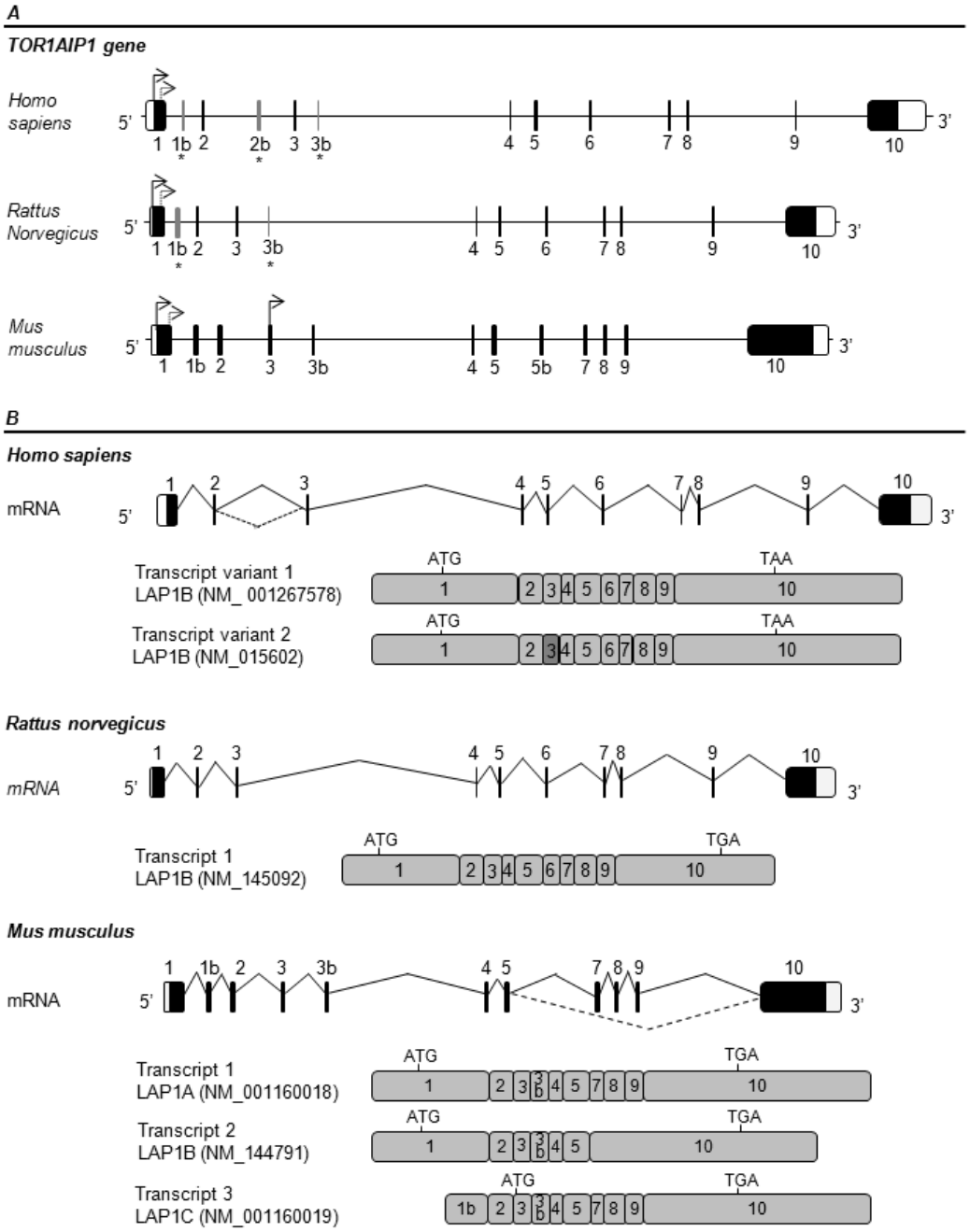

Figure III.2. Gene structure and splice variants of human, rat and mouse *TOR1AIP1*. A- Structure of the human, rat and mouse *TOR1AIP1* gene. Non-coding sequences in exons are represented by open boxes and coding exons are represented by black filled boxes. Predicted exons 1b and 3b in human and rat genes, and exon 2b in human gene are represented by grey boxes and denoted by an asterisk. The in-frame ATG codons are indicated by arrows. **B-** Schematic representation of the alternative splicing patterns and resulting LAP1 transcripts variants (human, rat and mouse). The translation initiation codons (ATG) and the stop codons (TAA or TGA in human and mouse/rat sequences, respectively) are indicated in each transcript. Human LAP1 transcripts variants differ only in exon 3 (dark grey) by three nucleotides through an alternative 3' splicing event.

Sequencing of rat LAP1C and partial characterization of rat LAP1A and LAP1B suggested that rat LAP1 family members arise from alternative splicing (Martin et al., 1995). However, despite what is reported in the literature, it was only found one Reference Sequence (RefSeq) transcript in GenBank that corresponds to rat LAP1B isoform (Fig. III.2B) [GenBank:NM_145092]. Nevertheless, two related sequences (non-RefSeq sequences) were found in GenBank: U20286 (transcript 2), a transcript that lacks an N-terminal segment and U19614 (transcript 3), a transcript that lacks an internal segment (Figure III.2). Alignment of the rat LAP1 genomic sequence with the known rat LAP1B transcript, using the BLAST algorithm, revealed the presence of 10 exons (Fig. III.3). Taking into account the exon structure of rat LAP1 transcripts, we infer that U20286 has a truncated exon 1 in the N-terminal, while in the U19614 transcript, exon 5 was skipped.

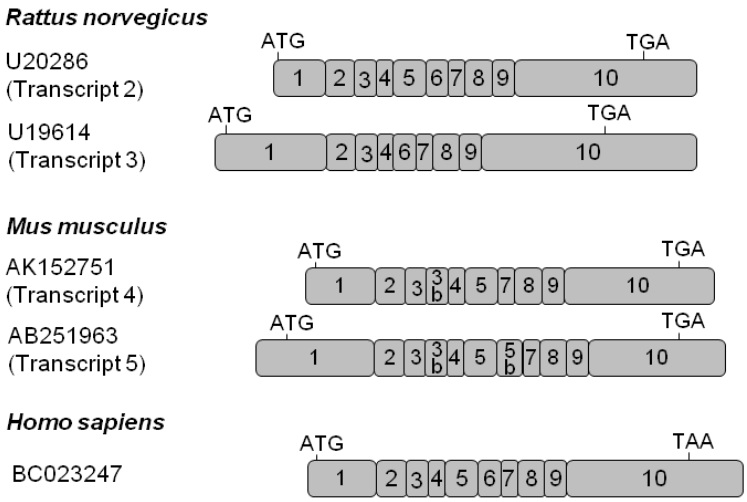

Figure III.3. Schematic representation of LAP1 non-RefSeq transcripts. The translation initiation codons (ATG) and the stop codons (TAA or TGA in human and mouse/rat sequences, respectively) are indicated in each transcript.

For mouse there are three RefSeq records corresponding to three different mouse LAP1 transcripts: transcript 1 [GenBank: NM_001160018] that represents the longest transcript; transcript 2 [GenBank: NM _144791] that is shorter than transcript 1 and lacks an internal segment; and transcript 3 [GenBank: NM_001160019] that represents the smallest transcript and lacks the N-terminus (Fig. III.2B). Additionally, we found other related sequences corresponding to two different mouse LAP1 transcripts in

GenBank: AK152751 (transcript 4), a transcript that lacks an N-terminal segment and AB251963 (transcript 5), a transcript that has an additional internal segment (Figure III.3). Alignment of the mouse LAP1 genomic sequence with the known transcripts revealed the presence of 12 exons (Fig. III.2). Taking into account the exon structure of mouse LAP1 transcripts, we showed that exon 7, 8 and 9 are absent in transcript 2. Transcript 3 lacks exon 1, but has an additional first exon, that we termed exon 1b. However translation is not initiated at the exon 1b, but exon 3 does have an in frame ATG, encoding for a protein with a different N-terminal. Transcript 4 has a truncated exon 1 in the N-terminal and transcript 5 has an alternative exon 5b that is not found in any of the other transcripts. Of note, the C-terminal (exon 10) seems to be the most conserved region among mouse LAP1 isoforms.

In order to predict alternative exons, which would lead to distinct human LAP1 isoforms, we aligned mouse LAP1 transcripts against the genomic sequence of the *TOR1AIP1 gene*, using BLAST algorithm. Further, we identified intron-exon junctions by comparing genomic and cDNA sequences and making use of *in silico* tools NNSPLICE and GENSCAN (Table III.1). The alignment revealed high identity between exons 1-5 and 7-10, while exon 6 of human gene does not align with any mouse transcript. Moreover, mouse transcripts have three different exons (that we termed 1b, 3b and 5b) that are not found in the human LAP1B transcripts. The alignment of mouse exons 1b and 3b against the human genomic sequence revealed the presence of putative alternative exons 1b and 3b in the human gene (Fig. III.2A). In the GenBank database, a human expressed sequence tag (EST) was found [GenBank: DB454036], which shares homology with exon 1b. Alignment of this EST with human genomic sequence also revealed the presence of an alternative exon, that we termed exon 2b (Fig. III.2B). This exon is not conserved in mouse or rat genomic sequences (Table III.1). In contrast, a human EST (GenBank: CX760895) encoding an exon with high homology with mouse exon 3b was found in the GenBank database. The splice sites of putative exon 2b and 3b are according to the consensus rules (GT/AG).

Table III.1. Intron/exon junctions in the *TOR1AIP1* gene.

	Intron 3'end	5'end – Exon size (bp) – 3'end	Intron 5'end
Exon 1			
Human		ACTGCCTC – 936 - CTCTGAAG	GTgaggac
Mouse		CGG*AG** - 723 - *CGCG***	**a*cagt
Rat		*AAA*ACA – 672 – *CGC*G**	**a*cagt
Exon 1b			
*Human		ATAGTTTG - 92 - TCGTGAAG	GTactgac
Mouse		GA*CAGGA – 137 – *TT**G*T	***ag**g
*Rat		AA*GAGGA – 136 - *TT**A*T	***ac**g
Exon 2			
Human	tttttttAG	AGGATGAA – 78 - GGCTCCAG	GTaagaat
Mouse	*gc*g***	******** – 75 - ****T***	*******g
Rat	*gc*a***	******** – 75 - *A**T***	*******t
Exon 2b			
*Human	ttctctAG	CTGCTGTA – 131 - AAAGAAGG	GTacttga
Mouse	–	–	–
Rat	–	–	–
Exon 3			
Human	tatattAG	CAGTGAGT – 60 - AAGATATG	GTaagaga
Mouse	**c*cc**	G*TGA*TG – 60 - ****CT**	******t*
Rat	**t*cc**	TGATG*GT – 60 - ****CC**	******g*
Exon 3b			
*Human	tcttgcAG	ATTCGACA – 45 - TTAATTAT	GTtcgttt
Mouse	****a***	****A*** – 45 – *G**AG*G	***t****
*Rat	ct*ata**	**C*A*** - 45 – GC*CAAGT	**GT**GC
Exon 4			
Human	tcttctAG	AAGCCACC – 42 - TGAAGAAG	GTatttta
Mouse	********	****T*CC – 39 – C*******	***a***c
Rat	********	*C**TT** - 39 – GC*GTTT*	***a***t
Exon 5			
Human	ctctttAG	GAGAAAAC – 87 - ATCTGGAG	GTaatatt
Mouse	*ct*g***	******C* - 81 – G**AA***	*****g**
Rat	*ct*g***	******C* – 81 – G***A***	****ca**
Exon 5b			
Human	–	–	–
Mouse	tggtttAG	ATGAAGCC - 56 - GCCACACA	GTtaagta
Rat	–	–	–
Exon 6			
Human	atttttAG	ATAAAACC – 57 - ATCACAAA	GTaagtaa
Rat	g****c**	**G**G** – 57 - *C****C*	*******c
Mouse	–	–	–
Exon 7			
Human	tgtttcAG	GTCAAAAC – 42 - AGTGCTAA	GTaagtag
Mouse	****ct**	A***GG** – 42 – *C****G*	******tc
Rat	****ct**	***GGGGG – 45 – *C****GC	******gc
Exon 8			
Human	tgcttcAG	GCTCAGGA – 69 - GATGCAAA	GTaagtag
Mouse	********	C******* - 69 – A***GCGT	********
Rat	********	C*A***** - 69 – A***GC*T	********
Exon 9			
Human	accattAG	ATGGCAGC – 57 - CAGCCGAC	GTaagttt
Mouse	tatt****	**AA**A* – 57 – ***G*C**	******c*
Rat	tatt****	**AA**A* – 57 – ***G*A*G	********
Exon 10			
Human	ctgagtAG	AAGTGACT – 2624 - ATACTCTC	
Mouse	*****c**	**TC*G** – 3111 - **GT*A*A	
Rat	*****c**	**GCAG** – 1547 - *AAG*T*T	

Nucleotides sequences of the 5' and 3' end of exons and the donor and acceptor sites at the intron/exon junctions (in upper case) of the human, mouse and rat *TOR1AIP1* genes are deduced from the *TOR1AIP1* genomic sequences. Sequences of intron ends are given in lower case, except for the donor and acceptor sites in upper case. Exons and introns are numbered as referred in Fig. III.1 and exon sizes are given. Homologies between human and mouse/rat sequences are shown by asterisks. Exon 1b and 3b in human and rat sequences and exon 2b in the human sequence are putative exons.

Additionally, search in Genbank database for human ESTs and alignments of detected human ESTs against the genomic sequence of human LAP1 was performed, in order to identify alternative exons. It was found that the 3' end of exon 8, exon 9 and the 5´end of exon 10 were skipped in one EST [GenBank: AU154882]. Furthermore, a non-RefSeq protein record [GenBank: EAW91067] that matches with this EST was found. Finally, several human ESTs (e.g. AL530866, BM907999, DA552747 and DA539545) and non-RefSeq mRNAs records (BC023247, AK023204 and AK021613) that lack the 5' end region of exon 1 were found in GenBank. These sequences lack the start codon present in LAP1B but have an additional in frame ATG, 363 nucleotides downstream of the first one (Fig. III.2A). This second in frame ATG is conserved between species (human, mouse and rat). Once more the analysis of the identified transcripts reveals that the C-terminal region of LAP1 transcripts remains highly conserved.

III.3.3.Analysis of LAP1 transcripts

III.3.3.1. RT-PCR

Given that two human LAP1 immunoreactive bands were detected (Fig. III.1) and since there is evidences that LAP1 isoforms are originated by alternative splicing (Fig. III.2), we went on to test if the smaller LAP1 transcript (putative LAP1C) has alternative exons, using RT-PCR. Briefly, cDNA was synthetized from adult brain poly A+ RNA using a reverse primer in the 3' UTR of exon 10 (E10RV) of human LAP1B or an oligo$(dT)_{20}$ primer that aligned with the poly A+ tail of mRNAs (Fig. III.4A). Subsequent amplification reactions were carried out using different primer pairs. The primer set E1FW (targeted to exon 1) and E10BRV (targeted to exon 10) amplified a fragment of 1.86 Kb (Fig. III.4B). This PCR fragment was ligated into the Nzy-blunt vector and the insert fully sequenced. Sequence results showed that the PCR fragment corresponds to the LAP1B transcript already described, as it was expected by its size. Given that only one fragment was amplified, using primers that aligned in exon 1 and 10, one can deduce that the N- or the C-terminal of the putative LAP1C transcript should be different. Additionally, and in order to exclude the possibility of internal alternative exons, the cDNA was also amplified using the following primer sets: E2FW (targeted to the boundary between exon 1 and 2) and E10BRV (targeted to exon 10); E5FW (targeted to exon 5) and E10CRV (targeted to an internal region of exon 10). The

first primer set (E2FW+E10BRV) used, generated a fragment of 1.34 kb (Fig. III.4C), which corresponds to the expected size of the transcript without alternative exons. Additionally, a larger fragment of 1.6 kb was also obtained which, after sequencing analysis, corresponded to an unspecific band. The second primer set (E5FW+E10CRV) used, generated a fragment of 0.58 kb (Fig. III.4D) that matched with the expected transcript without alternative exons. In addition, total RNA from SH-SY5Y cells was extracted and RT-PCR was perfomed using the oligo(dT)$_{20}$ primer. The synthesized cDNA was amplified using the primers E1FW and E10BRV and once more a single PCR fragment of 1.86 kb was obtained, corresponding to the LAP1B transcript (Fig. III.4E).

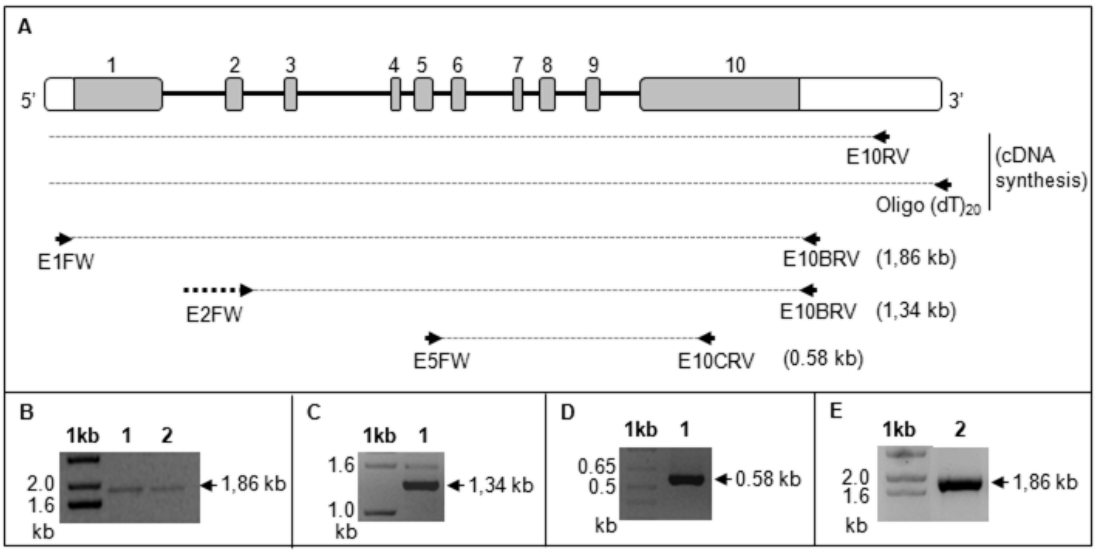

Figure III.4. RT-PCR of human LAP1. A- Localization of the primers used for RT-PCR on human *TOR1AIP1* gene. The cDNA was synthesized from adult brain poly A+ RNA (Clontech) (B, C and D) or SH-SY5Y cell total RNA (E) using a reverse primer targeted to exon 10 (E10RV) or an oligo(dT)$_{20}$ primer. Amplification of the cDNA was performed using specific primer pairs. **B-** cDNA amplification using primers E1FW (targeted to exon 1) and E10BRV (targeted to exon 10). **C-** cDNA amplification using primers E2FW (targeted to exon 1/2) and E10BRV (targeted to exon 10). **D-** cDNA amplification using primers E5FW (targeted to exon 5) and E10CRV (targeted to the middle of exon 10). **E-** cDNA amplification using primers E1FW (targeted to exon 1) and E10BRV (targeted to exon 10). 1kb, DNA size marker 1kb ladder (Invitrogen); 1, cDNA synthesized using E10RV primer; 2, cDNA synthetized using oligo(dT)$_{20}$ primer.

III.3.3.2. Northern Blot

The RT-PCR methodology did not produce a transcript corresponding to the putative LAP1C isoform, nor did it corroborate the presence of alternative exons that would lead to the translation of LAP1C. Consequently, in order to test whether different mRNAs or a single mRNA encodes LAP1 isoforms, Northern blot analysis was performed. If a single RNA is present, LAP1 isoforms could be generated by an alternative translation initiation mechanism, instead of alternative transcription. Hence, a probe was designed, directed against a region of exon 10 (span nucleotides 1602-2265) that is conserved in LAP1 isoforms. Total RNA from SH-SY5Y cells was isolated, given that this cell line expresses high levels of the putative LAP1C isoform (Fig. III.1B). Both undifferentiated and differentiated (with 10 µM retinoic acid for 4 days) SH-SY5Y cells were used to isolate total RNA. The results showed that the probe hybridized with two bands in both conditions (Fig. III.5). The higher band corresponds to the LAP1B transcript but appears to migrate slower than expected, bearing in mind its characterized mRNA size of 4.05 kb (GenBank: NM_001267578). The presence of a lower band is consistent with the existence of a second LAP1 transcript, corresponding to putative LAP1C transcript. Both RNAs appear to be of similar abundance in SH-SY5Y cells, which is not in direct proportion to the protein levels of LAP1B and putative LAP1C isoforms detected by immunoblotting. A probe directed to human β-actin was used as a control and hybridized to a single band bellow 3.7 kb (Fig. III.5), as expected.

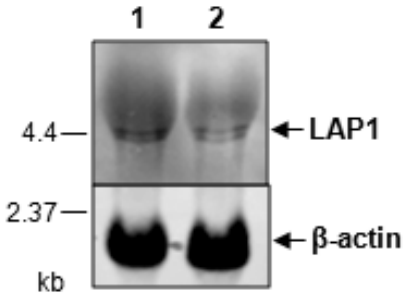

Figure III.5. Northern blot analysis of LAP1 RNAs in SH-SY5Y cells. A- Total RNA was isolated from SH-SY5Y cells and membranes hybridized with a biotinylated probe directed against exon 10 of LAP1. β-actin was probed as control. RNA size markers are depicted on the left. 1, RNA isolated from SH-SY5Y cells non-differentiated; 2, RNA isolated from SH-SY5Y celsl differentiated with retinoic acid.

Additionally, we showed that *in vitro* translation of LAP1B does not generate any low molecular weight protein, indicating that LAP1C is not generated by alternative translational initiation (Fig. III.6)

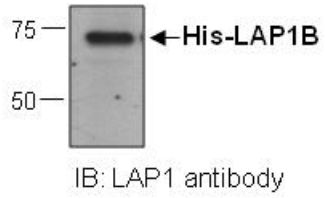

Figure III.6. *In vitro* translation (IVT) of LAP1B. IVT of pET-LAP1B generates only His-tagged LAP1B.

III.3.4. Identification of LAP1C isoform liquid chromatography-mass spectrometry

Northern blot analysis supported the existence of two LAP1 isoforms in human cell lines, but data was not as clear from the other methodologies, as described above. Thus, HPLC-MS analysis was employed. Two approaches were used for enrichment of LAP1 peptides. In the first procedure, membrane proteins from SH-SY5Y cells were enriched by centrifugation in 50 mM Tris-HCl buffer (insoluble fraction, pellet) and in the second, SH-SY5Y cell lysates were immunoprecipitated with the LAP1 specific antibody. SH-SY5Y total cell lysates were also employed for HPLC-MS analysis. All three samples were loaded on SDS-PAGE followed by Coomassie blue colloidal staining. The bands corresponding to LAP1B (68 kDa) and LAP1C (56 kDa) were excised and analyzed by HPLC-MS. Following careful excision, bands were tryptically digested, and the resulting peptides analysed in a nano-HPLC system online coupled to a Q Exactive mass spectrometer (Thermo Fisher Scientific, Germany). Overall, 80 unique peptides of LAP1B/LAP1C were identified, for all the conditions analysed. Immunoprecipitation of LAP1 and isolation of membrane proteins showed to be efficient techniques for the enrichment of LAP1 isoforms, since a large number of peptides were identified in comparison with the number of peptides identified from total cell lysates (Table III.2).

Table III.2. LAP1 peptides identified by mass spectrometry analysis.

	68 kDa band (LAP1B)			56 kDa band (LAP1C)		
Peptides	**Lysate**	**Membrane fraction**	**IP**	**Lysate**	**Membrane fraction**	**IP**
EGWGVYVTPR		x	x			
LAPQNGGSSDAPAYR			x			
FSDEPPEVYGDFEPLVAK		x	x			
LQQQHSEQPPLQPSPVMTR	x	x		x	x	x
LQQQHSEQPPLQPSPVMTRR					x	
DSHSSEEDEASSQTDLSQTISK		x	x			x
DSHSSEEDEASSQTDLSQTISKK			x			x
SIQEAPVSEDLVIR	x	x	x	x	x	x
RPPLRYPR				x	x	
VNFSEEGETEEDDQDSSHSSVTTVK		x	x	x		x
SSSQYIESFWQSSQSQNFTAHDK						x
QPSVLSSGYQK			x			x
TPQEWAPQTAR					x	x
TRMQNDSILKSELGNQSPSTSSR					x	
MQNDSILKSELGNQSPSTSSR				x	x	x
QVTGQPQNASFVK	x	x	x	x	x	x
QVTGQPQNASFVKR		x	x	x	x	x
NKYQGQDEKLWK				x	x	
SQPAILLLTAAR		x	x		x	x
SQPAILLLTAARDAEEALR				x	x	
IDGTDKATQDSDTVKLEVDQELSNGFK						x
ATQDSDTVKLEVDQELSNGFK		x	x		x	x
LEVDQELSNGFK			x		x	x
FESFPAGSTLIFYK		x	x		x	x
DVALVLTVLLEEETLGTSLGLK						x
FTNSNTPNSYNHMDPDKLNGLWSR					x	
ISHLVLPVQPENALKR	x	x		x	x	x
ISHLVLPVQPENALK	x	x		x	x	x
Nº peptides	5	13	14	11	18	19

Three different samples were analyzed by mass spectrometry analysis: total cell lysates, membrane containing-fraction and LAP1 immunoprecipitates (IP), as described in the methods section. Samples were loaded on SDS-PAGE, gels stained with Coomassie blue colloidal and 68 kDa and 56 kDa bands (corresponding to LAP1B and LAP1C, respectively) excised from the gel before mass spectrometry analysis. The different peptides identified are listed on the right and the presence of the peptides in each condition analyzed (lysate, membrane fraction or IP) is marked by an x. The number of peptides identified in each condition is also shown. In total, 80 unique peptides were identified, taking in account all conditions analyzed.

After comparison of all peptides, 28 different peptides of LAP1B/LAP1C were identified. Overall, only 3 peptides were specifically identified in the 68 kDa band (LAP1B) and 11 peptides were only found in the 56 kDa (LAP1C) band. However, all these 11 peptides also match with the known sequence of LAP1B (Table III.3). The overall sequence coverage was 47% for LAP1B and 75.3% for LAP1C. Since the LAP1C protein is more abundant in SH-SY5Y cells than LAP1B, it was expected that more peptides in the 56 kDa band (LAP1C) would be identified. Taking into account the exons boundaries of LAP1B represented in table 1, it is reasonable to conclude that the three unique peptides found in the LAP1B-containing bands correspond to the 5' end region of exon 1. Moreover, we identified peptides that aligned fully or partially with the 10 exons of LAP1B (Table III.3). Moreover, we identified a methionine at position 122, which is a few amino acids upstream of the location of the first peptide identified in the LAP1C-containing bands (Table III.3), indicating a potential start codon for LAP1C translation. This data is in agreement with GenBank AAH23247 sequence, in which the amino acid sequence was deduced by conceptual translation of the BC023247 mRNA sequence. When these values are compared with the expected molecular weight of LAP1 isoforms (Table III.4), one can conclude that the band migrating at 56 kDa is consistent with the existence of a LAP1 isoform with a truncated exon 1 (LAP1C). Therefore, the newly identified LAP1C has a shorter exon 1 when compared to LAP1B, generating an N-terminal truncated protein. Given its molecular weight similarity with rat LAP1C the authors propose that the new human LAP1 isoform should also have the designation LAP1C.

Table III.3. LAP1B and LAP1C peptides identified by liquid chromatography-mass spectrometry.

	Peptides	Position of peptides in the known LAP1B sequence
Peptides identified in the 68 kDa band (LAP1B)	EGWGVYVTPR LAPQNGGSSDAPAYR FSDEPPEVYGDFEPLVAK LQQQHSEQPPLQPSPVMTR DSHSSEEDEASSQTDLSQTISK DSHSSEEDEASSQTDLSQTISKK SIQEAPVSEDLVIR VNFSEEGETEEDDQDSSHSSVTTVK QPSVLSSGYQK QVTGQPQNASFVK QVTGQPQNASFVKR SQPAILLLTAAR ATQDSDTVKLEVDQELSNGFK LEVDQELSNGFK FESFPAGSTLIFYK ISHLVLPVQPENALK ISHLVLPVQPENALKR	1 magdgrraea vregwgvyvt prapiregrg rlapqnggss dapayrtpps rqgrrevrfs 61 deppevygdf eplvakersp vgkrtrleef rsdsakeevr esayylrsrq rrqprpqete 121 emktrrttrl qqqhseqppl qpspvmtrrg lrdshsse**E**d eassqtdlsq tiskktvrsi 181 qeap**A**vsedl virlrrpplr ypry**E**atsvq qkvnfsee**G**e teeddqdssh ssvttvkars 241 rdsdesg**D**kt trsssqyies fwqssq**S**qnf tahdkqpsvl **S**sgyqktpqe wapqtarirt 301 rmq**N**dsilks elgnqspsts sr**Q**vtgqpqn asfvkrnrww llpliaalas gsfwffstpe 361 vettavqefq nqmnqlknky qgqdeklwkr sqtflekhln sshprsqpai llltaardae 421 ealrclseqi adayssfrsv rairidgtdk atqdsdtvkl evdqelsngf kngqnaavvh 481 rfesfpagst lifykycdhe naafkdvalv ltvlleeetl gtslglkeve ekvrdflkvk 541 ftnsntpnsy nhmdpdklng lwsrishlvl pvqpenalkr gicl
Peptides identified in the 56 kDa band (LAP1C)	LQQQHSEQPPLQPSPVMTR LQQQHSEQPPLQPSPVMTRR DSHSSEEDEASSQTDLSQTISK DSHSSEEDEASSQTDLSQTISKK SIQEAPVSEDLVIR RPPLRYPR VNFSEEGETEEDDQDSSHSSVTTVK SSSQYIESFWQSSQSQNFTAHDK QPSVLSSGYQK TPQEWAPQTAR TRMQNDSILKSELGNQSPSTSSR MQNDSILKSELGNQSPSTSSR QVTGQPQNASFVK QVTGQPQNASFVKR NKYQGQDEKLWK SQPAILLLTAAR SQPAILLLTAARDAEEALR IDGTDKATQDSDTVKLEVDQELSNGFK ATQDSDTVKLEVDQELSNGFK LEVDQELSNGFK FESFPAGSTLIFYK DVALVLTVLLEEETLGTSLGLK FTNSNTPNSYNHMDPDKLNGLWSR ISHLVLPVQPENALK ISHLVLPVQPENALKR	1 magdgrraea vregwgvyvt prapiregrg rlapqnggss dapayrtpps rqgrrevrfs 61 deppevygdf eplvakersp vgkrtrleef rsdsakeevr esayylrsrq rrqprpqete 121 em[ ]ktrrttrl qqqhseqppl qpspvmtrrg lrdshsse**E**d eassqtdlsq tiskktvrsi 181 qeap**A**vsedl virlrrpplr ypry**E**atsvq qkvnfsee**G**e teeddqdssh ssvttvkars 241 rdsdesg**D**kt trsssqyies fwqssq**S**qnf tahdkqpsvl **S**sgyqktpqe wapqtarirt 301 rmq**N**dsilks elgnqspsts sr**Q**vtgqpqn asfvkrnrww llpliaalas gsfwffstpe 361 vettavqefq nqmnqlknky qgqdeklwkr sqtflekhln sshprsqpai llltaardae 421 ealrclseqi adayssfrsv rairidgtdk atqdsdtvkl evdqelsngf kngqnaavvh 481 rfesfpagst lifykycdhe naafkdvalv ltvlleeetl gtslglkeve ekvrdflkvk 541 ftnsntpnsy nhmdpdklng lwsrishlvl pvqpenalkr gicl

The peptides identified in the 68 kDa band (corresponding to LAP1B) and in the 56 kDa band (corresponding to LAP1C) are listed. The localization of those peptides (highlighted in grey) is shown in the amino acid sequence of the known LAP1B for comparative analysis. Amino acids located in exon boundaries are represented in upper case and underlined. A second methione, that may represent the translation start site of LAP1C, is boxed.

Table III.4. Human LAP1 transcripts and isoforms.

	Human LAP1 transcripts					
	LAP1B (variant 1)		LAP1B (variant 2)		LAP1C	
Exon	Total	Coding	Total	Coding	Total	Coding
1	936	475	693	475	NC	112
2	78	78	78	78	78	78
3	60	60	57	57	60	60
4	42	42	42	42	42	42
5	87	87	87	87	87	87
6	57	57	57	57	57	57
7	42	42	42	42	46	46
8	69	69	69	69	69	69
9	57	57	57	57	57	57
10	2624	785	2624	785	2624	785
mRNA size (bp)	4054	1752	4051	1749	> 3358	1386
	Human LAP1 isoforms					
Nº of amino acids	584		583		462	
Calculated MW (kDa)	66.3		65.6		52.5	
Migration in SDS-PAGE (kDa)	68		68		56	

Organization and exon size (bp) of the previously described LAP1B transcripts and the new LAP1C transcript is described. The number of amino acids, calculated molecular weight (MW) and MW inferred through migration in SDS-PAGE gel of LAP1 isoforms are also shown. NC, not confirmed. The full size of exon 1 and the mRNA of LAP1C was not confirmed.

III.3.5. Identification of a putative promoter in LAP1C sequence

This study clearly demonstrates that two LAP1 isoforms are present in human cells and are most likely generated by the translation of two different mRNAs. Therefore, the regulatory mechanism underlying the expression of two LAP1 isoforms may be due to the transcriptional regulation of LAP1. Therefore, we analyzed the genomic sequence of the first exon of the human *TOR1AIP1* gene in order to find putative alternative promoters that would lead to a downstream alternative transcription initiation and produce the smaller LAP1C transcript. NNPP and TSSG programs permitted the search for candidate promoters. These programs predicted a promoter in the region downstream of the translation initiation site of LAP1B and upstream of the translation initiation site of LAP1C (Fig. III.7). A putative TATA box was predicted 29 nucleotides downstream from the predicted transcription initiation site, using the TSSG program.

Furthermore, the region of the predicted transcription initiation site is conserved between species (Fig. III.7).

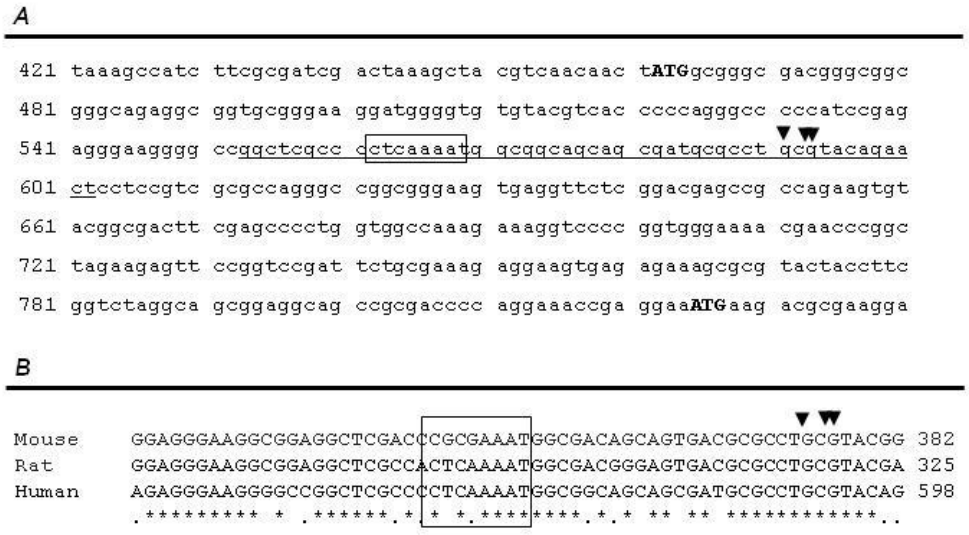

Figure III.7. Predicted promoter and alternative transcription initiation site of human LAP1C. A- Localization of a predicted promoter in the *TOR1AIP1* genomic sequence. The promoter region predicted using the NNPP program is underlined. The transcription initiation site predicted by the TSSG program is indicated by an arrow and the one predicted by the NNPP program is indicated by a double arrow. The putative TATA box predicted using the TSSG program is indicated by a box. **B-** Alignment of the predicted human promoter region with the homologous mouse and rat sequences.

III.3.6.Functional characterization of LAP1 isoforms

III.3.6.1. Solubilization properties of LAP1 isoforms

Analysis of the subcellular localization of different LAP1B deletion mutants demonstrated that only constructs with the whole nucleoplasmic domain were fully resistant to extraction with triton X-100. Deletion mutants containing only a part of the nucleoplasmic domain were extractable using this detergent (Kondo et al., 2002). Furthermore, it was also reported that most of rat LAP1C is solubilized using triton X-100 plus 100 mM NaCl, while LAP1A and LAP1B remain in the pellet (insoluble fraction) as well as lamins (Foisner and Gerace, 1993). Therefore, we went on to test if the human LAP1C isoform is less resistant to extraction from nuclear membranes using triton X-100 and increasing salt concentrations (NaCl). Our results showed that LAP1C is partially solubilized after triton X-100 addition, while LAP1B remains in the pellet (Fig. III.8). Furthermore, the majority of LAP1C is solubilized after extraction with triton X-100 plus 50 mM NaCl and it is not found in the pellet using high salt

concentration (500 mM). In contrast, LAP1B is only fully solubilized after extraction with triton X-100 plus 500 mM NaCl (Fig III.8). Lamin B1 and β-tubulin were used as controls. As expected, lamin B1 is found in the pellet fraction while β-tubulin is found in the supernatant in all conditions analyzed (Fig. III.8). There is just a minor amount of β-tubulin in the pellet fraction when neither triton nor NaCl are added. These results are in agreement with the fact that human LAP1C differs from LAP1B in the first exon located in the nucleoplasmic domain.

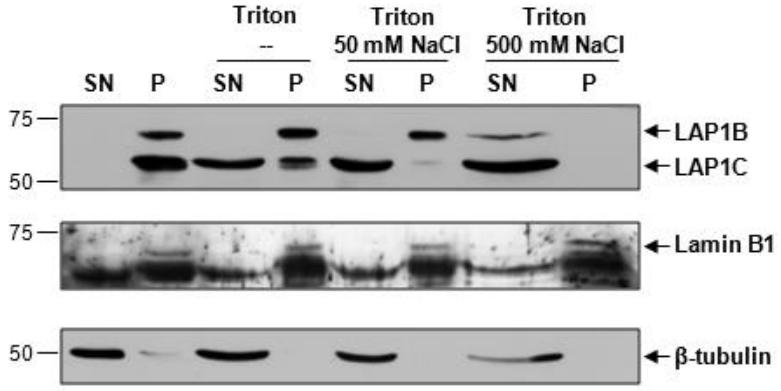

Figure III.8. Solubilization properties of human LAP1 isoforms. Solubilization of LAP1 in Tris-HCl buffer or Tris-HCl buffer containing 1% triton X-100, 1% triton X-100 and 50 mM NaCl or 500 mM NaCl. Equal fractions of supernatant (SN) and pellet (P) were loaded. IB, immunoblotting.

III.3.6.2. Cell and tissue specific expression pattern of LAP1 isoforms

It was previously reported that rat LAP1A is the major isoform identified in rat liver tissue, while LAP1C is highly expressed in cultured cells (Senior and Gerace, 1988). Therefore, immunoblotting with LAP1 antibody in human samples was performed, in order to establish if human LAP1 isoforms are differentially expressed in human cell lines and distinct tissues. In fact for the different human cell lines (HeLa, SKMEL-28 and SH-SY5Y cells, derived from a cervical cancer, skin melanoma and neuroblatoma, respectively) tested, LAP1C protein is more abundant than LAP1B (Fig. III.9A), in agreement with previous reports. In rat, LAP1C is the major isoform in the pheochromocytoma rat cell line PC12, while in rat cortex lysates, the ratio between LAP1C and LAP1B decreases (Fig. III.9A), although in the latter case expression of both isoforms is quite similar. In contrast, LAP1B and LAP1C expression profiles, in human tissues, appear to be dependent on the specific tissue (Fig. III.9B). LAP1C has

higher expression levels in lung, kidney and spleen, compared to LAP1B. In contrast, LAP1B is the major isoform present in liver, brain and heart, while in ovary, testis and pancreas the expression of both LAP1B and C is quite similar. An interesting aspect is the fact that in human brain, the expression of LAP1B is higher than LAP1C. Other bands appear in these blots and their significance deserves further attention.

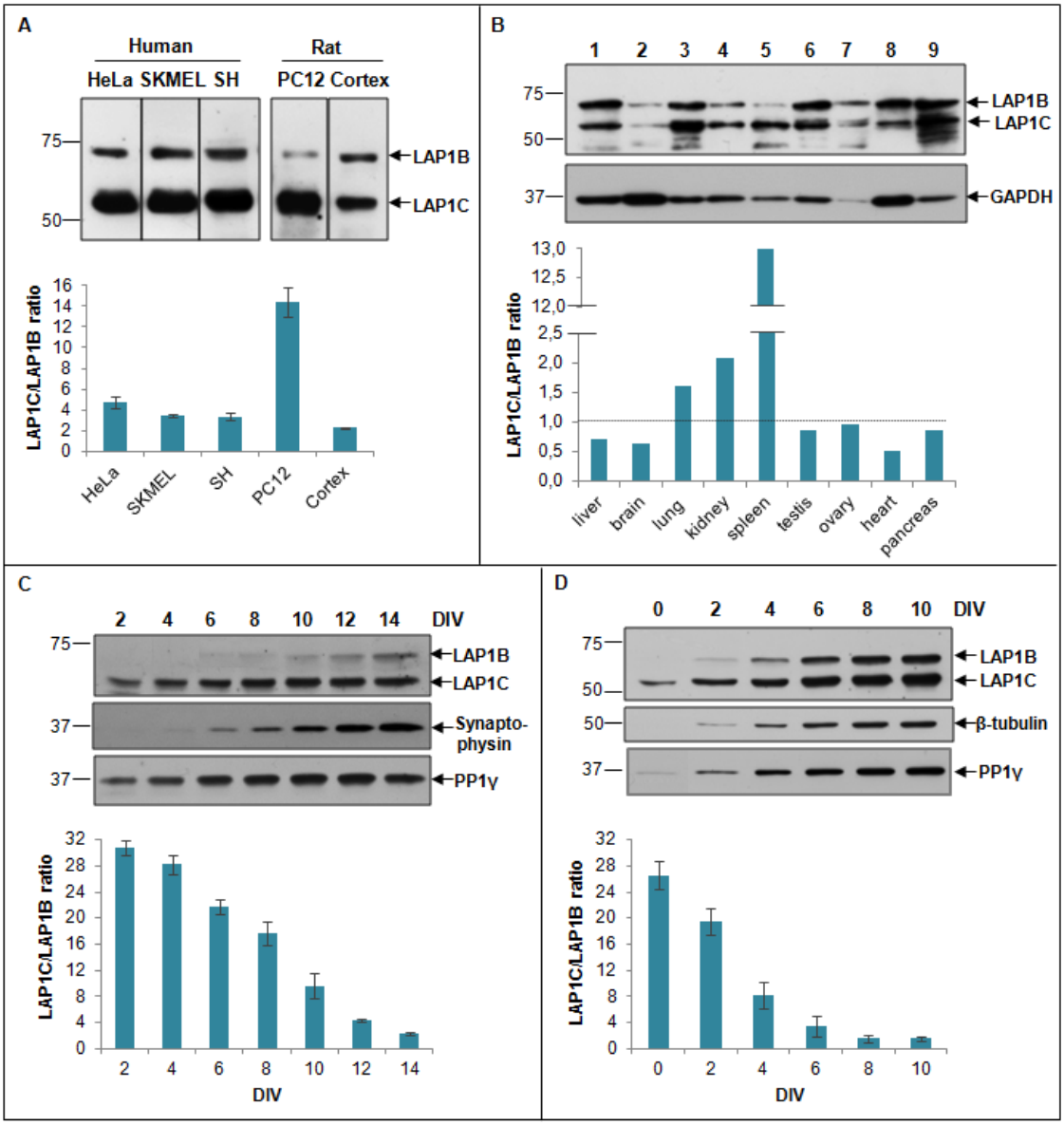

Figure III.9. **LAP1 expression in different cell lines and tissues**. **A-** Endogenous LAP1 isoforms were detected in HeLa, SKMEL-28 and SH-SY5Y human cells and in rat PC12 cell line and rat cortex lysates. **B-** Human tissue blot (Clontech) was immunoblotted with LAP1 antibody. 1, liver; 2, brain; 3, lung; 4, kidney; 5, spleen; 6, testis; 7, ovary; 8, heart, 9, pancreas. **C-** Endogenous expression of LAP1 isoforms was detected in primary cortical neurons for 14 DIV, using a LAP1 antibody. Synaptophysin and PP1γ were used as controls for expressing patterns **D-** Endogenous expression of LAP1 isoforms was detected in SH-SY5Y cells differentiated with retinoic acid for 10 DIV using a LAP1 antibody. β-tubulin and PP1γ were used as controls.

Previous reports suggested that the expression of the three mouse LAP1 isoforms seems to be developmentally regulated. By comparing the mouse P19 teratocarcinoma cell line and the differentiated P19MES line, mouse LAP1A and LAP1B were strongly expressed only in the differentiated cells, while LAP1C was found in both cell types (Martin et al., 1995). Therefore, we also analyzed the expression pattern of LAP1 isoforms during the establishment of cortical primary cultures for 14 days *in vitro* (DIV). Our data showed that LAP1B and LAP1C expression increases during neuronal development (Figure 7C). However, LAP1C expression in cortical neurons reaches a maximum a 10 DIV and remains almost constant thereafter. In contrast, LAP1B is expressed at very low levels until 10 DIV and increases over 14 DIV (Fig. III.9C). LAP1B is barely detected at 2 and 4 DIV, in comparative terms (longer exposure times will produce more intense bands). The pre-synaptic marker synaptophysin and PP1γ were used as controls. These results indicate that LAP1B is highly expressed in functional mature neurons since its intracellular levels correlate very well with synaptophysin levels, a pre-synaptic marker.

Similar results were obtained when SH-SY5Y cells were differentiated. Briefly, SH-SY5Y cells were plated at a density of 1 x 10^5 and grown for 10 days in MEM/F12 medium with 10% FBS in the presence of 10 μM retinoic acid. Under the experimental conditions tested, the expression of both LAP1B and LAP1C increased during differentiation (Fig. III.9D). However the increase of LAP1B levels were more marked than LAP1C levels, as demonstrated by the ratio between both proteins (Fig. III.9D) and its intracellular levels are high when the cells are differentiated. Of note, undifferentiated SH-SY5Y cells also express the LAP1B isoform and it was visible when membranes were exposed for longer periods of time.

III.3.7. Regulation of both isoforms by pos-translational modifications

We have recently reported that human LAP1B is dephosphorylated *in vitro* by PP1 (Santos et al., 2013). Protein phosphorylation is a crucial mechanism for signal transduction that regulates the biological activity of diverse proteins (Barford et al., 1998; Cohen, 1989). Thus, it is important to understand if human LAP1C is likewise regulated by protein phosphorylation and if PP1 is responsible for its dephosphorylation, as occurs with LAP1B. Hence we performed an assay similar to that previously reported by us and developed for LAP1B (Santos et al., 2013). Hence, SH-SY5Y cells were incubated with two different concentrations of OA (0.25 nM and 500 nM that inhibit PP2A and PP1/PP2A, respectively) and cell lysates were further incubated with 100 ng of recombinant purified PP1γ1 protein (Fig. III.10A). The results showed that after addition of purified PP1γ1 an increase in the migration of both LAP1 isoforms is detected (Fig. III.10A), consistent with the dephosphorylation of these proteins by PP1γ1. Therefore, it appears that both human LAP1B and LAP1C are desphosphorylated by PP1.

Further, HPLC-MS analysis unequivocally showed that both isoforms are regulated by protein phosphorylation. SH-SY5Y cells were incubated with 0.25 nM OA or 500 nM OA. A control, i.e. cells not treated with OA, was also included in the experiment. Then cells were lysed and immunoprecipitated with LAP1 specific antibody. Immunoprecipitates were loaded on SDS-PAGE and 68 kDa and 56 kDa bands (corresponding to LAP1B and LAP1C, respectively) were excised and subsequently analysed by nanoHPLC-MS in a Q Exactive mass spectrometer. In total, four phosphorylated residues (Ser216, Ser306, Ser310, and Thr221) were identified in the peptides resultant from digestion of LAP1C protein (Fig. III.10B). Since LAP1B protein sequence is equal to LAP1C, with the exception of a longer N-terminal, we infer that LAP1B could be also phosphorylated in the same residues. Thus, the numeration of the residues is relative to the human LAP1B protein sequence for comparative analysis. Peptides phosphorylated on Ser216 and Thr221 residues were identified in the control condition (without OA treatment) and also when PP1 was inhibited (500 nM OA treatment). Moreover, two additional residues, Ser 306 and Ser310, were found to be phosphorylated specifically in the latter condition (Fig. III.10B). These results demonstrated that PP1 is likely involved in the dephosphorylation of Ser306 and Ser310, since these residues were not found to be phosphorylated in the control

condition (without OA treatment) neither in the PP2A-inhibited condition (0.25 nM OA treatment). Further, membrane enriched fraction from SH-SY5Y cells, acquired as previously described, was also loaded on SDS-PAGE and the LAP1B and LAP1C bands analysed by HPLC-MS following the same procedures described above. This analysis resulted in the identification of one additional phosphorylated LAP1B/C residue: Ser143 (Fig. III.10B). From overall, we identified 5 different phosphorylated residues of LAP1B/C, but only Ser306 and Ser310 residues were associated with PP1 activity. Furthermore, Ser143, Thr221 and Ser310 residues are conserved between human, rat and mouse species while Ser216 and Ser306 are not conserved (Fig. III.10B).

Additionally, another post-translational modification of human LAP1B and LAP1C was identified by HPLC-MS. Three methionines (Met146, Met302 and Met553) were modified by the addition of oxygen (Fig. III.10B). None of these methionines serves as an initiation site for LAP1B or LAP1C proteins synthesis. Furthermore, Met146 residue is not conserved, but Met302 and Met553 residues are conserved between human, rat and mouse species (Fig. III.10B)

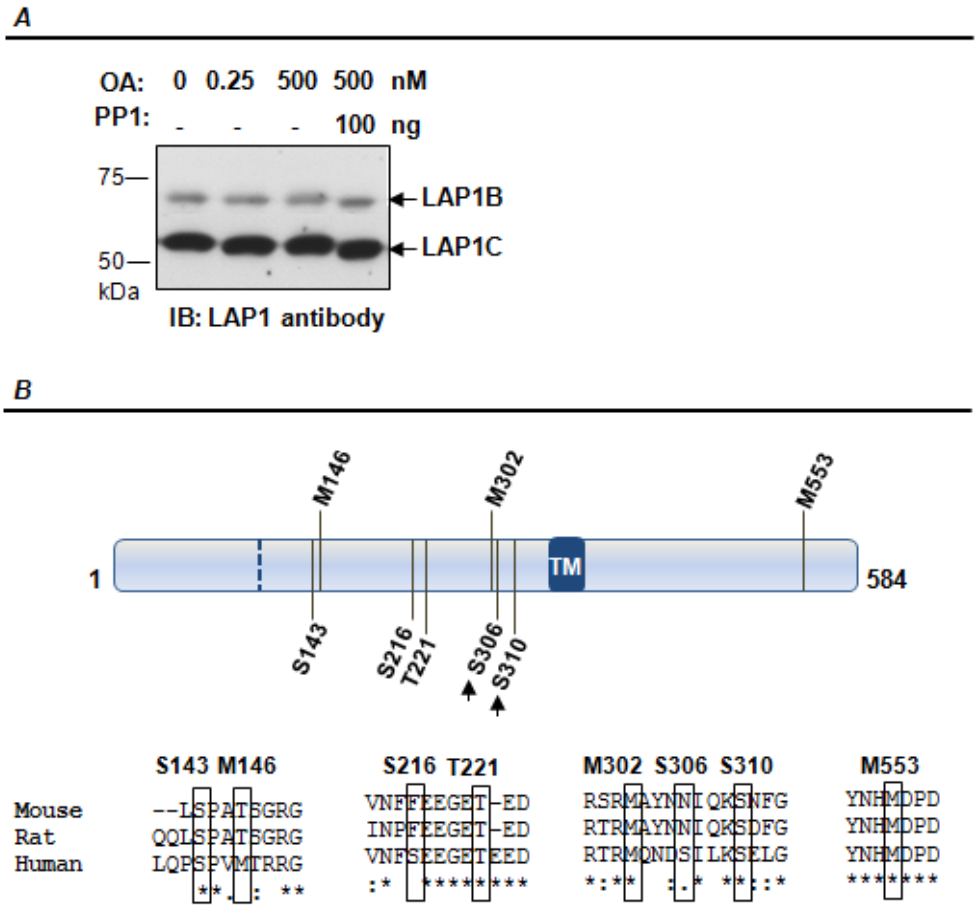

Figure III.10. Human LAP1 post-translational modifications. A- SH-SY5Y cells were incubated with 0, 0.25 or 500 nM okadaic acid (OA) for 3 hours. Lysates were incubated at 30ºC for 1 hour with or without 100 ng of PP1γ1 protein. **B-**. LAP1 isoforms are phosphorylated on Ser 143, Ser 216, Thr 221, Ser 306 and Ser 310 residues. PP1 was found to be responsible for Ser 306 and Ser 310 residues dephosphorylaton (indicated by arrows). Methionine residues 146, 302 and 553 residues were found to be oxidized. Post-translational modified residues and flanking regions were aligned against others species using Clustal Omega algorithm. The residues numeration is relative to the LAP1B sequence and the translation initiation site of LAP1C is indicated by a dashed line. IB, immunoblotting.

.

III.4. DISCUSSION

The work here presented permitted the identification of a novel LAP1 isoform (LAP1C) in human cells using a variety of methods and confirmed by HPLC-MS analysis. LAP1C has a short N-terminal domain, when compared to LAP1B. Furthermore it appears that human LAP1 isoforms (LAP1B and LAP1C) are regulated at the transcriptional level and can be subject to post-translational modifications, namely protein phosphorylation and methione oxidation. Additionally we established that PP1 mediates the dephosphorylation of LAP1C and B at Ser306 and Ser310 residues.

The genomic structure of *TOR1AIP1* genes from human, rat and mouse species is conserved. Indeed, human and rat *TOR1AIP1* genes have 10 conserved exons, while mouse has 12 exons in total and 9 exons present high identity compared to rat and human exons (Fig. III.1). Additional exons 1b, 3b and 5b were found in mouse transcripts. Alignment of these exons against the human and rat genomic sequences revealed the presence of putative alternative exons 1b and 3b in the respective genes. However, we were not able to identify alternative exons in human transcripts by RT-PCR (Fig. III.4). However, our *in silico* data suggest that potential new isoforms of LAP1 could be generated by alternative splicing. In eukaryotes, transcript variants arise from a combination of alternative transcription start sites selection, alternative splicing and differential usage of polyadenylation sites (Carninci et al., 2005). It was previously reported that rat LAP1 isoforms are generated by alternative splicing (Martin et al., 1995). In addition to alternative splicing, our data also suggests that alternative transcription start sites or alternative promoters could generate distinct LAP1 isoforms. We found non-RefSeq mRNAs and ESTs in GenBank that lack the 5´end region of exon 1, thereby they do not have the first translation start site present in the full-length exon 1- transcripts. This is common to the three species analyzed (human, rat and mouse). A significant number of genes use one or more alternative promoters. The usage of alternative promoters can induce alterations in the N-terminal of the protein coding sequence or create alternative ORFs, thereby potentiating the diversity of eukaryotic genome expression (Landry et al., 2003; Trinklein et al., 2003; Zhang et al., 2007). Moreover, alternative promoters are also functionally correlated with alternative

splicing. Thus alternative promoter usage and alternative splicing are two major mechanisms for increasing transcript diversity (Meshorer et al., 2004; Xin et al., 2008).

Although we were unable to produce an additional LAP1 human transcript by RT-PCR we showed that an alternative LAP1 transcript exists in human cells given that: (i) transfecting SH-SY5Y cells with two specific LAP1 shRNAs resulted in the knockdown of two LAP1 immunoreactive bands (68 and 56 kDa) (Fig. III.1); (ii) the lower band of 56 kDa has the same molecular weight as the rat LAP1C isoform; (iii) Northern blot analysis revealed the presence of two differently sized RNAs (Fig. III.5); (iv) alternative exons were found by *in silico* analysis. Furthermore and conclusively, the SDS-PAGE extracted 56 kDa protein (LAP1C), when analyzed by HPLC-MS, was shown to be 1 exon shorter when compared to LAP1B, thus generating an N-terminal truncated protein. A methionine at position 122 (relative to LAP1B sequence) was also identified, indicating a potential start codon for LAP1C translation (Table 3). The non-RefSeq mRNAs present in GenBank have different N-terminal sequences thus excluding the start codon used for LAP1B. Consistently, the downstream in frame start codon is present at position 122, in agreement with our HPLC-MS results. Moreover, the theoretical molecular weight of the identified LAP1C isoform (Table 4) is in agreement with the band of 56 kDa identified by immunoblotting using the LAP1 antibody.

Previous reports showed that deletion of a part of the nucleoplasmic domain of LAP1B increase the solubilization of this protein after detergent addition (Kondo et al., 2002). Hence, the resistance of the LAP1 isoforms (in particular LAP1C) to extraction from nuclear membranes was tested, using triton X-100 and increasing salt concentrations (NaCl). We demonstrated that LAP1C is more easily solubilized (Fig. III.8) than LAP1B, in agreement with the observation that human LAP1C differs from LAP1B in the 5´end region of the first exon located in the nucleoplasmic domain. Although it becomes clear that human LAP1 isoforms contain different N-termini, the origin of these proteins has to be established. The identification of two human LAP1 RNAs by Northern blot analysis and the existence of non-RefSeq mRNAs matching with the putative LAP1C sequence in GenBank, suggests that LAP1B and LAP1C are products of different RNAs and thereby their generation is regulated at the transcriptional level. Therefore, LAP1 isoforms could arise from alternative splicing or alternative promoter usage and consequently use an alternative transcription initiation site. Database searches for alternative promoters, identified an upstream putative LAP1C translation initiation site (Fig. III.7). Despite this, resolution of this question

will require additional experiments. Several reports showed that the 5' UTR region is shorter in certain mRNAs and arise via alternative splicing or activation of a downstream alternative promoter. Normally, this process leads to the increased synthesis of a specific protein, meaning that the translation of short 5' UTR mRNAs is more efficient in those cases. On the other hand, extension of the 5' UTR may provide a more complex and controlled regulation of gene expression (Charron et al., 1998; Han et al., 2003; Meshorer et al., 2004). It will also be interesting to understand the consequences in the lost of the N-terminal domain of LAP1C in protein-protein interactions. Previous reports suggested that rat LAP1C has a weaker interaction with the nuclear lamina in comparison with rat LAP1A and LAP1B (Foisner and Gerace, 1993; Senior and Gerace, 1988). Moreover, rat LAP1A and LAP1B were found to bind directly to lamins A, C and B1 *in vitro* and probably indirectly to chromosomes (Foisner and Gerace, 1993), while rat LAP1A/C was found to immunoprecipitate with B-type lamins (Maison et al., 1997).

We have recently reported that LAP1B is dephosphorylated *in vitro* by PP1 (Santos et al., 2013). Protein phosphorylation is a major signaling mechanism in eukaryotic cells that is able to regulate the biological activity of diverse proteins (Barford et al., 1998; Cohen, 1989), including proteins involved in pathological conditions (Fardilha et al., 2010; Rebelo et al., 2013; Rebelo et al., 2007; Vieira et al., 2010). In the work here described, the newly identified human LAP1C isoform was shown to be also dephosphorylated by PP1 (Fig. III.10). In addition, phosphorylation sites were mapped by HPLC-MS. Five phosphorylated residues were identified (Ser143, Ser216, Thr221, Ser306 and Ser310) in LAP1B/LAP1C and PP1 was shown to be associated with the dephosphorylation of two of these residues (Ser306 and Ser310, the numeration of the residues is relative to the human LAP1B protein sequence). Moreover, Ser143, Thr221 and Ser310 residues are conserved between the species analysed. Functional phosphorylation sites are more conserved during evolution than sites without characterized function (Landry et al., 2009). Therefore, it will be interesting to understand the effects of reversible protein phosphorylation on LAP1 function. In addition, we found that LAP1 is also post-translationally modified by methionine oxidation. Methionine is oxidized to methionine sulfoxide by the addition of an extra oxygen atom (methionine oxidation) and this process may function as a protein regulatory mechanism (reviewed in Kim et al., 2013).

LAP1 is ubiquitously expressed in neuronal and non-neuronal tissues (Goodchild and Dauer, 2005; Goodchild et al., 2005). Previous reports also showed that LAP1A, B and C are all detected in liver, spleen, brain and kidney rat tissues, but LAP1A seems to be the major isoform present in rat liver. In contrast, LAP1C is the major isoform found in rat cultured cells (Senior and Gerace, 1988). Our results are in agreement with previous data, since we detected higher expression of human LAP1C isoform in different cultured cells in comparison to LAP1B (Fig. III.9A). However, when we analyzed human tissues we found that the expression of LAP1B/LAP1C is dependent on the specific tissue (Fig. III.9B). Nevertheless, the human LAP1 isoform with higher molecular weight identified so far, LAP1B, is more abundant in liver than the smallest LAP1C isoform, in agreement with previous studies in rat liver tissue. Of particular interest is the profile of LAP1 expression in brain. LAP1 was found to interact with torsinA, the protein involved in the neurological disorder DYT1 dystonia. LAP1 is able to relocate torsinA to the NE, although the latter is normally found in ER (Goodchild and Dauer, 2005). The torsinA mutant form, which is present in DYT1 dystonia patients, is also primarily relocated to the NE (Goodchild and Dauer, 2004; Naismith et al., 2004). Therefore, it was suggested that abnormal accumulation of torsinA in the nuclear envelope may lead to a nuclear envelope dysfunction through LAP1 binding, thus contributing to DYT1 dystonia pathogenesis.

Furthermore, the expression of the LAP1 isoforms seems to be regulated during mouse spinal cord development and maturation (Goodchild et al., 2005). In order to understand if LAP1 isoforms are also differentially regulated in neuronal models, its expression profile during neuronal differentiation of SH-SY5Y cells (0-10 DIVs) (Fig. III.9D) and during maturation of rat cortical primary cultures (2-14 DIVs) (Fig. III.9C) was analyzed. Thus, we showed that in both models, LAP1C is already detected at 0/2 DIV while LAP1B is barely detected at this time point. However, the expression differences between LAP1C/LAP1B decrease during DIVs, which means that LAP1B is upregulated later when compared to LAP1C. Moreover, the expression of LAP1C is maintained at late DIVs while LAP1B continues to increase. Previous studies reported that LAP1A and LAP1B are strongly expressed in mouse liver cells and differentiated P19MES cells, while in mouse embryonic 3T3 cells and undifferentiated P19 cells LAP1A and LAP1B are barely detected. In contrast LAP1C is expressed in all cells (Martin et al., 1995). In our work, we provide a link between LAP1 expression and the state of neuronal differentiation of SH-SY5Y cells and maturation of neurons,

suggesting that LAP1 may play a role in those processes. It was previously reported that knockout of *TOR1AIP1* gene in mouse results in perinatal lethality and the nuclear membranes of various tissues and cultured neurons of those mouse embryos showed severe abnormalities (Kim et al., 2010a). Therefore, disturbances in the expression of LAP1 may compromise neuronal survival.

In conclusion, this is the first report of human LAP1C isoform recovery from human cells. Some related mRNA sequences have been already described in GenBank, however they were not identified as splice variants of human LAP1. Moreover, this work provides new insights with respect to *TOR1AIP1* genomic structure, potential transcripts and protein isoforms. Our data suggest that new potential human LAP1 isoforms could be generated by alternative splicing and deserve further investigation. We also showed that human LAP1B and LAP1C isoforms are differentially expressed and post-translationally regulated by protein phosphorylation and methionine oxidation. Finally, it was shown that PP1 is likely involved in the dephosphorylation of at least two LAP1B/LAP1C residues (Ser306 and Ser310).

CHAPTER IV - POTENTIAL ROLE OF LAP1 IN NUCLEAR ENVELOPE DYNAMICS

LAP1 was one of the first lamin associated proteins identified (Senior and Gerace, 1988), however its function remains poorly understood. Nevertheless, LAP1 is probably involved in the regulation of the NE structure and mitosis progression. Thus the work described in chapter IV provides particular insights with respect to the localization and phosphorylation state of LAP1 during the cell cycle and its importance for nuclear integrity and cell cycle progression. The results presented in this chapter provide a basis for future studies and will be submitted for publication in the *Molecular and Cellular Biochemistry* journal, and the manuscript (manuscript 3) is entitled: "Cell cycle progression is LAP1 dependent".

"Cell cycle progression is LAP1 dependent"

Mariana Santos[1], Patrícia Costa[1], Filipa Martins[1], Edgar F. Da Cruz e Silva[1], Odete A. da Cruz e Silva[1], Sandra Rebelo[1]

[1] Health Sciences, Centre for Cell Biology, Neuroscience Laboratory, University of Aveiro, Aveiro, Portugal

Abstract

Cell division in eukaryotes requires the disassembly of the nuclear envelope (NE) when cells enter mitosis and reassembly at the end of mitosis. These processes are complex and involve coordinated steps where NE proteins have a crucial role. Lamina associated polypeptide 1 (LAP1) is an inner nuclear membrane protein that is potentially associated with cell cycle-dependent events. In support of this role, LAP1 has been implicated in the regulation of the NE reassembly (Gerace and Foisner, 1994; Martin et al., 1995) and assembly of the mitotic spindle (Neumann et al., 2010) during mitosis. In this study, we demonstrated that LAP1 intracellular levels vary during the cell cycle in SH-SY5Y cells, and that LAP1 is highly phosphorylated during mitosis. We also observed that LAP1 co-localized with α-tubulin acetylated in the mitotic spindle and with γ-tubulin in centrosomes (main microtubule organizing center) in mitotic cells. Moreover, LAP1 knockdown resulted in decrease number of mitotic cells and decrease levels of α-tubulin acetylated (marker of microtubules stability) and lamin B1. These findings place LAP1 at a key position to participate in the maintenance of the NE structure and progression of cell cycle.

IV.1. INTRODUCTION

In eukaryotes, chromosomes are enclosed in the nucleus by the nuclear envelope (NE) that separates the nuclear content from the cytoplasm one. During mitosis, the NE remains intact ("closed mitosis") in organisms such as yeast, or is only partially disrupted at later stages of mitosis, as it happens in *Caenorhabditis elegans* and *Drosophila melanogaster*. In sharp contrast, in most higher eukaryotes, the NE is completely disassembled at the onset of mitosis and reassembled at the end of mitosis ("open mitosis"). Microtubules that form the mitotic spindle are exclusively cytoplasmic but have to come in contact with chromosomes for correct chromosome segregation during cell division. Thereby, NE breakdown allows the access of spindle microtubules to chromosomes (reviewed in Arnone et al., 2013; Foisner, 2003; Guttinger et al., 2009). The NE breakdown involves the disassembly of the nuclear pore complex (NPCs), depolymerization of lamins, and spreading of most NE soluble components and inner nuclear membrane (INM) proteins to the cytoplasm and ER networking, respectively. The NE is reassembled at the end of mitosis by the concentration of INM proteins and lamins on the decondensing chromatin, lamin polymerization and NPCs assembly (Guttinger et al., 2009; Moir et al., 2000).

One of the first lamin associated proteins identified was the lamina associated polypeptide 1 (LAP1) (Senior and Gerace, 1988), which is a type II transmembrane protein of the INM (Kondo et al., 2002; Martin et al., 1995). In interphase cells LAP1 is located at the INM in association with lamins and chromosomes. The interaction between LAP1 and lamins during the interphase might be important for targeting lamins to the NE and thereby contributing for the maintenance of the NE architecture. However, when the NE is disassembled during prometaphase, LAP1 seems to be redistributed through the ER, losing its association with chromosomes and lamins, thereby contributing to the NE breakdown. (Foisner and Gerace, 1993; Martin et al., 1995; Senior and Gerace, 1988; Yang et al., 1997). Moreover, it seems that LAP1 is regulated by protein phosphorylation during mitosis, as it happens for other nuclear proteins (Dephoure et al., 2008; Olsen et al., 2010). Protein phosphorylation represents a pivotal regulatory mechanism in diverse aspects of cell cycle progression (Bollen et al., 2009; Guttinger et al., 2009). More recently, Neumann *et al* reported that LAP1 may play a role in the the assembly of the mitotic spindle and consequently in mitosis

progression (Neumann et al., 2010). Nevertheless, the role of LAP1 during mitosis is not yet well defined.

In this study, the intracellular levels and localization of human LAP1 was analyzed in cell cycle-synchronized SH-SY5Y cells. Given that phosphorylation is a crucial regulatory mechanism for cell cycle progression, the phosphorylation state of human LAP1 was also evaluated. Moreover, we established a relation between LAP1 deficiency and decrease intracellular levels of acetylated α-tubulin which in turn correlates with decrease microtubules stability. This study provides a basis for a detailed analysis of the role of LAP1 in NE structure at interphase and dynamics during cell cycle.

IV.2. MATERIALS AND METHODS

IV.2.1. Antibodies

The primary antibodies used were rabbit polyclonal LAP1 (Goodchild and Dauer, 2005); mouse monoclonal α-tubulin (Zymed), mouse monoclonal acetylated α-tubulin (Sigma), mouse monoclonal γ–tubulin (Sigma), rabbit polyclonal lamin B1 (Santa Cruz Biotechnology) and histone H3 Ser10 (Genetex). The secondary antibodies used were anti-mouse and anti-rabbit horseradish peroxidase-linked antibodies (GE Healthcare) for ECL detection. Alexa 488-conjugated anti-mouse IgG and Alexa 594-conjugated anti-rabbit IgG (Molecular Probes) were used for the immunolocalization studies.

IV.2.2. Cell culture and cell cycle arrest

SH-SY5Y cells (ATCC CRL-2266) were grown in Minimal Essential Medium (MEM) supplemented with F-12 Nutrient Mixture (Gibco, Invitrogen), 10% fetal bovine serum (FBS, Gibco, Invitrogen), 1.5 mM L-glutamine, 100 U/mL penicillin and 100 mg/mL streptomycin (Gibco, Invitrogen). Cell cycle arrest at G0/G1 was achieved by removing serum from the culture medium for 48 hours. For synchronization in mitosis, SH-SY5Y cells were accumulated in prometaphase by adding 100 ng/ml nocodazole to complete medium for 18 hours. Cells were selectively harvested by mechanical shock, washed and resuspended in nocodazole-free medium for 30 minutes for expression and phosphorylation studies. For immunolocalization studies, cells were washed and nocodazole-free medium was added to let cell cycle to progress for 1h. After that period the SH-SY5Y cells were harvested or fixed using 4% paraformaldehyde and preceded for immunocytochemistry analysis.

IV.2.3. Immunocytochemistry

Once fixed as described above, SH-SY5Y cells were permeabilized with triton X-100 for 10 minutes, washed with PBS 1x and then blocked in 3% BSA/PBS 1x for 1 hour. Cells were incubated with the primary antibodies for 2 hours, followed by secondary antibodies for 1 hour. Preparations were washed with PBS, mounted using

Vectashield mounting media with DAPI (Vector). Preparations were visualized using an Olympus IX81 epifluoresence microscope (Olympus, Optical Co. GmbH) equipped with the appropriate filter combinations and a 100×objective (Plan-Neofluar, 100x/1.35 oil objective). Images were acquired with an F-view II CCD camera (Soft Imaging System GmbH, Münster, Germany) driven by Soft Imaging software. Alternatively, preparations were also visualized using an LSM510-Meta confocal microscope (Zeiss), as previously described (Rebelo et al., 2013; Santos et al., 2013).

IV.2.4. LAP1 knockdown

The knockdown of endogenous LAP1 in SH-SY5Y cells was achieved using a short hairpin RNA (shRNA) strategy as previously described (Santos, 2014). Briefly, SH-SY5Y cells were transiently transfected with both pSIREN-LAP1-C1 and pSIREN-LAP1-C2 plasmids or with the pSIREN-CMS (negative control).

IV.2.5. Protein phosphorylation analysis

Cellular lysates were resolved in 7.5% SDS-PAGE containing 50 μM Phos-tag (AAL-107, Wako) and 100 μM $MnCl_2$. After protein electrophoresis, Phos-tag acrylamide gels were washed with transfer buffer (25 mM Tris, 192 mM glycine and 20% methanol) containing 10 mM EDTA for 10 min to chelate $MnCl_2$ and then with transfer buffer without EDTA for 10 min according to the manufacturer's protocol.

IV.2.6. SDS-PAGE and immunoblotting

Samples were separated on SDS-PAGE and electrophoretically transferred onto nitrocellulose membranes. Nitrocellulose membranes were incubated in Ponceau S solution for 5 minutes and then scanned in a GS-800 calibrated imaging densitometer (Bio-Rad), in order to assess equal gel loading. Membranes were washed in TBST 1x to remove Ponceau S staining, followed by immunological detection with specific antibodies as indicated. Membranes were saturated in 5% non-fat dry milk in TBS-T and further incubated with primary antibodies. Detection was achieved using horseradish peroxidase-conjugated anti-rabbit or anti-mouse IgGs as secondary antibodies and proteins visualized by ECL (GE Healthcare).

IV.2.7. Quantification and Statistical Analysis

Autoradiograms were scanned in a GS-800 calibrated imaging densitometer (Bio-Rad) and protein bands quantified using the Quantity One densitometry software (Bio-Rad). Data were expressed as mean ± SEM of at least three independent experiments. Statistical significance analysis was conducted by Student's test, with the level of statistical significance being considered $P < 0.05$.

IV.3. RESULTS

IV.3.1. Intracellular levels and phosphorylation state of LAP1 during mitosis

A large number of genes are differentially expressed throughout the cell cycle (Cho et al., 2001; Shedden and Cooper, 2002). Interestingly, expression of genes encoding nuclear proteins (e.g. lamins) increases at the end of mitosis and beginning of G1 phase (van der Meijden et al., 2002). Moreover, cell cycle progression is tightly regulated by protein phosphorylation and several nuclear proteins were found to be highly phosphorylated specifically during mitosis (Dephoure et al., 2008; Olsen et al., 2010). Therefore, we tested if LAP1 is regulated in a similar manner. For that, SH-SY5Y cells were arrested in G0/G1 phase by incubation in serum-free medium for 48 hours and in mitosis by treatment with nocodazole for 18h, followed by incubation in nocodazole-free medium for additional 30 minutes. Firstly, we analyzed the intracellular levels of both human LAP1 isoforms (LAP1B and LAP1C) by immunoblotting using a specific LAP1 antibody (Goodchild and Dauer, 2005). Our results showed that the intracellular levels of both LAP1 isoforms were significantly higher in G0/G1-arrested cells (G0/1), compared to non-synchronized (NS) cells and mitosis-arrested cells (M; Fig. IV.1A). Moreover, opposite results were observed when cells were arrested in mitosis where significantly lower intracellular levels of both LAP1 isoforms were detected. The intracellular levels of LAP1 increased approximately 24% in G0/G1-arrested cells and decreases by 36% in mitosis-arrested cells when compared to NS cells (Fig. IV.1A). The cell cycle arresting in prometaphase using nocodozale was confirmed by detection of histone H3 phosphorylated at Ser10 (Fig. IV.1A), which was previously shown elevated during mitosis (Hendzel et al., 1997). Ponceau S staining was used as loading control (data not shown). Further, non-synchronized and synchronized SH-SY5Y cells were loaded on Phos-tag polyacrylamide gels in order to analyze the phosphorylation state of LAP1 proteins. In SDS-PAGE with polyacrylamide-bound Mn^2-Phos-tag, phosphorylated proteins are trapped by the Phos-tag sites, thus delaying their migration (Hosokawa et al., 2010; Kinoshita et al., 2006). Therefore, in Phos-tag SDS-PAGE, LAP1 was separated into multiple bands in non-synchronized and synchronized cells, indicating as expected that LAP1 is a multiphosphorylated protein (Fig. IV.1B). In fact, our previous report indicated that LAP1 is multiphosphorylated in NS cells (Santos, 2014). Moreover, an upward shift is visible in mitosis-arrested cells

(Fig. IV.1B). The two faster-migrating bands were barely detected in mitosis-arrested cells, while the other bands appear to have the same intensity of that seen in non-synchronized cells (Fig. IV.1B). In addition one slower-migrating band was detected in mitosis-arrested cells. Thus, our results showed that LAP1 was phosphorylated during both interphase and mitosis, but seems to be highly phosphorylated during mitosis, in agreement with previous reports (Dephoure et al., 2008; Olsen et al., 2010).

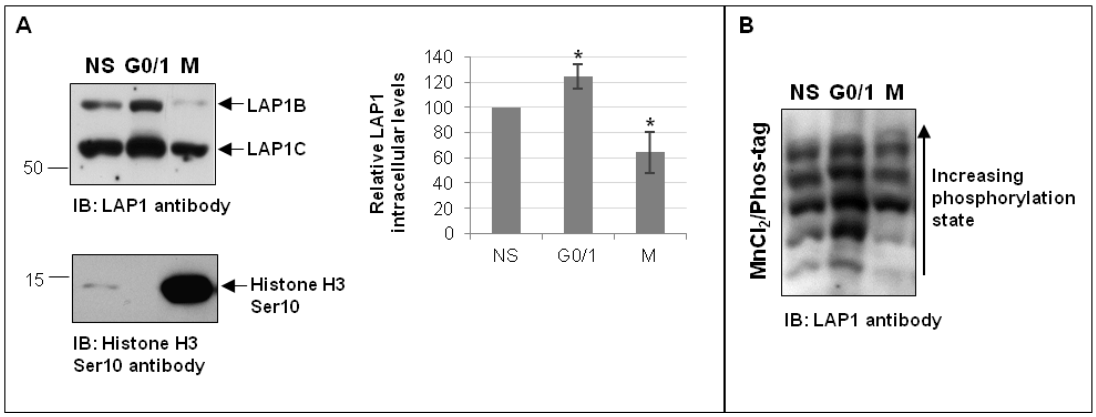

Figure IV.1. Detection of LAP1 proteins in cell cycle- synchronized cells**. A-** Quantification of LAP1B and LAP1C intracellular levels in NS cells, G0/1 and M-synchronized cells. Immunoblotting with histone H3 Ser10 antibody was performed to confirm mitosis arresting. Data are presented as mean ± SEM of at least three independent experiments. Statistically different from NS cells, * $p < 0.05$**. B-** Detection of phosphorylated LAP1 in non-synchronized (NS) cells, G0- and mitosis (M)- synchronized SH-SY5Y cells by the Phos-tag reagent. Proteins were separated in SDS-PAGE containing 50 µM Phos-tag and 100 µM MnCl2 or containing only MnCl2 for comparative analysis.

IV.3.2. Localization of LAP1 during mitosis

During mitosis, LAP1 is dispersed throughout ER membranes and is found in mitotic vesicles that associate transiently with the mitotic spindle (Maison et al., 1997; Yang et al., 1997). In this study, the distribution of human LAP1 during cell cycle was analyzed by immunofluorescence using a specific LAP1 antibody (Goodchild and Dauer, 2005) in the neuronal-like SH-SY5Y cells. Acetylated α-tubulin antibody was used to label the microtubules/mitotic spindle during mitosis. Our results showed that during interphase LAP1 localizes at the nuclear periphery in accordance with its known localization at the INM (Fig. IV.2). At metaphase, LAP1 is distributed throughout the cell in a punctuate pattern, excluding the chromosomal area, and this is also seen at anaphase and initial stages of telophase. In some points, LAP1 co-localized with

acetylated α-tubulin in the mitotic spindle and also in the mid-body (Fig. IV.2), in agreement with previous reports (Maison et al., 1997). At late telophase, LAP1 is clearly detected encircling the chromosomes (Fig. IV.2), even when chromosomes are still not decondensed.

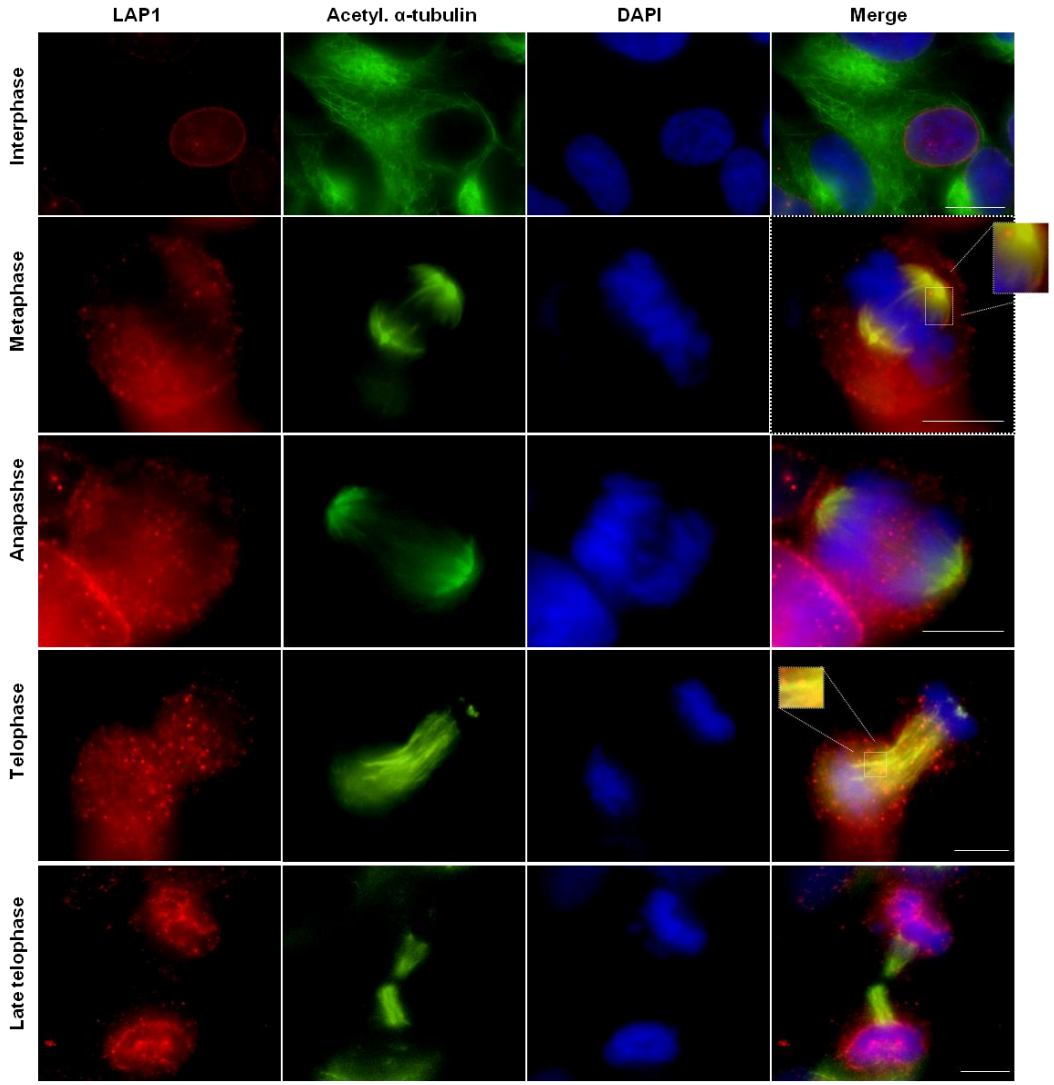

Figure IV.2. Immunolocalization of LAP1 during cell cycle in SH-SY5Y cells. Acetylated α-tubulin (α-tubulin acet.) labels the microtubules/mitotic spindles. Specific primary antibody for endogenous LAP1 was detected with Alexa Fluor 594-conjugated secondary antibody (red) and α-tubulin acetylated was detected with Alexa Fluor 488-conjugated secondary antibody (green). DNA was stained with DAPI (blue). The higher magnification view shows in more detail the co-localization of LAP1 and acetylated α-tubulin in the mitotic spindle. Photographs were acquired using an Olympus epifluoresence microscope. Bars, 10 µm.

Additionally, we performed imunofluorescence analysis using an antibody against γ-tubulin, a marker for centrosomes. The results showed that a fraction of LAP1 co-localize with γ-tubulin in centrosomes during metaphase and anaphase (Fig. IV.3).

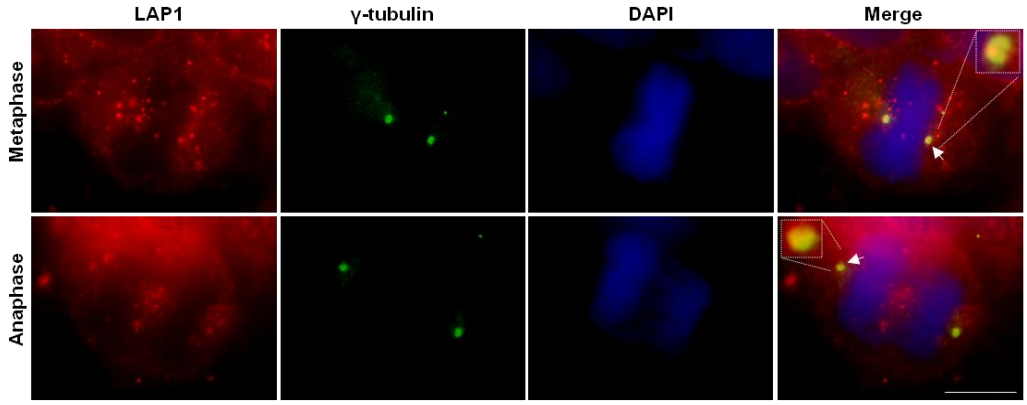

Figure IV.3. Co-localization of LAP1 and γ-tubulin during mitosis in SH-SY5Y cells. γ-tubulin labels the centrosomes. Specific primary antibody for endogenous LAP1 was detected with Alexa Fluor 594-conjugated secondary antibody (red) and γ-tubulin was detected with Alexa Fluor 488-conjugated secondary antibody (green). DNA was stained with DAPI (blue). The higher magnification view shows in more detail the co-localization of LAP1 γ-tubulin in centrosomes. Photographs were acquired using an Olympus epifluoresence microscope. Bars, 10 μm.

IV.3.3. Effects of LAP1 knockdown

During mitosis, LAP1 has been implicated in the assembly of the mitotic spindle (Neumann et al., 2010) and in the reassembly of the NE; the latter mainly due to the association with chromosomes at the end of mitosis (Gerace and Foisner, 1994; Martin et al., 1995). However, the specific role of LAP1 association with microtubules/mitotic spindle was not yet established. In order to determine the functional impact of LAP1 and alpha-tubulin association, LAP1 was down regulated in SH-SY5Y cells using specific LAP1-shRNAs. Cells were transfected with two different LAP1-shRNAs (pSIREN-LAP1 plasmids) or with the negative control, the pSIREN-CMS plasmid. Then immunofluorescence analysis was performed using LAP1 and acetylated α-tubulin antibodies and DAPI (nuclear marker) to monitor cell cycle phases. Microscopic visualization of LAP1-negative and –positive labeled cells, leads us to confirm that LAP1 levels were reduced by 36%. Afterward, we analyzed and count mitotic cells in pSIREN-CMS and pSIREN-LAP1 transfected cells. The results showed that the percentage of mitotic figures in control cells is about 3.39% but this number decreases

to 2.37% in LAP1-deficient cells (Fig. IV.4A). This mean that the number of mitotic cells significantly decrease (around 30% less) after LAP1 knockdown. Moreover, the nucleus of LAP1-negative labeled interphase cells presented an abnormal morphology (Fig. IV.4B). The distribution of acetylated α-tubulin was also altered in those cells. Acetylated α-tubulin was either concentrated around the nucleus or barely detected (Fig. IV.4B), thus suggesting that the levels of acetylated α-tubulin decreased in LAP1-depleted cells. In addition, the effects of LAP1 knockdown were analyzed by immunoblotting. Since the nuclei of LAP1-depleted cells have abnormal morphology, we performed immunoblotting with lamin B1 antibody to infer about nuclear lamina integrity. Our results showed that LAP1 knockdown lead to decrease levels of lamin B1 (approximately 33%). In agreement with immunofluorescence observations, we also showed that LAP1-deficient cells presented lower levels of acetylated α-tubulin, thereby resulting in a decrease of approximately 27% in the ratio acetylated α-tubulin/total tubulin (Fig. IV.4C). Moreover, the levels of histone H3 phosphorylated at Ser10 were reduced approximately 41% in LAP1-deficient cells (Fig. IV.4C), in agreement with the lower number of mitotic cells detected by microscopic visualization (Fig. IV.4A).

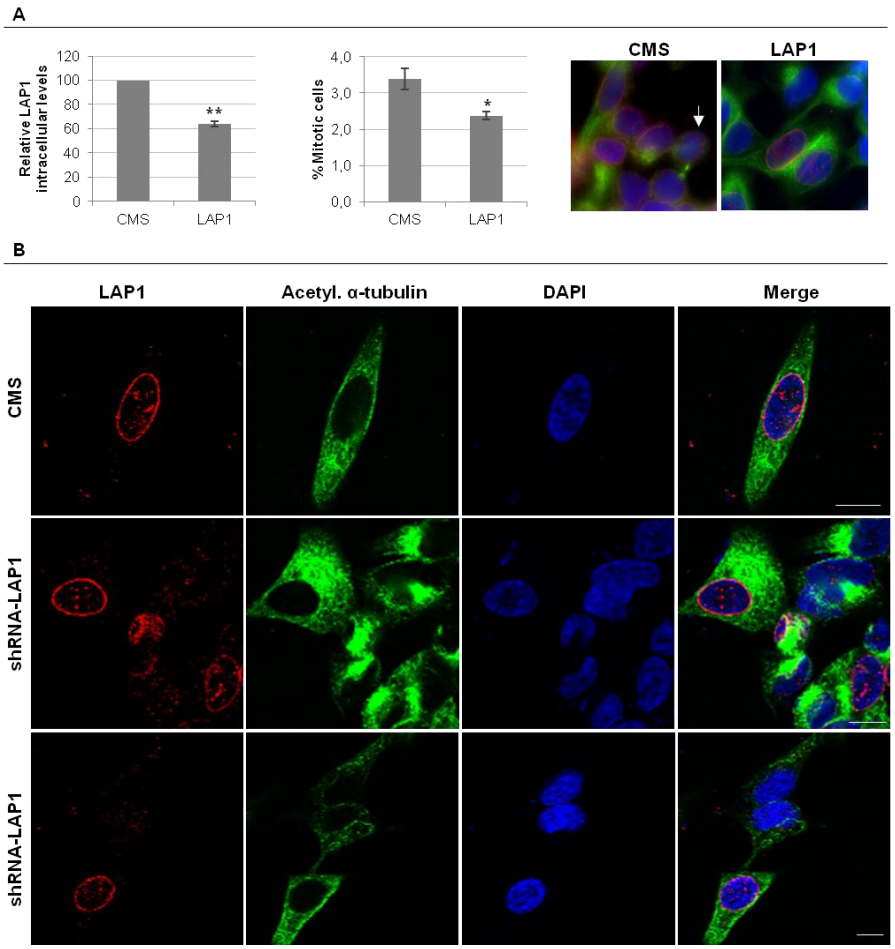

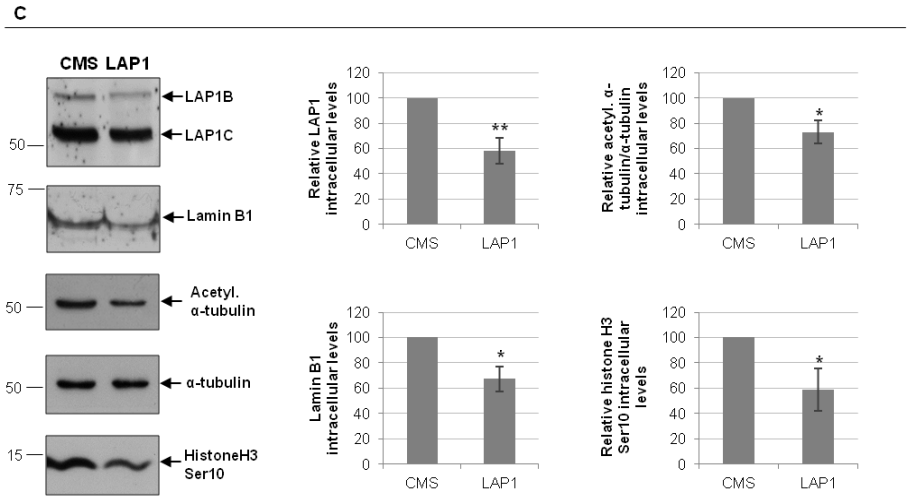

Figure IV.4. Effects of shRNA knockdown of human LAP1. SH-SY5Y cells were transfected with two specific LAP1 shrnas (LAP1) or a control missense shRNA (CMS) **A-** Analysis of the number of cells in mitosis after LAP1 knockdown. The analysis of LAP1 expression (on the left) and % of mitotic cells (on the right) was performed by microscopic visualization. Representative microscopic images are also shown. The arrow indicates the presence of a mitotic figure. **B-** Microscopic visualization of shRNA-LAP1 and CMS transfected cells. Specific primary antibody for endogenous LAP1 was detected with Alexa Fluor 594-conjugated secondary antibody (red) and α-tubulin acetylated was detected with Alexa Fluor 488-conjugated secondary antibody (green). DNA was stained with DAPI. Photographs were acquired using a LSM 510-Meta confocal microscope. Bars, 10 µm**. C-** Analysis of the expression of acetylated α-tubulin/total tubulin ratio, lamin B1 and histone H3 phosphorylated at Ser10 in LAP1-deficient cells by immunoblotting. Data are presented as mean ± SEM of at least three independent experiments. Statistically different from CMS transfected cells, $^{*}p < 0.05$, $^{**}p < 0.01$.

IV.4. DISCUSSION

LAP1 was one of the first lamin associated proteins identified (Senior and Gerace, 1988), however its function remains poorly understood. Despite that, LAP1 has been implicated in the regulation of the NE reassembly (Gerace and Foisner, 1994; Martin et al., 1995) and assembly of the mitotic spindle (Neumann et al., 2010) during mitosis. In this study, we used the neuronal-like SH-SY5Y cells as a model to study the intracellular levels and potential role of human LAP1 during mitosis. Our results revealed that LAP1 is differentially expressed in SH-SY5Y cells during the cell cycle. LAP1 expression is reduced in mitosis-arrested cells, whereas is upregulated in G0/G1-arrest cells after serum deprivation (Fig. IV.1A). Several genes are differentially expressed throughout cell cycle, thereby contributing to the regulation of specific processes (Cho et al., 2001; Shedden and Cooper, 2002). In agreement with our findings, genes encoding nuclear proteins, such as lamins, were found to be upregulated at the end of mitosis and beginning of G1 phase (van der Meijden et al., 2002). These facts underline the importance of LAP1 and other nuclear proteins for the regulation of NE synthesis at the end of mitosis. Furthermore, the association of LAP1 with chromosomes at late anaphase/telophase may contribute to the NE reassembly, possibly by targeting lamins and membrane vesicles to chromosomes surface and/or anchoring chromatin to the NE (Gerace and Foisner, 1994; Martin et al., 1995). Others INM proteins such as LBR, emerin and LAP2 were also found to accumulate on the surface of chromatin during anaphase/telophase *in vivo* (Foisner and Gerace, 1993; Haraguchi et al., 2000). Thus, the binding of INM proteins to chromatin accompanies NE assembly at the end of mitosis, while dissociation is required for NE breakdown.

NE breakdown and reassembly are complex processes that require the action of several cellular activities such as reversible protein phosphorylation (Bollen et al., 2009; Guttinger et al., 2009). Our results also showed that LAP1 is regulated by phosphorylation during both interphase and mitosis, but seems to be highly phosphorylated during mitosis (Fig. IV.1B). Indeed, it was previously shown that several nuclear proteins are highly phosphorylated during mitosis (Dephoure et al., 2008; Olsen et al., 2010). Nevertheless, LAP1 could be (de)phosphorylated in a cell cycle-dependent manner at specific residues, as it happens with lamins. Phosphorylation of lamins at different residues might play specific roles throughout the cell cycle. For example, phosphorylation of lamin B2 at Ser17 is specifically involved in lamin

depolymerization and NE disassembly (Kuga et al., 2010). Nevertheless, it has been accepted that phosphorylation of lamins is an important mechanism for lamin depolymerization when the NE is disassembled, whereas dephosphorylation leads to lamin polymerization and the end of mitosis (Thompson et al., 1997). Recently, we have reported that LAP1B is dephosphorylated by PP1 (Santos et al., 2013), a phosphatase that is responsible for the dephosphorylation of several proteins in association with cell cycle events (Bollen et al., 2009). Another interesting fact is that phosphorylation can abolish the binding of INM proteins, such as LBR and LAP2β, to chromatin (Foisner and Gerace, 1993; Pyrpasopoulou et al., 1996; Takano et al., 2004). Thus, the effects of LAP1 (de)phosphorylation on chromatin binding and its role on NE dynamics should be addressed.

Furthermore, one report uncovered a potential function for LAP1 in the assembly of the mitotic spindle (Neumann et al., 2010). Downregulation of LAP1 led to the formation of defective mitotic spindles and thereby aberrant mitotic exit and cell death (Neumann et al., 2010). Defects in mitotic spindle integrity can affect the stability of microtubules and therefore the levels of microtubules acetylation. In this study, we were not able to identify defective mitotic spindles; however we observed a decrease in the number of mitotic figures after LAP1 knockdown (Fig. IV.4A), concomitant with decrease phosphorylation of histone H3 at Ser10. Histone H3 phosphorylation has been correlated with chromosome condensation during mitosis (Hendzel et al., 1997). Therefore, decrease number of mitotic figures could be result of the inhibition of cell cycle progression to the mitosis phase. Moreover, we showed that LAP1 co-localize with acetylated α-tubulin in the mitotic spindle and mid-body (Fig. IV.2), and also co-localize with γ-tubulin at some points in centrosomes (Fig. IV. 3), the main microtubule organizing centre. Maison *et al* reported that LAP1C and lamin B colocalize in mitotic vesicles that associate transiently with the mitotic spindle (Maison et al., 1997), however the localization of LAP1 in centrosomes has never been shown. Interestingly, emerin and the novel INM protein SAMP1 are involved in centrosome positioning and connection to the NE (Buch et al., 2009; Salpingidou et al., 2007).

Additionally, depletion of LAP1 also affected the levels of tubulin acetylation, lamin B1 and the morphology of the nucleus in interphase cells (Fig. IV.4B and C). Decrease levels of tubulin acetylation could be result of microtubules instability due to disruption of NE integrity. Cytoskeleton elements as tubulin are connected to the NE

through interaction with nesprins (proteins of the ONM), binding partners of SUN proteins in the INM, which is turn bind to lamins, thereby forming the LINC complex (Crisp et al., 2006; Haque et al., 2006). Depletion of LAP1 from the INM may cause disruption of protein interactions at the NE and loss of the LINC complex, and thereby lead to a deregulation of microtubules dynamics. In a similar manner, it was previously reported that lamin A/C depletion lead to the disturbance of actin, vimentin and tubulin organization (Broers et al., 2004). Interestingly, mutations in some genes encoding NE proteins cause different NE-related diseases, often associated with reduced expression levels of those proteins (reviewed in Dauer and Worman, 2009). Currently, disease associated-LAP1 mutations have not been reported. Nevertheless, Kim *et al* reported that various tissues and cultured neurons of *TOR1AIP1* knockout mice embryos exhibit NE abnormalities and these mice usually dye on the last prenatal day or first postnatal day (Kim et al., 2010a). More recently, LAP1 was found to interact with the INM protein emerin. Emerin loss of function causes X-linked Emery-Dreifuss muscular dystrophy in humans. Similarly, conditional depletion of LAP1 from mouse striated muscle causes muscular dystrophy leading to early lethality (Shin et al., 2013). Furthermore, LAP1 has been associated with DYT1 dystonia due to its interaction with torsinA (Goodchild and Dauer, 2005). The NE of torsinA null fibroblasts is normal, but reducing LAP1 levels in those cell causes NE abnormalities, thus suggesting that these proteins are functionally related (Kim et al., 2010a). Therefore, several evidences suggest that LAP1 is a crucial protein for the maintenance of the NE structure and regulation of cell-cycle dynamics.

CHAPTER V - NOVEL INSIGHTS INTO DYT1 DYSTONIA PATHOPHYSIOLOGY BASED ON TORSINA

TorsinA is primarily located in the endoplasmic reticulum (ER) lumen and nuclear envelope (NE), while the DYT1 dystonia mutant (ΔE-torsinA) is abnormally concentrated in the NE (Gonzalez-Alegre and Paulson, 2004; Goodchild and Dauer, 2004; Naismith et al., 2004), where it interacts with LAP1 (Goodchild and Dauer, 2005). The accumulation of ΔE-torsinA causes NE abnormalities, presence of inclusions and seems to affect the cytoskeleton structure (Gonzalez-Alegre and Paulson, 2004; Goodchild et al., 2005; Hewett et al., 2000; Nery et al., 2008). Therefore, the work described in chapter V was designed so as to provide novel insights into DYT1 dystonia pathophysiology based on torsinA.

Chapter V is subdivided in three sections. In section V.A., the distribution of wt-torsinA and ΔE-torsinA in non-neuronal and neuronal cells was analyzed, with the intent of choosing an adequate DYT1 dystonia cellular model. The aim of section V.B. was to evaluate the effects of ΔE-torsinA overexpression in cytoskeleton dynamics. Finally, the aim of section V.C. was to validate and characterize the interaction between PP1, LAP1 and torsinA. Two of these sections (V.B and V.C) are being prepared as manuscripts for publication.

Section V.A.:
"Characterization of DYT1 dystonia cellular models"

Section V.B. (Manuscript 4):
"DYT1 dystonia-associated mutant affects cytoskeletal dynamics", submitted for publication in the *Microscopy and Mycroanalysis* journal.

Section V.C. (Manuscript 5):
"Protein phosphorylation regulates a novel torsinA trimeric complex", will be submitted for publication in the *Frontiers in Cellular Neuroscience* journal.

CHAPTER V.A – CHARACTERIZATION OF DYT1 DYSTONIA CELLULAR MODELS

Mariana Santos[1], Sandra Rebelo[1], Edgar F. da Cruz e Silva[1], Odete A. da Cruz e Silva[1]

[1] Health Sciences, Centre for Cell Biology, Neuroscience Laboratory, University of Aveiro, Aveiro, Portugal

Abstract

TorsinA is the central protein in DYT1 dystonia, since a mutation of one glutamic acid within the C-terminal of this protein (ΔE302/303, also referred to as ΔE) was found in most cases of DYT1 dystonia. Wt-torsinA protein is primarily located in the endoplasmic reticulum (ER) lumen and nuclear envelope (NE), while ΔE-torsinA protein is abnormally concentrated in the NE. However, the ΔE-torsinA cellular phenotype appears to be specific to neuronal cells. Therefore, in order to establish an adequate cellular model for the study of DYT1 dystonia, we analyzed the distribution of wt- and ΔE-torsinA in non-neuronal cells (COS-7) and neuronal-like cells (SH-SY5Y). Our results suggest that ΔE-torsinA is specifically enriched in the NE in neuronal cells, in agreement with previous reports. Thus, the SH-SY5Y cell line will be used as a DYT1 dystonia cellular model to study the molecular and cellular mechanisms associated with ΔE-torsinA mutation.

V.A.1. INTRODUCTION

TorsinA and its related family members belong to the ATPases associated with a variety of cellular activities (AAA^+) superfamily. TorsinA has been the most studied torsin family member because of its association with DYT1 dystonia. A mutation of a single glutamic acid within the C-terminal of torsinA (ΔE302/303, also referred to as ΔE) was found in most cases of DTY1 dystonia (Ozelius et al., 1997). TorsinA is primarily located in the ER lumen and NE, while ΔE-torsinA is abnormally concentrated in the NE (Gonzalez-Alegre and Paulson, 2004; Goodchild and Dauer, 2004; Naismith et al., 2004). Neurons from ΔE-torsinA knockin mice present severe NE abnormalities and vesicles in the lumen of the NE, although non-neuronal cells appears to be normal (Goodchild et al., 2005). Indeed, Giles *et al* reported that the accumulation of ΔE-torsinA in the NE may be specific for neuronal cells (Giles et al., 2008). At the NE, torsinA was found to interact with LAP1 (Goodchild and Dauer, 2005), SUN1 (Jungwirth et al., 2011) and nesprin-1, -2 and -3 proteins (Nery et al., 2008). The discovery that torsinA not only resides in the ER but also in the NE, suggested that torsinA plays a role in the NE. Therefore, we addressed the distribution of wt- and ΔE-torsinA in non-neuronal cells (COS-7) and neuronal-like cells (SH-SY5Y) in order to test if both cell lines present the phenotypes previously reported.

.

V.A.2. MATERIAL AND METHODS

V.A.2.1. Antibodies

The primary antibodies used were rabbit polyclonal LAP1 (Goodchild and Dauer, 2005) and rabbit polyclonal calnexin (StressGen Bioreagents Corp.). The secondary antibody used was Alexa 594-conjugated anti-rabbit IgG (Molecular Probes).

V.A.2.2. Expression vectors and DNA constructs

GFP-tagged wt-torsinA and ΔE-torsinA constructs were kindly provided by Dr. William Dauer. Briefly, wt-torsinA and ΔE-torsinA cDNAs were cloned into pcDNA3.1 vector and GFP was introduced between residues 21 and 22 of torsinA (immediately following the N-terminal signal sequence cleavage), as previously described (Goodchild and Dauer, 2004).

V.A.2.3. Cell culture and transfection

COS-7 (ATCC CRL-1651) cells were grown in Dulbecco's modified Eagle's medium (DMEM) supplemented with 10% Fetal Bovine Serum (FBS), 100 U/ml penicillin, 100 mg/ml streptomycin and 3.7 g/l $NaHCO_3$ (Complete DMEM). SH-SY5Y cells (ATCC CRL-2266) were grown in Minimal Essential Medium (MEM) supplemented with F-12 Nutrient Mixture (Gibco, Invitrogen), 10% fetal bovine serum (FBS, Gibco, Invitrogen), 1.5 mM L-glutamine, 100 U/mL penicillin and 100 mg/mL streptomycin (Gibco, Invitrogen). Cells were seeded onto 6-well plates (area of 10 cm^2 per well) to be at 80-90 % confluency at the time of transfection. Rat hippocampal primary cultures were established from embryonic day 18 embryos as previously described (Henriques et al., 2007). Briefly, after dissociation with 0.75 mg/ml trypsin, cells were plated onto poly-D-lysine-coated dishes at a density of $1.0x10^5$ cells/cm^2 in B27-supplemented Neurobasal medium (GIBCO) (Brewer et al., 1993). The medium was supplemented with glutamine (0.5 mM), gentamicin (60 µg/ml) and glutamate (25 µM). Cultures were maintained in an atmosphere of 5% CO_2 at 37ºC until 10 days *in vitro* (DIV) before transfection.

Transient transfections were performed using TurboFect (Thermo Scientific) according to the manufacturer's protocols. After 24 hours of transfection, the cells were fixed using 4% paraformaldehyde and further subjected to immunocytochemical analysis.

V.A.2.4. Immunocytochemistry

Once fixed as described above, cells were permeabilized with triton X-100 for 10 minutes and further incubated with the primary antibodies for 2 hours followed by incubation with Alexa 594-conjugated secondary antibody for 1 hour. GFP was directly visualized using the adequate filter settings. Preparations were washed with PBS, mounted using Vectashield mounting media with DAPI (Vector). Preparations were visualized using an Olympus IX81 epifluoresence microscope (Olympus, Optical Co. GmbH) as previously described in chapter IV.

V.A.2.5. Statistical Analysis

Data were expressed as mean ± SEM of at least three independent experiments. Statistical significance analysis was conducted by Student's t-test, with the level of statistical significance being considered $P < 0.05$.

V.A.3. RESULTS

Several studies reported that overexpression of ΔE-torsinA in cultured cells leads to the relocalization of torsinA from the ER to the NE, namely in cells expressing low ΔE-torsinA levels. However, in cells expressing high levels of ΔE-torsinA, the protein is also present in the ER and forms inclusions (Goodchild and Dauer, 2004, 2005; Naismith et al., 2004). Moreover, it seems that ΔE-torsinA abnormally accumulates in the NE in neuronal cells (Giles et al., 2008; Goodchild et al., 2005) rather than other cell types. Thus, before proceeding to further studies, we tested two cellular models for the study of DYT1 dystonia. Non-neuronal cells (COS-7) and neuronal-like cells (SH-SY5Y cells) were transfected with different amounts (0.5, 1, 2 and 4 μg) of GFP-tagged wt-torsinA (GFP-wt-torsinA) or ΔE-torsinA (GFP-ΔE-torsinA) cDNAs. In COS-7 cells, wt- and ΔE-torsinA are both distributed throughout the ER in all cells analyzed (Fig. V.A.1A), and are also found in a perinuclear localization. Moreover, the localization of both proteins was not dependent on the amount of transfected cDNAs. We also observed that both wt- and ΔE-torsinA transfected cells present inclusions, some located in the ER/cytoplasm and others around the NE (Fig. V.A.1A). From the cells analyzed about 31-45 % and 29-39 % of wt- and ΔE-torsinA transfected cells presented inclusions, respectively (Fig. V.A.1B). Moreover the number of inclusions significantly increased with increasing amounts of transfected cDNAs (Fig. V.A.1B), being statistically significant when we compared cells transfected with 0.5 μg of torsinA cDNAs with cells transfected with 2 and 4 μg (Fig. V.A.1B). The localization of both wt- and ΔE-torsinA proteins was confirmed using an ER marker (calnexin). We were able to determine that, in fact, both wt- and ΔE-torsinA proteins co-localize with calnexin (Fig. V.A.2, upper panel), which is not only an ER marker but also a binding protein of torsinA (Naismith et al., 2009a; Zhao et al., 2013b). Further, we labeled cells with LAP1 antibody and showed that both wt- and ΔE-torsinA co-localize with LAP1 (Fig. V.A.2, lower panel), thus demonstrating that torsinA proteins are also localized in the NE.

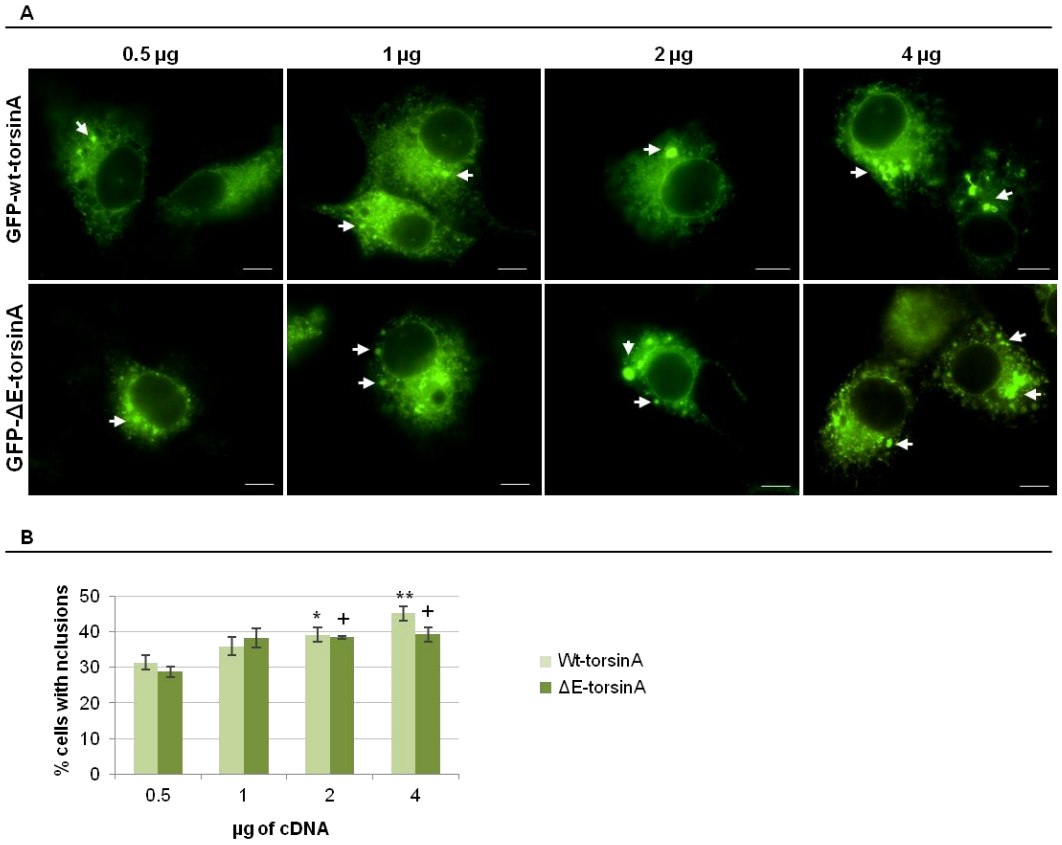

Figure V.A.1. Localization of wt- and ΔE-torsinA in non-neuronal cells (COS-7 cells). **A-** Localization of torsinA proteins in COS-7 cells upon transfection with 0.5, 1, 2 or 4 µg of GFP-wt-torsinA or GFP-ΔE-torsinA cDNAs. GFP-tagged torsinA proteins were directly visualized. Presence of inclusions is marked by arrows. **B-** Percentage of wt- and ΔE-torsinA transfected cells that present inclusions. Values are mean ± SEM, n=3 (20 cells analyzed in each experiment). Statistically different from 0.5 µg wt-torsinA transfected cells, ***** $p < 0.05$, ****** $p < 0.01$. Statistically different from 0.5 µg ΔE-torsinA transfected cells, $^{+}$ $p < 0.05$. Photographs were acquired using an Olympus epifluoresence microscope. Bars, 10 µm.

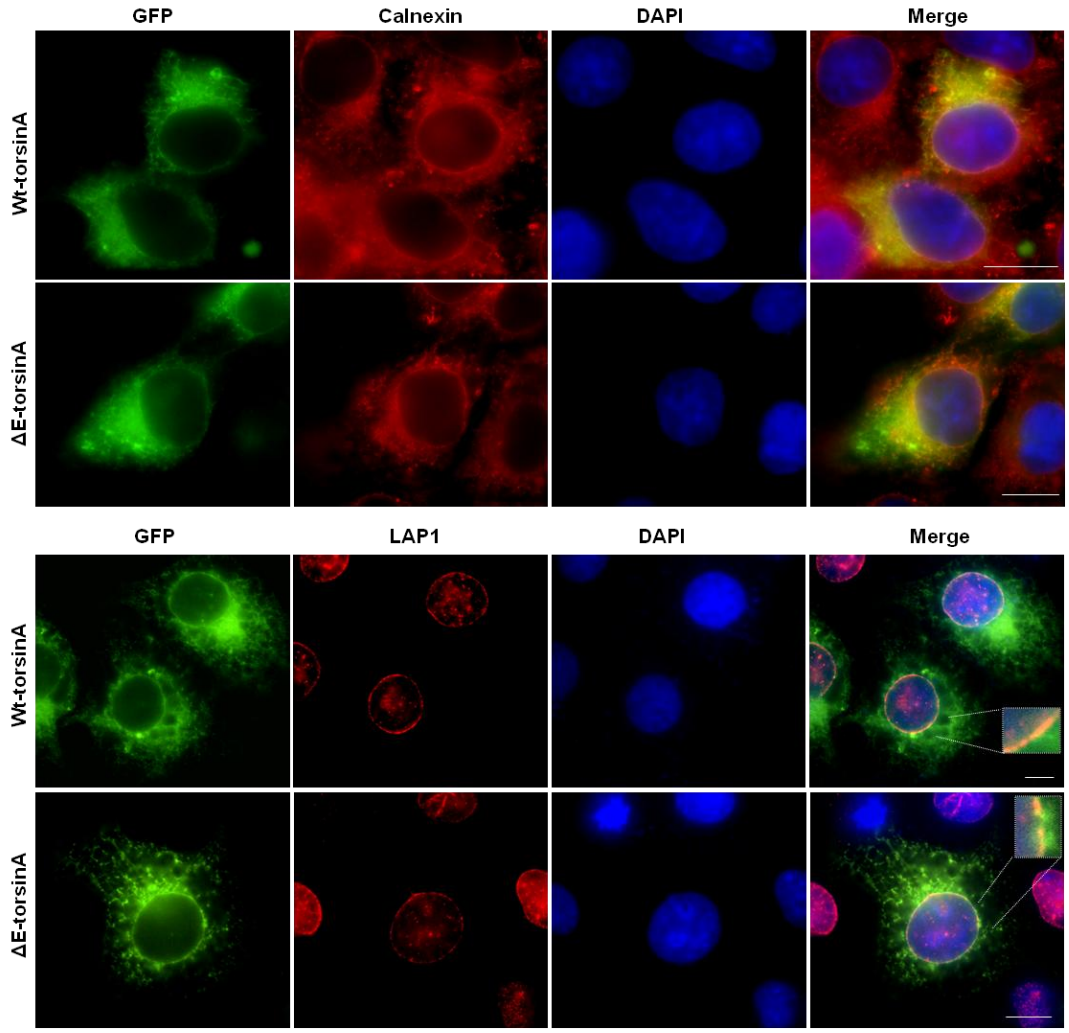

Figure V.A.2. Co-localization of torsinA proteins with calnexin and LAP1 in COS-7 cells. COS-7 cells were transfected with 0.5 µg of GFP-wt-torsinA or GFP-ΔE-torsinA cDNAs. Specific primary antibodies for endogenous calnexin (upper panel) and LAP1 (lower panel) were detected with Alexa Fluor 594-conjugated secondary antibody (red). DNA was stained with DAPI (blue). GFP-tagged torsinA proteins were directly visualized. Photographs were acquired using an Olympus epifluoresence microscope. Bars, 10 µm.

In contrast, in SH-SY5Y cells, a considerable number of ΔE-torsinA transfected cells revealed concentrated perinuclear localization (NE localization), while wt-torsinA is found throughout the cell body and processes and in the NE (Fig. V.A.3). Further, we observed increased labeling of the cytoplasm (presumably ER) upon transfection with increasing amounts of ΔE-torsinA cDNA (Fig. V.A.3B). Indeed, the percentage of cells with specific NE immunoreactivity is about 43% upon transfection with 0.5 µg of ΔE-torsinA cDNA, but this percentage decrease to 31%, 27% and 26 % after transfection with 1, 2 and 4 µg of ΔE-torsinA cDNA, respectively.

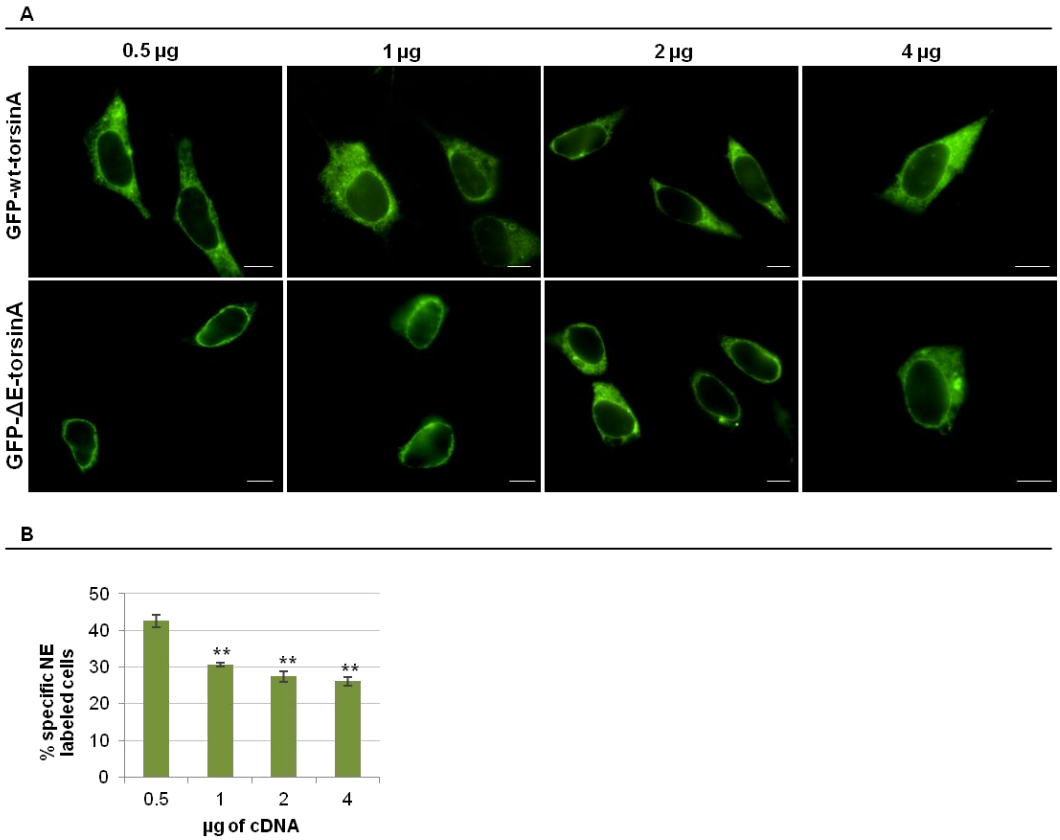

Figure V.A.3. Localization of wt- and ΔE-torsinA in SH-SY5Y cells. **A-** Localization of torsinA proteins in SH-SY5Y cells upon transfection with 0.5, 1, 2 or 4 µg of GFP-wt-torsinA or GFP-ΔE-torsinA cDNAs. GFP-tagged torsinA proteins were directly visualized. **B-** Percentage of ΔE-torsinA transfected cells that present specific perinuclear labeling. Values are mean ± SEM, n=3 (20 cells analyzed in each experiment). Statistically different from 0.5 µg transfected cells, ****** $p < 0.01$. Photographs were acquired using an Olympus epifluoresence microscope. Bars, 10 µm.

Moreover, only a small percentage of cells (around 1-10 %) expressing either wt- or ΔE-torsinA present inclusions. Further, we labeled cells with calnexin and the results revealed that both wt-torsinA and ΔE-torsinA co-localizes with calnexin in the ER (Fig. V.A.4, upper panel). The localization of both torsinA proteins in the NE of SH-SY5Y cells was evidenced by the co-localization of those proteins with LAP1 (Fig. V.A.4, lower panel).

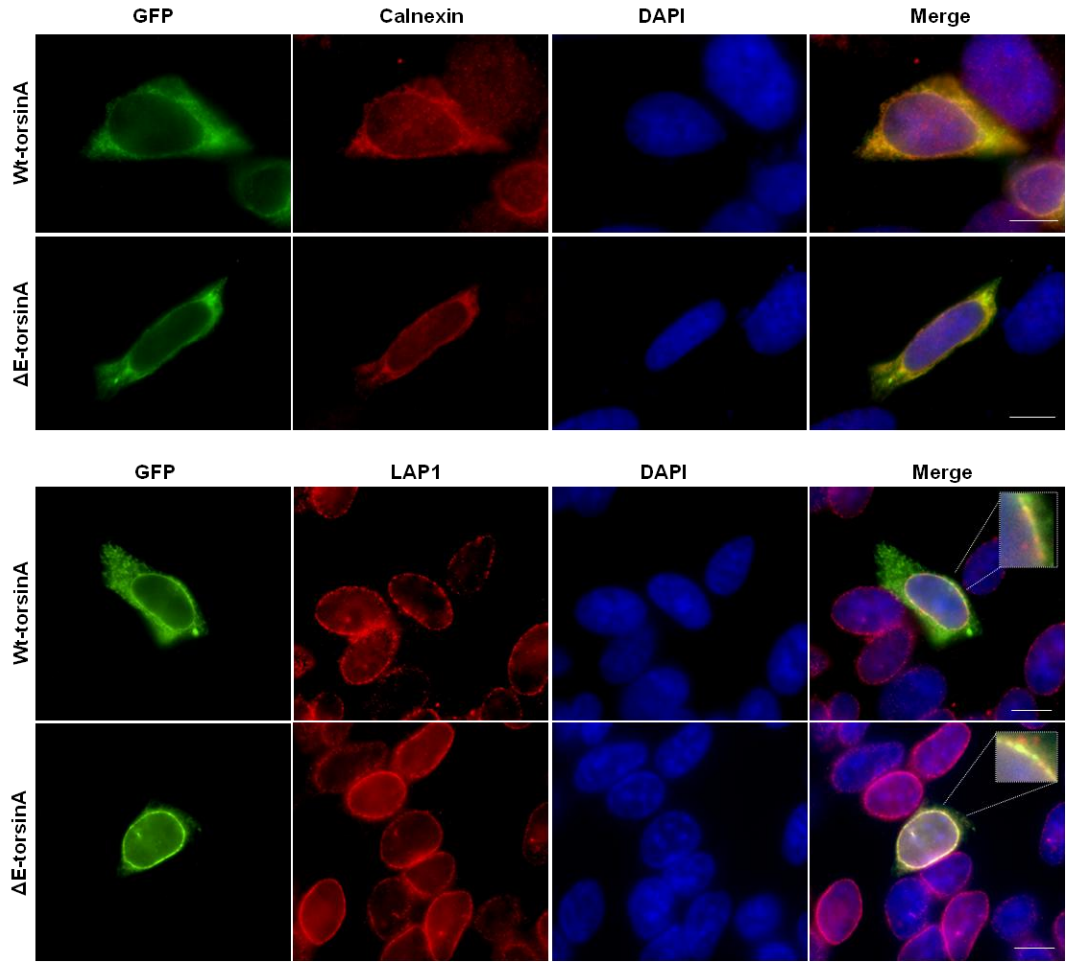

Figure V.A.4. Co-localization of torsinA proteins with calnexin and LAP1 in neuronal-like cells (SH-SY5Y cells). SH-SY5Y cells were transfected with 0.5 µg of GFP-wt-torsinA or GFP-ΔE-torsinA cDNAs. Specific primary antibodies for endogenous calnexin (upper panel) and LAP1 (lower panel) were detected with Alexa Fluor 594-conjugated secondary antibody (red). DNA was stained with DAPI (blue). GFP-tagged torsinA proteins were directly visualized. Photographs were acquired using an Olympus epifluoresence microscope. Bars, 10 µm.

Additionally, rat hippocampal neurons were transfected with wt- or ΔE-torsinA cDNAs (0.5 µg). As expected, wt-torsinA localized throughout the cell body and extends to neuritis, while ΔE-torsinA appears to be specifically concentrated in the NE and co-localizes with LAP1 (Fig. V.A.5). However, due to low levels of transfection, we were not able to perform a quantitative analysis regarding specific localization of torsinA proteins as previously described. Nevertheless, these results confirmed that ΔE-torsinA mutation induces relocalization of torsinA from the ER to the NE in neuronal cells but not in non-neuronal cells.

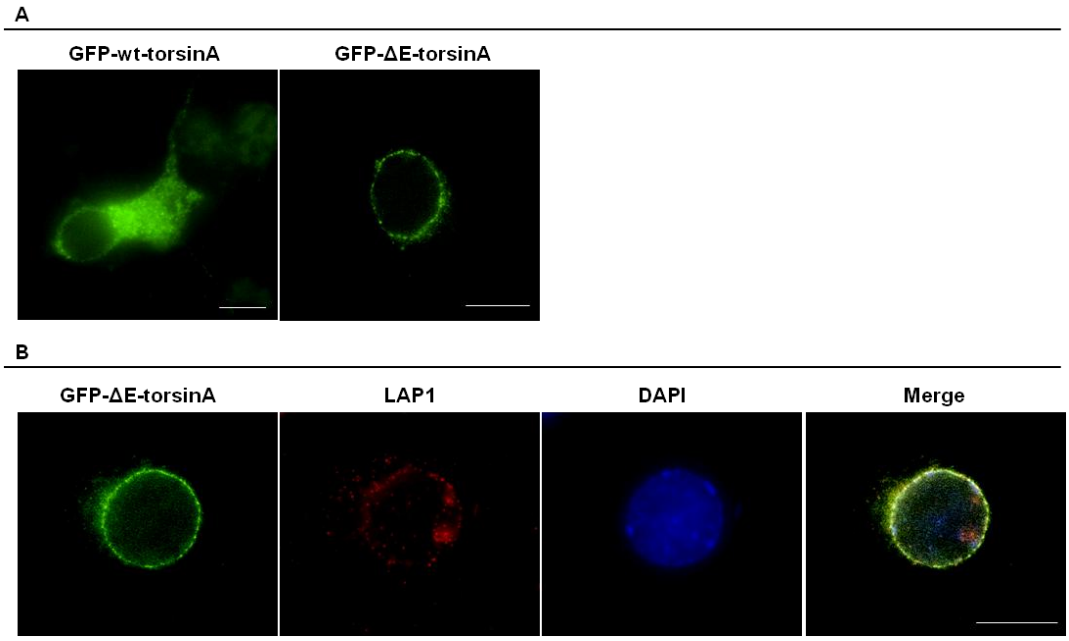

Figure V.A.5. Distribution of wt- and ΔE-torsinA in rat primary hippocampal neurons.A. Hippocampal neurons were transfected with 0.5 µg of GFP-wt-torsinA or GFP-ΔE-torsinA cDNAs. **B.** Co-localization of ΔE-torsinA with LAP1. Specific primary antibody for endogenous LAP1 was detected with Alexa Fluor 594-conjugated secondary antibody (red). DNA was stained with DAPI (blue). GFP-tagged torsinA proteins were directly visualized. Photographs were acquired using an Olympus epifluoresence microscope. Bars, 10 µm.

V.A.4. DISCUSSION

TorsinA is expressed in both neuronal and non-neuronal tissues (Ozelius et al., 1997), however it is unclear why DYT1 dystonia-associated mutation leads to a neuronal phenotype. ΔE-torsinA mutation drives torsinA to relocalize to the NE, which may also result in inclusion formation, in different cell types (Gonzalez-Alegre and Paulson, 2004; Goodchild and Dauer, 2004; Hewett et al., 2000; Naismith et al., 2004). Nevertheless, a study which provides a quantitative analysis of the relative NE/ER distribution, reported that accumulation of ΔE-torsinA in the NE is specific of neuronal cells (Giles et al., 2008). Moreover, torsinA null mice and ΔE-torsinA knock-in mice present an abnormal NE, with blebs and herniations in the perinuclear space, in cultured neurons, but not in non-neuronal cells (Goodchild et al., 2005; Kim et al., 2010a). Despite the ubiquitous presence of torsinA, high expression levels of torsinA are found within the brain (Ozelius et al., 1997). In contrast, another torsin family member-torsinB, has high expression levels in non-neuronal tissues, which could explain why torsinA depletion specifically affects neuronal tissues (Jungwirth et al., 2010; Kim et al., 2010a). Indeed, depletion of torsinB in torsinA knock-in mouse embryonic fibroblasts also leads to NE abnormalities in non-neuronal cells (Kim et al., 2010a).

Our results are in agreement with the hypothesis that ΔE-torsinA phenotype is quite different between neuronal and non-neuronal cells. Indeed, it seems that ΔE-torsinA is specifically recruited to the NE in neuronal-like cells (SH-SY5Y cells) at moderate expression levels, but not in non-neuronal cells (COS-7). Abnormal accumulation of torsinA in the NE suggests that a NE dysfunction may contribute to DYT1 dystonia pathogenesis. At the NE, torsinA was found to interact with LAP1 (Goodchild and Dauer, 2005) and SUN1 (Jungwirth et al., 2011), proteins of the INM, and nesprins (Nery et al., 2008) located in the ONM. The results also revealed that both wt- and ΔE-torsinA appears to accumulate in inclusions in COS-7 cells (Fig. V.A.1). In contrast, the presence of inclusions was rarely seen in SH-SY5Y cells. These inclusions were previously reported in cells expressing higher levels of ΔE-torsinA (Goodchild and Dauer, 2004, 2005; Naismith et al., 2004). This could mean that, under our experimental conditions, COS-7 cells are expressing high levels of torsinA proteins. Moreover, as the level of expression increased, the labeling of ΔE-torsinA in the ER of SH-SY5Y cells also increased (Fig. V.A.3), as is characteristic of highly expressed NE proteins (Schirmer et al., 2003). These findings underline the importance of choosing an

adequate DYT1 dystonia cellular model to study the molecular and cellular mechanisms associated with ΔE-torsinA mutation.

From the results here presented, SH-SY5Y cells were used as the model system for the study of DYT1 dystonia in further experiments. Another important aspect is that the levels of torsinA proteins should not be extremely high, in order to preserve proper cellular distribution of those proteins. Hence, we decided to transfect SH-SY5Y cells with 0.5 µg of wt-torsinA or ΔE-torsinA cDNAs per well of a 6-well plate (area of 10 cm^2) in subsequent studies.

CHAPTER V.B – DYT1 DYSTONIA-ASSOCIATED MUTANT AFFECTS CYTOSKELETAL DYNAMICS

The work described in chapter V.B was included in the following extended abstract, submitted for publication in the *Microscopy and Mycroanalysis* journal:

"DYT1 dystonia-associated mutant affects cytoskeletal dynamics"

Santos, M.[*], Rebelo, S.[*], da Cruz e Silva, E. F.[*], da Cruz e Silva, O. A. B.[*]

[*]Center for Cell Biology, Health Sciences and Biology Department, University of Aveiro, Campus de Santiago, 3810-193 Aveiro, Portugal

Extended abstract

TorsinA and its related family members belong to the ATPases associated with a variety of cellular activities (AAA^+) superfamily. TorsinA has been the most studied torsin family member due to its association with DYT1 dystonia. A mutation of a single glutamic acid within the C-terminal of torsinA (ΔE302/303, also referred to as ΔE) was found in most cases of DTY1 dystonia. TorsinA is primarily located in the endoplasmic reticulum (ER) lumen and nuclear envelope (NE), while ΔE-torsinA is abnormally concentrated in the NE. TorsinA has been implicated in cytoskeleton dynamics through interaction with different binding partners. However, it seems that the ΔE-torsinA mutation interferes with cytoskeleton dynamics. Therefore, we analyzed cytoskeleton alterations associated with the ΔE-torsinA mutation. In order to achieve this goal, we transfected SH-SY5Y cells with GFP-wt-torsinA or GFP-ΔE-torsinA and performed immunofluorescence analysis with β-tubulin and acetylated α-tubulin specific antibodies and with phalloidin that binds to F-actin. We showed that in wt-torsinA transfected cells, β-tubulin, acetylated α-tubulin and F-actin were distributed throughout the cytoplasm, in a manner similar to non-transfected cells. In contrast, in some ΔE-torsinA transfected cells, the distribution of those markers is altered, being more restricted to the NE, and cells seem to be less intensely labeled. Moreover, in some cells, β-tubulin co-localized with ΔE-torsinA positive inclusions. Further, when we quantified the fluorescence intensity (FI) of β-tubulin, we detected a slight decrease of the FI in ΔE-torsinA transfected cells compared to wt-torsinA transfected cells. In the

same way, ΔE-torsinA transfected cells have lower levels of acetylated α-tubulin, which is a marker for microtubules stability, suggesting that microtubule dynamics may be compromised by the ΔE-torsinA mutation. Furthermore, we observed a loss of F-actin stress fibers in ΔE-torsinA transfected cells. Indeed, we showed that F-actin FI decrease from 1.03 to 0.83 (around 20%) in ΔE-torsinA transfected cells compared with wt-torsinA transfected cells. Our results are in agreement with previous reports where it was reported that the expression of ΔE-torsinA altered the localization of vimentin to the NE, KLC to inclusions and nesprin-3 to the ER. Nesprins in the outer nuclear membrane bind to actin, microtubules and intermediate filaments, thus forming a complex that links the nucleoskeleton and cytoskeleton (the LINC complex). Therefore, torsinA and its binding partners may have a role in modulating the LINC complex. Disruption of the LINC complex may contribute to the development of muscular dystrophies and cardiomyopathies.

V.B.1. INTRODUCTION

TorsinA has been shown to be involved in several cellular processes by interacting with different binding proteins (reviewed in Granata et al., 2009). Interestingly, torsinA has been implicated in cytoskeleton dynamics through interaction with nesprins, vimentin, KLC and tau. Nesprins in the ONM bind to actin filaments, microtubules and intermediate filaments, thus forming the LINC complex (Crisp et al., 2006; Haque et al., 2006). When torsinA is depleted, nesprin-3 is redistributed to the ER, indicating that torsinA is important for the proper localization of nesprin-3 and participates in the LINC complex (Nery et al., 2008). Furthermore, immunoprecipitation of vimentin not only brings down torsinA, but also other cytoskeleton components such as α-tubulin, kinesin and actin and the NE protein LAP1 (Hewett et al., 2006). Further, overerexpression of ΔE-torsinA alters the localization of vimentin to the NE (Hewett et al., 2006) and KLC to inclusions (Kamm et al., 2004). Therefore, it is important to analyze not only the physiological function of torsinA in cytoskeleton dynamics, but also the alterations associated with the ΔE-torsinA mutation. In order to achieve this goal, we transfected SH-SY5Y cells with wt-torsinA or ΔE-torsinA and further analyzed it by immunofluorescence. The effects of ΔE-torsinA mutation in the distribution of cytoskeletal elements (β-tubulin, acetylated α-tubulin and F-actin) were determined.

V.B.2. Material and methods

V.B.2.1. Antibodies and drugs

The primary antibodies used were mouse monoclonal β-tubulin (Invitrogen) and mouse monoclonal acetylated α-tubulin (Sigma). The secondary antibody used was Alexa 594-conjugated anti-mouse IgG (Molecular Probes). Alexa Fluor 594-conjugated phalloidin (Molecular Probes) was used to label F-actin.

V.B.2.2. Expression vectors and DNA constructs

GFP-tagged wt-torsinA and ΔE-torsinA constructs were kindly provided by Dr. William Dauer (Goodchild and Dauer, 2004).

V.B.2.3. Cell culture and transfection

SH-SY5Y cells (ATCC CRL-2266) were grown in Minimal Essential Medium (MEM) supplemented with F-12 Nutrient Mixture (Gibco, Invitrogen), 10% fetal bovine serum (FBS, Gibco, Invitrogen), 1.5 mM L-glutamine, 100 U/mL penicillin and 100 mg/mL streptomycin (Gibco, Invitrogen).

Transient transfections were performed using TurboFect (Thermo Scientific) according to the manufacturer's protocols. After 24 hours of transfection, the cells were fixed using 4% paraformaldehyde and further subjected to immunocytochemical analysis.

V.B.2.4. Immunocytochemistry

Once fixed as described above, cells were permeabilized with triton X-100 for 10 minutes and further incubated with the primary antibodies for 2 hours followed by incubation with Alexa 594-conjugated secondary antibody for 1 hour. Cells were incubated with phalloidin for 30 minutes. Preparations were washed with PBS, mounted using Vectashield mounting media with DAPI (Vector) and visualized using an

LSM510-Meta confocal microscope (Zeiss) as previously described (Santos et al., 2013).

V.B.2.5. Statistical Analysis

Statistical significance analysis was conducted by Student's t-test, with the level of statistical significance being considered $P < 0.05$. Data were expressed as mean ± SEM

V.B.3. RESULTS

There is significant evidence for a role of torsinA in cytoskeleton dynamics, mainly because of its interaction with different cytoskeletal proteins. Moreover depletion of endogenous torsinA or overerexpression of ΔE-torsinA alters the localization of some proteins such nesprin-3, vimentin and KLC (Hewett et al., 2006; Kamm et al., 2004; Nery et al., 2008). Therefore, we decided to analyze if the ΔE-torsinA mutation alters the distribution/expression of other cytoskeletal elements. In order to achieve this goal, we transiently transfected SH-SY5Y cells with wt-torsinA or ΔE-torsinA and performed immunofluorescence with β-tubulin and acetylated α-tubulin specific antibodies and phalloidin that binds to F-actin. We showed that in cells overexpressing wt-torsinA, both β-tubulin and acetylated α-tubulin were distributed throughout the cytoplasm, in the same way as non-transfected (NT) cells (Fig. V.B.1A). In contrast, we noticed that some ΔE-torsinA transfected cells were weakly stained with β-tubulin and acetylated α-tubulin antibodies, and in some cells this proteins were found located around the NE (Fig. V.B.1A). In order to clearly establish if wt- and ΔE-torsinA transfected cells present different levels of β-tubulin and acetylated α-tubulin, we measure the fluorescence intensity (FI) of all cells and transfected cells, labeled with those antibodies, in various fields. Then we compared the ratio transfected cells FI/total cells FI of wt- and ΔE-torsinA transfected cells (Fig. V.B.1B). This analysis was performed using a specific software (Zeiss LSM 510 4.0 software). Thus, we showed that β-tubulin and acetylated α-tubulin FI was more intense in wt-torsinA transfected cells (1.05 and 0.98, respectively) than ΔE-torsinA transfected cells (0.99 and 0.89, respectively). Thus β-tubulin and acetylated α-tubulin FI in ΔE-torsinA transfected cells only decrease around 6.5% and 9.3%, respectively, when compared to wt-torsinA transfected cells. Moreover, we also observed that β-tubulin co-localized with ΔE-torsinA positive inclusions (higher magnification view in Fig. V.B.1A).

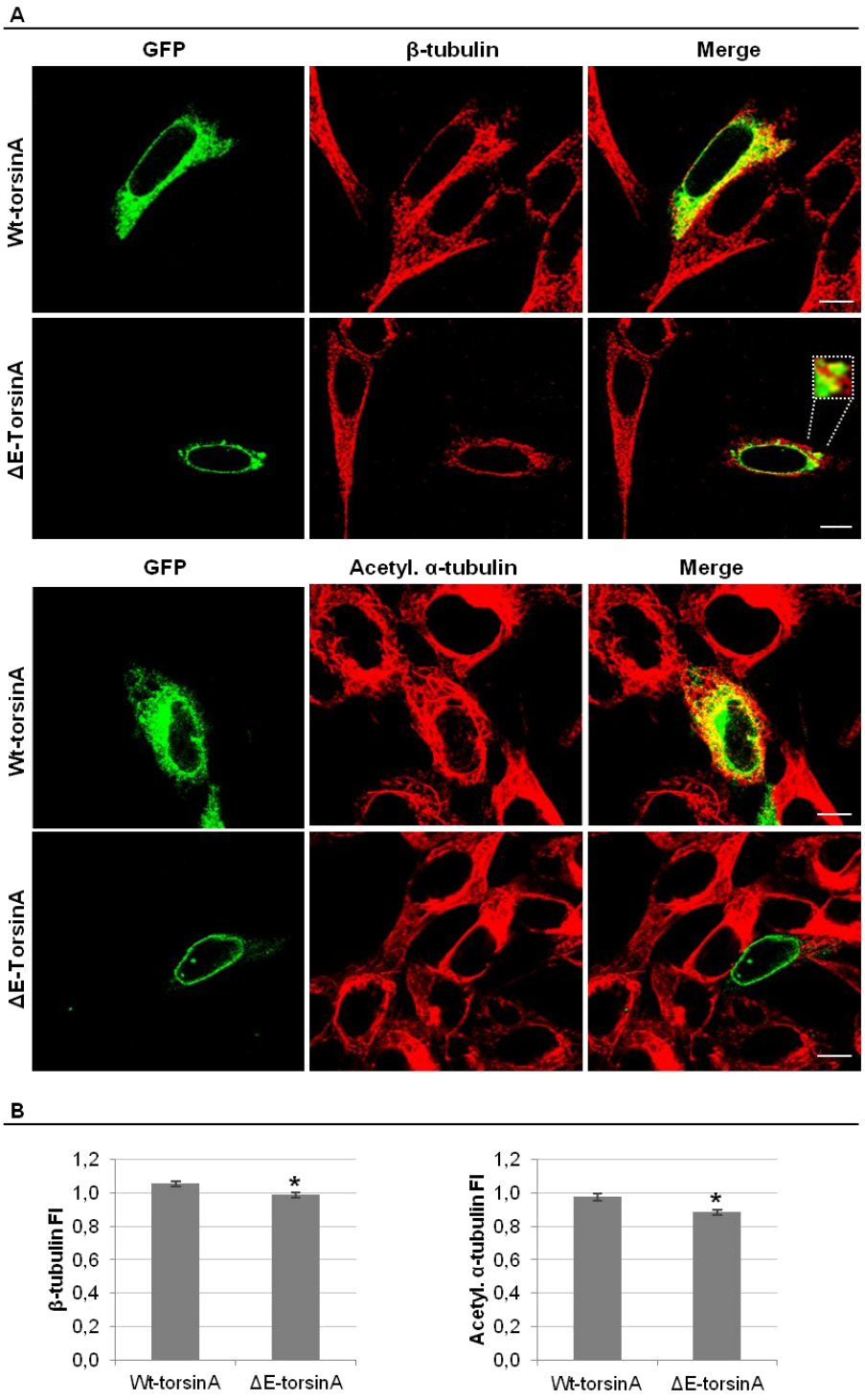

Figure V.B.1. Distribution of β-tubulin and acetylated α-tubulin in wt- and ΔE-torsinA transfected cells. **A-** SH-SY5Y cells were transfected with GFP-wt-torsinA or GFP-ΔE-torsinA. Specific primary antibodies for endogenous β-tubulin and acetylated α-tubulin (acetyl. α-tubulin) were detected with Alexa Fluor 594-conjugated secondary antibody (red). The higher magnification view shows in more detail the co-localization of ΔE-torsinA and β-tubulin in inclusions. **B-** Quantification of β-tubulin and acetyl. α-tubulin fluorescence intensity (FI), which represents the ratio transfected cells FI/total cells FI, in wt- and ΔE-torsinA transfected cells. Values are mean ± SEM, n= 22 cells (for β-tubulin) and 30 cells (acetyl. α-tubulin). Statistically different from wt-torsinA transfected cells, *****$p < 0.05$. Photographs were acquired using a LSM 510-Meta confocal microscope. Bars, 10 μm.

Further, we observed that F-actin was distributed throughout the cytoplasm in wt-torsinA transfected cells and NT cells. In contrast, ΔE-torsinA transfected cells seem to be less intensely labeled with phalloidin, thus showing a lost of F-actin stress fibers (Fig.V.B.2A). Indeed, F-actin FI was more intense in wt-torsinA transfected cells (1.03) than ΔE-torsinA transfected cells (0.83) (Fig. V.B.2B). Thus F-actin FI in ΔE-torsinA transfected cells decrease around 20% in comparison with wt-torsinA transfected cells.

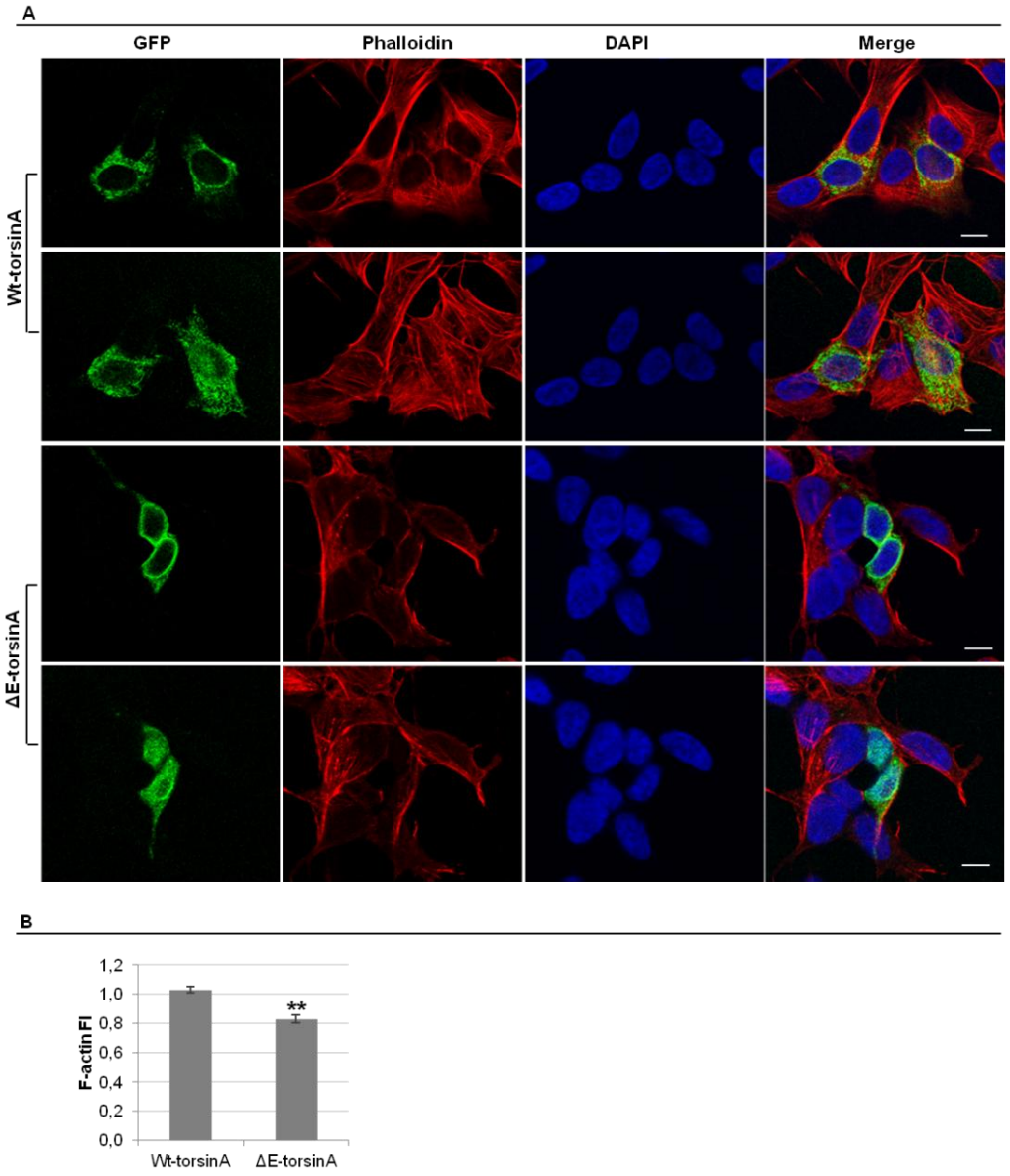

Figure V.B.2. Distribution of F-actin in wt- and ΔE-torsinA transfected cells. **A-** SH-SY5Y cells were transfected with GFP-wt-torsinA or GFP-ΔE-torsinA cDNAs and labeled with phalloidin (that binds to F-actin) conjugated with Alexa Fluor 594 (red). Two different focal planes are shown for each image. DNA was stained with DAPI (blue). **B-** Quantification of F-actin fluorescence intensity (FI), which represents the ratio transfected cells FI/total cells FI, in wt- and ΔE-torsinA transfected cells. Values are mean ± SEM, n= 20 cells. Statistically different from wt-torsinA transfected cells, **$p < 0.01$. Photographs were acquired using a LSM 510-Meta confocal microscope. Bars, 10 µm.

V.B.4. DISCUSSION

TorsinA has several potential functions and among them is cytoskeletal regulation. In this work we showed that ΔE-torsinA could potentially lead to a decrease in the intracellular levels and distribution of β-tubulin and acetylated α-tubulin (Fig. V.B.1). However, the effects of ΔE-torsinA mutation were more pronounced when we evaluated the intracellular levels of F-actin. Indeed, it seems that ΔE-torsinA mutation lead to a decrease in the intracellular levels of F-actin (Fig. V.B.2), possibly related with a loss of stress fibers.

TorsinA was found to interact with different cytoskeleton elements such as vimentin, KLC and tau. Co-immunoprecipitation studies also showed that vimentin and torsinA are in a complex that includes other cytoskeleton components such as α-tubulin, kinesin and actin (Hewett et al., 2006). However, it seems that ΔE-torsinA mutation interferes with cytoskeleton dynamics. Expression of ΔE-torsinA altered the localization of vimentin to the NE (Hewett et al., 2006) and KLC to inclusions (Kamm et al., 2004). Moreover, fractioning studies suggested that ΔE-torsinA associates to a lesser degree with the cytoskeleton when compared with wt-torsinA (Hewett et al., 2006). However, no consistent alterations were seen in the distribution of actin and tubulin in DYT1 fibroblasts compared to control fibroblasts. Nevertheless, when we quantified the FI of β-tubulin, we detected a slight decrease of the FI in ΔE-torsinA transfected cells compared to wt-torsinA transfected cells (Fig.V.B.1B). In the same way, ΔE-torsinA transfected cells seem to have lower intracellular levels of acetylated α-tubulin (Fig. V.B.1B), which is a marker for microtubules stability, suggesting that microtubule dynamics may be compromised by the ΔE-torsinA mutation. Furthermore, we observed a loss of F-actin stress in ΔE-torsinA transfected cells (Fig. V.B.2A). Indeed, we showed that F-actin FI decrease around 20% in ΔE-torsinA transfected cells compared with wt-torsinA transfected cells (Fig. V.B.2B).

The localization of torsinA, and particularly ΔE-torsinA, at the NE suggests that a NE dysfunction may contribute to DYT1 dystonia pathogenesis. Moreover, the NE localization of torsinA and its binding to NE proteins make torsinA a candidate for establishing a link between the NE and cytoskeleton. At the NE, torsinA was found to interact with LAP1 (Goodchild and Dauer, 2005) and SUN1 (Jungwirth et al., 2011), proteins of the INM, and nesprins (Nery et al., 2008) located in the ONM. SUN proteins have a NE lumenal domain that interacts with nesprins, which form a functional link

with intermediate filaments, microtubules and actin, thereby forming the LINC complex (Crisp et al., 2006; Haque et al., 2006). SUN1 is required for torsinA localization in the NE (Jungwirth et al., 2011). Moreover, torsinA depletion appears to remove nesprin-3 from the NE, suggesting that torsinA is important for the proper maintenance of the LINC complex (Nery et al., 2008). In other hand, overexpression of ΔE-torsinA altered the localization of vimentin to the NE (Hewett et al., 2006). Nesprin-3 binds to vimentin through plectin and all three proteins were found to co-immunoprecipitate with torsinA. Therefore, torsinA and its NE binding partners may have a role in modulating the LINC complex, enabling proper nuclei positioning. It was reported that disruption of the LINC complex results in the impairment of nuclear positioning and cell polarization and may contribute to the development of muscular dystrophies and cardiomyopathies (Lombardi et al., 2011).

CHAPTER V.C – IDENTIFICATION OF THE NOVEL LAP1/PP1/TORSINA COMPLEX

The work described in chapter V.C was included in the following manuscript, which will be submitted for publication in the *Frontiers in Cellular Neuroscience* journal:

"Protein phosphorylation regulates a novel torsinA trimeric complex"

Mariana Santos[1], Sandra Rebelo[1], Filipa Martins[1], Patrícia Costa[1], William T. Dauer[2], Edgar F. da Cruz e Silva[1], Odete A. da Cruz e Silva[1]

[1]Health Sciences, Centre for Cell Biology, Neuroscience Laboratory, University of Aveiro, Aveiro, Portugal

[2]Departments of Neurology and Cell & Developmental Biology, University of Michigan Medical School, Ann Arbor, Michigan, USA

Abstract

DYT1 dystonia is the most common form of early onset isolated dystonia and is caused by a mutation in the *DYT1* gene, resulting in the loss of a single glutamic acid (ΔE) within the torsinA protein. Several functions have been proposed for torsinA including nuclear envelope (NE) and endoplamic reticulum (ER) dynamics, secretory protein trafficking, transport of secretory vesicles and response to stress, possibly acting as a chaperone at several subcellular compartments through interaction with specific binding partners. TorsinA is localized in the contiguous lumen of the ER and NE, however the mutant form, ΔE torsinA, concentrates in the perinuclear space of the NE. At the NE, torsinA interacts with others proteins, including the lamina associated polypeptide 1 (LAP1). We have recently reported that LAP1 also interacts with protein phosphatase 1 (PP1). PP1 is a ser/thr phosphatase that dephosphorylates about a third of all proteins in eukaryotic cells. PP1 regulates several functions by associating with different binding partners. Like torsinA, PP1 is expressed virtually in all tissues but has higher expression levels in the brain. The work here presented confirms the occurrence of the trimeric complex PP1/LAP1/torsinA in rat brain and cellular models. Moreover, results from blot overlay assays, suggest that torsinA and PP1 do not bind directly but via LAP1. Significantly, results showed that torsinA proteins (wt- and ΔE-torsinA) can

be dephosphorylated by PP1, as well as LAP1. Furthermore, knockdown of the bridging protein LAP1 leads to reduced intracellular levels of both PP1 and torsinA proteins. Localization studies for LAP1 and PP1 in a cellular model of DYT1 dystonia were also conducted. The identification of this novel trimeric complex provides new insights for DYT1 dystonia, where protein phosphorylation may represent a pivotal regulatory mechanism.

V.C.1. INTRODUCTION

Dystonia is a movement disorder characterized by sustained or intermittent muscle contractions causing abnormal, often repetitive, movements, postures, or both (Albanese et al., 2013). Several genes have been mapped for dystonia, though dystonia associated with the *DYT1* gene, encoding torsinA protein, is the most common and severe form of hereditary isolated dystonia. DYT1 dystonia is an autosomal dominant disease with penetrance of around 30% and it is caused by a 3 bp (GAG) deletion in the coding region of the *DYT1* (*TOR1A*) gene. This deletion results in the loss of a single glutamic acid in the C-terminal of torsinA protein (ΔE-torsinA) (Ozelius et al., 1997). Three other variations in torsinA have been found, but none has been unequivocally associated with the disease (Kabakci et al., 2004; Kock et al., 2006; Leung et al., 2001; Ozelius et al., 1997). TorsinA and its related family members belong to the ATPases associated with a variety of cellular activities (AAA^+) superfamily (Ozelius et al., 1997). These proteins typically act as chaperones and are involved in several functions, such as, protein folding and degradation, membrane trafficking, DNA replication and repair, cytoskeletal regulation and mitosis (reviewed in Ogura and Wilkinson, 2001; Vale, 2000). The predicted structure of torsinA contains a single AAA^+ domain, which includes Walker A and Walker B nucleotide binding motifs, and the α-helical domains sensor-1 and sensor-2, which are important for the ATPase activity (Iyer et al., 2004; Neuwald et al., 1999; Ogura and Wilkinson, 2001).

TorsinA resides in the endoplasmic reticulum (ER) lumen (Hewett et al., 2003; Kustedjo et al., 2000), but it is also located in the nuclear envelope (NE) (Goodchild and Dauer, 2004; Naismith et al., 2004). Additionally, the ΔE-torsinA mutation was found to be abnormally concentrated in the NE of cultured cells, neurons and DYT1 patient-derived fibroblasts (Goodchild and Dauer, 2004). Furthermore, a mutation in the Walker B domain (E171Q-torsinA) inhibits ATP hydrolysis and results in an ATP-bound state, causing high affinity substrate interactions. This mutation causes a redistribution of torsinA from the ER to the NE (Goodchild and Dauer, 2004; Naismith et al., 2004). Abnormal accumulation of ΔE-torsinA in the NE suggests that a NE dysfunction may, in turn, contribute to DYT1 dystonia pathogenesis. The accumulation of torsinA in the NE led to the discovery of lamina associated polypeptide 1 (LAP1) or torsinA interacting protein 1 (TOR1AIP1) as a binding partner of torsinA (Goodchild and Dauer, 2005). LAP1 is a type II transmembrane protein of the inner nuclear

membrane (INM), containing a nucleoplasmic N-terminal domain, a single transmembrane domain and a lumenal C-terminal domain located in the perinuclear space (Martin et al., 1995). The latter domain in conserved between LAP1 family members (LAP1A, B and C) (Martin et al., 1995) and mediates the interaction with torsinA (Goodchild and Dauer, 2005). Moreover, LAP1 was found to relocate torsinA to the NE in a perinuclear distribution (Goodchild and Dauer, 2005). Additionally, torsinA was found to interact with others NE proteins such as SUN1 and nesprin-1, -2 and -3 (Jungwirth et al., 2011; Nery et al., 2008). Recent work from our laboratory, established that LAP1B interacts with protein phosphatase 1 (PP1) in the nucleoplasm and it is dephosphorylated *in vitro* by PP1γ1 (Santos et al., 2013). In mammalian cells three genes (*PPP1CA*, *PPP1CB* and *PPP1CC*) encode four PP1 isoforms: PP1alpha (PP1α), PP1beta/delta (PP1β/δ), PP1gamma1 (PP1γ1) and PP1gamma2 (PP1γ2) (da Cruz e Silva et al., 1995b; Sasaki et al., 1990). PP1 proteins are predicted to catalyze the majority of protein dephosphorylation events in eukaryotic cells (Bollen et al., 2010; Heroes et al., 2013). The versatility of PP1 is largely determined by the binding of its catalytic subunit to different specific regulatory subunits. Close to 200 PP1 interacting proteins have thus far been identified (Esteves et al., 2012a; Esteves et al., 2012b; Fardilha et al., 2011; Heroes et al., 2013).

TorsinA, LAP1 and PP1 are ubiquitously expressed (da Cruz e Silva et al., 1995b; Goodchild and Dauer, 2005; Ozelius et al., 1997), but PP1 and torsinA both exhibit high levels of expression in the brain (Augood et al., 1999; da Cruz e Silva et al., 1995b; Ozelius et al., 1997). Moreover, within cells, torsinA interacts with LAP1 in the perinuclear space (Goodchild and Dauer, 2005), which in turn binds to PP1 in the nucleoplasm (Santos et al., 2013). Thereby it is plausible that these three proteins co-exist in a complex. In fact, the data here presented show that both wt-torsinA and ΔE-torsinA form a complex with LAP1 and PP1. Moreover, it is possible to infer that torsinA and PP1 do not bind directly but instead via LAP1. Nevertheless, torsinA was found to be dephosphorylated by PP1, as well as LAP1. Therefore, the functionally consequences of reversible protein phosphorylation on torsinA and its potential role in DYT1 dystonia pathogenesis is an avenue that should be explored in future studies.

V.C.2. MATERIALS AND METHODS

V.C.2.1. Antibodies

The primary antibodies used were rabbit polyclonal LAP1 (Goodchild and Dauer, 2005); rabbit polyclonal CBC2C and CBC3C, that recognize the C-terminal of PP1α and PP1γ, respectively (da Cruz e Silva et al., 1995b); mouse monoclonal torsinA (Milipore); rabbit polyclonal torsinA (ab76133, Abcam); mouse monoclonal JL-8 antibody (BD Biosciences) that recognizes GFP-fusion proteins and Myc-tag antibody (Cell Signaling) that recognizes Myc-fusion proteins. The secondary antibodies used were anti-mouse and anti-rabbit horseradish peroxidase-linked antibodies (GE Healthcare) for ECL detection, and Alexa 594-conjugated anti-rabbit IgG (Molecular Probes) and Alexa 350-conjugated anti-mouse for co-localization studies.

V.C.2.2. Expression vectors and DNA constructs

pcDNA3.1-GFP-wt-torsinA and pcDNA3.1-GFP-ΔE-torsinA constructs have been previously described (Goodchild and Dauer, 2004), as well as, pET-LAP1B and Myc-LAP1B (Santos et al., 2013). The pSIREN-RetroQ vector was kindly provided by Dr. Celso Cunha from the *Instituto de Higiene e Medicina Tropical*, Lisbon (Casaca et al., 2011)

V.C.2.3. Cell culture and transfection

SH-SY5Y cells (ATCC CRL-2266) were grown in Minimal Essential Medium (MEM) supplemented with F-12 Nutrient Mixture (Gibco, Invitrogen), 10% FBS (Gibco, Invitrogen), 1.5 mM L-glutamine, 100 U/mL penicillin and 100 mg/mL streptomycin (Gibco, Invitrogen). Transient transfections were performed using TurboFect (Thermo Scientific) according to the manufacture's protocol. After 24 hours of transfection, cells were harvested for subsequent immunoprecipitation experiments or fixed, using 4% paraformaldehyde for immunocytochemical analysis.

V.C.2.4. Brain dissection

Winstar rats (9-12 weeks) were obtained from Harlan Interfaune Ibérica, SL. All experimental procedures observed the European legislation for animal experimentation (2010/63/EU). No specific ethics approval under EU guidelines was required for this project, since the rats were only euthanized, by cervical stretching followed by decapitation, for brain removal. This is within the European law (Council Directive 86/609/EEC) and during this procedure all steps were taken to ameliorate animal suffering and the minimum number of possible animals were used. The procedures were approved and supervised by our Institutional Animal Care and Use Committee (IACUC): Comissão Responsável pela Experimentação e Bem-Estar Animal (CREBEA).

Briefly, animals were euthanized by cervical stretching followed by decapitation and the cerebellum was dissected out on ice. The tissue was then homogenized on ice, in non-denaturing lysis buffer (50 mM Tris-HCl pH 8.0, 120 mM NaCl, 4% CHAPS) containing protease inhibitors (1 mM PMSF, 10 mM Benzamidine, 2 µM Leupeptin, 1.5 µM Aprotinin, 5 µM Pepstatin A), with a Potter-Elvehjem tissue homogenizer with 10-15 pulses at 650-750 rpm (Rebelo et al., 2013). Resulting tissue extracts were used for IP analysis using Dynabeads Protein G (Dynal, Invitrogen) as previously described (Santos et al., 2013).

V.C.2.5. Co-immunoprecipitation

SH-SY5Y cells were transfected with wt-torsinA or ΔE-torsinA were collected in lysis buffer (50 mM Tris-HCl pH 8, 120 mM NaCl, 4% CHAPS) containing protease inhibitors (1 mM PMSF, 10 mM Benzamidine, 2 µM Leupeptin, 1.5 µM Aprotinin, 5 µM Pepstatin A). Immunoprecipitations were carried using Dynabeads Protein G (Dynal, Invitrogen) as previously described (Santos et al., 2013).

V.C.2.6. Blot overlay assay

LAP1B, wt-torsinA and ΔE-torsinA proteins were generated by *in vitro* transcription/ translation (IVT) from pET-LAP1B, pcDNA3.1-GFP-wt-torsinA and

pcDNA3.1-GFP-ΔE-torsinA expression vectors, respectively, using the TnT-coupled transcription/translation kit (Promega), according to the manufactures' instructions. For the overlay assays, four samples of 250 ng of purified recombinant PP1γ1 protein (Watanabe et al., 2003) were separated on a 12% SDS-PAGE. All proteins were transferred onto a nitrocellulose membrane and overlaid with either LAP1B-IVT, wt-torsinA-IVT, ΔE-torsinA-IVT or negative control of IVT. The bound proteins were detected by incubating the membrane with JL-8 (GFP) antibody and developed by ECL.

V.C.2.7. Immunocytochemistry

Once fixed as described above, SH-SY5Y cells were permeabilized with triton X-100 for 10 min. Cells were first incubated with one of the primary antibodies for 2 hours, followed by the secondary antibody for 1 hour. After washing with 1x PBS, cells were subsequently incubated with a second primary antibody for 2 hours, followed by the secondary antibody for 1 hour. GFP was visualized directly. Preparations were washed with PBS, mounted using Vectashield mounting media (Vector) or Vectashield mounting media with DAPI (Vector). Preparations were visualized using an Olympus IX81 epifluoresence microscope (Olympus, Optical Co. GmbH) equipped with the appropriate filter combinations and a 100×objective (Plan-Neofluar, 100x/1.35 oil objective). Images were acquired with an F-view II CCD camera (Soft Imaging System GmbH, Münster, Germany) driven by Soft Imaging software.

V.C.2.8. Detection of protein phosphorylation

SH-SY5Y cells were transfected with wt- or ΔE-torsinA cDNAs and treated with 0.25 nM or 500 nM okadaic acid (OA) for 3 hours. Then, cells were collected in PP1 buffer (50 mM Tris-HCl pH 7.5, 0.1 mM EGTA, 1 mM $MnCl_2$ and 5 mM DTT) and lysates incubated at 30ºC for 1 hour with or without 100 ng of purified PP1γ1 protein. Proteins were resolved in 7.5% SDS-PAGE containing 50 μM Phos-tag (AAL-107, Wako) and 100 μM $MnCl_2$. After electrophoresis, Phos-tag acrylamide gels were washed with transfer buffer (25 mM Tris, 192 mM glycine and 20% methanol) containing 10 mM EDTA for 10 min to chelate $MnCl_2$ and then with transfer buffer without EDTA for 10 min according to the manufacturer's protocol.

V.C.2.9. LAP1 knockdown

Knockdown of endogenous LAP1 in SH-SY5Y cells was achieved using a short hairpin RNA (shRNA) strategy as previously described (Santos, 2014). SH-SY5Y cells were transfected with both pSIREN-LAP1-C1 and pSIREN-LAP1-C2 plasmids or with the pSIREN-CMS (negative control).

V.C.2.10. SDS-PAGE and immunoblotting

Samples were separated on SDS-PAGE and electrophoretically transferred onto nitrocellulose. Nitrocellulose membranes were incubated in Ponceau S solution for 5 minutes and then scanned in a GS-800 calibrated imaging densitometer (Bio-Rad), in order to assess equal gel loading. Membranes were washed in TBST 1x to remove Ponceau S staining, followed by immunological detection with specific antibodies as indicated. Membranes were saturated in 5% non-fat dry milk in TBS-T for 2 hours and further incubated with primary antibodies. The incubations with the CBC2C, CBC3C and torsinA were performed overnight while LAP1 and GFP antibodies were incubated for 3 hours. Detection was achieved using horseradish peroxidase-conjugated anti-rabbit or anti-mouse IgGs as secondary antibodies and proteins visualized by ECL (GE Healthcare).

V.C.2.11. Quantification and Statistical Analysis

Autoradiograms were scanned in a GS-800 calibrated imaging densitometer (Bio-Rad) and protein bands quantified using the Quantity One densitometry software (Bio-Rad). Data were expressed as mean ± SEM of at least three independent experiments. Statistical significance analysis was conducted by Student's test, with the level of statistical significance being considered $P < 0.05$

V.C.3. RESULTS

V.C.3.1. Identification of the novel LAP1/PP1/TorsinA complex

Given that torsinA binds to the lumenal domain of LAP1 in the perinuclear space (Goodchild and Dauer, 2005), while PP1 binds to the nucleoplasmic domain of LAP1 inside the nucleus (Santos et al., 2013), it is reasonable to deduce that these proteins could form a trimeric complex. Moreover, PP1 and torsinA are both particularly abundant within the brain (Augood et al., 1999; da Cruz e Silva et al., 1995b; Ozelius et al., 1997). Hence, co-immunoprecipitations of rat cerebellum extracts using LAP1, PP1α, PP1γ and torsinA specific antibodies were performed (Fig. V.C.1). Upon immunoprecipitation with LAP1 and torsinA antibodies, bands of approximately 37 kDa corresponding to PP1α and PP1γ were identified (Fig. V.C.1). Further, when immunoprecipitations were carried out with PP1α, PP1γ or torsinA antibodies, a band below 75 kDa corresponding to the higher LAP1 isoform (LAP1B) was clearly indentified. The smaller LAP1 isoform (LAP1C) seems to be co-immunoprecipitated, but the band is obscured by the antibody's IgG heavy chain (Fig. V.C.1). Using the same methodology, similar results were detected in other brain regions, namely striatum and cortex (data not shown) that are, in addition to the cerebellum, implicated in dystonia pathogenesis.

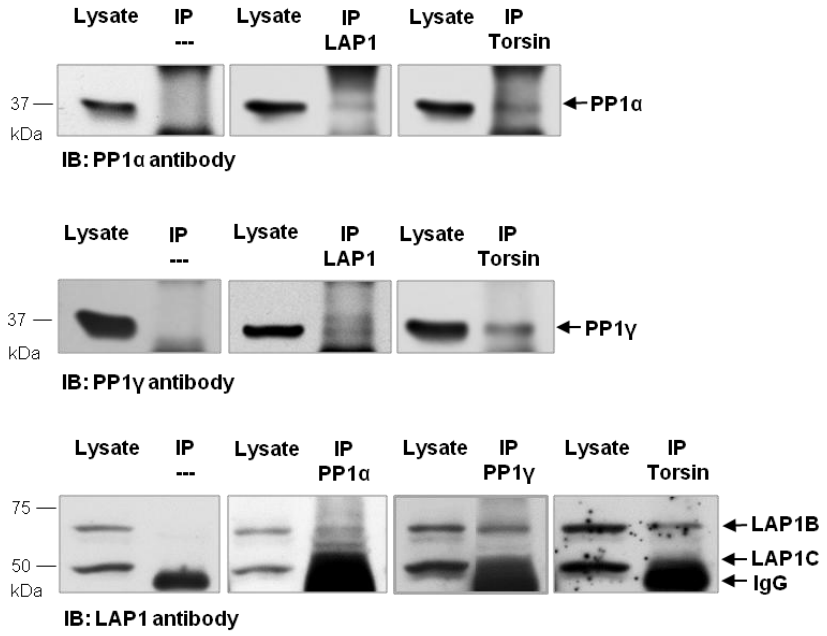

Figure V.C.1. Co-immunoprecipitation of the PP1/LAP1/TorsinA complex in rat cerebellum. Rat cerebellum extracts were immunoprecipitated with PP1α, PP1γ, LAP1 or torsinA antibibodies bound to protein G- Dynabeads. Negative controls were performed by incubating cell extracts with beads. IP, immunoprecipitation. IB, immunobloting.

Having shown that endogenous torsinA (wt-torsinA) forms a complex with LAP1 and PP1, we went on to test if the same happen with ΔE-torsinA mutant. Thus, SH-SY5Y cells overexpressing GFP-wt-torsinA or GFP-ΔE-torsinA were immunoprecipitated using specific LAP1, PP1α or PP1γ antibodies (Fig. V.C.2A). Upon PP1α and PP1γ immunoprecipitation, immunoblotting with GFP antibody was performed in order to detect wt- and ΔE-torsinA in fusion with GFP-tag, and also with LAP1 antibody to detect endogenous LAP1. The results showed that PP1 antibodies immunoprecipitated both wt- and ΔE-torsinA and also LAP1. Moreover, when the immunoprecipitation was carried out with the LAP1 antibody, wt- and ΔE-torsinA and PP1γ could be decteted (Fig. V.C.2B). In addition, similar results were obtained in COS-7 cells using the same methodology (data not shown).

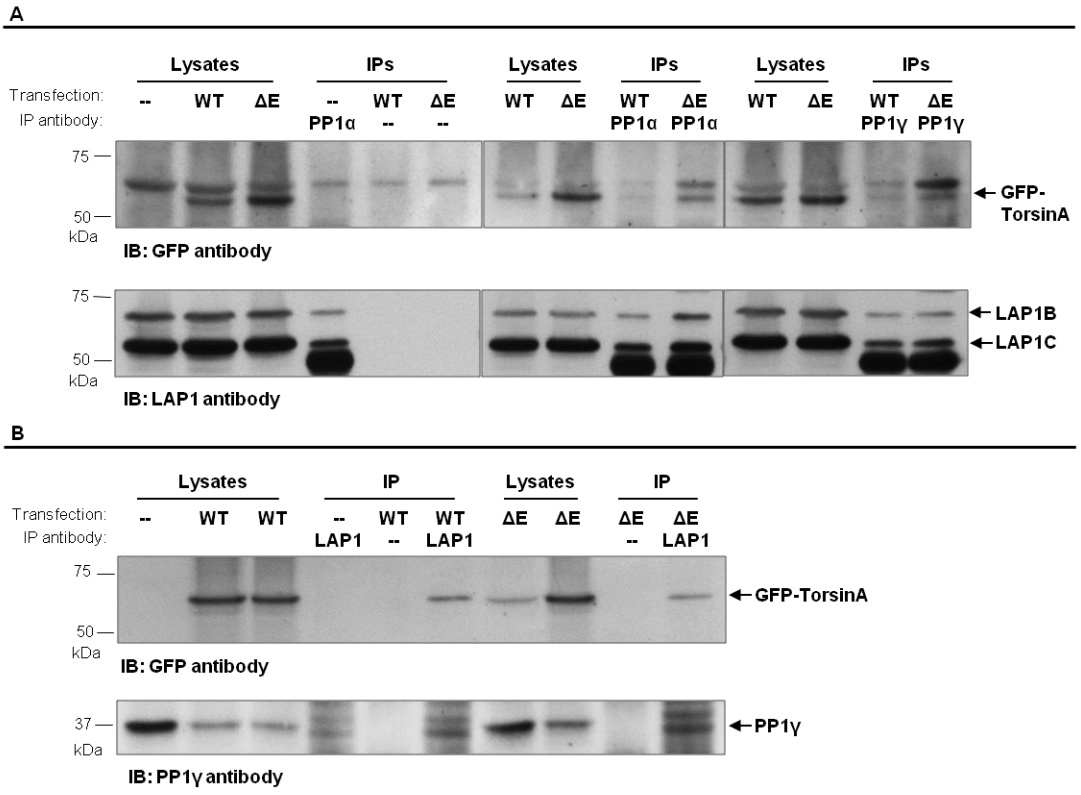

Figure V.C.2. Wt-torsinA and ΔE-torsinA form a complex with LAP1 and PP1. A- SH-SY5Y cells were transfected with GFP-Wt-torsinA or GFP-ΔE-torsinA and immunoprecipitated with PP1α and PP1γ antibodies bound to protein G- Dynabeads. **B-** SH-SY5Y cells were transfected with GFP-wt-torsinA or GFP-ΔE-torsinA and immunoprecipitated with LAP1 antibody bound to protein G- Dynabeads. Negative controls were performed by incubating cell extracts with beads. IP, immunoprecipitation. IB, immunobloting.

V.C.3.2. Localization of the trimeric complex

Having established that PP1, LAP1 and torsinA form a trimeric complex of potential physiological relevance, it is important to unravel its subcellular localization. Thus, SH-SY5Y cells were transfected with GFP-wt-torsinA or GFP-ΔE-torsinA, followed by immunofluorescence analysis using LAP1 and PP1γ specific antibodies (Fig. V.3A and B). Individually, all proteins have the expected subcellular distribution. Namely, GFP-wt-torsinA was found throughout the ER and encircling the nucleus, while GFP-ΔE-torsinA was mainly found in a perinuclear distribution. LAP1 was located in the NE and PP1γ was predominantly found in the nucleus, including the nucleolus, and throughout the cytoplasm. As expected, both torsinA proteins (wt and ΔE) clearly co-localized with LAP1 in the NE, as is evident by the yellow color in the merge images (Fig. V.3A). PP1γ co-localized with wt-torsinA at some points in the

ER/cytoplasm and with both wt- and ΔE-torsinA near the NE (Fig. V.3B), probably at the outer membrane of the NE (cytoplasmic side). Furthermore, SH-SY5Y cells were transfected with Myc-LAP1B followed by immunofluorescence analysis using Myc-tag and PP1γ antibodies. As previously reported by us (Santos et al., 2013), LAP1B and PP1γ co-localize at specific points within the nucleus and near the inner side of the NE (nucleoplasmic side). These results indicate that the common location for PP1, LAP1 and torsinA proteins is the NE, presumably the perinuclear space.

Additionally, SH-SY5Y cells were co-transfected with GFP-wt-torsinA or GFP-ΔE-torsinA plus Myc-LAP1B followed by immunofluorescence analysis using Myc-tag and PP1γ antibodies. The results show that the overexpression of LAP1B and one of the torsinA proteins caused nuclear abnormalities and invaginations of the NE (Fig. V.3C).

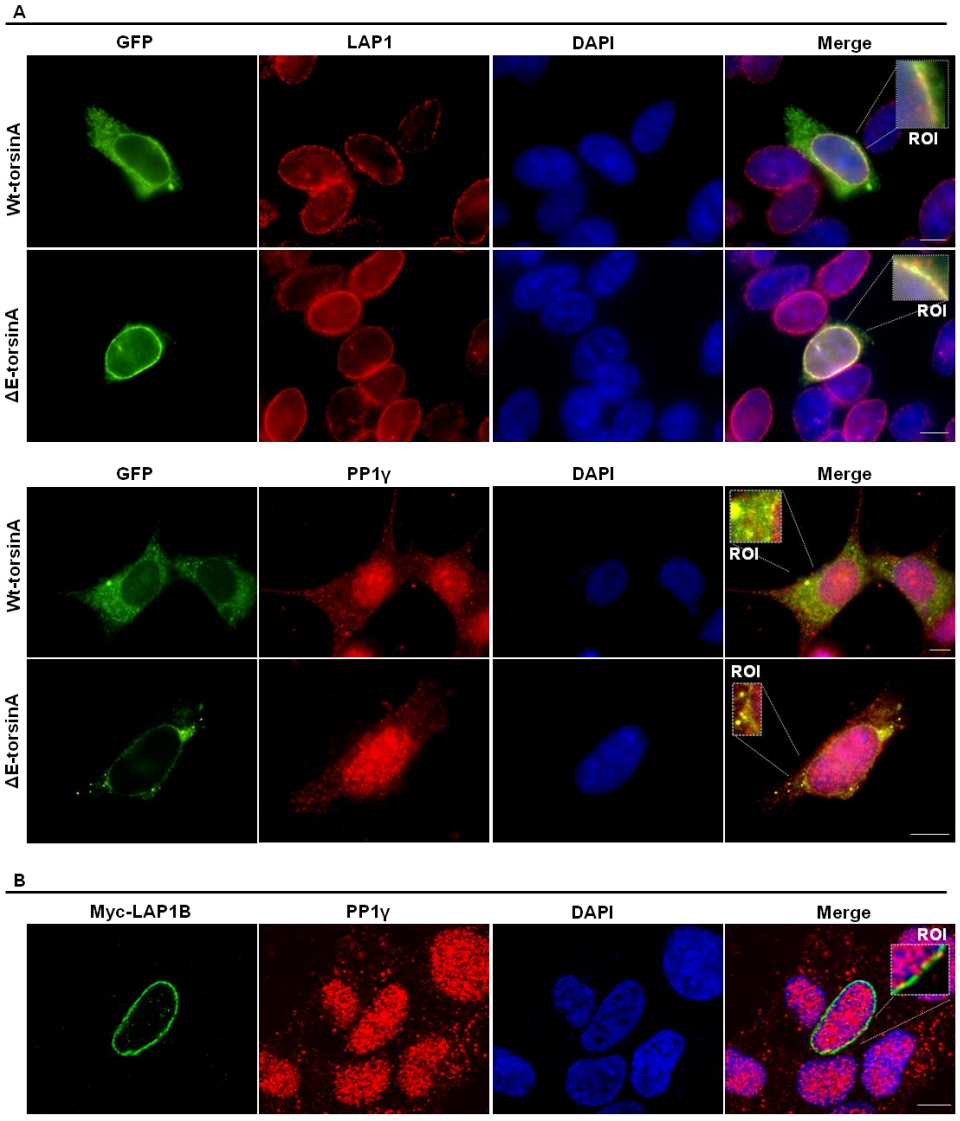

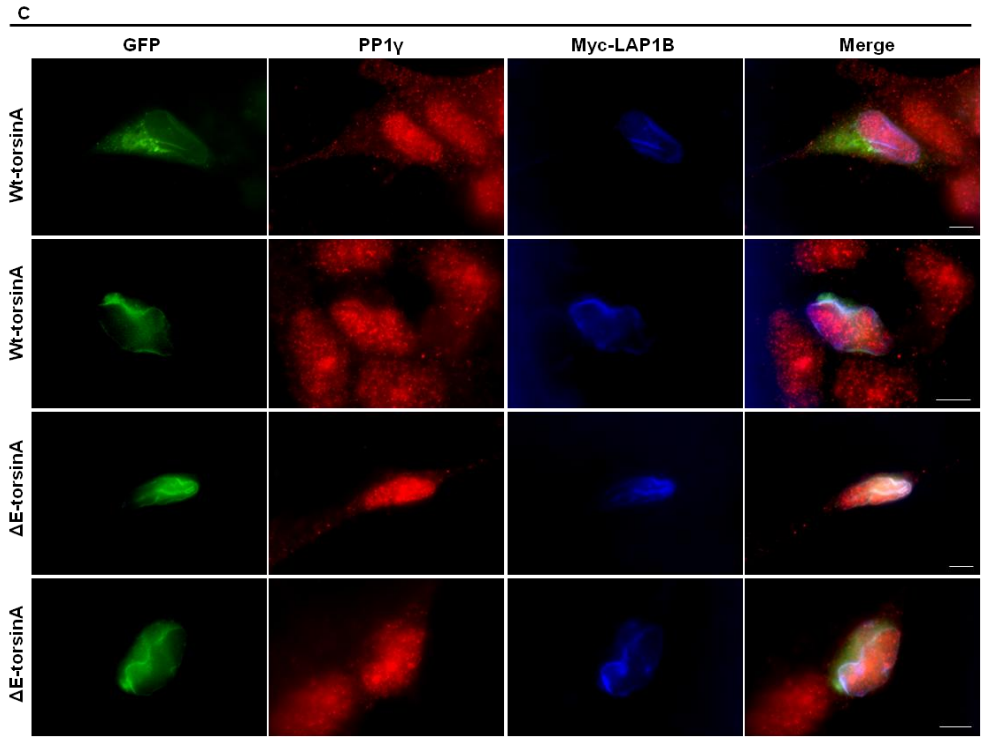

Figure V.C.3. Localization of the PP1/LAP1/TorsinA complex in SH-SY5Y cells. A- Co-localization of overexpressed GFP-wt-torsinA or GFP-ΔE-torsinA with endogenous LAP1 or PP1γ. **B-** Immunolocalization of Myc-LAP1B and endogenous PP1γ. The presence of the complexes is evidenced by the ROI (region of interest). **C-** Nuclear defects were observed in cells overexpressing GFP-wt-torsinA or GFP-ΔE-torsinA plus Myc-LAP1B. GFP was directly visualized. Specific primary antibodies for endogenous LAP1 and PP1γ were detected with Alexa Fluor 594 conjugated secondary antibody (red) and a specific primary antibody for the Myc-tag was detected with Alexa Fluor 350 conjugated secondary antibody (blue). DNA was stained with DAPI. Photographs were acquired using an Olympus epifluoresence microscope. Bars, 10 µm.

V.C.3.3. LAP1 as a bridging protein between torsinA and PP1

LAP1 binds directly to torsinA in the perinuclear space (Goodchild and Dauer, 2005) and to PP1α and γ isoforms in the nucleoplasm (Santos et al., 2013). Thus, it is possible that LAP1 may be a bridging protein between PP1 (inside the nucleus) and torsinA (in the perinuclear space). Moreover, none of the documented PP1 binding motifs (Ayllon et al., 2002; Hendrickx et al., 2009; Meiselbach et al., 2006; Wakula et al., 2003) were identified in torsinA by *in silico* analysis. Nonetheless, in order to understand wheter wt- and ΔE-torsinA bind directly to PP1 or via LAP1, an *in vitro* blot overlay assay was performed. Firstly, human LAP1B, wt-torsinA and ΔE-torsinA proteins were generated by *in vitro* translation (IVT). Subsequently, membranes containing recombinant purified PP1γ1 protein were overlaid with the negative control

of IVT, wt-torsinA or ΔE-torsinA or with LAP1B and then with wt-torsinA or ΔE-torsinA IVTs. Further, immunoblotting was performed using GFP antibody to detect wt- and ΔE-torsinA in fusion with GFP-tag. Upon incubation with LAP1B and subsequently with wt- or ΔE-torsinA, a band of approximately 37 kDa was clearly decteted, which corresponds to the molecular weight of PP1γ1 (Fig. V.C.4). This was not observed when PP1γ1 was directly overlaid with wt- and ΔE-torsinA (in the absence of LAP1B); however a very faint band was detected (Fig. V.C.4). Thus, one cannot indubitable confirm that wt- and ΔE-torsinA do not bind directly to PP1, but LAP1B clearly strengths the binding between these proteins. Moreover, LAP1B binds directly to both wt- and ΔE-torsinA *in vitro* and seems to link torsinA with PP1.

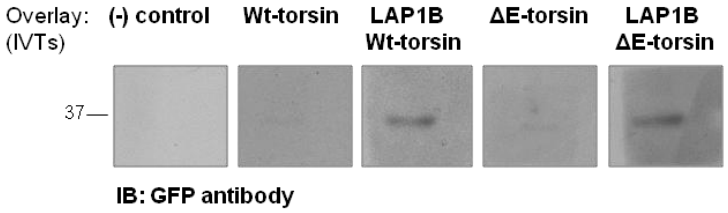

Figure V.C.4. Blot overlay assay. Five samples of purified recombinant PP1γ1 protein were separated by SDS-PAGE and the resulting blot was overlaid with the negative control of IVT [(-) control], wt-torsinA-IVT, ΔE-torsinA-IVT or overlaid with LAP1B-IVT followed by a second overlay with wt-torsinA-IVT or ΔE-torsinA-IVT. IB, immunobloting.

V.C.3.4. TorsinA is dephosphorylated by PP1

TorsinA has several potential phosphorylation sites and at least two residues (Thr 215 and Ser 224) were found to be phosphorylated, as determined by mass spectrometry analysis (Oppermann et al., 2012). Given that torsinA interacts with PP1, it is plausible that this phosphatase is responsible for dephosphorylating torsinA. Hence, SH-SY5Y cells were transfected with GFP-wt-torsinA or GFP-ΔE-torsinA and then incubated with two different concentrations of OA: 0.25 nM or 500 nM that inhibit PP2A and PP2A/PP1, respectively. Cell lysates were further incubated with or without 100 ng of recombinant purified PP1γ1 protein. Proteins were resolved in $MnCl_2$/Phos-tag SDS-PAGE in order to analyze the phosphorylation state of torsinA proteins (Hosokawa et al., 2010; Kinoshita et al., 2006) and in $MnCl_2$ SDS-PAGE for comparative analysis. In the Phos-tag SDS-PAGE, GFP-torsinA proteins apparently migrated as two bands (Fig.

V.C.5C, immunoblotting with GFP antibody). However, it is not clear in the images if the upper (slower migrating) band(s) detected after PP2A/PP1 inhibition (500 nM OA treatment) is a single diffuse band or a doublet. Nevertheless, PP2/PP1 inhibition considerable produces an upward shift of those bands (that are also more intense), which was not seen when PP2A alone was inhibited (0.25 nM OA treatment). Moreover, these effects were reversed upon PP1γ1 incubation *in vitro*; thus showing that the slower migrating bands are phosphorylated species and that PP1γ1 is involved in the dephosphorylation of GFP-wt-torsinA and GFP-ΔE-torsinA proteins. In addition, immunoblotting with torsinA antibody (Fig.V.C.5D) was performed, in order to analyze the phosphorylation state of endogenous torsinA. The results showed that endogenous torsinA migrated as three bands in Phos-tag SDS-PAGE. Moreover, the slower migrating band is only detectable after 500 nM OA treatment in both wt- and ΔE-torsinA transfected cells, in agreement with our previous results. This band is still detectable upon PP1γ1 incubation *in vitro*, but the intensity of the band decreased (Fig. V.C.5D). These results showed that endogenous torsinA is also phosphorylated and is dephosphorylated to some extent by PP1γ1.

Additionally, the phosphorylation state of LAP1 was also analyzed. In $MnCl_2$ SDS-PAGE (Fig. V.C.5B), a slight downward shift of LAP1 was detected in wt-torsinA transfected cells upon incubation with PP1γ1 *in vitro*, but this shift was not so evident in ΔE-torsinA transfected cells (Fig. V.C.5B). Nevertheless, in Phos-tag SDS-PAGE (V.C.5E), LAP1 was separated into several bands with large mobility differences. Interestingly, upon PP2A/PP1 inhibition (500 nM OA) a considerable upward shift of LAP1 was detected, which was not observed when PP2A alone was inhibited (0.25 nM OA). Moreover, this shift was reversed after PP1γ1 incubation in *vitro*, in agreement with our previous studies (Santos et al., 2013). The changes in the phosphorylation state of LAP1 were observed in both wt- and ΔE-torsinA transfected cells; thus showing that the pathogenic ΔE-torsinA mutation does not seem to affect the phosphatase activity of PP1 toward its substrates.

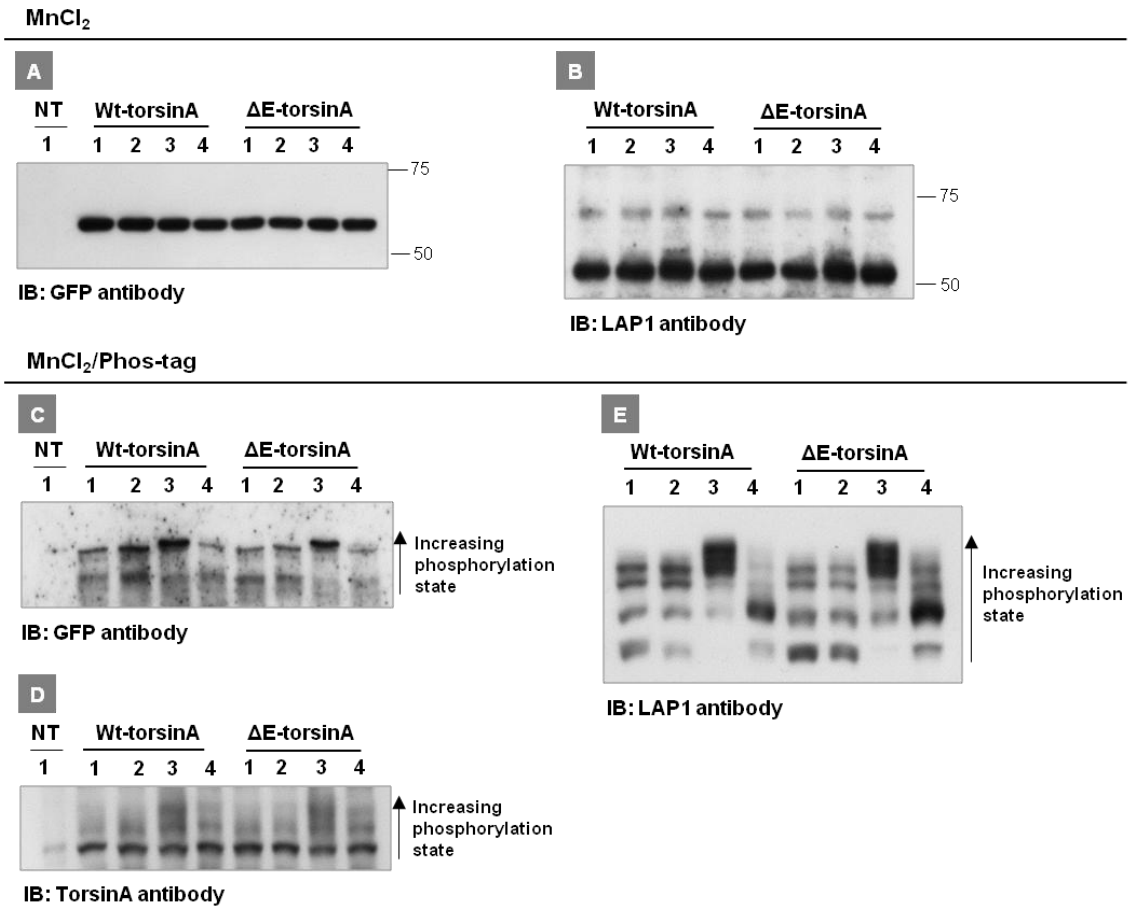

Figure V.C.5. Detection of phosphorylated torsinA proteins. SH-SY5Y cells were transfected with GFP-wt-torsinA or GFP-ΔE-torsinA. Transfected cells were left untreated (lane 1) or treated with 0.25 nM OA (lane 2) or 500 nM OA (lanes 3 and 4) for 3 hours. Cell lysates were then incubated *in vitro* with (lane 4) or without (lanes 1, 2 and 3) purified PP1γ1. Proteins were resolved in SDS-PAGE containing $MnCl_2$ (upper panel, A and B) or 50 µM Phos-tag plus 100 µM $MnCl_2$ (lower panel, C, D and E) for comparative analysis. 1, without OA; 2, 0.25 nM OA; 3, 500 nM OA; 4, 500 nM OA plus PP1γ1 addition. IB, immunoblotting; NT, non-transfected cells.

V.C.3.5. Effects of LAP1 knockdown

To further investigate the physiological relevance of the trimeric complex, down regulation of the bridging protein, LAP1, was performed using specific LAP1-shRNAs. SH-SY5Y cells were transfected with two different pSIREN-LAP1 plasmids (previously described), in order to induce LAP1 knockdown, or with the pSIREN-CMS plasmid as the negative control. Interestingly, reducing the levels of LAP1 (decrease by 42%) resulted in a significant decrease in the expression levels of both PP1γ and torsinA (31% and 40%, respectively) (Fig. V.C.6). Ponceau S staining was used as a loading control.

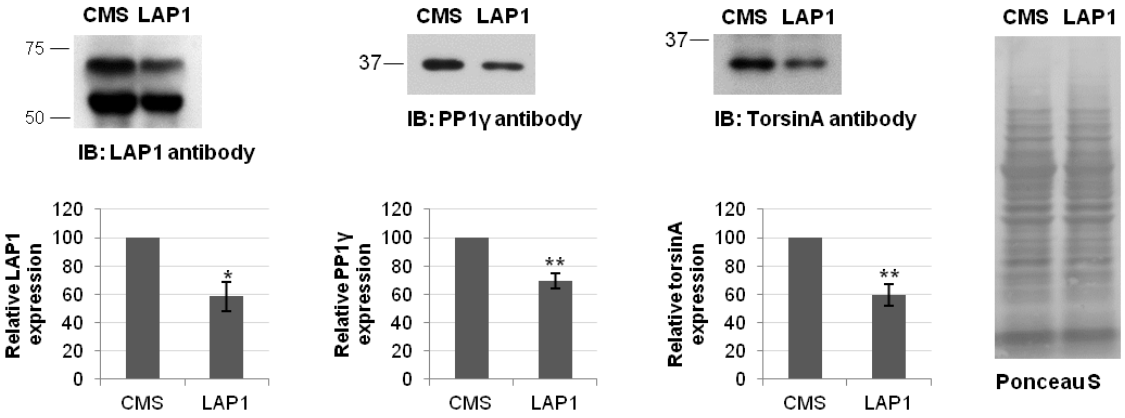

Figure V.C.6. Effects of LAP1 knockdown. SH-SY5Y cells were transfected with two specific LAP1-shRNAs (LAP1) or a control missense shRNA (CMS). Data are presented as mean ± SEM of at least three independent experiments. Statistically different from CMS transfected cells, *****$p < 0.05$, $^{**}p < 0.01$. IB, immunoblotting.

V.C.4. DISCUSSION

TorsinA is localized at different subcellular compartments (ER and NE and cell body and processes of neuronal cells), interacting with different proteins. Consequently, several potential functions have been attributed to torsinA, such as organization of the NE and ER, regulation of the cytoskeleton network, protein processing in the secretory pathway, synaptic vesicle recycling and response to stress (reviewed in Granata et al., 2009). LAP1 was the first binding protein of torsinA identified in the NE (Goodchild and Dauer, 2005). Of note, overexpressed LAP1 was able to recruit wt-torsinA to the NE, while other NE proteins did not produce the same effect. We have recently reported that LAP1 binds to PP1 in the nucleoplasm (Santos et al., 2013).

In this study, LAP1, torsinA and PP1 were shown to form a trimeric complex (Fig. V.C.1, V.C.2 and V.C4). Several immunoprecipitations using specific antibodies directed against these proteins were performed, thereby confirming that LAP1, torsinA and PP1γ and PP1α isoforms are all part of a complex in rat brain (Fig. V.C.1). In order to establish the potential relevance of the latter complex for DYT1 dystonia, the relative association of wt-torsinA and DYT1 dystonia mutant (ΔE-torsinA) in this complex was evaluated. Thus, both wt-torsinA and ΔE-torsinA were found to be in a complex with LAP1 and PP1 isoforms in SH-SY5Y cells (Fig. V.C.2). Conversely, ΔE-torsinA was previously reported to compromise the binding of torsinA ATP-hydrolysis mutant (E171Q-torsinA) with LAP1 (Naismith et al., 2009a; Zhao et al., 2013b). In the absence of ΔE-torsinA, E171Q-torsinA mutant showed high affinity for substrate binding and was found to strongly co-immunoprecipitate with LAP1 (Goodchild and Dauer, 2005). Nevertheless, the results showed that ΔE-torsinA mutant is able to interact with both LAP1 and PP1 (Fig. V.C.2 and V.C.3) in a manner similar to wt-torsinA. This is the first time that torsinA was reported to bind to a protein phosphatase. However, torsinA/PP1 interaction may be indirect and mediated by LAP1 (Fig. V.C.4). Indeed, torsinA does not have any of the canonical PP1 binding motifs previously described (Ayllon et al., 2002; Hendrickx et al., 2009; Meiselbach et al., 2006; Wakula et al., 2003). Most PP1 binding proteins interact with the PP1 catalytic subunit through a conserved PP1 binding motif termed the RVxF motif (Meiselbach et al., 2006; Wakula et al., 2003). Additionally, other PP1 binding motifs have been reported, such as the SILK and the MyPhoNE motifs (Hendrickx et al., 2009) and the apoptotic signature F-X-X-[KR]-X-[KR] (Ayllon et al., 2002). Nevertheless, some proteins bind to PP1

through additional docking motifs. For example, iASPP (inhibitory member of the apoptosis-stimulating proteins of the p53 family) lacks a canonical RVxF binding motif but binds to PP1 through a noncanonical motif (RNYF) (Llanos et al., 2011), and the leucine-rich repeats of sds22 protein are essential for binding to PP1 (Ceulemans et al., 2002b). Thus, one can not exclude the possibility that torsinA interacts directly with PP1, but the overlay assay (Fig. V.C.4) strongly suggests that LAP1 is a bridging protein between PP1 and wt- and ΔE-torsinA proteins.

Reversible protein phosphorylation is a crucial mechanism for signal transduction, regulating the biological activity of diverse proteins (Barford et al., 1998; Cohen, 1989). TorsinA has several potential sites for phosphorylation and two residues (Thr 215 and Ser 224) can be phosphorylated (Oppermann et al., 2012). In addition, another torsin family member, torsinB, seems to also be regulated by phosphorylation (Olsen et al., 2010). However, the involvement of specific kinases and/or phosphatases had not previosuly been documented. The work here described established that torsinA associates with PP1, and is plausible that torsinA can be dephosphorylated by the latter. PP1 catalyzes the majority of protein dephosphorylation events in eukaryotic cells (Bollen et al., 2010; Heroes et al., 2013) and its action is largely determined by binding to different regulatory subunits. These regulatory subunits can be inhibitors of the catalytic activity, substrate-specifying subunits, targeting subunits or substrates of PP1 (Bollen et al., 2009; Bollen et al., 2010). In order to determine if torsinA is a substrate of PP1, Phos-tag SDS-PAGE methodology was applied in order to analyze the phosphorylation state of torsinA. Results showed that the phosphorylated forms of torsinA were upregulated after PP1 inhibition *in vivo* and this effect was reversed upon PP1 addition *in vitro* (Fig. V.C.5). These results were similar for GFP-wt-torsinA, GFP-ΔE-torsinA and endogenous torsinA; thus arguing that torsinA is a substrate of PP1. Moreover, it seems that the presence of ΔE-torsinA mutant does not affect the phosphatase activity of PP1 toward its substrates (torsinA and LAP1). Some PP1 substrates can be either activated by dephosphorylation, as is the case of focal adhesion kinase and caspase 2 (Bollen et al., 2010) or inactivated, as it happens with NEK2 and Aurora-A (Mi et al., 2007). Thus, it will be interesting to understand the effects of PP1 dephosphorylation on torsinA function.

Protein phosphorylation regulates the enzymatic activities and modulates protein-protein interactions (Barford et al., 1998), thereby it is plausible that LAP1 and torsinA (de)phosphorylation events can regulate the interaction between those proteins.

Interestingly, protein phosphorylation has been linked to the regulation of the interaction between NE components during mitosis (Bollen et al., 2009; Guttinger et al., 2009). For example, phosphorylation of lamins is important for lamin depolymerization and NE breakdown (Kuga et al., 2010), while dephosphorylation of lamin B by PP1 leads to lamin polymerization and accompanies NE reassembly (Thompson et al., 1997). Moreover, protein phosphorylation can also regulate the interaction of NE proteins with chromatin (Foisner and Gerace, 1993; Pyrpasopoulou et al., 1996; Takano et al., 2004) and chromatin regulators such as BAF (Hirano et al., 2005). Therefore, LAP1 and torsinA dephosphorylation by PP1 may regulate LAP1 and torsinA interactions at the NE in order to preserve the NE integrity, which may be compromised in DYT1 dystonia. Additionally, aberrant protein phosphorylation of key proteins has been linked to many diseases and dysfunctional states (da Cruz e Silva et al., 1995a; Delobel et al., 2002b; Fardilha et al., 2010; Rebelo et al., 2013; Rebelo et al., 2007; Vieira et al., 2010). Regarding INM proteins, it was reported that mutated forms of emerin found in Emery-Dreifuss muscular dystrophy patients exhibited abnormal cell-cycle dependent phosphorylation forms and altered nuclear lamina interaction (Ellis et al., 1998). Interestingly, emerin was recently found to bind to LAP1 and conditional depletion of LAP1 from mouse striated muscle caused muscular dystrophy (Shin et al., 2013). In closing, given that LAP1 and torsinA are regulated by reversible protein phosphorylation, and that PP1 dephosphorylates both proteins, this provides novel insights into DYT1 dystonia and other NE-related diseases pathogenesis.

CHAPTER VI - DISCUSSION AND CONCLUDING REMARKS

VI.1. LAP1B, A NOVEL PP1 BINDING PROTEIN

Several clones encoding human LAP1B (NM_001267578) were identified in YTH screens of a human brain cDNA library using PP1 α, γ1 and γ2 isoforms as baits (Esteves et al., 2012a; Esteves et al., 2013a; Santos et al., 2013). The interaction between LAP1B and PP1 was validated using different techniques (yeast co-transformation, blot overlay assay and co-immunoprecipitations). Moreover, the LAP1B/PP1 binding is direct as confirmed *in vitro* by blot overlay assay. LAP1B interacts with PP1 through a conserved RVxF-like motif (REVRF) located in the nucleoplasmic domain. Microscopic analysis confirmed the association between LAP1 and PP1 in the nucleoplasm and near the INM. Furthermore, LAP1B is a substrate of PP1, since PP1 dephosphorylated LAP1B *in vitro*. From these results we were able to describe a novel PP1 regulatory protein.

Interestingly, the majority of PP1 binding proteins are located in the nucleus, cytoplasm and plasma membrane (Esteves et al., 2013a; Heroes et al., 2013). However, LAP1B (Santos et al., 2013) and AKAP1-149 (Steen et al., 2000) are the only PP1 binding proteins specifically located at the NE. AKAP-149 functions as a PP1 targeting protein by recruiting PP1 to the NE upon NE assembly and promoting lamin B dephosphorylation and polymerization (Steen and Collas, 2001; Steen et al., 2000; Thompson et al., 1997). LAP1B also binds to lamins, thereby it is plausible that LAP1B also function as a PP1 targeting protein in order to promote lamins or other NE proteins dephosphorylation. In addition, PP1-mediated dephosphorylation of LAP1B may also regulate the function of the latter or even the interaction between LAP1B and other NE proteins or chromatin. Dephosphorylation of NE proteins is an important mechanism that promotes NE reassembly at the end of mitosis (Bollen et al., 2009; Guttinger et al., 2009). Thus, dephosphorylation of LAP1B by PP1 may present itself as an important regulatory mechanism for NE reassembly during mitosis.

VI.2. IDENTIFICATION OF A NOVEL HUMAN LAP1 ISOFORM (LAP1C)

The complexity of the NE components and protein composition increased throughout evolution. Several INM proteins were first found in metazoans and some proteins such as LAP1 were found, thus far, only in vertebrates. It would appear that the emergence of INM proteins such as LAP1 probably conferred a selective advantage to vertebrates (Cohen et al., 2001; Mans et al., 2004). In rat, the LAP1 gene (*TOR1AIP1*) undergoes alternative splicing to originate three LAP1 isoforms (LAP1A, B and C) (Martin et al., 1995; Senior and Gerace, 1988). *In silico* analysis of mouse LAP1 transcripts present in the GenBank database showed that, at least, three LAP1 isoforms are originated by alternative splicing of mouse *TOR1AIP1* gene. However, it remained unclear, until this work, if the same occurs with the human *TOR1AIP1* gene. Previous results had identified only the LAP1B isoform in human cells (Kondo et al., 2002). Moreover, all clones identified in our previous YTH screen (using PP1 isoforms as baits) corresponded to the LAP1B isoform (Esteves et al., 2012a; Esteves et al., 2013a; Santos et al., 2013). Nevertheless, given the diversity of LAP1 isoforms identified in other species, we decided to further clarify the existence of additional human LAP1 family members.

ShRNA-mediated knockdown of LAP1 in human cells resulted in specific reductions of the expression of two proteins: a higher molecular weight protein (approximately 68 kDa), which corresponds to the known LAP1B isoform, and a lower molecular weight protein (approximately 56 kDa). Mass spectrometry analysis of these proteins, revealed that the 56 kDa protein is N-terminally truncated compared to the LAP1B isoform. Given its molecular weight similarity with rat LAP1C, we designated the newly identified human LAP1 isoform as LAP1C. Moreover, LAP1B and LAP1C were shown to be products of different RNAs and thereby their generation must be regulated at the transcriptional level, possibly by alternative promoter usage. The existence of non-RefSeq mRNAs matching with the LAP1C sequence in GenBank corroborates this hypothesis.

The newly identified human LAP1C has a shorter nucleoplasmic domain. Thereby, LAP1C was more easily solubilized after detergent/salt treatment, compared to LAP1B, in agreement with previous reports regarding rat LAP1 isoforms (Foisner and Gerace, 1993). Kondo *et al* reported that the entire nucleoplasmic domain of human LAP1B may be required for full retention at the INM (Kondo et al., 2002). Therefore, a

fraction of LAP1C may reside in other subcellular compartments in addition to the INM. Moreover, the lost of the N-terminal nucleoplasmic domain may affect protein-protein interactions; consequently LAP1C and LAP1B may have different binding partners. For example, LAP1C lacks the PP1 binding motif (REVRF) present in LAP1B. Nevertheless, PP1 was able to dephosphorylate LAP1C, as well as LAP1B, under our experimental conditions. This could happen due to an indirect interaction between LAP1C and PP1, probably via other nuclear proteins such as lamins, or even via LAP1B. Furthermore, functional characterization of both human LAP1 isoforms showed that they are differentially expressed across diverse human cell lines and tissues. LAP1C was the major isoform detected in different cultured cell lines in agreement with previous reports regarding rat LAP1C (Senior and Gerace, 1988). In contrast, the abundance of LAP1B/LAP1C in human tissues is dependent on the specific tissue. Interestingly, human LAP1B is more abundant in brain and is upregulated later during SH-SY5Y cells differentiation when compared to LAP1C. Moreover, the expression levels of rat LAP1B/LAP1C during maturation of rat cortical primary cultures correlate well with those observed for human LAP1B in differentiated SH-SY5Y cells.

VI.3. POTENTIAL ROLE OF LAP1 PROTEINS DURING CELL CYCLE

The association of LAP1 proteins with lamins and chromatin (Foisner and Gerace, 1993) suggests that LAP1 is involved in the positioning of lamins and chromatin in close proximity to the NE, thereby contributing to the maintenance of the NE structure (Gerace and Huber, 2012; Martin et al., 1995). Moreover, Kim *et al* reported that various tissues and cultured neurons of *TOR1AIP1* knockout mice embryos exhibit NE abnormalities such as “blebs – vesicle-appearing structures” in the perinuclear space (Kim et al., 2010a), thus arguing that LAP1 is a key protein in the NE. In support of this role, we showed that downregulation of human LAP1 proteins (LAP1B and LAP1C) in SH-SY5Y cells cause nuclear abnormalities and decrease expression of lamins and acetylated α-tubulin. Decreased levels of tubulin acetylation could be the result of microtubule instability due to disruption of NE integrity and loss of connection between the nucleoplasm and the cytoskeleton (disruption of the LINC complex).

In addition, LAP1 co-localized with acetylated α-tubulin in the mitotic spindle and midbody microtubules, suggesting that LAP1 and microtubules are functionally associated during mitosis. In agreement wih this, Neumann *et al* reported that downregulation of LAP1 led to the formation of defective mitotic spindles and thereby aberrant mitotic exit (Neumann et al., 2010). Moreover, LAP1 also co-localized with γ-tubulin in centrosomes. Other NE proteins, such as emerin and SAMP1, were found to be involved in centrosome positioning and connection to the NE (Buch et al., 2009; Salpingidou et al., 2007).

Furthermore, cell cycle-dependent phosphorylation of LAP1 proteins could regulate LAP1 function and interactions. In agreement with mass spectrometry data (Dephoure et al., 2008; Olsen et al., 2010), we showed that LAP1 proteins are highly phosphorylated during mitosis using the Phos-tag SDS-PAGE method. Interestingly, the activity of PP1, which is responsible for the dephosphorylation of LAP1 proteins, seems to be repressed at early-mid mitosis (Kwon et al., 1997).

VI.4. RELEVANCE OF PP1/LAP1/TORSINA COMPLEX IN DYT1 DYSTONIA

The finding that PP1 interacts with LAP1, which in turn binds to torsinA, opens a new perspective in the study of DYT1 dystonia. PP1 interacts with the nucleoplasmic domain of LAP1B (Santos et al., 2013), while torsinA binds to the lumenal domain of LAP1 in the perinuclear space (Goodchild and Dauer, 2005). The lumenal domain of LAP1 is conserved between LAP1 isoforms, thus it is reasonable to deduce that torsinA interacts with all LAP1 isoforms. In this study, the interaction between PP1, LAP1 and torsinA proteins was confirmed by co-immunoprecipitation in rat brain and human SH-SY5Y cells and by an *in vitro* blot overlay assay. Moreover, both wt-torsinA and DYT1 dystonia mutant (ΔE-torsinA) were found to interact with PP1 and LAP1. Therefore, we identified a novel trimeric complex composed by PP1, LAP1 and torsinA. In this trimeric complex, LAP1 seems to function as a bridging protein to bring PP1 into close proximity with torsinA that lacks a canonical PP1 binding motif. Furthermore, torsinA was shown to be regulated by reversible protein phosphorylation and PP1 is able to dephosphorylate torsinA.

VI.4.1. DYT1 dystonia, a nuclear envelope-related disease

Mutations in genes encoding NE proteins have been associated with increasing number of diseases referred to as laminopathies or nuclear envelopathies. The molecular mechanisms underlying these diseases are still not clearly understood. However, some proposed mechanisms that explain how these mutations cause disease are loss of assembly or stability of protein complexes, disruption of lamin-cytoskeleton interactions, altered gene expression and cell cycle abnormalities (Dauer and Worman, 2009; Dorner et al., 2007; Wilkie et al., 2011). These diseases result from mutations in genes encoding widely expressed proteins of the nuclear envelope and many have tissue-selective effects (Dauer and Worman, 2009). DYT1 dystonia is a CNS selective nuclear envelopathy caused by a mutation in the *TOR1A* gene encoding torsinA protein (Ozelius et al., 1997). Wt-torsinA has been localized in the ER and between the inner and outer nuclear membranes, while DYT1 dystonia mutant (ΔE-torsinA) abnormally concentrate between the NE membranes (Goodchild et al., 2005; Hewett et al., 2003; Kustedjo et al., 2000; Naismith et al., 2004). The accumulation of torsinA in the NE results in abnormal morphology of the NE and the presence of inclusions (Gonzalez-Alegre and Paulson, 2004; Goodchild et al., 2005; Hewett et al., 2000). However this phenotype seems to be specific of neuronal cells. ΔE-torsinA knock-in mice exhibit abnormalities in the NE membranes specifically in neurons. Moreover, neurons from torsinA knockout mice display similar NE abnormalities, although non-neuronal cell types appear normal (Goodchild et al., 2005). However, reducing LAP1 levels in torsinA null fibroblasts causes NE abnormalities, thus suggesting that these proteins are functionally related (Kim et al., 2010a).

VI.4.2. Potential role of the PP1/LAP1/TorsinA complex in NE dynamics

PP1 has several regulatory binding subunits in the nucleus; thereby PP1 can regulate different nuclear functions such as mRNA processing, transcription and cell cycle events (reviewed in Bollen and Beullens, 2002; Ceulemans and Bollen, 2004). During cell cycle, PP1 is particularly important in the reformation of the NE (Steen and Collas, 2001; Steen et al., 2000; Thompson et al., 1997). Indeed, NE breakdown and reassembly are complex processes that are regulated by reversible protein

phosphorylation (Bollen et al., 2009; Guttinger et al., 2009). LAP1 and torsinA dephosphorylation by PP1 may promote NE reformation and regulate LAP1 and torsinA interactions at the NE in order to preserve NE integrity. LAP1 and torsinA seem to be functionally related in the maintenance of the NE structure in neurons, since both *TOR1AIP1* and *TOR1A* knockout mice display similar NE abnormalities (Kim et al., 2010a). Interestingly, another AAA^+ protein termed p97 was found to be involved in the final phases of NE reformation in order to form a sealed NE *in vitro*, presumably in association with a receptor protein in the NE (Burke and Ellenberg, 2002; Hetzer et al., 2001).

LAP1 and torsinA may participate in the regulation of the LINC complex which is required to maintain the structure and integrity of the NE as well as the nuclear size, shape and positioning of nuclei (reviewed in Rothballer and Kutay, 2013). LAP1 binds to lamins and may contribute to its positioning in close proximity with the NE. As previously described, downregulation of LAP1 in SH-SY5Y cells caused decreased expression levels of lamin B1 and acetylated α-tubulin (Chapter IV). In addition, downregulation of LAP1 caused a decrease in the expression levels of its binding partners torsinA and PP1. Moreover, LAP1 depletion in fibroblasts caused the mislocalization of emerin (Shin et al., 2013), which can bind directly to microtubules and actin (Holaska et al., 2004; Salpingidou et al., 2007). TorsinA interacts with the LINC components nesprins (Nery et al., 2008) and SUN proteins (Jungwirth et al., 2011). Depletion of torsinA caused mislocalization of nesprin-3 to the ER and affects the positioning of the nucleus (Nery et al., 2008), while ΔE-torsinA overexpression lead to the accumulation of vimentin, which binds to nesprin-3 through plectin, around the nucleus (Hewett et al., 2006). In addition, our results provided evidence that ΔE-torsinA overexpression affects the expression/localization of tubulin and F-actin.

Reversible protein phosphorylation is a mechanism capable of modulating protein-protein interactions (Barford et al., 1998), thereby it is plausible that LAP1 and torsinA (de)phosphorylation events contribute to the maintenance of the NE structure through regulation of protein-protein interactions at the NE. Moreover protein phosphorylation can regulate the interaction of NE proteins with chromatin (Foisner and Gerace, 1993; Pyrpasopoulou et al., 1996; Takano et al., 2004) and chromatin regulators such as BAF (Hirano et al., 2005). Additionally, aberrant protein phosphorylation on key proteins has been linked to many diseases and dysfunctional states (da Cruz e Silva et al., 1995a; Delobel et al., 2002a). For example, neurofibrillary tangles found in

Alzheimer's disease patients are composed of a hyperphosphorylated form of the microtubule-stabilizing protein tau. Inhibition of PP1 and PP2A could lead to the hiperphosphorylation of tau (Malchiodi-Albedi et al., 1997). Regarding INM proteins, it was reported that mutated forms of emerin found in Emery-Dreifuss muscular dystrophy patients exhibited abnormal cell-cycle dependent phosphorylation forms and altered nuclear lamina interaction (Ellis et al., 1998).

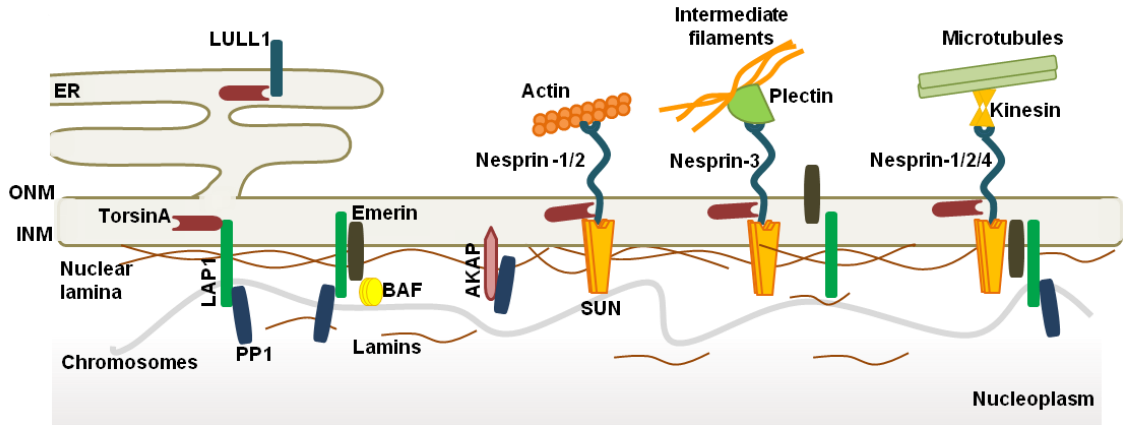

Figure VI.1. Schematic illustration of LAP1, PP1 and torsinA interactions at the nuclear envelope. TorsinA can be found in both the endoplasmic reticulum (ER), where it interacts with LULL1, and lumen of the perinuclear space. In the nuclear envelope torsinA can bind to proteins of the inner nuclear membrane (INM) like LAP1 and SUN and to nesprins located in the outer nuclear membrane (ONM). SUN proteins bind to lamins and to nesprins, which in turn bind to cytoskeleton elements (F-actin, kinesin/microtubules and plectin/intermediate filaments). LAP1 is located in the INM where it binds to both torsinA (in the perinuclear space) and PP1 in the nucleoplasm. LAP1 can also bind to lamins, chromosomes and emerin. The latter can be localized in both the inner and outer nuclear membranes and interacts directly with lamins, SUN, nesprins and chromatin associated protein BAF. PP1 is highly abundant in the nucleus and is linked to the NE through interaction with AKAP-149, lamins and LAP1.

VI.4.3. Abnormal dopamine signaling in DYT1 dystonia

TorsinA, LAP1 and PP1 are ubiquitously expressed (da Cruz e Silva et al., 1995b; Goodchild and Dauer, 2005; Ozelius et al., 1997), but PP1 and torsinA are both present at high levels of expression in the brain (Augood et al., 1999; da Cruz e Silva et al., 1995b; Ozelius et al., 1997). Moreover, ΔE-torsinA has a specific neurological phenotype (Giles et al., 2008; Goodchild et al., 2005), suggesting that torsinA plays a specific role in selected neuronal cells. In support of this, torsinA is expressed at high levels within dopaminergic neurons of the substantia nigra pars compacta. PP1α and PP1γ1 have the highest levels of expression in the striatum, where they were shown to be relatively enriched in the medium-sized spiny neurons (da Cruz e Silva et al., 1995b; Ouimet et al., 1995), which express DARPP-32 (Ouimet et al., 1984). DARPP-32 has a crucial role in dopaminergic transmission and is a potent inhibitor of PP1 when phosphorylated at Thr34. The state of (de)phosphorylation of DARPP-32 is modulated by dopamine and other neurotransmitters in the striatum. Dopamine, acting on D1 receptors, causes activation of PKA and phosphorylation of DARPP-32 on Thr 34. Conversely, dopamine, acting on D2 receptors, causes the dephosphorylation of DARPP-32, through inhibition of PKA and activation of PP2B (Greengard et al., 1999). Several studies in mouse models have provided evidence that DYT1 dystonia is related with impaired dopaminergic and cholinergic signalling. Particularly, reduced D2 receptor activity and function have been documented (Dang et al., 2012; Giannakopoulou et al., 2010; Napolitano et al., 2010; Pisani et al., 2006; Yokoi et al., 2011). Therefore, D2-deficiency may alter the rate of phosphorylation of DARPP-32, resulting in reduced activity of PP1, which controls the state of phosphorylation and the physiological activity of several neuronal phosphoproteins. The hypothesis that PP1 and/or abnormal protein phosphorylation may have a key role in DYT1 dystonia seems worthwhile exploring in the future.

VI.5. CONCLUDING REMARKS

LAP1 was identified in 1988 but its function remains poorly understood. Later, LAP1 was found to interact with torsinA, which abnormally concentrates in the NE, indicating that LAP1 is involved in the pathogenesis of DYT1 dystonia. Nevertheless, the molecular mechanisms underlying the neuropathology of DYT1 dystonia are not clearly understood.The work included in this thesis provides important new insights into the biological properties of LAP1 proteins and LAP1 proteins complexes.

In conclusion this work resulted in:

- the validation of LAP1B as a novel PP1 binding protein in the nuclear envelope;
- the identification and characterization of the novel human LAP1C isoform;
- the uncovering of the potential role of LAP1 proteins during cell cycle;
- the identification of the novel PP1/LAP1/torsinA complex;
- the identification of LAP1 and torsinA (wt- and ΔE-torsinA) as phosphoproteins and substrates of PP1.

The fact that LAP1 and torsinA are regulated by reversible protein phosphorylation, and that PP1 dephosphorylates both proteins, opens a new perspective in the study of DYT1 dystonia. Altough the findings presented here do not provide a definitive role for protein phosphorylation/PP1 in DYT1 dystonia pathogenesis, they do provide a basis for futures studies. Moreover, our work suggests that the function of protein complexes in the nuclear envelope, particular LAP1 complexes, may underlie the pathology of nuclear envelope-related diseases such as DYT1 dystonia. Thereby, the functional relevance of these complexes should be pursued in the future.

REFERENCES

Abdelmohsen, K., Srikantan, S., Yang, X., Lal, A., Kim, H.H., Kuwano, Y., Galban, S., Becker, K.G., Kamara, D., de Cabo, R., *et al.* (2009). Ubiquitin-mediated proteolysis of HuR by heat shock. EMBO J *28*, 1271-1282.

Adolph, K.W. (1987). ADPribosylation of nuclear proteins labeled with [3H]adenosine: changes during the HeLa cycle. Biochimica et biophysica acta *909*, 222-230.

Aebi, U., Cohn, J., Buhle, L., and Gerace, L. (1986). The nuclear lamina is a meshwork of intermediate-type filaments. Nature *323*, 560-564.

Ajuh, P.M., Browne, G.J., Hawkes, N.A., Cohen, P.T., Roberts, S.G., and Lamond, A.I. (2000). Association of a protein phosphatase 1 activity with the human factor C1 (HCF) complex. Nucleic acids research *28*, 678-686.

Albanese, A., Bhatia, K., Bressman, S.B., Delong, M.R., Fahn, S., Fung, V.S., Hallett, M., Jankovic, J., Jinnah, H.A., Klein, C., *et al.* (2013). Phenomenology and classification of dystonia: A consensus update. Movement disorders : official journal of the Movement Disorder Society.

Allen, P.B., Kwon, Y.G., Nairn, A.C., and Greengard, P. (1998). Isolation and characterization of PNUTS, a putative protein phosphatase 1 nuclear targeting subunit. J Biol Chem *273*, 4089-4095.

Allen, P.B., Ouimet, C.C., and Greengard, P. (1997). Spinophilin, a novel protein phosphatase 1 binding protein localized to dendritic spines. Proc Natl Acad Sci U S A *94*, 9956-9961.

Altschul, S.F., Gish, W., Miller, W., Myers, E.W., and Lipman, D.J. (1990). Basic local alignment search tool. Journal of molecular biology *215*, 403-410.

Andreassen, P.R., Lacroix, F.B., Villa-Moruzzi, E., and Margolis, R.L. (1998). Differential subcellular localization of protein phosphatase-1 alpha, gamma1, and delta isoforms during both interphase and mitosis in mammalian cells. J Cell Biol *141*, 1207-1215.

Arnone, J.T., Walters, A.D., and Cohen-Fix, O. (2013). The dynamic nature of the nuclear envelope: lessons from closed mitosis. Nucleus *4*, 261-266.

Asanuma, K., Ma, Y., Okulski, J., Dhawan, V., Chaly, T., Carbon, M., Bressman, S.B., and Eidelberg, D. (2005). Decreased striatal D2 receptor binding in non-manifesting carriers of the DYT1 dystonia mutation. Neurology *64*, 347-349.

Augood, S.J., Hollingsworth, Z., Albers, D.S., Yang, L., Leung, J.C., Muller, B., Klein, C., Breakefield, X.O., and Standaert, D.G. (2002). Dopamine transmission in DYT1 dystonia: a biochemical and autoradiographical study. Neurology *59*, 445-448.

Augood, S.J., Keller-McGandy, C.E., Siriani, A., Hewett, J., Ramesh, V., Sapp, E., DiFiglia, M., Breakefield, X.O., and Standaert, D.G. (2003). Distribution and ultrastructural localization of torsinA immunoreactivity in the human brain. Brain research *986*, 12-21.

Augood, S.J., Martin, D.M., Ozelius, L.J., Breakefield, X.O., Penney, J.B., Jr., and Standaert, D.G. (1999). Distribution of the mRNAs encoding torsinA and torsinB in the normal adult human brain. Annals of neurology *46*, 761-769.

Augood, S.J., Penney, J.B., Jr., Friberg, I.K., Breakefield, X.O., Young, A.B., Ozelius, L.J., and Standaert, D.G. (1998). Expression of the early-onset torsion dystonia gene (DYT1) in human brain. Annals of neurology *43*, 669-673.

Ayllon, V., Cayla, X., Garcia, A., Fleischer, A., and Rebollo, A. (2002). The anti-apoptotic molecules Bcl-xL and Bcl-w target protein phosphatase 1alpha to Bad. European journal of immunology *32*, 1847-1855.

Ayllon, V., Cayla, X., Garcia, A., Roncal, F., Fernandez, R., Albar, J.P., Martinez, C., and Rebollo, A. (2001). Bcl-2 targets protein phosphatase 1 alpha to Bad. J Immunol *166*, 7345-7352.

Balcioglu, A., Kim, M.O., Sharma, N., Cha, J.H., Breakefield, X.O., and Standaert, D.G. (2007). Dopamine release is impaired in a mouse model of DYT1 dystonia. J Neurochem *102*, 783-788.

Bao, L., Patel, J.C., Walker, R.H., Shashidharan, P., and Rice, M.E. (2010). Dysregulation of striatal dopamine release in a mouse model of dystonia. J Neurochem *114*, 1781-1791.

Barascu, A., Le Chalony, C., Pennarun, G., Genet, D., Imam, N., Lopez, B., and Bertrand, P. (2012). Oxidative stress induces an ATM-independent senescence pathway through p38 MAPK-mediated lamin B1 accumulation. EMBO J *31*, 1080-1094.

Barford, D., Das, A.K., and Egloff, M.P. (1998). The structure and mechanism of protein phosphatases: insights into catalysis and regulation. Annual review of biophysics and biomolecular structure *27*, 133-164.

Barker, H.M., Brewis, N.D., Street, A.J., Spurr, N.K., and Cohen, P.T. (1994). Three genes for protein phosphatase 1 map to different human chromosomes: sequence, expression and gene localisation of protein serine/threonine phosphatase 1 beta (PPP1CB). Biochimica et biophysica acta *1220*, 212-218.

Barker, H.M., Craig, S.P., Spurr, N.K., and Cohen, P.T. (1993). Sequence of human protein serine/threonine phosphatase 1 gamma and localization of the gene (PPP1CC) encoding it to chromosome bands 12q24.1-q24.2. Biochimica et biophysica acta *1178*, 228-233.

Basham, S.E., and Rose, L.S. (2001). The Caenorhabditis elegans polarity gene ooc-5 encodes a Torsin-related protein of the AAA ATPase superfamily. Development *128*, 4645-4656.

Baucum, A.J., 2nd, Strack, S., and Colbran, R.J. (2012). Age-dependent targeting of protein phosphatase 1 to Ca2+/calmodulin-dependent protein kinase II by spinophilin in mouse striatum. PloS one *7*, e31554.

Bauman, A.L., Goehring, A.S., and Scott, J.D. (2004). Orchestration of synaptic plasticity through AKAP signaling complexes. Neuropharmacology *46*, 299-310.

Bengtsson, L., and Otto, H. (2008). LUMA interacts with emerin and influences its distribution at the inner nuclear membrane. J Cell Sci *121*, 536-548.

Bennecib, M., Gong, C.X., Grundke-Iqbal, I., and Iqbal, K. (2000). Role of protein phosphatase-2A and -1 in the regulation of GSK-3, cdk5 and cdc2 and the phosphorylation of tau in rat forebrain. FEBS Lett *485*, 87-93.

Berger, R., Theodor, L., Shoham, J., Gokkel, E., Brok-Simoni, F., Avraham, K.B., Copeland, N.G., Jenkins, N.A., Rechavi, G., and Simon, A.J. (1996). The characterization and localization of the mouse thymopoietin/lamina-associated polypeptide 2 gene and its alternatively spliced products. Genome Res *6*, 361-370.

Bibb, J.A., Snyder, G.L., Nishi, A., Yan, Z., Meijer, L., Fienberg, A.A., Tsai, L.H., Kwon, Y.T., Girault, J.A., Czernik, A.J., *et al.* (1999). Phosphorylation of DARPP-32 by Cdk5 modulates dopamine signalling in neurons. Nature *402*, 669-671.

Bione, S., Maestrini, E., Rivella, S., Mancini, M., Regis, S., Romeo, G., and Toniolo, D. (1994). Identification of a novel X-linked gene responsible for Emery-Dreifuss muscular dystrophy. Nat Genet *8*, 323-327.

Blethrow, J.D., Glavy, J.S., Morgan, D.O., and Shokat, K.M. (2008). Covalent capture of kinase-specific phosphopeptides reveals Cdk1-cyclin B substrates. Proc Natl Acad Sci U S A *105*, 1442-1447.

Blitzer, R.D., Connor, J.H., Brown, G.P., Wong, T., Shenolikar, S., Iyengar, R., and Landau, E.M. (1998). Gating of CaMKII by cAMP-regulated protein phosphatase activity during LTP. Science *280*, 1940-1942.

Bollen, M. (2001). Combinatorial control of protein phosphatase-1. Trends Biochem Sci *26*, 426-431.

Bollen, M., and Beullens, M. (2002). Signaling by protein phosphatases in the nucleus. Trends Cell Biol *12*, 138-145.

Bollen, M., Gerlich, D.W., and Lesage, B. (2009). Mitotic phosphatases: from entry guards to exit guides. Trends Cell Biol *19*, 531-541.

Bollen, M., Peti, W., Ragusa, M.J., and Beullens, M. (2010). The extended PP1 toolkit: designed to create specificity. Trends in biochemical sciences *35*, 450-458.

Bonne, G., Di Barletta, M.R., Varnous, S., Becane, H.M., Hammouda, E.H., Merlini, L., Muntoni, F., Greenberg, C.R., Gary, F., Urtizberea, J.A., *et al.* (1999). Mutations in the

gene encoding lamin A/C cause autosomal dominant Emery-Dreifuss muscular dystrophy. Nat Genet *21*, 285-288.

Bordelon, J.R., Smith, Y., Nairn, A.C., Colbran, R.J., Greengard, P., and Muly, E.C. (2005). Differential localization of protein phosphatase-1alpha, beta and gamma1 isoforms in primate prefrontal cortex. Cereb Cortex *15*, 1928-1937.

Boudrez, A., Beullens, M., Groenen, P., Van Eynde, A., Vulsteke, V., Jagiello, I., Murray, M., Krainer, A.R., Stalmans, W., and Bollen, M. (2000). NIPP1-mediated interaction of protein phosphatase-1 with CDC5L, a regulator of pre-mRNA splicing and mitotic entry. J Biol Chem *275*, 25411-25417.

Brachner, A., and Foisner, R. (2011). Evolvement of LEM proteins as chromatin tethers at the nuclear periphery. Biochemical Society transactions *39*, 1735-1741.

Bragg, D.C., Armata, I.A., Nery, F.C., Breakefield, X.O., and Sharma, N. (2011). Molecular pathways in dystonia. Neurobiol Dis *42*, 136-147.

Bragg, D.C., Kaufman, C.A., Kock, N., and Breakefield, X.O. (2004). Inhibition of N-linked glycosylation prevents inclusion formation by the dystonia-related mutant form of torsinA. Molecular and cellular neurosciences *27*, 417-426.

Breakefield, X.O., Blood, A.J., Li, Y., Hallett, M., Hanson, P.I., and Standaert, D.G. (2008). The pathophysiological basis of dystonias. Nature reviews. Neuroscience *9*, 222-234.

Bressman, S.B., and Saunders-Pullman, R. (2013). Primary dystonia: Moribund or viable. Movement disorders : official journal of the Movement Disorder Society *28*, 906-913.

Brewer, G.J., Torricelli, J.R., Evege, E.K., and Price, P.J. (1993). Optimized survival of hippocampal neurons in B27-supplemented Neurobasal, a new serum-free medium combination. J Neurosci Res *35*, 567-576.

Bridger, J.M., Kill, I.R., O'Farrell, M., and Hutchison, C.J. (1993). Internal lamin structures within G1 nuclei of human dermal fibroblasts. J Cell Sci *104 (Pt 2)*, 297-306.

Broers, J.L., Peeters, E.A., Kuijpers, H.J., Endert, J., Bouten, C.V., Oomens, C.W., Baaijens, F.P., and Ramaekers, F.C. (2004). Decreased mechanical stiffness in LMNA-/- cells is caused by defective nucleo-cytoskeletal integrity: implications for the development of laminopathies. Human molecular genetics *13*, 2567-2580.

Buch, C., Lindberg, R., Figueroa, R., Gudise, S., Onischenko, E., and Hallberg, E. (2009). An integral protein of the inner nuclear membrane localizes to the mitotic spindle in mammalian cells. J Cell Sci *122*, 2100-2107.

Burdette, A.J., Churchill, P.F., Caldwell, G.A., and Caldwell, K.A. (2010). The early-onset torsion dystonia-associated protein, torsinA, displays molecular chaperone activity in vitro. Cell stress & chaperones *15*, 605-617.

Burge, C., and Karlin, S. (1997). Prediction of complete gene structures in human genomic DNA. Journal of molecular biology *268*, 78-94.

Burke, B., and Ellenberg, J. (2002). Remodelling the walls of the nucleus. Nat Rev Mol Cell Biol *3*, 487-497.

Burke, B., and Stewart, C.L. (2013). The nuclear lamins: flexibility in function. Nat Rev Mol Cell Biol *14*, 13-24.

Butler, A.G., Duffey, P.O., Hawthorne, M.R., and Barnes, M.P. (2004). An epidemiologic survey of dystonia within the entire population of northeast England over the past nine years. Adv Neurol *94*, 95-99.

Caldwell, G.A., Cao, S., Sexton, E.G., Gelwix, C.C., Bevel, J.P., and Caldwell, K.A. (2003). Suppression of polyglutamine-induced protein aggregation in Caenorhabditis elegans by torsin proteins. Hum Mol Genet *12*, 307-319.

Callan, A.C., Bunning, S., Jones, O.T., High, S., and Swanton, E. (2007). Biosynthesis of the dystonia-associated AAA+ ATPase torsinA at the endoplasmic reticulum. Biochem J *401*, 607-612.

Canettieri, G., Morantte, I., Guzman, E., Asahara, H., Herzig, S., Anderson, S.D., Yates, J.R., 3rd, and Montminy, M. (2003). Attenuation of a phosphorylation-dependent activator by an HDAC-PP1 complex. Nature structural biology *10*, 175-181.

Cao, S., Gelwix, C.C., Caldwell, K.A., and Caldwell, G.A. (2005). Torsin-mediated protection from cellular stress in the dopaminergic neurons of Caenorhabditis elegans. The Journal of neuroscience : the official journal of the Society for Neuroscience *25*, 3801-3812.

Carbon, M., Niethammer, M., Peng, S., Raymond, D., Dhawan, V., Chaly, T., Ma, Y., Bressman, S., and Eidelberg, D. (2009). Abnormal striatal and thalamic dopamine neurotransmission: Genotype-related features of dystonia. Neurology *72*, 2097-2103.

Cardinali, B., Cohen, P.T., and Lamond, A.I. (1994). Protein phosphatase 1 can modulate alternative 5' splice site selection in a HeLa splicing extract. FEBS Lett *352*, 276-280.

Carlezon, W.A., Jr., Duman, R.S., and Nestler, E.J. (2005). The many faces of CREB. Trends in neurosciences *28*, 436-445.

Carninci, P., Kasukawa, T., Katayama, S., Gough, J., Frith, M.C., Maeda, N., Oyama, R., Ravasi, T., Lenhard, B., Wells, C., *et al.* (2005). The transcriptional landscape of the mammalian genome. Science *309*, 1559-1563.

Casaca, A., Fardilha, M., da Cruz, E.S.E., and Cunha, C. (2011). In Vivo Interaction of the Hepatitis Delta Virus Small Antigen with the ELAV-Like Protein HuR. The open virology journal *5*, 12-21.

Ceulemans, H., and Bollen, M. (2004). Functional diversity of protein phosphatase-1, a cellular economizer and reset button. Physiol Rev *84*, 1-39.

Ceulemans, H., and Bollen, M. (2006). A tighter RVxF motif makes a finer Sift. Chem Biol *13*, 6-8.

Ceulemans, H., Stalmans, W., and Bollen, M. (2002a). Regulator-driven functional diversification of protein phosphatase-1 in eukaryotic evolution. Bioessays *24*, 371-381.

Ceulemans, H., Vulsteke, V., De Maeyer, M., Tatchell, K., Stalmans, W., and Bollen, M. (2002b). Binding of the concave surface of the Sds22 superhelix to the alpha 4/alpha 5/alpha 6-triangle of protein phosphatase-1. J Biol Chem *277*, 47331-47337.

Charron, M., Shaper, J.H., and Shaper, N.L. (1998). The increased level of beta1,4-galactosyltransferase required for lactose biosynthesis is achieved in part by translational control. Proc Natl Acad Sci U S A *95*, 14805-14810.

Chen, C.Y., Chi, Y.H., Mutalif, R.A., Starost, M.F., Myers, T.G., Anderson, S.A., Stewart, C.L., and Jeang, K.T. (2012). Accumulation of the inner nuclear envelope protein Sun1 is pathogenic in progeric and dystrophic laminopathies. Cell *149*, 565-577.

Cheng, A., Dean, N.M., and Honkanen, R.E. (2000). Serine/threonine protein phosphatase type 1gamma1 is required for the completion of cytokinesis in human A549 lung carcinoma cells. J Biol Chem *275*, 1846-1854.

Chi, Y., Welcker, M., Hizli, A.A., Posakony, J.J., Aebersold, R., and Clurman, B.E. (2008). Identification of CDK2 substrates in human cell lysates. Genome biology *9*, R149.

Cho, R.J., Huang, M., Campbell, M.J., Dong, H., Steinmetz, L., Sapinoso, L., Hampton, G., Elledge, S.J., Davis, R.W., and Lockhart, D.J. (2001). Transcriptional regulation and function during the human cell cycle. Nat Genet *27*, 48-54.

Chu, L., Su, M.Y., Maggi, L.B., Jr., Lu, L., Mullins, C., Crosby, S., Huang, G., Chng, W.J., Vij, R., and Tomasson, M.H. (2012). Multiple myeloma-associated chromosomal translocation activates orphan snoRNA ACA11 to suppress oxidative stress. The Journal of clinical investigation *122*, 2793-2806.

Ciechanover, A. (1994). The ubiquitin-proteasome proteolytic pathway. Cell *79*, 13-21.

Clements, L., Manilal, S., Love, D.R., and Morris, G.E. (2000). Direct interaction between emerin and lamin A. Biochem Biophys Res Commun *267*, 709-714.

Cohen, M., Lee, K.K., Wilson, K.L., and Gruenbaum, Y. (2001). Transcriptional repression, apoptosis, human disease and the functional evolution of the nuclear lamina. Trends Biochem Sci *26*, 41-47.

Cohen, P. (1989). The structure and regulation of protein phosphatases. Annu Rev Biochem *58*, 453-508.

Cohen, P. (2002a). Protein kinases--the major drug targets of the twenty-first century? Nature reviews. Drug discovery *1*, 309-315.

Cohen, P.T. (1997). Novel protein serine/threonine phosphatases: variety is the spice of life. Trends Biochem Sci *22*, 245-251.

Cohen, P.T. (2002b). Protein phosphatase 1--targeted in many directions. J Cell Sci *115*, 241-256.

Crisp, M., Liu, Q., Roux, K., Rattner, J.B., Shanahan, C., Burke, B., Stahl, P.D., and Hodzic, D. (2006). Coupling of the nucleus and cytoplasm: role of the LINC complex. J Cell Biol *172*, 41-53.

da Cruz e Silva, E.F., da Cruz e Silva, O.A., Zaia, C.T., and Greengard, P. (1995a). Inhibition of protein phosphatase 1 stimulates secretion of Alzheimer amyloid precursor protein. Mol Med *1*, 535-541.

da Cruz e Silva, E.F., Fox, C.A., Ouimet, C.C., Gustafson, E., Watson, S.J., and Greengard, P. (1995b). Differential expression of protein phosphatase 1 isoforms in mammalian brain. J Neurosci *15*, 3375-3389.

da Cruz e Silva, O.A., Fardilha, M., Henriques, A.G., Rebelo, S., Vieira, S., and da Cruz e Silva, E.F. (2004). Signal transduction therapeutics: relevance for Alzheimer's disease. Journal of molecular neuroscience : MN *23*, 123-142.

Dang, M.T., Yokoi, F., Cheetham, C.C., Lu, J., Vo, V., Lovinger, D.M., and Li, Y. (2012). An anticholinergic reverses motor control and corticostriatal LTD deficits in Dyt1 DeltaGAG knock-in mice. Behavioural brain research *226*, 465-472.

Dang, M.T., Yokoi, F., McNaught, K.S., Jengelley, T.A., Jackson, T., Li, J., and Li, Y. (2005). Generation and characterization of Dyt1 DeltaGAG knock-in mouse as a model for early-onset dystonia. Exp Neurol *196*, 452-463.

Dang, M.T., Yokoi, F., Pence, M.A., and Li, Y. (2006). Motor deficits and hyperactivity in Dyt1 knockdown mice. Neuroscience research *56*, 470-474.

Dauer, W.T., and Worman, H.J. (2009). The nuclear envelope as a signaling node in development and disease. Developmental cell *17*, 626-638.

Dechat, T., Adam, S.A., Taimen, P., Shimi, T., and Goldman, R.D. (2010). Nuclear lamins. Cold Spring Harbor perspectives in biology *2*, a000547.

Dechat, T., Korbei, B., Vaughan, O.A., Vlcek, S., Hutchison, C.J., and Foisner, R. (2000). Lamina-associated polypeptide 2alpha binds intranuclear A-type lamins. J Cell Sci *113 Pt 19*, 3473-3484.

Delobel, P., Flament, S., Hamdane, M., Delacourte, A., Vilain, J.P., and Buee, L. (2002a). Modelling Alzheimer-specific abnormal Tau phosphorylation independently of GSK3beta and PKA kinase activities. FEBS Lett *516*, 151-155.

Delobel, P., Flament, S., Hamdane, M., Mailliot, C., Sambo, A.V., Begard, S., Sergeant, N., Delacourte, A., Vilain, J.P., and Buee, L. (2002b). Abnormal Tau phosphorylation of the Alzheimer-type also occurs during mitosis. J Neurochem *83*, 412-420.

Dephoure, N., Zhou, C., Villen, J., Beausoleil, S.A., Bakalarski, C.E., Elledge, S.J., and Gygi, S.P. (2008). A quantitative atlas of mitotic phosphorylation. Proceedings of the National Academy of Sciences of the United States of America *105*, 10762-10767.

Devaul, N., Wang, R., and Sperry, A.O. (2013). PPP1R42, a PP1 binding protein, regulates centrosome dynamics in ARPE-19 cells. Biology of the cell / under the auspices of the European Cell Biology Organization.

Dorner, D., Gotzmann, J., and Foisner, R. (2007). Nucleoplasmic lamins and their interaction partners, LAP2alpha, Rb, and BAF, in transcriptional regulation. The FEBS journal *274*, 1362-1373.

Dreesen, O., Chojnowski, A., Ong, P.F., Zhao, T.Y., Common, J.E., Lunny, D., Lane, E.B., Lee, S.J., Vardy, L.A., Stewart, C.L., *et al.* (2013). Lamin B1 fluctuations have differential effects on cellular proliferation and senescence. J Cell Biol *200*, 605-617.

Dreuillet, C., Tillit, J., Kress, M., and Ernoult-Lange, M. (2002). In vivo and in vitro interaction between human transcription factor MOK2 and nuclear lamin A/C. Nucleic acids research *30*, 4634-4642.

Dwyer, N., and Blobel, G. (1976). A modified procedure for the isolation of a pore complex-lamina fraction from rat liver nuclei. J Cell Biol *70*, 581-591.

Eckersley-Maslin, M.A., Bergmann, J.H., Lazar, Z., and Spector, D.L. (2013). Lamin A/C is expressed in pluripotent mouse embryonic stem cells. Nucleus *4*, 53-60.

Egloff, M.P., Cohen, P.T., Reinemer, P., and Barford, D. (1995). Crystal structure of the catalytic subunit of human protein phosphatase 1 and its complex with tungstate. Journal of molecular biology *254*, 942-959.

Egloff, M.P., Johnson, D.F., Moorhead, G., Cohen, P.T., Cohen, P., and Barford, D. (1997). Structural basis for the recognition of regulatory subunits by the catalytic subunit of protein phosphatase 1. EMBO J *16*, 1876-1887.

Ellenberg, J., Siggia, E.D., Moreira, J.E., Smith, C.L., Presley, J.F., Worman, H.J., and Lippincott-Schwartz, J. (1997). Nuclear membrane dynamics and reassembly in living cells: targeting of an inner nuclear membrane protein in interphase and mitosis. J Cell Biol *138*, 1193-1206.

Ellis, J.A., Craxton, M., Yates, J.R., and Kendrick-Jones, J. (1998). Aberrant intracellular targeting and cell cycle-dependent phosphorylation of emerin contribute to the Emery-Dreifuss muscular dystrophy phenotype. J Cell Sci *111 (Pt 6)*, 781-792.

Emanuele, M.J., Lan, W., Jwa, M., Miller, S.A., Chan, C.S., and Stukenberg, P.T. (2008). Aurora B kinase and protein phosphatase 1 have opposing roles in modulating kinetochore assembly. J Cell Biol *181*, 241-254.

Espona-Fiedler, M., Soto-Cerrato, V., Hosseini, A., Lizcano, J.M., Guallar, V., Quesada, R., Gao, T., and Perez-Tomas, R. (2012). Identification of dual mTORC1 and mTORC2 inhibitors in melanoma cells: prodigiosin vs. obatoclax. Biochemical pharmacology *83*, 489-496.

Esteves, S.L., Domingues, S.C., da Cruz e Silva, O.A., Fardilha, M., and da Cruz e Silva, E.F. (2012a). Protein phosphatase 1alpha interacting proteins in the human brain. Omics : a journal of integrative biology *16*, 3-17.

Esteves, S.L., Korrodi-Gregorio, L., Cotrim, C.Z., van Kleeff, P.J., Domingues, S.C., da Cruz e Silva, O.A., Fardilha, M., and da Cruz e Silva, E.F. (2013a). Protein phosphatase 1gamma isoforms linked interactions in the brain. Journal of molecular neuroscience : MN *50*, 179-197.

Esteves, S.L., Korrodi-Gregorio, L., Cotrim, C.Z., van Kleeff, P.J., Domingues, S.C., da Cruz, E.S.O.A., Fardilha, M., and da Cruz, E.S.E.F. (2012b). Protein Phosphatase 1gamma Isoforms Linked Interactions in the Brain. Journal of molecular neuroscience : MN.

Esteves, S.L., Korrodi-Gregorio, L., Cotrim, C.Z., van Kleeff, P.J., Domingues, S.C., da Cruz, E.S.O.A., Fardilha, M., and da Cruz, E.S.E.F. (2013b). Protein phosphatase 1gamma isoforms linked interactions in the brain. Journal of molecular neuroscience : MN *50*, 179-197.

Fahn, S. (1988). Concept and classification of dystonia. Adv Neurol *50*, 1-8.

Fahn, S. (2011). Classification of movement disorders. Movement disorders : official journal of the Movement Disorder Society *26*, 947-957.

Fahn, S., Bressman, S.B., and Marsden, C.D. (1998). Classification of dystonia. Adv Neurol *78*, 1-10.

Fahrenkrog, B., and Aebi, U. (2003). The nuclear pore complex: nucleocytoplasmic transport and beyond. Nat Rev Mol Cell Biol *4*, 757-766.

Fardilha, M., Esteves, S.L., Korrodi-Gregorio, L., da Cruz e Silva, O.A., and da Cruz e Silva, F.F. (2010). The physiological relevance of protein phosphatase 1 and its interacting proteins to health and disease. Current medicinal chemistry *17*, 3996-4017.

Fardilha, M., Esteves, S.L., Korrodi-Gregorio, L., Vintem, A.P., Domingues, S.C., Rebelo, S., Morrice, N., Cohen, P.T., da Cruz e Silva, O.A., and da Cruz e Silva, E.F. (2011). Identification of the human testis protein phosphatase 1 interactome. Biochemical pharmacology *82*, 1403-1415.

Fardilha, M., Wu, W., Sa, R., Fidalgo, S., Sousa, C., Mota, C., da Cruz e Silva, O.A., and da Cruz e Silva, E.F. (2004). Alternatively spliced protein variants as potential therapeutic targets for male infertility and contraception. Annals of the New York Academy of Sciences *1030*, 468-478.

Farinelli, M., Heitz, F.D., Grewe, B.F., Tyagarajan, S.K., Helmchen, F., and Mansuy, I.M. (2012). Selective regulation of NR2B by protein phosphatase-1 for the control of the NMDA receptor in neuroprotection. PloS one *7*, e34047.

Farmer, S.F., Sheean, G.L., Mayston, M.J., Rothwell, J.C., Marsden, C.D., Conway, B.A., Halliday, D.M., Rosenberg, J.R., and Stephens, J.A. (1998). Abnormal motor unit synchronization of antagonist muscles underlies pathological co-contraction in upper limb dystonia. Brain *121 (Pt 5)*, 801-814.

Feng, J., Yan, Z., Ferreira, A., Tomizawa, K., Liauw, J.A., Zhuo, M., Allen, P.B., Ouimet, C.C., and Greengard, P. (2000). Spinophilin regulates the formation and function of dendritic spines. Proc Natl Acad Sci U S A *97*, 9287-9292.

Fernandez, A., Brautigan, D.L., and Lamb, N.J. (1992). Protein phosphatase type 1 in mammalian cell mitosis: chromosomal localization and involvement in mitotic exit. J Cell Biol *116*, 1421-1430.

Ferrari-Toninelli, G., Paccioretti, S., Francisconi, S., Uberti, D., and Memo, M. (2004). TorsinA negatively controls neurite outgrowth of SH-SY5Y human neuronal cell line. Brain research *1012*, 75-81.

Foisner, R. (2003). Cell cycle dynamics of the nuclear envelope. TheScientificWorldJournal *3*, 1-20.

Foisner, R., and Gerace, L. (1993). Integral membrane proteins of the nuclear envelope interact with lamins and chromosomes, and binding is modulated by mitotic phosphorylation. Cell *73*, 1267-1279.

Foulds, P.G., Mitchell, J.D., Parker, A., Turner, R., Green, G., Diggle, P., Hasegawa, M., Taylor, M., Mann, D., and Allsop, D. (2011). Phosphorylated alpha-synuclein can be detected in blood plasma and is potentially a useful biomarker for Parkinson's disease. FASEB J *25*, 4127-4137.

Funabiki, H., and Wynne, D.J. (2013). Making an effective switch at the kinetochore by phosphorylation and dephosphorylation. Chromosoma *122*, 135-158.

Furukawa, K., and Hotta, Y. (1993). cDNA cloning of a germ cell specific lamin B3 from mouse spermatocytes and analysis of its function by ectopic expression in somatic cells. EMBO J *12*, 97-106.

Furukawa, K., Inagaki, H., and Hotta, Y. (1994). Identification and cloning of an mRNA coding for a germ cell-specific A-type lamin in mice. Exp Cell Res *212*, 426-430.

Furukawa, Y., Hornykiewicz, O., Fahn, S., and Kish, S.J. (2000). Striatal dopamine in early-onset primary torsion dystonia with the DYT1 mutation. Neurology *54*, 1193-1195.

Garibotto, V., Romito, L.M., Elia, A.E., Soliveri, P., Panzacchi, A., Carpinelli, A., Tinazzi, M., Albanese, A., and Perani, D. (2011). In vivo evidence for GABA(A) receptor changes in the sensorimotor system in primary dystonia. Movement disorders : official journal of the Movement Disorder Society *26*, 852-857.

Gautier, V.W., Gu, L., O'Donoghue, N., Pennington, S., Sheehy, N., and Hall, W.W. (2009). In vitro nuclear interactome of the HIV-1 Tat protein. Retrovirology *6*, 47.

Gerace, L., and Blobel, G. (1980). The nuclear envelope lamina is reversibly depolymerized during mitosis. Cell *19*, 277-287.

Gerace, L., and Burke, B. (1988). Functional organization of the nuclear envelope. Annu Rev Cell Biol *4*, 335-374.

Gerace, L., and Foisner, R. (1994). Integral membrane proteins and dynamic organization of the nuclear envelope. Trends Cell Biol *4*, 127-131.

Gerace, L., and Huber, M.D. (2012). Nuclear lamina at the crossroads of the cytoplasm and nucleus. Journal of structural biology *177*, 24-31.

Ghilardi, M.F., Carbon, M., Silvestri, G., Dhawan, V., Tagliati, M., Bressman, S., Ghez, C., and Eidelberg, D. (2003). Impaired sequence learning in carriers of the DYT1 dystonia mutation. Annals of neurology *54*, 102-109.

Giannakopoulou, D., Armata, I., Mitsacos, A., Shashidharan, P., and Giompres, P. (2010). Modulation of the basal ganglia dopaminergic system in a transgenic mouse exhibiting dystonia-like features. J Neural Transm *117*, 1401-1409.

Giles, L.M., Chen, J., Li, L., and Chin, L.S. (2008). Dystonia-associated mutations cause premature degradation of torsinA protein and cell-type-specific mislocalization to the nuclear envelope. Hum Mol Genet *17*, 2712-2722.

Giles, L.M., Li, L., and Chin, L.S. (2009). Printor, a novel torsinA-interacting protein implicated in dystonia pathogenesis. J Biol Chem *284*, 21765-21775.

Glass, J.R., and Gerace, L. (1990). Lamins A and C bind and assemble at the surface of mitotic chromosomes. J Cell Biol *111*, 1047-1057.

Godet, A.N., Guergnon, J., Maire, V., Croset, A., and Garcia, A. (2010). The combinatorial PP1-binding consensus Motif (R/K)x((0,1))V/IxFxx(R/K)x(R/K) is a new apoptotic signature. PloS one *5*, e9981.

Goldberg, J., Huang, H.B., Kwon, Y.G., Greengard, P., Nairn, A.C., and Kuriyan, J. (1995). Three-dimensional structure of the catalytic subunit of protein serine/threonine phosphatase-1. Nature *376*, 745-753.

Goldstein, L.S., and Philp, A.V. (1999). The road less traveled: emerging principles of kinesin motor utilization. Annual review of cell and developmental biology *15*, 141-183.

Gonzalez-Alegre, P., and Paulson, H.L. (2004). Aberrant cellular behavior of mutant torsinA implicates nuclear envelope dysfunction in DYT1 dystonia. The Journal of neuroscience : the official journal of the Society for Neuroscience *24*, 2593-2601.

Goodchild, R.E., and Dauer, W.T. (2004). Mislocalization to the nuclear envelope: an effect of the dystonia-causing torsinA mutation. Proceedings of the National Academy of Sciences of the United States of America *101*, 847-852.

Goodchild, R.E., and Dauer, W.T. (2005). The AAA+ protein torsinA interacts with a conserved domain present in LAP1 and a novel ER protein. J Cell Biol *168*, 855-862.

Goodchild, R.E., Kim, C.E., and Dauer, W.T. (2005). Loss of the dystonia-associated protein torsinA selectively disrupts the neuronal nuclear envelope. Neuron *48*, 923-932.

Granata, A., Schiavo, G., and Warner, T.T. (2009). TorsinA and dystonia: from nuclear envelope to synapse. Journal of neurochemistry *109*, 1596-1609.

Granata, A., Watson, R., Collinson, L.M., Schiavo, G., and Warner, T.T. (2008). The dystonia-associated protein torsinA modulates synaptic vesicle recycling. J Biol Chem *283*, 7568-7579.

Greengard, P., Allen, P.B., and Nairn, A.C. (1999). Beyond the dopamine receptor: the DARPP-32/protein phosphatase-1 cascade. Neuron *23*, 435-447.

Gros-Louis, F., Dupre, N., Dion, P., Fox, M.A., Laurent, S., Verreault, S., Sanes, J.R., Bouchard, J.P., and Rouleau, G.A. (2007). Mutations in SYNE1 lead to a newly discovered form of autosomal recessive cerebellar ataxia. Nat Genet *39*, 80-85.

Grossman, S.D., Hsieh-Wilson, L.C., Allen, P.B., Nairn, A.C., and Greengard, P. (2002). The actin-binding domain of spinophilin is necessary and sufficient for targeting to dendritic spines. Neuromolecular medicine *2*, 61-69.

Grundmann, K., Glockle, N., Martella, G., Sciamanna, G., Hauser, T.K., Yu, L., Castaneda, S., Pichler, B., Fehrenbacher, B., Schaller, M., *et al.* (2012). Generation of a novel rodent model for DYT1 dystonia. Neurobiol Dis *47*, 61-74.

Grundmann, K., Reischmann, B., Vanhoutte, G., Hubener, J., Teismann, P., Hauser, T.K., Bonin, M., Wilbertz, J., Horn, S., Nguyen, H.P., *et al.* (2007). Overexpression of human wildtype torsinA and human DeltaGAG torsinA in a transgenic mouse model causes phenotypic abnormalities. Neurobiol Dis *27*, 190-206.

Guttinger, S., Laurell, E., and Kutay, U. (2009). Orchestrating nuclear envelope disassembly and reassembly during mitosis. Nat Rev Mol Cell Biol *10*, 178-191.

Hagiwara, M., Alberts, A., Brindle, P., Meinkoth, J., Feramisco, J., Deng, T., Karin, M., Shenolikar, S., and Montminy, M. (1992). Transcriptional attenuation following cAMP induction requires PP-1-mediated dephosphorylation of CREB. Cell *70*, 105-113.

Han, B., Dong, Z., Liu, Y., Chen, Q., Hashimoto, K., and Zhang, J.T. (2003). Regulation of constitutive expression of mouse PTEN by the 5'-untranslated region. Oncogene *22*, 5325-5337.

Han, G., Ye, M., Liu, H., Song, C., Sun, D., Wu, Y., Jiang, X., Chen, R., Wang, C., Wang, L., *et al.* (2010). Phosphoproteome analysis of human liver tissue by long-gradient nanoflow LC coupled with multiple stage MS analysis. Electrophoresis *31*, 1080-1089.

Haque, F., Lloyd, D.J., Smallwood, D.T., Dent, C.L., Shanahan, C.M., Fry, A.M., Trembath, R.C., and Shackleton, S. (2006). SUN1 interacts with nuclear lamin A and cytoplasmic

nesprins to provide a physical connection between the nuclear lamina and the cytoskeleton. Molecular and cellular biology *26*, 3738-3751.

Haraguchi, T., Koujin, T., Hayakawa, T., Kaneda, T., Tsutsumi, C., Imamoto, N., Akazawa, C., Sukegawa, J., Yoneda, Y., and Hiraoka, Y. (2000). Live fluorescence imaging reveals early recruitment of emerin, LBR, RanBP2, and Nup153 to reforming functional nuclear envelopes. Journal of cell science *113 (Pt 5)*, 779-794.

Harris, C.A., Andryuk, P.J., Cline, S., Chan, H.K., Natarajan, A., Siekierka, J.J., and Goldstein, G. (1994). Three distinct human thymopoietins are derived from alternatively spliced mRNAs. Proc Natl Acad Sci U S A *91*, 6283-6287.

Havugimana, P.C., Hart, G.T., Nepusz, T., Yang, H., Turinsky, A.L., Li, Z., Wang, P.I., Boutz, D.R., Fong, V., Phanse, S., *et al.* (2012). A census of human soluble protein complexes. Cell *150*, 1068-1081.

Hellemans, J., Preobrazhenska, O., Willaert, A., Debeer, P., Verdonk, P.C., Costa, T., Janssens, K., Menten, B., Van Roy, N., Vermeulen, S.J., *et al.* (2004). Loss-of-function mutations in LEMD3 result in osteopoikilosis, Buschke-Ollendorff syndrome and melorheostosis. Nat Genet *36*, 1213-1218.

Hemmings, H.C., Jr., Greengard, P., Tung, H.Y., and Cohen, P. (1984). DARPP-32, a dopamine-regulated neuronal phosphoprotein, is a potent inhibitor of protein phosphatase-1. Nature *310*, 503-505.

Hendrickx, A., Beullens, M., Ceulemans, H., Den Abt, T., Van Eynde, A., Nicolaescu, E., Lesage, B., and Bollen, M. (2009). Docking motif-guided mapping of the interactome of protein phosphatase-1. Chemistry & biology *16*, 365-371.

Hendzel, M.J., Wei, Y., Mancini, M.A., Van Hooser, A., Ranalli, T., Brinkley, B.R., Bazett-Jones, D.P., and Allis, C.D. (1997). Mitosis-specific phosphorylation of histone H3 initiates primarily within pericentromeric heterochromatin during G2 and spreads in an ordered fashion coincident with mitotic chromosome condensation. Chromosoma *106*, 348-360.

Henriques, A.G., Vieira, S.I., Rebelo, S., Domingues, S.C., da Cruz e Silva, E.F., and da Cruz e Silva, O.A. (2007). Isoform specific amyloid-beta protein precursor metabolism. Journal of Alzheimer's disease : JAD *11*, 85-95.

Heroes, E., Lesage, B., Gornemann, J., Beullens, M., Van Meervelt, L., and Bollen, M. (2013). The PP1 binding code: a molecular-lego strategy that governs specificity. The FEBS journal *280*, 584-595.

Hetzer, M., Meyer, H.H., Walther, T.C., Bilbao-Cortes, D., Warren, G., and Mattaj, I.W. (2001). Distinct AAA-ATPase p97 complexes function in discrete steps of nuclear assembly. Nature cell biology *3*, 1086-1091.

Hewett, J., Gonzalez-Agosti, C., Slater, D., Ziefer, P., Li, S., Bergeron, D., Jacoby, D.J., Ozelius, L.J., Ramesh, V., and Breakefield, X.O. (2000). Mutant torsinA, responsible for early-onset torsion dystonia, forms membrane inclusions in cultured neural cells. Human molecular genetics *9*, 1403-1413.

Hewett, J., Johanson, P., Sharma, N., Standaert, D., and Balcioglu, A. (2010). Function of dopamine transporter is compromised in DYT1 transgenic animal model in vivo. J Neurochem *113*, 228-235.

Hewett, J., Ziefer, P., Bergeron, D., Naismith, T., Boston, H., Slater, D., Wilbur, J., Schuback, D., Kamm, C., Smith, N., *et al.* (2003). TorsinA in PC12 cells: localization in the endoplasmic reticulum and response to stress. Journal of neuroscience research *72*, 158-168.

Hewett, J.W., Zeng, J., Niland, B.P., Bragg, D.C., and Breakefield, X.O. (2006). Dystonia-causing mutant torsinA inhibits cell adhesion and neurite extension through interference with cytoskeletal dynamics. Neurobiology of disease *22*, 98-111.

Hirano, Y., Segawa, M., Ouchi, F.S., Yamakawa, Y., Furukawa, K., Takeyasu, K., and Horigome, T. (2005). Dissociation of emerin from barrier-to-autointegration factor is regulated through mitotic phosphorylation of emerin in a xenopus egg cell-free system. J Biol Chem *280*, 39925-39933.

Hofemeister, H., and O'Hare, P. (2005). Analysis of the localization and topology of nurim, a polytopic protein tightly associated with the inner nuclear membrane. J Biol Chem *280*, 2512-2521.

Hoffmann, K., Dreger, C.K., Olins, A.L., Olins, D.E., Shultz, L.D., Lucke, B., Karl, H., Kaps, R., Muller, D., Vaya, A., *et al.* (2002). Mutations in the gene encoding the lamin B receptor produce an altered nuclear morphology in granulocytes (Pelger-Huet anomaly). Nat Genet *31*, 410-414.

Hoger, T.H., Zatloukal, K., Waizenegger, I., and Krohne, G. (1990). Characterization of a second highly conserved B-type lamin present in cells previously thought to contain only a single B-type lamin. Chromosoma *99*, 379-390.

Holaska, J.M., Kowalski, A.K., and Wilson, K.L. (2004). Emerin caps the pointed end of actin filaments: evidence for an actin cortical network at the nuclear inner membrane. PLoS biology *2*, E231.

Honkanen, R.E., and Golden, T. (2002). Regulators of serine/threonine protein phosphatases at the dawn of a clinical era? Current medicinal chemistry *9*, 2055-2075.

Hosokawa, T., Saito, T., Asada, A., Fukunaga, K., and Hisanaga, S. (2010). Quantitative measurement of in vivo phosphorylation states of Cdk5 activator p35 by Phos-tag SDS-PAGE. Molecular & cellular proteomics : MCP *9*, 1133-1143.

Hsu, J.Y., Sun, Z.W., Li, X., Reuben, M., Tatchell, K., Bishop, D.K., Grushcow, J.M., Brame, C.J., Caldwell, J.A., Hunt, D.F., *et al.* (2000). Mitotic phosphorylation of histone H3 is governed by Ipl1/aurora kinase and Glc7/PP1 phosphatase in budding yeast and nematodes. Cell *102*, 279-291.

Huang, H.B., Horiuchi, A., Watanabe, T., Shih, S.R., Tsay, H.J., Li, H.C., Greengard, P., and Nairn, A.C. (1999). Characterization of the inhibition of protein phosphatase-1 by DARPP-32 and inhibitor-2. J Biol Chem *274*, 7870-7878.

Huang, H.S., Pozarowski, P., Gao, Y., Darzynkiewicz, Z., and Lee, E.Y. (2005). Protein phosphatase-1 inhibitor-3 is co-localized to the nucleoli and centrosomes with PP1gamma1 and PP1alpha, respectively. Arch Biochem Biophys *443*, 33-44.

Hutchins, J.R., Toyoda, Y., Hegemann, B., Poser, I., Heriche, J.K., Sykora, M.M., Augsburg, M., Hudecz, O., Buschhorn, B.A., Bulkescher, J., *et al.* (2010). Systematic analysis of human protein complexes identifies chromosome segregation proteins. Science *328*, 593-599.

Ilardi, J.M., Mochida, S., and Sheng, Z.H. (1999). Snapin: a SNARE-associated protein implicated in synaptic transmission. Nature neuroscience *2*, 119-124.

Ito, H., Koyama, Y., Takano, M., Ishii, K., Maeno, M., Furukawa, K., and Horigome, T. (2007). Nuclear envelope precursor vesicle targeting to chromatin is stimulated by protein phosphatase 1 in Xenopus egg extracts. Exp Cell Res *313*, 1897-1910.

Iyer, L.M., Leipe, D.D., Koonin, E.V., and Aravind, L. (2004). Evolutionary history and higher order classification of AAA+ ATPases. Journal of structural biology *146*, 11-31.

Jagatheesan, G., Thanumalayan, S., Muralikrishna, B., Rangaraj, N., Karande, A.A., and Parnaik, V.K. (1999). Colocalization of intranuclear lamin foci with RNA splicing factors. J Cell Sci *112 (Pt 24)*, 4651-4661.

Jankovic, J. (2013). Medical treatment of dystonia. Movement disorders : official journal of the Movement Disorder Society *28*, 1001-1012.

Johnson, S.A., and Hunter, T. (2005). Kinomics: methods for deciphering the kinome. Nature methods *2*, 17-25.

Jungwirth, M., Dear, M.L., Brown, P., Holbrook, K., and Goodchild, R. (2010). Relative tissue expression of homologous torsinB correlates with the neuronal specific importance of DYT1 dystonia-associated torsinA. Human molecular genetics *19*, 888-900.

Jungwirth, M.T., Kumar, D., Jeong, D.Y., and Goodchild, R.E. (2011). The nuclear envelope localization of DYT1 dystonia torsinA-DeltaE requires the SUN1 LINC complex component. BMC cell biology *12*, 24.

Kabakci, K., Hedrich, K., Leung, J.C., Mitterer, M., Vieregge, P., Lencer, R., Hagenah, J., Garrels, J., Witt, K., Klostermann, F., *et al.* (2004). Mutations in DYT1: extension of the phenotypic and mutational spectrum. Neurology *62*, 395-400.

Kamm, C., Boston, H., Hewett, J., Wilbur, J., Corey, D.P., Hanson, P.I., Ramesh, V., and Breakefield, X.O. (2004). The early onset dystonia protein torsinA interacts with kinesin light chain 1. The Journal of biological chemistry *279*, 19882-19892.

Kavanagh, D.M., Powell, W.E., Malik, P., Lazou, V., and Schirmer, E.C. (2007). Organelle proteome variation among different cell types: lessons from nuclear membrane proteins. Sub-cellular biochemistry *43*, 51-76.

Kawabe, T., Muslin, A.J., and Korsmeyer, S.J. (1997). HOX11 interacts with protein phosphatases PP2A and PP1 and disrupts a G2/M cell-cycle checkpoint. Nature *385*, 454-458.

Kim, C.E., Perez, A., Perkins, G., Ellisman, M.H., and Dauer, W.T. (2010a). A molecular mechanism underlying the neural-specific defect in torsinA mutant mice. Proceedings of the National Academy of Sciences of the United States of America *107*, 9861-9866.

Kim, G., Weiss, S.J., and Levine, R.L. (2013). Methionine oxidation and reduction in proteins. Biochimica et biophysica acta.

Kim, W., Bennett, E.J., Huttlin, E.L., Guo, A., Li, J., Possemato, A., Sowa, M.E., Rad, R., Rush, J., Comb, M.J., *et al.* (2011). Systematic and quantitative assessment of the ubiquitin-modified proteome. Molecular cell *44*, 325-340.

Kim, Y., Holland, A.J., Lan, W., and Cleveland, D.W. (2010b). Aurora kinases and protein phosphatase 1 mediate chromosome congression through regulation of CENP-E. Cell *142*, 444-455.

Kim, Y.M., Watanabe, T., Allen, P.B., Lee, S.J., Greengard, P., Nairn, A.C., and Kwon, Y.G. (2003). PNUTS, a protein phosphatase 1 (PP1) nuclear targeting subunit. Characterization of its PP1- and RNA-binding domains and regulation by phosphorylation. J Biol Chem *278*, 13819-13828.

King, M.C., Lusk, C.P., and Blobel, G. (2006). Karyopherin-mediated import of integral inner nuclear membrane proteins. Nature *442*, 1003-1007.

Kinoshita, E., Kinoshita-Kikuta, E., Takiyama, K., and Koike, T. (2006). Phosphate-binding tag, a new tool to visualize phosphorylated proteins. Molecular & cellular proteomics : MCP *5*, 749-757.

Kock, N., Naismith, T.V., Boston, H.E., Ozelius, L.J., Corey, D.P., Breakefield, X.O., and Hanson, P.I. (2006). Effects of genetic variations in the dystonia protein torsinA: identification of polymorphism at residue 216 as protein modifier. Hum Mol Genet *15*, 1355-1364.

Konakova, M., Huynh, D.P., Yong, W., and Pulst, S.M. (2001). Cellular distribution of torsin A and torsin B in normal human brain. Archives of neurology *58*, 921-927.

Kondo, Y., Kondoh, J., Hayashi, D., Ban, T., Takagi, M., Kamei, Y., Tsuji, L., Kim, J., and Yoneda, Y. (2002). Molecular cloning of one isotype of human lamina-associated polypeptide 1s and a topological analysis using its deletion mutants. Biochem Biophys Res Commun *294*, 770-778.

Korrodi-Gregorio, L., Ferreira, M., Vintem, A.P., Wu, W., Muller, T., Marcus, K., Vijayaraghavan, S., Brautigan, D.L., da Cruz, E.S.O.A., Fardilha, M., *et al.* (2013). Identification and characterization of two distinct PPP1R2 isoforms in human spermatozoa. BMC cell biology *14*, 15.

Kreivi, J.P., Trinkle-Mulcahy, L., Lyon, C.E., Morrice, N.A., Cohen, P., and Lamond, A.I. (1997). Purification and characterisation of p99, a nuclear modulator of protein phosphatase 1 activity. FEBS Lett *420*, 57-62.

Kuga, T., Nozaki, N., Matsushita, K., Nomura, F., and Tomonaga, T. (2010). Phosphorylation statuses at different residues of lamin B2, B1, and A/C dynamically and independently change throughout the cell cycle. Experimental cell research *316*, 2301-2312.

Kuner, R., Teismann, P., Trutzel, A., Naim, J., Richter, A., Schmidt, N., von Ahsen, O., Bach, A., Ferger, B., and Schneider, A. (2003). TorsinA protects against oxidative stress in COS-1 and PC12 cells. Neuroscience letters *350*, 153-156.

Kuret, J., Bell, H., and Cohen, P. (1986). Identification of high levels of protein phosphatase-1 in rat liver nuclei. FEBS Lett *203*, 197-202.

Kustedjo, K., Bracey, M.H., and Cravatt, B.F. (2000). Torsin A and its torsion dystonia-associated mutant forms are lumenal glycoproteins that exhibit distinct subcellular localizations. J Biol Chem *275*, 27933-27939.

Kutuzov, M.A., Solov'eva, O.V., Andreeva, A.V., and Bennett, N. (2002). Protein Ser/Thr phosphatases PPEF interact with calmodulin. Biochem Biophys Res Commun *293*, 1047-1052.

Kwon, Y.G., Lee, S.Y., Choi, Y., Greengard, P., and Nairn, A.C. (1997). Cell cycle-dependent phosphorylation of mammalian protein phosphatase 1 by cdc2 kinase. Proc Natl Acad Sci U S A *94*, 2168-2173.

Landry, C.R., Levy, E.D., and Michnick, S.W. (2009). Weak functional constraints on phosphoproteomes. Trends in genetics : TIG *25*, 193-197.

Landry, J.R., Mager, D.L., and Wilhelm, B.T. (2003). Complex controls: the role of alternative promoters in mammalian genomes. Trends in genetics : TIG *19*, 640-648.

Landsverk, H.B., Kirkhus, M., Bollen, M., Kuntziger, T., and Collas, P. (2005). PNUTS enhances in vitro chromosome decondensation in a PP1-dependent manner. Biochem J *390*, 709-717.

Le, A.V., Tavalin, S.J., and Dodge-Kafka, K.L. (2011). Identification of AKAP79 as a protein phosphatase 1 catalytic binding protein. Biochemistry *50*, 5279-5291.

Lee, K.K., Haraguchi, T., Lee, R.S., Koujin, T., Hiraoka, Y., and Wilson, K.L. (2001). Distinct functional domains in emerin bind lamin A and DNA-bridging protein BAF. J Cell Sci *114*, 4567-4573.

Lee, O.H., Kim, H., He, Q., Baek, H.J., Yang, D., Chen, L.Y., Liang, J., Chae, H.K., Safari, A., Liu, D., *et al.* (2011). Genome-wide YFP fluorescence complementation screen identifies new regulators for telomere signaling in human cells. Molecular & cellular proteomics : MCP *10*, M110 001628.

Lesage, B., Beullens, M., Pedelini, L., Garcia-Gimeno, M.A., Waelkens, E., Sanz, P., and Bollen, M. (2007). A complex of catalytically inactive protein phosphatase-1 sandwiched between Sds22 and inhibitor-3. Biochemistry *46*, 8909-8919.

Leung, J.C., Klein, C., Friedman, J., Vieregge, P., Jacobs, H., Doheny, D., Kamm, C., DeLeon, D., Pramstaller, P.P., Penney, J.B., *et al.* (2001). Novel mutation in the TOR1A (DYT1) gene in atypical early onset dystonia and polymorphisms in dystonia and early onset parkinsonism. Neurogenetics *3*, 133-143.

Libotte, T., Zaim, H., Abraham, S., Padmakumar, V.C., Schneider, M., Lu, W., Munck, M., Hutchison, C., Wehnert, M., Fahrenkrog, B., *et al.* (2005). Lamin A/C-dependent localization of Nesprin-2, a giant scaffolder at the nuclear envelope. Mol Biol Cell *16*, 3411-3424.

Lievens, J.C., Woodman, B., Mahal, A., and Bates, G.P. (2002). Abnormal phosphorylation of synapsin I predicts a neuronal transmission impairment in the R6/2 Huntington's disease transgenic mice. Molecular and cellular neurosciences *20*, 638-648.

Lin, F., Blake, D.L., Callebaut, I., Skerjanc, I.S., Holmer, L., McBurney, M.W., Paulin-Levasseur, M., and Worman, H.J. (2000). MAN1, an inner nuclear membrane protein that shares the LEM domain with lamina-associated polypeptide 2 and emerin. J Biol Chem *275*, 4840-4847.

Lin, F., and Worman, H.J. (1993). Structural organization of the human gene encoding nuclear lamin A and nuclear lamin C. J Biol Chem *268*, 16321-16326.

Lin, F., and Worman, H.J. (1995). Structural organization of the human gene (LMNB1) encoding nuclear lamin B1. Genomics *27*, 230-236.

Lin, Q., Buckler, E.S.t., Muse, S.V., and Walker, J.C. (1999). Molecular evolution of type 1 serine/threonine protein phosphatases. Molecular phylogenetics and evolution *12*, 57-66.

Liu, C.W., Wang, R.H., Dohadwala, M., Schonthal, A.H., Villa-Moruzzi, E., and Berndt, N. (1999). Inhibitory phosphorylation of PP1alpha catalytic subunit during the G(1)/S transition. J Biol Chem *274*, 29470-29475.

Liu, D., Davydenko, O., and Lampson, M.A. (2012). Polo-like kinase-1 regulates kinetochore-microtubule dynamics and spindle checkpoint silencing. J Cell Biol *198*, 491-499.

Liu, D., Vleugel, M., Backer, C.B., Hori, T., Fukagawa, T., Cheeseman, I.M., and Lampson, M.A. (2010). Regulated targeting of protein phosphatase 1 to the outer kinetochore by KNL1 opposes Aurora B kinase. J Cell Biol *188*, 809-820.

Liu, L., Xie, N., Rennie, P., Challis, J.R., Gleave, M., Lye, S.J., and Dong, X. (2011). Consensus PP1 binding motifs regulate transcriptional corepression and alternative RNA splicing activities of the steroid receptor coregulators, p54nrb and PSF. Mol Endocrinol *25*, 1197-1210.

Liu, Z., Zolkiewska, A., and Zolkiewski, M. (2003). Characterization of human torsinA and its dystonia-associated mutant form. Biochem J *374*, 117-122.

Llanos, S., Royer, C., Lu, M., Bergamaschi, D., Lee, W.H., and Lu, X. (2011). Inhibitory member of the apoptosis-stimulating proteins of the p53 family (iASPP) interacts with protein phosphatase 1 via a noncanonical binding motif. J Biol Chem *286*, 43039-43044.

Lombardi, M.L., Jaalouk, D.E., Shanahan, C.M., Burke, B., Roux, K.J., and Lammerding, J. (2011). The interaction between nesprins and sun proteins at the nuclear envelope is critical for force transmission between the nucleus and cytoskeleton. The Journal of biological chemistry *286*, 26743-26753.

Luo, X., Fang, G., Coldiron, M., Lin, Y., Yu, H., Kirschner, M.W., and Wagner, G. (2000). Structure of the Mad2 spindle assembly checkpoint protein and its interaction with Cdc20. Nature structural biology *7*, 224-229.

Machiels, B.M., Henfling, M.E., Schutte, B., van Engeland, M., Broers, J.L., and Ramaekers, F.C. (1996). Subcellular localization of proteasomes in apoptotic lung tumor cells and persistence as compared to intermediate filaments. Eur J Cell Biol *70*, 250-259.

Maison, C., Pyrpasopoulou, A., Theodoropoulos, P.A., and Georgatos, S.D. (1997). The inner nuclear membrane protein LAP1 forms a native complex with B-type lamins and partitions with spindle-associated mitotic vesicles. The EMBO journal *16*, 4839-4850.

Makino, S., Kaji, R., Ando, S., Tomizawa, M., Yasuno, K., Goto, S., Matsumoto, S., Tabuena, M.D., Maranon, E., Dantes, M., *et al.* (2007). Reduced neuron-specific expression of the TAF1 gene is associated with X-linked dystonia-parkinsonism. American journal of human genetics *80*, 393-406.

Malchiodi-Albedi, F., Petrucci, T.C., Picconi, B., Iosi, F., and Falchi, M. (1997). Protein phosphatase inhibitors induce modification of synapse structure and tau

hyperphosphorylation in cultured rat hippocampal neurons. Journal of neuroscience research *48*, 425-438.

Malenka, R.C. (1994). Synaptic plasticity in the hippocampus: LTP and LTD. Cell *78*, 535-538.

Malik, P., Korfali, N., Srsen, V., Lazou, V., Batrakou, D.G., Zuleger, N., Kavanagh, D.M., Wilkie, G.S., Goldberg, M.W., and Schirmer, E.C. (2010). Cell-specific and lamin-dependent targeting of novel transmembrane proteins in the nuclear envelope. Cell Mol Life Sci *67*, 1353-1369.

Manilal, S., Recan, D., Sewry, C.A., Hoeltzenbein, M., Llense, S., Leturcq, F., Deburgrave, N., Barbot, J., Man, N., Muntoni, F., *et al.* (1998). Mutations in Emery-Dreifuss muscular dystrophy and their effects on emerin protein expression. Hum Mol Genet *7*, 855-864.

Mans, B.J., Anantharaman, V., Aravind, L., and Koonin, E.V. (2004). Comparative genomics, evolution and origins of the nuclear envelope and nuclear pore complex. Cell Cycle *3*, 1612-1637.

Mansharamani, M., and Wilson, K.L. (2005). Direct binding of nuclear membrane protein MAN1 to emerin in vitro and two modes of binding to barrier-to-autointegration factor. J Biol Chem *280*, 13863-13870.

Martella, G., Tassone, A., Sciamanna, G., Platania, P., Cuomo, D., Viscomi, M.T., Bonsi, P., Cacci, E., Biagioni, S., Usiello, A., *et al.* (2009). Impairment of bidirectional synaptic plasticity in the striatum of a mouse model of DYT1 dystonia: role of endogenous acetylcholine. Brain *132*, 2336-2349.

Martin, L., Crimaudo, C., and Gerace, L. (1995). cDNA cloning and characterization of lamina-associated polypeptide 1C (LAP1C), an integral protein of the inner nuclear membrane. J Biol Chem *270*, 8822-8828.

Maske, C.P., Hollinshead, M.S., Higbee, N.C., Bergo, M.O., Young, S.G., and Vaux, D.J. (2003). A carboxyl-terminal interaction of lamin B1 is dependent on the CAAX endoprotease Rce1 and carboxymethylation. J Cell Biol *162*, 1223-1232.

Mattout-Drubezki, A., and Gruenbaum, Y. (2003). Dynamic interactions of nuclear lamina proteins with chromatin and transcriptional machinery. Cell Mol Life Sci *60*, 2053-2063.

McAvoy, T., Allen, P.B., Obaishi, H., Nakanishi, H., Takai, Y., Greengard, P., Nairn, A.C., and Hemmings, H.C., Jr. (1999). Regulation of neurabin I interaction with protein phosphatase 1 by phosphorylation. Biochemistry *38*, 12943-12949.

McLean, P.J., Kawamata, H., Shariff, S., Hewett, J., Sharma, N., Ueda, K., Breakefield, X.O., and Hyman, B.T. (2002). TorsinA and heat shock proteins act as molecular chaperones: suppression of alpha-synuclein aggregation. J Neurochem *83*, 846-854.

McNaught, K.S., Kapustin, A., Jackson, T., Jengelley, T.A., Jnobaptiste, R., Shashidharan, P., Perl, D.P., Pasik, P., and Olanow, C.W. (2004). Brainstem pathology in DYT1 primary torsion dystonia. Annals of neurology *56*, 540-547.

Meadows, J.C., Shepperd, L.A., Vanoosthuyse, V., Lancaster, T.C., Sochaj, A.M., Buttrick, G.J., Hardwick, K.G., and Millar, J.B. (2011). Spindle checkpoint silencing requires association of PP1 to both Spc7 and kinesin-8 motors. Developmental cell *20*, 739-750.

Meiselbach, H., Sticht, H., and Enz, R. (2006). Structural analysis of the protein phosphatase 1 docking motif: molecular description of binding specificities identifies interacting proteins. Chemistry & biology *13*, 49-59.

Mermoud, J.E., Cohen, P., and Lamond, A.I. (1992). Ser/Thr-specific protein phosphatases are required for both catalytic steps of pre-mRNA splicing. Nucleic acids research *20*, 5263-5269.

Mermoud, J.E., Cohen, P.T., and Lamond, A.I. (1994). Regulation of mammalian spliceosome assembly by a protein phosphorylation mechanism. EMBO J *13*, 5679-5688.

Meshorer, E., Toiber, D., Zurel, D., Sahly, I., Dori, A., Cagnano, E., Schreiber, L., Grisaru, D., Tronche, F., and Soreq, H. (2004). Combinatorial complexity of 5' alternative acetylcholinesterase transcripts and protein products. J Biol Chem *279*, 29740-29751.

Mi, J., Guo, C., Brautigan, D.L., and Larner, J.M. (2007). Protein phosphatase-1alpha regulates centrosome splitting through Nek2. Cancer research *67*, 1082-1089.

Misbahuddin, A., Placzek, M.R., Taanman, J.W., Gschmeissner, S., Schiavo, G., Cooper, J.M., and Warner, T.T. (2005). Mutant torsinA, which causes early-onset primary torsion dystonia, is redistributed to membranous structures enriched in vesicular monoamine transporter in cultured human SH-SY5Y cells. Movement disorders : official journal of the Movement Disorder Society *20*, 432-440.

Mislow, J.M., Holaska, J.M., Kim, M.S., Lee, K.K., Segura-Totten, M., Wilson, K.L., and McNally, E.M. (2002). Nesprin-1alpha self-associates and binds directly to emerin and lamin A in vitro. FEBS Lett *525*, 135-140.

Moir, R.D., Montag-Lowy, M., and Goldman, R.D. (1994). Dynamic properties of nuclear lamins: lamin B is associated with sites of DNA replication. J Cell Biol *125*, 1201-1212.

Moir, R.D., Yoon, M., Khuon, S., and Goldman, R.D. (2000). Nuclear lamins A and B1: different pathways of assembly during nuclear envelope formation in living cells. The Journal of cell biology *151*, 1155-1168.

Moorhead, G.B., De Wever, V., Templeton, G., and Kerk, D. (2009). Evolution of protein phosphatases in plants and animals. Biochem J *417*, 401-409.

Moorhead, G.B., Trinkle-Mulcahy, L., and Ulke-Lemee, A. (2007). Emerging roles of nuclear protein phosphatases. Nat Rev Mol Cell Biol *8*, 234-244.

Morishita, W., Connor, J.H., Xia, H., Quinlan, E.M., Shenolikar, S., and Malenka, R.C. (2001). Regulation of synaptic strength by protein phosphatase 1. Neuron *32*, 1133-1148.

Mulkey, R.M., Endo, S., Shenolikar, S., and Malenka, R.C. (1994). Involvement of a calcineurin/inhibitor-1 phosphatase cascade in hippocampal long-term depression. Nature *369*, 486-488.

Munton, R.P., Vizi, S., and Mansuy, I.M. (2004). The role of protein phosphatase-1 in the modulation of synaptic and structural plasticity. FEBS Lett *567*, 121-128.

Naismith, T.V., Dalal, S., and Hanson, P.I. (2009a). Interaction of torsinA with its major binding partners is impaired by the dystonia-associated DeltaGAG deletion. J Biol Chem *284*, 27866-27874.

Naismith, T.V., Dalal, S., and Hanson, P.I. (2009b). Interaction of TorsinA with its major binding partners is impaired by the dystonia associated {Delta}GAG deletion. J Biol Chem.

Naismith, T.V., Heuser, J.E., Breakefield, X.O., and Hanson, P.I. (2004). TorsinA in the nuclear envelope. Proceedings of the National Academy of Sciences of the United States of America *101*, 7612-7617.

Napolitano, F., Pasqualetti, M., Usiello, A., Santini, E., Pacini, G., Sciamanna, G., Errico, F., Tassone, A., Di Dato, V., Martella, G., *et al.* (2010). Dopamine D2 receptor dysfunction is rescued by adenosine A2A receptor antagonism in a model of DYT1 dystonia. Neurobiol Dis *38*, 434-445.

Nery, F.C., Armata, I.A., Farley, J.E., Cho, J.A., Yaqub, U., Chen, P., da Hora, C.C., Wang, Q., Tagaya, M., Klein, C., *et al.* (2011). TorsinA participates in endoplasmic reticulum-associated degradation. Nature communications *2*, 393.

Nery, F.C., Zeng, J., Niland, B.P., Hewett, J., Farley, J., Irimia, D., Li, Y., Wiche, G., Sonnenberg, A., and Breakefield, X.O. (2008). TorsinA binds the KASH domain of nesprins and participates in linkage between nuclear envelope and cytoskeleton. Journal of cell science *121*, 3476-3486.

Neumann, B., Walter, T., Heriche, J.K., Bulkescher, J., Erfle, H., Conrad, C., Rogers, P., Poser, I., Held, M., Liebel, U., *et al.* (2010). Phenotypic profiling of the human genome by time-lapse microscopy reveals cell division genes. Nature *464*, 721-727.

Neuwald, A.F., Aravind, L., Spouge, J.L., and Koonin, E.V. (1999). AAA+: A class of chaperone-like ATPases associated with the assembly, operation, and disassembly of protein complexes. Genome research *9*, 27-43.

Novoyatleva, T., Heinrich, B., Tang, Y., Benderska, N., Butchbach, M.E., Lorson, C.L., Lorson, M.A., Ben-Dov, C., Fehlbaum, P., Bracco, L., *et al.* (2008). Protein phosphatase 1 binds to the RNA recognition motif of several splicing factors and regulates alternative pre-mRNA processing. Hum Mol Genet *17*, 52-70.

O'Connor, M.S., Safari, A., Liu, D., Qin, J., and Songyang, Z. (2004). The human Rap1 protein complex and modulation of telomere length. J Biol Chem *279*, 28585-28591.

Ogura, T., and Wilkinson, A.J. (2001). AAA+ superfamily ATPases: common structure--diverse function. Genes to cells : devoted to molecular & cellular mechanisms *6*, 575-597.

Okochi, M., Walter, J., Koyama, A., Nakajo, S., Baba, M., Iwatsubo, T., Meijer, L., Kahle, P.J., and Haass, C. (2000). Constitutive phosphorylation of the Parkinson's disease associated alpha-synuclein. J Biol Chem *275*, 390-397.

Olsen, J.V., Blagoev, B., Gnad, F., Macek, B., Kumar, C., Mortensen, P., and Mann, M. (2006). Global, in vivo, and site-specific phosphorylation dynamics in signaling networks. Cell *127*, 635-648.

Olsen, J.V., Vermeulen, M., Santamaria, A., Kumar, C., Miller, M.L., Jensen, L.J., Gnad, F., Cox, J., Jensen, T.S., Nigg, E.A., *et al.* (2010). Quantitative phosphoproteomics reveals widespread full phosphorylation site occupancy during mitosis. Science signaling *3*, ra3.

Oppermann, F.S., Grundner-Culemann, K., Kumar, C., Gruss, O.J., Jallepalli, P.V., and Daub, H. (2012). Combination of chemical genetics and phosphoproteomics for kinase signaling analysis enables confident identification of cellular downstream targets. Molecular & cellular proteomics : MCP *11*, O111 012351.

Ouimet, C.C., da Cruz e Silva, E.F., and Greengard, P. (1995). The alpha and gamma 1 isoforms of protein phosphatase 1 are highly and specifically concentrated in dendritic spines. Proc Natl Acad Sci U S A *92*, 3396-3400.

Ouimet, C.C., Miller, P.E., Hemmings, H.C., Jr., Walaas, S.I., and Greengard, P. (1984). DARPP-32, a dopamine- and adenosine 3':5'-monophosphate-regulated phosphoprotein enriched in dopamine-innervated brain regions. III. Immunocytochemical localization. The Journal of neuroscience : the official journal of the Society for Neuroscience *4*, 111-124.

Ozelius, L.J., and Bressman, S.B. (2011). Genetic and clinical features of primary torsion dystonia. Neurobiol Dis *42*, 127-135.

Ozelius, L.J., Hewett, J.W., Page, C.E., Bressman, S.B., Kramer, P.L., Shalish, C., de Leon, D., Brin, M.F., Raymond, D., Corey, D.P., *et al.* (1997). The early-onset torsion dystonia gene (DYT1) encodes an ATP-binding protein. Nat Genet *17*, 40-48.

Ozelius, L.J., Page, C.E., Klein, C., Hewett, J.W., Mineta, M., Leung, J., Shalish, C., Bressman, S.B., de Leon, D., Brin, M.F., *et al.* (1999). The TOR1A (DYT1) gene family and its role in early onset torsion dystonia. Genomics *62*, 377-384.

Padiath, Q.S., Saigoh, K., Schiffmann, R., Asahara, H., Yamada, T., Koeppen, A., Hogan, K., Ptacek, L.J., and Fu, Y.H. (2006). Lamin B1 duplications cause autosomal dominant leukodystrophy. Nat Genet *38*, 1114-1123.

Page, M.E., Bao, L., Andre, P., Pelta-Heller, J., Sluzas, E., Gonzalez-Alegre, P., Bogush, A., Khan, L.E., Iacovitti, L., Rice, M.E., *et al.* (2010). Cell-autonomous alteration of

dopaminergic transmission by wild type and mutant (DeltaE) TorsinA in transgenic mice. Neurobiology of disease *39*, 318-326.

Pathak, R.K., Luskey, K.L., and Anderson, R.G. (1986). Biogenesis of the crystalloid endoplasmic reticulum in UT-1 cells: evidence that newly formed endoplasmic reticulum emerges from the nuclear envelope. J Cell Biol *102*, 2158-2168.

Perry, R.L., Yang, C., Soora, N., Salma, J., Marback, M., Naghibi, L., Ilyas, H., Chan, J., Gordon, J.W., and McDermott, J.C. (2009). Direct interaction between myocyte enhancer factor 2 (MEF2) and protein phosphatase 1alpha represses MEF2-dependent gene expression. Molecular and cellular biology *29*, 3355-3366.

Pestov, N.B., Ahmad, N., Korneenko, T.V., Zhao, H., Radkov, R., Schaer, D., Roy, S., Bibert, S., Geering, K., and Modyanov, N.N. (2007). Evolution of Na,K-ATPase beta m-subunit into a coregulator of transcription in placental mammals. Proc Natl Acad Sci U S A *104*, 11215-11220.

Peti, W., Nairn, A.C., and Page, R. (2013). Structural basis for protein phosphatase 1 regulation and specificity. The FEBS journal *280*, 596-611.

Phukan, J., Albanese, A., Gasser, T., and Warner, T. (2011). Primary dystonia and dystonia-plus syndromes: clinical characteristics, diagnosis, and pathogenesis. Lancet neurology *10*, 1074-1085.

Pisani, A., Martella, G., Tscherter, A., Bonsi, P., Sharma, N., Bernardi, G., and Standaert, D.G. (2006). Altered responses to dopaminergic D2 receptor activation and N-type calcium currents in striatal cholinergic interneurons in a mouse model of DYT1 dystonia. Neurobiol Dis *24*, 318-325.

Planel, E., Yasutake, K., Fujita, S.C., and Ishiguro, K. (2001). Inhibition of protein phosphatase 2A overrides tau protein kinase I/glycogen synthase kinase 3 beta and cyclin-dependent kinase 5 inhibition and results in tau hyperphosphorylation in the hippocampus of starved mouse. J Biol Chem *276*, 34298-34306.

Puckelwartz, M.J., Kessler, E., Zhang, Y., Hodzic, D., Randles, K.N., Morris, G., Earley, J.U., Hadhazy, M., Holaska, J.M., Mewborn, S.K., *et al.* (2009). Disruption of nesprin-1 produces an Emery Dreifuss muscular dystrophy-like phenotype in mice. Hum Mol Genet *18*, 607-620.

Pyrpasopoulou, A., Meier, J., Maison, C., Simos, G., and Georgatos, S.D. (1996). The lamin B receptor (LBR) provides essential chromatin docking sites at the nuclear envelope. EMBO J *15*, 7108-7119.

Qian, J., Lesage, B., Beullens, M., Van Eynde, A., and Bollen, M. (2011). PP1/Repo-man dephosphorylates mitotic histone H3 at T3 and regulates chromosomal aurora B targeting. Current biology : CB *21*, 766-773.

Rebelo, S., Domingues, S.C., Santos, M., Fardilha, M., Esteves, S.L., Vieira, S.I., Vintem, A.P., Wu, W., da Cruz, E.S.E.F., and da Cruz, E.S.O.A. (2013). Identification of a Novel Complex AbetaPP:Fe65:PP1 that Regulates AbetaPP Thr668 Phosphorylation Levels. Journal of Alzheimer's disease : JAD *35*, 761-775.

Rebelo, S., Henriques, A.G., da Cruz e Silva, E.F., and da Cruz e Silva, O.A. (2004). Effect of cell density on intracellular levels of the Alzheimer's amyloid precursor protein. Journal of neuroscience research *76*, 406-414.

Rebelo, S., Vieira, S.I., Esselmann, H., Wiltfang, J., da Cruz e Silva, E.F., and da Cruz e Silva, O.A. (2007). Tyrosine 687 phosphorylated Alzheimer's amyloid precursor protein is retained intracellularly and exhibits a decreased turnover rate. Neuro-degenerative diseases *4*, 78-87.

Reese, M.G. (2001). Application of a time-delay neural network to promoter annotation in the Drosophila melanogaster genome. Computers & chemistry *26*, 51-56.

Reese, M.G., Eeckman, F.H., Kulp, D., and Haussler, D. (1997). Improved splice site detection in Genie. Journal of computational biology : a journal of computational molecular cell biology *4*, 311-323.

Riz, I., and Hawley, R.G. (2005). G1/S transcriptional networks modulated by the HOX11/TLX1 oncogene of T-cell acute lymphoblastic leukemia. Oncogene *24*, 5561-5575.

Rober, R.A., Weber, K., and Osborn, M. (1989). Differential timing of nuclear lamin A/C expression in the various organs of the mouse embryo and the young animal: a developmental study. Development *105*, 365-378.

Robinson, A., Partridge, D., Malhas, A., De Castro, S.C., Gustavsson, P., Thompson, D.N., Vaux, D.J., Copp, A.J., Stanier, P., Bassuk, A.G., *et al.* (2013). Is LMNB1 a susceptibility gene for neural tube defects in humans? Birth defects research. Part A, Clinical and molecular teratology *97*, 398-402.

Rocha, J.F., Vieira, S.I., and Silva, O.A.B.D.E. (2012). APP phosphorylation at S655 correlates with F-actin cytoskeleton dynamics - relevance in neuronal differentiation. Microsc Microanal *18*, 57-58.

Rostasy, K., Augood, S.J., Hewett, J.W., Leung, J.C., Sasaki, H., Ozelius, L.J., Ramesh, V., Standaert, D.G., Breakefield, X.O., and Hedreen, J.C. (2003). TorsinA protein and neuropathology in early onset generalized dystonia with GAG deletion. Neurobiol Dis *12*, 11-24.

Rothballer, A., and Kutay, U. (2013). The diverse functional LINCs of the nuclear envelope to the cytoskeleton and chromatin. Chromosoma *122*, 415-429.

Roux, K.J., Crisp, M.L., Liu, Q., Kim, D., Kozlov, S., Stewart, C.L., and Burke, B. (2009). Nesprin 4 is an outer nuclear membrane protein that can induce kinesin-mediated cell polarization. Proc Natl Acad Sci U S A *106*, 2194-2199.

Rubin, E., Mittnacht, S., Villa-Moruzzi, E., and Ludlow, J.W. (2001). Site-specific and temporally-regulated retinoblastoma protein dephosphorylation by protein phosphatase type 1. Oncogene *20*, 3776-3785.

S. Rebelo., S.C.D., S. Mariana, M. Fardilha, S. L. C. Esteves, S. I. Vieira, A. P. B. Vintém, W. Wu, E. F. da Cruz e Silva and O. A. B. da Cruz e Silva (2013). Identification of a novel complex APP:Fe65:PP1 that regulates APP Thr668 phosphorylation levels. JAD (submitted).

Salpingidou, G., Smertenko, A., Hausmanowa-Petrucewicz, I., Hussey, P.J., and Hutchison, C.J. (2007). A novel role for the nuclear membrane protein emerin in association of the centrosome to the outer nuclear membrane. J Cell Biol *178*, 897-904.

Santos, M. (2009). Validation of LAP1B as a novel Protein Phosphatase 1 regulator. Biology Department, University of Aveiro, Aveiro.

Santos, M., Domingues, C.S., Costa, P., Muller, T., Galozzi, S., Marcus, K., da Cruz e Silva, E.F., da Cruz e Silva, O.A.B, Rebelo, S. (2014). Identification of a novel human LAP1 isoform that is regulated by protein phosphorylation. Submitted to PlosOne.

Santos, M., Rebelo, S., Van Kleeff, P.J., Kim, C.E., Dauer, W.T., Fardilha, M., da Cruz, E.S.O.A., and da Cruz, E.S.E.F. (2013). The Nuclear Envelope Protein, LAP1B, Is a Novel Protein Phosphatase 1 Substrate. PloS one *8*, e76788.

Sasaki, K., Shima, H., Kitagawa, Y., Irino, S., Sugimura, T., and Nagao, M. (1990). Identification of members of the protein phosphatase 1 gene family in the rat and enhanced expression of protein phosphatase 1 alpha gene in rat hepatocellular carcinomas. Jpn J Cancer Res *81*, 1272-1280.

Scaffidi, P., and Misteli, T. (2005). Reversal of the cellular phenotype in the premature aging disease Hutchinson-Gilford progeria syndrome. Nature medicine *11*, 440-445.

Schirmer, E.C., Florens, L., Guan, T., Yates, J.R., 3rd, and Gerace, L. (2003). Nuclear membrane proteins with potential disease links found by subtractive proteomics. Science *301*, 1380-1382.

Schirmer, E.C., Florens, L., Guan, T., Yates, J.R., 3rd, and Gerace, L. (2005). Identification of novel integral membrane proteins of the nuclear envelope with potential disease links using subtractive proteomics. Novartis Foundation symposium *264*, 63-76; discussion 76-80, 227-230.

Schirmer, E.C., and Gerace, L. (2005). The nuclear membrane proteome: extending the envelope. Trends Biochem Sci *30*, 551-558.

Sciamanna, G., Bonsi, P., Tassone, A., Cuomo, D., Tscherter, A., Viscomi, M.T., Martella, G., Sharma, N., Bernardi, G., Standaert, D.G., *et al.* (2009). Impaired striatal D2 receptor function leads to enhanced GABA transmission in a mouse model of DYT1 dystonia. Neurobiol Dis *34*, 133-145.

Sciamanna, G., Hollis, R., Ball, C., Martella, G., Tassone, A., Marshall, A., Parsons, D., Li, X., Yokoi, F., Zhang, L., *et al.* (2012a). Cholinergic dysregulation produced by selective inactivation of the dystonia-associated protein torsinA. Neurobiol Dis *47*, 416-427.

Sciamanna, G., Tassone, A., Mandolesi, G., Puglisi, F., Ponterio, G., Martella, G., Madeo, G., Bernardi, G., Standaert, D.G., Bonsi, P., *et al.* (2012b). Cholinergic dysfunction alters synaptic integration between thalamostriatal and corticostriatal inputs in DYT1 dystonia. The Journal of neuroscience : the official journal of the Society for Neuroscience *32*, 11991-12004.

Senior, A., and Gerace, L. (1988). Integral membrane proteins specific to the inner nuclear membrane and associated with the nuclear lamina. J Cell Biol *107*, 2029-2036.

Shashidharan, P., Good, P.F., Hsu, A., Perl, D.P., Brin, M.F., and Olanow, C.W. (2000a). TorsinA accumulation in Lewy bodies in sporadic Parkinson's disease. Brain research *877*, 379-381.

Shashidharan, P., Kramer, B.C., Walker, R.H., Olanow, C.W., and Brin, M.F. (2000b). Immunohistochemical localization and distribution of torsinA in normal human and rat brain. Brain research *853*, 197-206.

Shashidharan, P., Sandu, D., Potla, U., Armata, I.A., Walker, R.H., McNaught, K.S., Weisz, D., Sreenath, T., Brin, M.F., and Olanow, C.W. (2005). Transgenic mouse model of early-onset DYT1 dystonia. Human molecular genetics *14*, 125-133.

Shedden, K., and Cooper, S. (2002). Analysis of cell-cycle-specific gene expression in human cells as determined by microarrays and double-thymidine block synchronization. Proc Natl Acad Sci U S A *99*, 4379-4384.

Shi, Y. (2009). Serine/threonine phosphatases: mechanism through structure. Cell *139*, 468-484.

Shin, J.Y., Mendez-Lopez, I., Wang, Y., Hays, A.P., Tanji, K., Lefkowitch, J.H., Schulze, P.C., Worman, H.J., and Dauer, W.T. (2013). Lamina-associated polypeptide-1 interacts with the muscular dystrophy protein emerin and is essential for skeletal muscle maintenance. Developmental cell *26*, 591-603.

Shumaker, D.K., Lee, K.K., Tanhehco, Y.C., Craigie, R., and Wilson, K.L. (2001). LAP2 binds to BAF.DNA complexes: requirement for the LEM domain and modulation by variable regions. EMBO J *20*, 1754-1764.

Sievers, F., and Higgins, D.G. (2014). Clustal omega, accurate alignment of very large numbers of sequences. Methods Mol Biol *1079*, 105-116.

Soderling, T.R., and Derkach, V.A. (2000). Postsynaptic protein phosphorylation and LTP. Trends in neurosciences *23*, 75-80.

Solovyev, V., and Salamov, A. (1997). The Gene-Finder computer tools for analysis of human and model organisms genome sequences. Proceedings / ... International Conference on Intelligent Systems for Molecular Biology ; ISMB. International Conference on Intelligent Systems for Molecular Biology *5*, 294-302.

Song, C.H., Bernhard, D., Bolarinwa, C., Hess, E.J., Smith, Y., and Jinnah, H.A. (2013). Subtle microstructural changes of the striatum in a DYT1 knock-in mouse model of dystonia. Neurobiol Dis *54*, 362-371.

Song, C.H., Fan, X., Exeter, C.J., Hess, E.J., and Jinnah, H.A. (2012). Functional analysis of dopaminergic systems in a DYT1 knock-in mouse model of dystonia. Neurobiol Dis *48*, 66-78.

Soullam, B., and Worman, H.J. (1995). Signals and structural features involved in integral membrane protein targeting to the inner nuclear membrane. J Cell Biol *130*, 15-27.

Stamelou, M., Edwards, M.J., Hallett, M., and Bhatia, K.P. (2012). The non-motor syndrome of primary dystonia: clinical and pathophysiological implications. Brain *135*, 1668-1681.

Standaert, D.G. (2011). Update on the pathology of dystonia. Neurobiol Dis *42*, 148-151.

Starr, D.A., and Han, M. (2002). Role of ANC-1 in tethering nuclei to the actin cytoskeleton. Science *298*, 406-409.

Steen, R.L., Beullens, M., Landsverk, H.B., Bollen, M., and Collas, P. (2003). AKAP149 is a novel PP1 specifier required to maintain nuclear envelope integrity in G1 phase. J Cell Sci *116*, 2237-2246.

Steen, R.L., and Collas, P. (2001). Mistargeting of B-type lamins at the end of mitosis: implications on cell survival and regulation of lamins A/C expression. J Cell Biol *153*, 621-626.

Steen, R.L., Martins, S.B., Tasken, K., and Collas, P. (2000). Recruitment of protein phosphatase 1 to the nuclear envelope by A-kinase anchoring protein AKAP149 is a prerequisite for nuclear lamina assembly. J Cell Biol *150*, 1251-1262.

Stewart, C., and Burke, B. (1987). Teratocarcinoma stem cells and early mouse embryos contain only a single major lamin polypeptide closely resembling lamin B. Cell *51*, 383-392.

Stewart, C.L., Roux, K.J., and Burke, B. (2007). Blurring the boundary: the nuclear envelope extends its reach. Science *318*, 1408-1412.

Stick, R., Angres, B., Lehner, C.F., and Nigg, E.A. (1988). The fates of chicken nuclear lamin proteins during mitosis: evidence for a reversible redistribution of lamin B2 between inner nuclear membrane and elements of the endoplasmic reticulum. J Cell Biol *107*, 397-406.

Strack, S., Barban, M.A., Wadzinski, B.E., and Colbran, R.J. (1997). Differential inactivation of postsynaptic density-associated and soluble Ca2+/calmodulin-dependent protein kinase II by protein phosphatases 1 and 2A. J Neurochem *68*, 2119-2128.

Strack, S., Kini, S., Ebner, F.F., Wadzinski, B.E., and Colbran, R.J. (1999). Differential cellular and subcellular localization of protein phosphatase 1 isoforms in brain. J Comp Neurol *413*, 373-384.

Svenningsson, P., Lindskog, M., Rognoni, F., Fredholm, B.B., Greengard, P., and Fisone, G. (1998). Activation of adenosine A2A and dopamine D1 receptors stimulates cyclic AMP-dependent phosphorylation of DARPP-32 in distinct populations of striatal projection neurons. Neuroscience *84*, 223-228.

Svenningsson, P., Tzavara, E.T., Liu, F., Fienberg, A.A., Nomikos, G.G., and Greengard, P. (2002). DARPP-32 mediates serotonergic neurotransmission in the forebrain. Proc Natl Acad Sci U S A *99*, 3188-3193.

Tadokoro, K., Yamazaki-Inoue, M., Tachibana, M., Fujishiro, M., Nagao, K., Toyoda, M., Ozaki, M., Ono, M., Miki, N., Miyashita, T., *et al.* (2005). Frequent occurrence of protein isoforms with or without a single amino acid residue by subtle alternative splicing: the case of Gln in DRPLA affects subcellular localization of the products. J Hum Genet *50*, 382-394.

Takano, M., Koyama, Y., Ito, H., Hoshino, S., Onogi, H., Hagiwara, M., Furukawa, K., and Horigome, T. (2004). Regulation of binding of lamin B receptor to chromatin by SR protein kinase and cdc2 kinase in Xenopus egg extracts. The Journal of biological chemistry *279*, 13265-13271.

Tan, S., Lyulcheva, E., Dean, J., and Bennett, D. (2008). Mars promotes dTACC dephosphorylation on mitotic spindles to ensure spindle stability. J Cell Biol *182*, 27-33.

Tanabe, L.M., Kim, C.E., Alagem, N., and Dauer, W.T. (2009). Primary dystonia: molecules and mechanisms. Nature reviews. Neurology *5*, 598-609.

Tanuma, N., Kim, S.E., Beullens, M., Tsubaki, Y., Mitsuhashi, S., Nomura, M., Kawamura, T., Isono, K., Koseki, H., Sato, M., *et al.* (2008). Nuclear inhibitor of protein phosphatase-1 (NIPP1) directs protein phosphatase-1 (PP1) to dephosphorylate the U2 small nuclear ribonucleoprotein particle (snRNP) component, spliceosome-associated protein 155 (Sap155). J Biol Chem *283*, 35805-35814.

Taylor, M.R., Slavov, D., Gajewski, A., Vlcek, S., Ku, L., Fain, P.R., Carniel, E., Di Lenarda, A., Sinagra, G., Boucek, M.M., *et al.* (2005). Thymopoietin (lamina-associated polypeptide 2) gene mutation associated with dilated cardiomyopathy. Human mutation *26*, 566-574.

Terrak, M., Kerff, F., Langsetmo, K., Tao, T., and Dominguez, R. (2004). Structural basis of protein phosphatase 1 regulation. Nature *429*, 780-784.

Terry-Lorenzo, R.T., Elliot, E., Weiser, D.C., Prickett, T.D., Brautigan, D.L., and Shenolikar, S. (2002). Neurabins recruit protein phosphatase-1 and inhibitor-2 to the actin cytoskeleton. J Biol Chem *277*, 46535-46543.

Terry-Lorenzo, R.T., Inoue, M., Connor, J.H., Haystead, T.A., Armbruster, B.N., Gupta, R.P., Oliver, C.J., and Shenolikar, S. (2000). Neurofilament-L is a protein phosphatase-1-binding protein associated with neuronal plasma membrane and post-synaptic density. J Biol Chem *275*, 2439-2446.

Thompson, L.J., Bollen, M., and Fields, A.P. (1997). Identification of protein phosphatase 1 as a mitotic lamin phosphatase. The Journal of biological chemistry *272*, 29693-29697.

Torres, G.E., Sweeney, A.L., Beaulieu, J.M., Shashidharan, P., and Caron, M.G. (2004). Effect of torsinA on membrane proteins reveals a loss of function and a dominant-negative phenotype of the dystonia-associated DeltaE-torsinA mutant. Proc Natl Acad Sci U S A *101*, 15650-15655.

Tran, H.T., Ulke, A., Morrice, N., Johannes, C.J., and Moorhead, G.B. (2004). Proteomic characterization of protein phosphatase complexes of the mammalian nucleus. Molecular & cellular proteomics : MCP *3*, 257-265.

Trinkle-Mulcahy, L., Ajuh, P., Prescott, A., Claverie-Martin, F., Cohen, S., Lamond, A.I., and Cohen, P. (1999). Nuclear organisation of NIPP1, a regulatory subunit of protein phosphatase 1 that associates with pre-mRNA splicing factors. J Cell Sci *112 (Pt 2)*, 157-168.

Trinkle-Mulcahy, L., Andersen, J., Lam, Y.W., Moorhead, G., Mann, M., and Lamond, A.I. (2006). Repo-Man recruits PP1 gamma to chromatin and is essential for cell viability. J Cell Biol *172*, 679-692.

Trinkle-Mulcahy, L., Andrews, P.D., Wickramasinghe, S., Sleeman, J., Prescott, A., Lam, Y.W., Lyon, C., Swedlow, J.R., and Lamond, A.I. (2003). Time-lapse imaging reveals dynamic relocalization of PP1gamma throughout the mammalian cell cycle. Mol Biol Cell *14*, 107-117.

Trinkle-Mulcahy, L., and Lamond, A.I. (2006). Mitotic phosphatases: no longer silent partners. Current opinion in cell biology *18*, 623-631.

Trinkle-Mulcahy, L., Sleeman, J.E., and Lamond, A.I. (2001). Dynamic targeting of protein phosphatase 1 within the nuclei of living mammalian cells. J Cell Sci *114*, 4219-4228.

Trinklein, N.D., Aldred, S.J., Saldanha, A.J., and Myers, R.M. (2003). Identification and functional analysis of human transcriptional promoters. Genome research *13*, 308-312.

Tsai, K.W., Tarn, W.Y., and Lin, W.C. (2007). Wobble splicing reveals the role of the branch point sequence-to-NAGNAG region in 3' tandem splice site selection. Molecular and cellular biology *27*, 5835-5848.

Tseng, L.C., and Chen, R.H. (2011). Temporal control of nuclear envelope assembly by phosphorylation of lamin B receptor. Mol Biol Cell *22*, 3306-3317.

Ulug, A.M., Vo, A., Argyelan, M., Tanabe, L., Schiffer, W.K., Dewey, S., Dauer, W.T., and Eidelberg, D. (2011). Cerebellothalamocortical pathway abnormalities in torsinA DYT1 knock-in mice. Proc Natl Acad Sci U S A *108*, 6638-6643.

Vale, R.D. (2000). AAA proteins. Lords of the ring. J Cell Biol *150*, F13-19.

Valente, E.M., Warner, T.T., Jarman, P.R., Mathen, D., Fletcher, N.A., Marsden, C.D., Bhatia, K.P., and Wood, N.W. (1998). The role of DYT1 in primary torsion dystonia in Europe. Brain *121 (Pt 12)*, 2335-2339.

van der Meijden, C.M., Lapointe, D.S., Luong, M.X., Peric-Hupkes, D., Cho, B., Stein, J.L., van Wijnen, A.J., and Stein, G.S. (2002). Gene profiling of cell cycle progression through S-phase reveals sequential expression of genes required for DNA replication and nucleosome assembly. Cancer research *62*, 3233-3243.

Vander Heyden, A.B., Naismith, T.V., Snapp, E.L., and Hanson, P.I. (2011). Static retention of the lumenal monotopic membrane protein torsinA in the endoplasmic reticulum. EMBO J *30*, 3217-3231.

Vasudevan, A., Breakefield, X.O., and Bhide, P.G. (2006). Developmental patterns of torsinA and torsinB expression. Brain research *1073-1074*, 139-145.

Vieira, S.I., Rebelo, S., Esselmann, H., Wiltfang, J., Lah, J., Lane, R., Small, S.A., Gandy, S., da Cruz, E.S.E.F., and da Cruz, E.S.O.A. (2010). Retrieval of the Alzheimer's amyloid precursor protein from the endosome to the TGN is S655 phosphorylation state-dependent and retromer-mediated. Molecular neurodegeneration *5*, 40.

Wagner, S.A., Beli, P., Weinert, B.T., Nielsen, M.L., Cox, J., Mann, M., and Choudhary, C. (2011). A proteome-wide, quantitative survey of in vivo ubiquitylation sites reveals widespread regulatory roles. Molecular & cellular proteomics : MCP *10*, M111 013284.

Wakula, P., Beullens, M., Ceulemans, H., Stalmans, W., and Bollen, M. (2003). Degeneracy and function of the ubiquitous RVXF motif that mediates binding to protein phosphatase-1. The Journal of biological chemistry *278*, 18817-18823.

Wang, B., Zhang, P., and Wei, Q. (2008a). Recent progress on the structure of Ser/Thr protein phosphatases. Science in China. Series C, Life sciences / Chinese Academy of Sciences *51*, 487-494.

Wang, W., Stukenberg, P.T., and Brautigan, D.L. (2008b). Phosphatase inhibitor-2 balances protein phosphatase 1 and aurora B kinase for chromosome segregation and cytokinesis in human retinal epithelial cells. Mol Biol Cell *19*, 4852-4862.

Wang, Z., Udeshi, N.D., Slawson, C., Compton, P.D., Sakabe, K., Cheung, W.D., Shabanowitz, J., Hunt, D.F., and Hart, G.W. (2010). Extensive crosstalk between O-GlcNAcylation and phosphorylation regulates cytokinesis. Science signaling *3*, ra2.

Washington, K., Ammosova, T., Beullens, M., Jerebtsova, M., Kumar, A., Bollen, M., and Nekhai, S. (2002). Protein phosphatase-1 dephosphorylates the C-terminal domain of RNA polymerase-II. J Biol Chem *277*, 40442-40448.

Watanabe, T., da Cruz e Silva, E.F., Huang, H.B., Starkova, N., Kwon, Y.G., Horiuchi, A., Greengard, P., and Nairn, A.C. (2003). Preparation and characterization of recombinant protein phosphatase 1. Methods in enzymology *366*, 321-338.

Waterham, H.R., Koster, J., Mooyer, P., Noort Gv, G., Kelley, R.I., Wilcox, W.R., Wanders, R.J., Hennekam, R.C., and Oosterwijk, J.C. (2003). Autosomal recessive HEM/Greenberg skeletal dysplasia is caused by 3 beta-hydroxysterol delta 14-reductase deficiency due to mutations in the lamin B receptor gene. American journal of human genetics *72*, 1013-1017.

Weber, C., Schreiber, T.B., and Daub, H. (2012). Dual phosphoproteomics and chemical proteomics analysis of erlotinib and gefitinib interference in acute myeloid leukemia cells. Journal of proteomics *75*, 1343-1356.

Westphal, R.S., Tavalin, S.J., Lin, J.W., Alto, N.M., Fraser, I.D., Langeberg, L.K., Sheng, M., and Scott, J.D. (1999). Regulation of NMDA receptors by an associated phosphatase-kinase signaling complex. Science *285*, 93-96.

Wichmann, T. (2008). Commentary: Dopaminergic dysfunction in DYT1 dystonia. Exp Neurol *212*, 242-246.

Wilhelmsen, K., Litjens, S.H., Kuikman, I., Tshimbalanga, N., Janssen, H., van den Bout, I., Raymond, K., and Sonnenberg, A. (2005). Nesprin-3, a novel outer nuclear membrane protein, associates with the cytoskeletal linker protein plectin. J Cell Biol *171*, 799-810.

Wilkie, G.S., Korfali, N., Swanson, S.K., Malik, P., Srsen, V., Batrakou, D.G., de las Heras, J., Zuleger, N., Kerr, A.R., Florens, L., *et al.* (2011). Several novel nuclear envelope transmembrane proteins identified in skeletal muscle have cytoskeletal associations. Molecular & cellular proteomics : MCP *10*, M110 003129.

Worman, H.J., and Courvalin, J.C. (2005). Nuclear envelope, nuclear lamina, and inherited disease. Int Rev Cytol *246*, 231-279.

Worman, H.J., Yuan, J., Blobel, G., and Georgatos, S.D. (1988). A lamin B receptor in the nuclear envelope. Proc Natl Acad Sci U S A *85*, 8531-8534.

Wu, J.Q., Guo, J.Y., Tang, W., Yang, C.S., Freel, C.D., Chen, C., Nairn, A.C., and Kornbluth, S. (2009). PP1-mediated dephosphorylation of phosphoproteins at mitotic exit is controlled by inhibitor-1 and PP1 phosphorylation. Nature cell biology *11*, 644-651.

Wu, W., Lin, F., and Worman, H.J. (2002). Intracellular trafficking of MAN1, an integral protein of the nuclear envelope inner membrane. J Cell Sci *115*, 1361-1371.

Xiao, J., Gong, S., Zhao, Y., and LeDoux, M.S. (2004). Developmental expression of rat torsinA transcript and protein. Brain research. Developmental brain research *152*, 47-60.

Xin, D., Hu, L., and Kong, X. (2008). Alternative promoters influence alternative splicing at the genomic level. PloS one *3*, e2377.

Yamashiro, S., Yamakita, Y., Totsukawa, G., Goto, H., Kaibuchi, K., Ito, M., Hartshorne, D.J., and Matsumura, F. (2008). Myosin phosphatase-targeting subunit 1 regulates mitosis by antagonizing polo-like kinase 1. Developmental cell *14*, 787-797.

Yan, Z., Hsieh-Wilson, L., Feng, J., Tomizawa, K., Allen, P.B., Fienberg, A.A., Nairn, A.C., and Greengard, P. (1999). Protein phosphatase 1 modulation of neostriatal AMPA channels: regulation by DARPP-32 and spinophilin. Nature neuroscience *2*, 13-17.

Yang, L., Guan, T., and Gerace, L. (1997). Integral membrane proteins of the nuclear envelope are dispersed throughout the endoplasmic reticulum during mitosis. The Journal of cell biology *137*, 1199-1210.

Yokoi, F., Dang, M.T., Li, J., and Li, Y. (2006). Myoclonus, motor deficits, alterations in emotional responses and monoamine metabolism in epsilon-sarcoglycan deficient mice. Journal of biochemistry *140*, 141-146.

Yokoi, F., Dang, M.T., Li, J., Standaert, D.G., and Li, Y. (2011). Motor deficits and decreased striatal dopamine receptor 2 binding activity in the striatum-specific Dyt1 conditional knockout mice. PloS one *6*, e24539.

Zeitlin, S.G., Shelby, R.D., and Sullivan, K.F. (2001). CENP-A is phosphorylated by Aurora B kinase and plays an unexpected role in completion of cytokinesis. J Cell Biol *155*, 1147-1157.

Zhang, L., Yokoi, F., Jin, Y.H., DeAndrade, M.P., Hashimoto, K., Standaert, D.G., and Li, Y. (2011). Altered dendritic morphology of Purkinje cells in Dyt1 DeltaGAG knock-in and purkinje cell-specific Dyt1 conditional knockout mice. PloS one *6*, e18357.

Zhang, Q., Skepper, J.N., Yang, F., Davies, J.D., Hegyi, L., Roberts, R.G., Weissberg, P.L., Ellis, J.A., and Shanahan, C.M. (2001). Nesprins: a novel family of spectrin-repeat-containing proteins that localize to the nuclear membrane in multiple tissues. J Cell Sci *114*, 4485-4498.

Zhang, S.X., Searcy, T.R., Wu, Y., Gozal, D., and Wang, Y. (2007). Alternative promoter usage and alternative splicing contribute to mRNA heterogeneity of mouse monocarboxylate transporter 2. Physiological genomics *32*, 95-104.

Zhang, Y.Q., and Sarge, K.D. (2008). Sumoylation regulates lamin A function and is lost in lamin A mutants associated with familial cardiomyopathies. J Cell Biol *182*, 35-39.

Zhao, C., Brown, R.S., Chase, A.R., Eisele, M.R., and Schlieker, C. (2013a). Regulation of Torsin ATPases by LAP1 and LULL1. Proc Natl Acad Sci U S A.

Zhao, C., Brown, R.S., Chase, A.R., Eisele, M.R., and Schlieker, C. (2013b). Regulation of Torsin ATPases by LAP1 and LULL1. Proc Natl Acad Sci U S A *110*, E1545-1554.

Zhao, Y., DeCuypere, M., and LeDoux, M.S. (2008a). Abnormal motor function and dopamine neurotransmission in DYT1 DeltaGAG transgenic mice. Exp Neurol *210*, 719-730.

Zhao, Y., Xiao, J., Ueda, M., Wang, Y., Hines, M., Nowak, T.S., Jr., and LeDoux, M.S. (2008b). Glial elements contribute to stress-induced torsinA expression in the CNS and peripheral nervous system. Neuroscience *155*, 439-453.

Zhen, Y.Y., Libotte, T., Munck, M., Noegel, A.A., and Korenbaum, E. (2002). NUANCE, a giant protein connecting the nucleus and actin cytoskeleton. J Cell Sci *115*, 3207-3222.

Zhu, L., Wrabl, J.O., Hayashi, A.P., Rose, L.S., and Thomas, P.J. (2008). The torsin-family AAA+ protein OOC-5 contains a critical disulfide adjacent to Sensor-II that couples redox state to nucleotide binding. Mol Biol Cell *19*, 3599-3612.

Zuleger, N., Kelly, D.A., Richardson, A.C., Kerr, A.R., Goldberg, M.W., Goryachev, A.B., and Schirmer, E.C. (2011). System analysis shows distinct mechanisms and common principles of nuclear envelope protein dynamics. J Cell Biol *193*, 109-123.

APPENDIX I – CULTURE MEDIA AND SOLUTIONS

Bacteria media

LB (Luria-Bertani) Medium

To 950 mL of deionised H_2O add:

LB 25 g

Agar 15 g (for plates only)

Shake until the solutes have dissolved. Adjust the volume of the solution to 1 L with deionised H_2O. Sterilize by autoclaving.

SOB Medium

To 950 mL of deionised H_2O add:

SOB Broth 25.5 g

Shake until the solutes have dissolved. Add 10 ml of a 250 mM KCl (prepared by dissolving 1.86 g of KCl in 100 mL of deionised H_2O). Adjust the pH to 7.0 with 5 N NaOH. Sterilize by autoclaving. Just prior to use add 5 ml of a sterile solution of 2 M $MgCl_2$ (prepared by dissolving 19 g of $MgCl_2$ in 100 mL of deionised H_2O and sterilize by autoclaving).

SOC Medium

SOC is identical to SOB except that it contains 20 mM glucose. After the SOB medium has been autoclaved, allow it to cool to 60ºC and add 20 mL of a sterile 1M glucose (this solution is made by dissolving 18 g of glucose in 90 mL of deionised H_2O; after the sugar has dissolved, adjust the volume of the solution to 100 mL with deionised H_2O and sterilize by filtration through a 0.22 µm filter).

100 mg/ml antibiotics stock solution (Ampicilin or Kanamycin)

Dissolve 1 g of the antibiotic in 10 mL of deionised H_2O. Mix until de solutes have dissolved, filter through a 0.22 µm filter, aliquot and store at -20ºC.

Competent cell solutions

Solution I (1L)

$MnCl_2.4H_2O$ 9.9 g

$CaCl_2.2H_2O$ 1.5 g

Glycerol 150 g

KHAc 1M 30 mL

Adjust the volume of the solution to 1 L with deionised H_2O. Adjust pH to 5.8, filter through a 0.2 μm filter and store at 4ºC.

Solution II (1L)

0.5 M MOPS (pH 6.8) 20 mL

RbCl 1.2 g

$CaCl_2.2H_2O$ 11g

Glycerol 150 g

Adjust the volume of the solution to 1 L with deionised H_2O. Filter through a 0.2 μm filter and store at 4ºC.

Solutions for DNA manipulation

50x TAE Buffer (1 L)

Tris base 242 g

Glacial acetic acid 57.1 ml

0.5 M EDTA (pH 8.0) 100 ml

TE Buffer (pH 7.5)

10 mM Tris-HCl pH 7.5

1 mM EDTA pH 8.0

6x loading Buffer (LB)

Bromophenol blue 0.25%

Glycerol 30%

Miniprep solutions

Cell resuspension solution

50 mM glucose

25 mM Tris-HCl pH 8.0

10 mM EDTA

Cell lysis solution

0.2 N NaOH

1% SDS

Neutralization solution

3 M potassium acetate

2 M glacial acetic acid

Maxiprep solutions

Cell Resuspension Solution

50 mM Tris-HCl (pH 7.5)

10 mM EDTA

100 µg/mL RNAase A

Cell Lysis Solution

0.2 M NaOH

1% SDS

Neutralization Solution

1.32 M potassium acetate pH 4.8

Column Wash Solution

80 mM potassium acetate

8.3 mM Tris-HCl (pH 7.5)

0.04 mM EDTA

55 % ethanol

Yeast Media

YPD medium

To 950 mL of deionised H_2O add:

YPD 50 g

Agar 15 g (for plates only)

Shake until the solutes have dissolved. Adjust the volume to 1 L with deionised H_2O and sterilize by autoclaving. Allow medium to cool to 60ºC and add glucose to 2% (50 ml of a sterile 40% stock solution).

10x Dropout solution (DO 10x)

This solution contains all but one or more of the following components:

	10x concentration (mg/L)	SIGMA #
L-Isoleucine	300	I-7383
L-Valine	1500	V-0500
L-Adenine hemisulfate salt	200	A-9126
L-Arginine HCl	200	A-5131
L-Histidine HCl monohydrate	200	H-9511
L-Leucine	1000	L-1512
L-Lysine HCl	300	L-1262
L-Methionine	200	M-9625
L-Phenylalanine	500	P-5030
L-Threonine	2000	T-8625
L-Tryptophan	200	T-0254
L-Tyrosine	300	T-3754
L-Uracil	200	U-0750

10x dropout supplements may be autoclaved and stored for up to 1 year.

Triple Drop Out: DO/-Leu/-Trp/-His

Quadruple Drop Out: DO/-Leu/-Trp/-His/-Ade

SD synthetic medium

To 800 mL of deionised H_2O add:

Yeast nitrogen base without amino acids (DIFCO) 6.7 g

Agar (for plates only) 15 g

Shake until the solutes have dissolved. Adjust the volume to 850 mL with deionised H_2O and sterilize by autoclaving. Allow medium to cool to 60ºC and add glucose to 2% (50 mL of a sterile 40% stock solution) and 100 mL of the appropriate 10x dropout solution.

Cell Culture Solutions and immunocytochemistry

PBS 1x

For a final volume of 500 mL, dissolve one pack of BupH Modified Dulbecco's Phosphate Buffered Saline Pack (Pierce) in deionised H_2O.

Final composition:

8 mM Sodium Phosphate

2 mM Potassium Phosphate

40 mM NaCl

10 mM KCl

Sterilize by filtering through a 0.2 μm filter and store at 4ºC

MEM + GLUTAMAX (HeLa cells)

For a final of 500 mL add:

Complete MEM + GLUTAMAX (Gibco, Invitrogen)

Fetal Bovine Serum (FBS) (Gibco, Invitrogen) 50 mL (10% v/v)

Non-Essential aminoacids (Gibco, Invitrogen) 5 mL (1% v/v)

100x Antibiotic-antimycotic (Gibco, Invitrogen) 5 mL (1% v/v)

Adjust the pH 7.4. Sterilize by filtering through a 0.2 μm filter and store at 4°C.

FBS is heat-inactivated for 30 min at 56ºC.

MEM + GLUTAMAX (HeLa cells)

For a final of 500 mL add:

Complete MEM + GLUTAMAX

Fetal Bovine Serum (FBS) (Gibco, Invitrogen) 50 mL (10% v/v)

Non-Essential aminoacids (Gibco, Invitrogen) 5 mL (1% v/v)

100x Antibiotic-antimycotic (Gibco, Invitrogen) 5 mL (1% v/v)

Adjust the pH 7.4. Sterilize by filtering through a 0.2 μm filter and store at 4°C.

FBS is heat-inactivated for 30 min at 56ºC.

DMEM medium (COS-7 cells and HEK193)

For a final volume of 1 L, dissolve one pack of DMEM powder (with L-glutamine and 4500 mg glucose/L, Sigma Aldrich) in deionised H_20 and add:

$NaHCO_3$ (Sigma) 3.7 g

FBS (Gibco, Invitrogen) 100 ml (10% v/v)

100x Antibiotic-antimycotic (Gibco, Invitrogen) 10 mL (1% v/v)

Adjust the pH 7.4. Sterilize by filtering through a 0.2 μm filter and store at 4°C.

FBS is heat-inactivated for 30 min at 56°C.

MEM/F12 medium (SH-SY5Y cells)

For a final volume of 1 L of deionized H_2O add:

MEM (Gibco, Invitrogen) 4.805 g

Ham's F12 (Gibco, Invitrogen) 5.315 g

$NaHCO_3$ (Sigma) 1.5 g

L-glutamine (200 mM stock solution) 2.5 mL

FBS (Gibco, Invitrogen) 100 mL (10% v/v)

100x Antibiotic-antimycotic (Gibco, Invitrogen) 10 mL (1% v/v)

Adjust the pH 7.4. Sterilize by filtering through a 0.2 μm filter and store at 4°C.

FBS is heat-inactivated for 30 min at 56°C.

RPMI medium (PC12 cells)

For a final volume of 1 L dissolve one pack of RPMI 1640 powder (with L-glutamine and 4500 mg/L glucose, Gibco) in deionized H_2O and add:

$NaHCO_3$ (Sigma) 0.85 g

FBS (Gibco, Invitrogen) 50 mL (5% v/v)

Horse serum (HS) 100 mL (10% v/v)
100x Antibiotic-antimycotic (Gibco, Invitrogen) 10 mL (1% v/v)
Adjust to pH 7.4. Sterilize by filtering through a 0.2 μm filter and store at 4°C.
FBS is heat-inactivated for 30 min at 56ºC.

Neurobasal medium (Cortical primary cultures)

The serum-free medium (Neurobasal; Gibco, Invitrogen) is supplemented with:
2% B27 Supplement (Gibco, Invitrogen)
0.5 mM L-glutamine
60 μg/ml Gentamicin (Gibco, Invitrogen)
0.001% Phenol Red (Sigma)
Sterilize by filtering through a 0.2 μm filter and store at 4°C

Hank's balanced salt solution (HBSS)

137 mM NaCl
5.36 mM KCl
0.44 mM KH_2PO_4
0.34 mM $Na_2HPO_42H_2O$
4.16 mM $NaHCO_3$
5 mM Glucose
1 mM Sodium pyruvate
10 mM HEPES
Adjust to pH 7.4. Sterilize by filtering through a 0.2 μm filter and store at 4°C.

Borate buffer

To a final volume of 1L, dissolve in deionised H_2O 9.28 g of boric acid (Sigma). Adjust to pH 8.2, sterilize by filtering through a 0.2 μm filter and store at 4°C.

1 mg/mL Poly-L-ornithine solution (10x)

To a final volume of 100 mL, dissolve in deionised H_2O 100 mg of poly-L-ornithine (Sigma-Aldrich).

10 mg/mL Poly-D-lysine solution (100x)

To a final volume of 10 mL, dissolve in deionised H_2O 100 mg of poly-D-lysine (Sigma-Aldrich).

4% Paraformaldehyde

For a final volume of 100 mL, add 4 g of paraformaldehyde to 25 mL deionised H_2O. Dissolve by heating the mixture at 58ºC while stirring. Add 1-2 drops of 1 M NaOH to clarify the solution and filter (0.2 μm filter). Add 50 mL of 2X PBS and adjust the volume to 100 mL with deionised H_2O.

Immunoprecipitation solutions

Lysis Buffer + Protease inhibitors

50 mM Tris-HCl (pH 8.0)
120 mM NaCl
4% CHAPS
1 mM PMSF
10 mM Benzamidine
2 μM Leupeptin
1.5 μM Aprotinin
5 μM Pepstatin A

SDS-PAGE and immunoblotting solutions

4x LGB (Lower Gel Buffer)

To 900 mL of deionised H_2O add:
Tris 181.65 g
SDS 4 g
Mix until the solutes have dissolved. Adjust the pH to 8.9 and adjust the volume to 1 L with deionised H_2O.

4x UGB (Upper Gel Buffer)

To 900 mL of deionised H_2O add:

Tris 75.69 g

Mix until the solute has dissolved. Adjust the pH to 6.8 and adjust the volume to 1 L with deionised H_2O.

30% Acrylamide/0.8% Bisacrylamide

To 70 mL of deionised H_2O add:

Acrylamide 29.2 g

Bisacrylamide 0.8 g

Mix until the solutes have dissolved. Adjust the volume to 100 mL with deionised H_2O. Filter through a 0.2 μm filter and store at 4°C.

10% APS

In 10 mL of deonised H_2O dissolve 1 g of APS.

Prepare fresh before use.

10% SDS

In 10 mL of deonised H_2O dissolve 1 g of SDS.

4x Loading Gel Buffer

1 M Tris solution pH 6.8	2.5 mL (250 mM)
SDS	0.8 g (8%)
Glycerol	4 mL (40%)
β-Mercaptoethanol	2 mL (2%)
Bromophenol blue	1 mg (0.01 %)

Adjust the volume to 10 mL with deionised H_2O. Store in darkness at room temperature.

1 M Tris pH 6.8 solution

To 150 mL of deonised H_2O add:

Tris base 30.3 g

Adjust the pH to 6.8 and adjust the final volume to 250 mL.

10x Running Buffer

To 800 mL of deionised H_2O add:

Tris 30.3 g (250 mM)

Glycine 144.2 g (2.5 M)

SDS 10 g (1%)

Adjust the pH to 8.3 and the final volume to 1 L.

1x Transfer buffer

To 600 ml of deionised H_2O add:

Tris 3.03 g (25 mM)

Glycine 14.41 g (192 mM)

Mix until solutes dissolution. Adjust the pH to 8.3 with HCl and the volume to 800 mL with deionised H_2O. Just prior to use add 200 mL of methanol (20%).

10x TBS (Tris buffered saline)

To 800 mL of deionised H_2O add:

Tris 12.11 g (10 mM)

NaCl 87.66 g (150 mM)

Adjust the pH to 8.0 with HCl and the final volume to 1 L with deionised H_2O.

10x TBST (TBS + Tween)

To 800 mL of deionised H_2O add:

Tris 12.11 g (10 mM)

NaCl 87.66 g (150 mM)

Tween 20 5 mL (0.05 %)

Adjust the pH to 8.0 with HCl and the final volume to 1 L with deionised H_2O.

Stripping solution

Tris 3.76 g (62.5 mM)

SDS 10 g (2%)

β-mercaptoethanol 3.5 mL (100 mM)

Dissolve Tris and SDS in deionised H_2O and adjust pH to 6.7. Add mercaptoethanol and ajust the volume to 500 ml.

Coomassie blue staining solutions

Staining solution

Coomassie Brilliant Blue	2 g
Methanol	500 mL
Acetic Acid	100 mL

Adjust the volume to 1 L with deionised H_2O.

Destaining solution

Methanol	250 mL
Acetic Acid	50 mL

Adjust the volume to 1 L with deionised H_2O.

APPENDIX II – PRIMERS

Oligo name	Sequence (5' - 3')	Target	RE
Gal4-AD FW	TACCACTACAATGGATG	pACT2	
Amplimer 3 RV	ATCGTAGATACTGAAAAACCCCGCAAGTTCAC	pACT2	
T7 promoter	TAATACGACTCACTATAGGG	T7 promoter	
LAP1B-BM1 FW	GGAATTCATATGGCGGGCGACGGG	LAP1B	EcoRI
LAP1B-BM1 RV	CCGCTCGAGTTAGACACTGGTGGCTTC	LAP1B	XhoI
LAP1B-BM2 FW	GGAATTCATATGGACGAGCCGCCAGAA	LAP1B	EcoRI
LAP1B-BM2 RV	CCGCTCGAGTTAGGCTACATCTTTGAAGGC	LAP1B	XhoI
LAP1B-BM1/2 FW	GGAATTCATATGGCGGGCGACGGG	LAP1B	EcoRI
LAP1B-BM1/2 RV	CCGCTCGAGTTAGACACTGGTGGCTTC	LAP1B	XhoI
LAP1B-BM3 FW	GGAATTCATATGGCCAGATCCAGGGAT	LAP1B	EcoRI
LAP1B-BM3 RV	CCTCGAGTTATAAGCAGATGCCCCT	LAP1B	XhoI
LAP1B-BM1/2+TM FW	GGAATTCATATGGCGGGCGACGGG	LAP1B	EcoRI
LAP1B-BM1/2+TM RV	CCTCGAGTTAGAACTCTTGAACAG	LAP1B	XhoI
LAP1B-BM1/2-TM RV	CCTCGAGTTACCGGTTCCTCTTGAC	LAP1B	XhoI
LAP1B-BM3+TM FW	GGAATTCATATGGTCAAGAGGACGG	LAP1B	EcoRI
LAP1B-BM3-TM FW	GGAATTCATATGGCTGTTCAAGTTC	LAP1B	EcoRI
LAP1B (ΔA185) FW	CATACAAGAGGCTCCAGTGAGTGAAGATCTTG	LAP1B	
LAP1B (ΔA185) RV	CAAGATCTTCACTCACTGGAGCCTCTTGTATG	LAP1B	
E1FW	CAGGAGAACCTAGGGTCCATAAAG	LAP1B	
E2FW	CATTCCTCTGAAGAGGATG	LAP1B	
E5FW	CTGAAGAAGATGATCAAGACAGCTC	LAP1B	
E10FW	CAAGGTCAAGATGAGAAGCTG	LAP1B	
E10RV	CTTGGCCTGACCTACTCTTAAGAC	LAP1B	
E10BRV	GTGAACAATTCTCAGAACTTGGGAC	LAP1B	
E10CRV	GTGAGCAGTAAGATAGCAGGCTG	LAP1B	
AFW	GCTCGTCGTCGACAACGGCTC	β-sctin	
ARV	CAAACATGATCTGGGTCATCTTCTC	β-actin	

APPENDIX III – BACTERIA AND YEAST STRAINS

Bacteria strains:

E. coli XL1-Blue: recA endA1 gyrA96 thi-1 hsdR17 supE44 relA1 lac[F' proAB lacZDM15 Tn10(Tetr)]

E. coli Rosetta (DE3) F^{-}ompT $hsdS_B(r_B^{-}m_B^{-})$ gal dcm (DE3) $pRARE^2$ (Cam^R)

Yeast strains:

S. cerevisiae AH109: MATa, trp1-901, leu2-3, 112 ura3-52, his3-200, gal4Δ, gal 80Δ, LYS2:: $GAL1_{UAS}$- $GAL1_{TATA}$-HIS3, $GAL2_{UAS}$-$GAL2_{TATA}$-ADE2, URA3::$MEL1_{UAS}$-$MEL1_{TATA}$-lacZ, MEL1

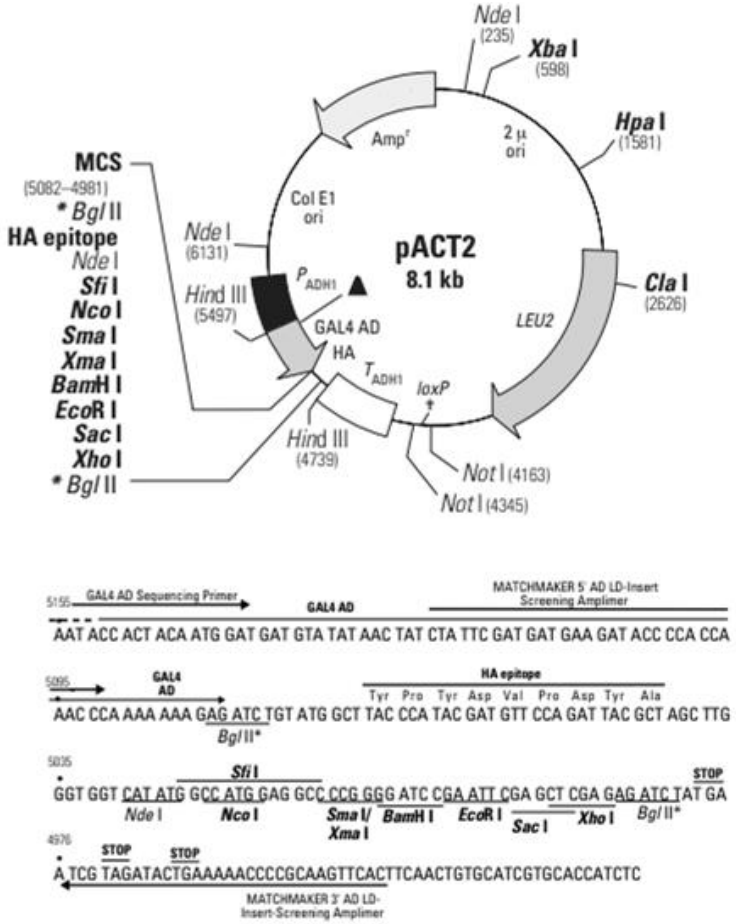

pACT2 (Clontech) map and multiple cloning sites. Unique sites are in bold. pACT2 is used to generate a hybrid containing the GAL4 AD, an epitope tag and a protein encoded by a cDNA in a fusion library. The hybrid protein is expressed at medium levels in yeast host cells from an enhanced, truncated ADH1 promoter and is targeted to the nucleus by the SV40 T-antigen nuclear localization sequence. pACT2 contains the *LEU2* gene for selection in Leu$^-$ auxotrophic yeast strains.

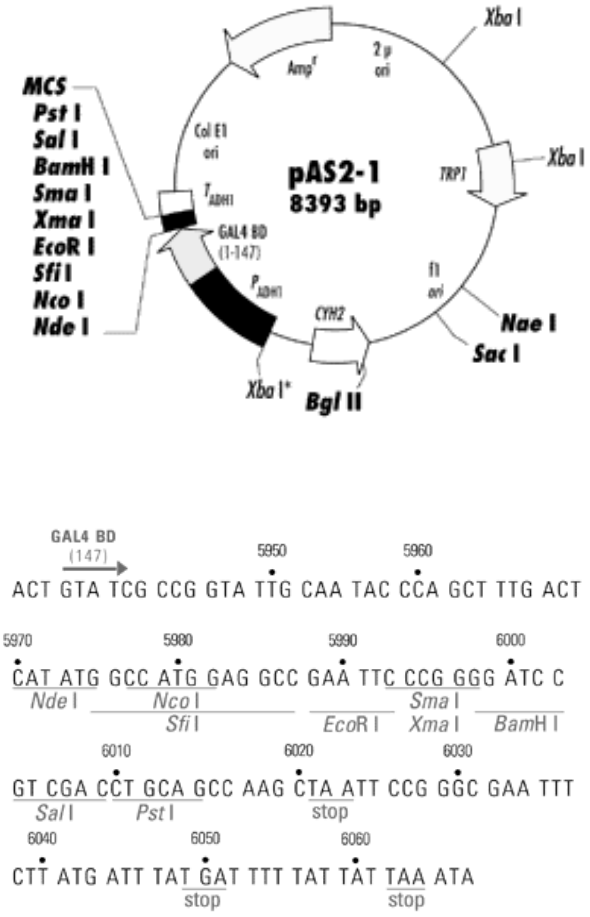

pAS2-1 (Clontech) map and multiple cloning sites. Unique restriction sites are coloured blue. pAS2-1 is a cloning vector used to generate fusions of a bait protein with the GAL4 DNA-BD. The hybrid protein is expressed at high levels in yeast host cells from the full-length ADH1 promoter. The hybrid protein is targeted to the yeast nucleus by nuclear localization sequences. pAS2-1 contains the *TRP1* gene for selection in Trp^- auxotrophic yeast strains.

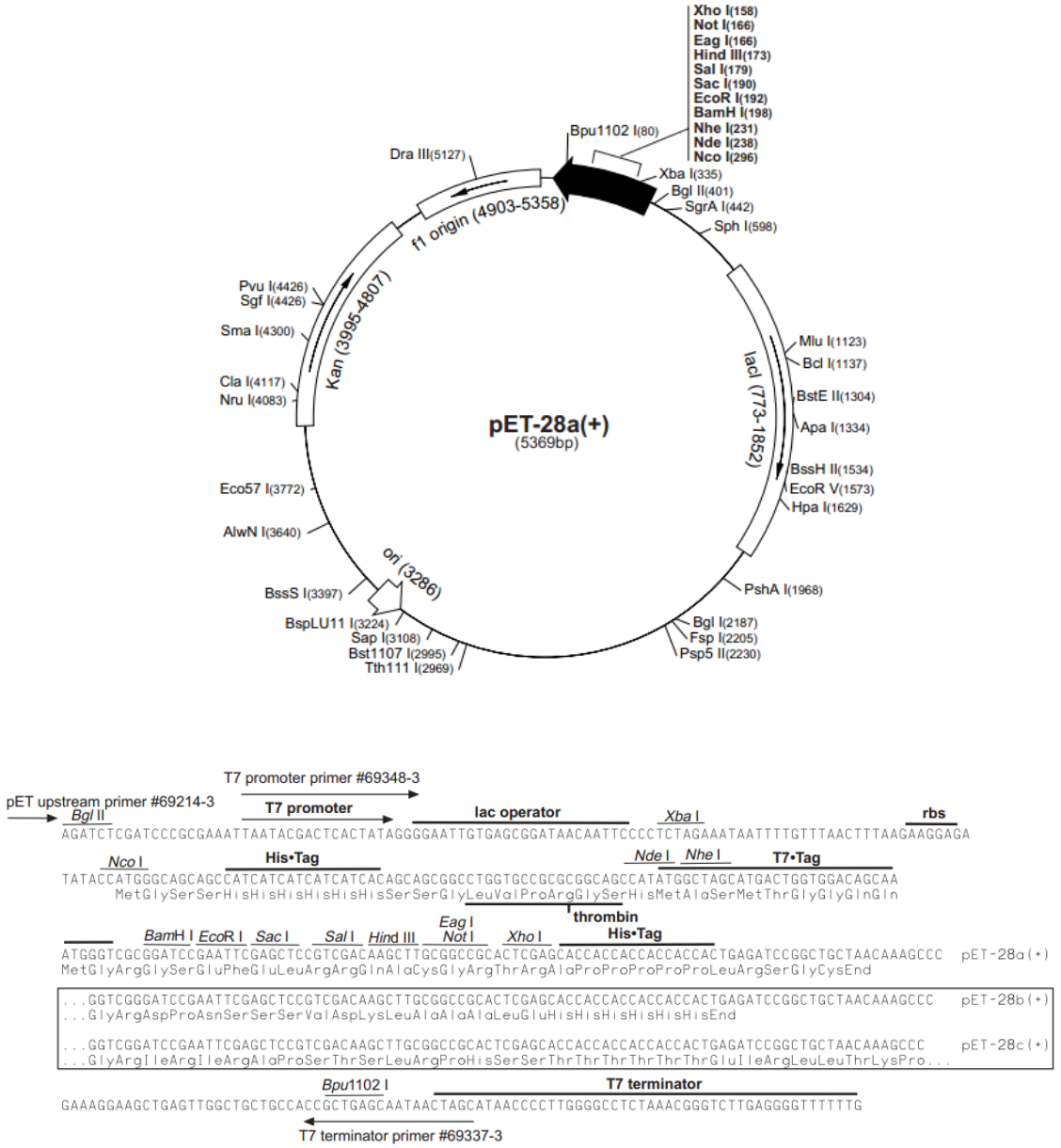

pET-28a-c(+) (Novagen) restriction map and multiple cloning sites. Unique sites are indicated on the circular map. pET-28a-c(+) is a *E. coli* expression vector with an N-terminal His tag/thrombin/T7 tag. This vector possesses the Kanamycin resistance gene.

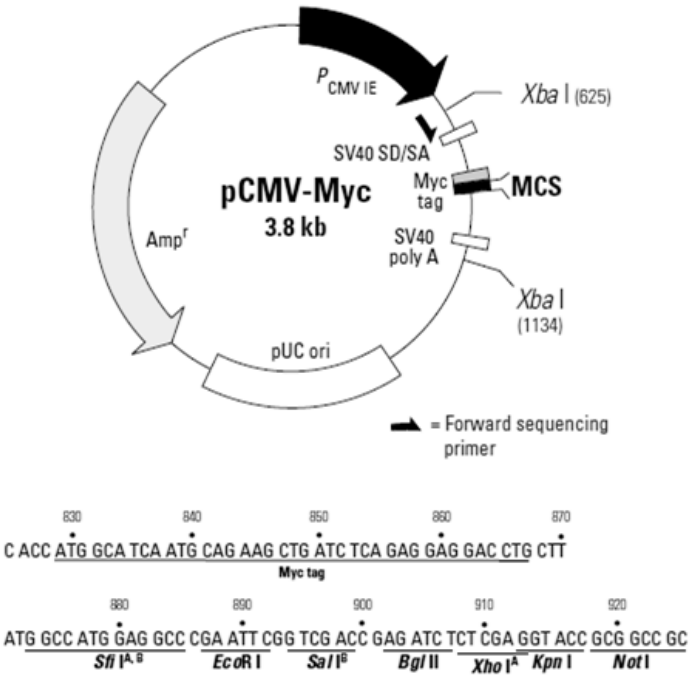

pCMV-Myc (Clontech) restriction map and multiple cloning sites. Unique restriction sites are in bold. pCMV-Myc is a mammalian expression vector with an N-terminal c-Myc epitope tag. This vector possesses the ampicillin resistance gene for selection in *E. coli*.

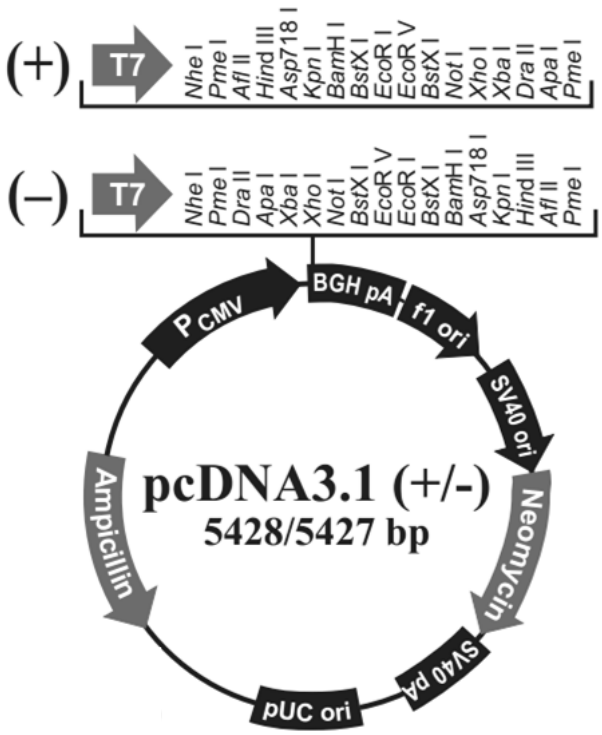

pcDNA3.1(Invitrogen) map and multiple cloning site. pcDNA3.1 is a mammalian expression vector. This vector possesses the ampicillin resistance gene for selection in *E. coli*.

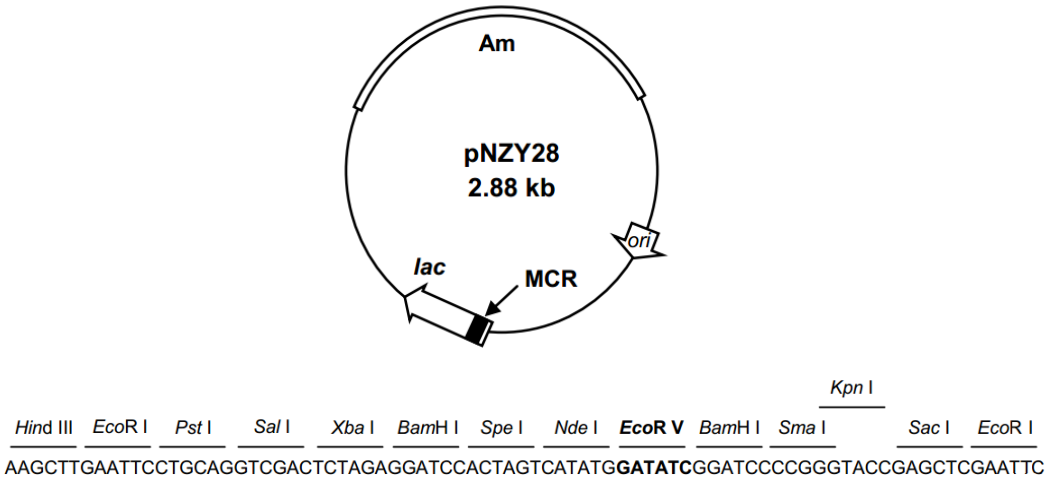

pNZYY28 (Nzytech) restriction map and multiple cloning region. The pNZY28 vector is provided linearized at the EcoRV site and allows the direct cloning of PCR products with blunt ends. This vector possesses the ampicillin resistance gene for selection in *E. coli*.

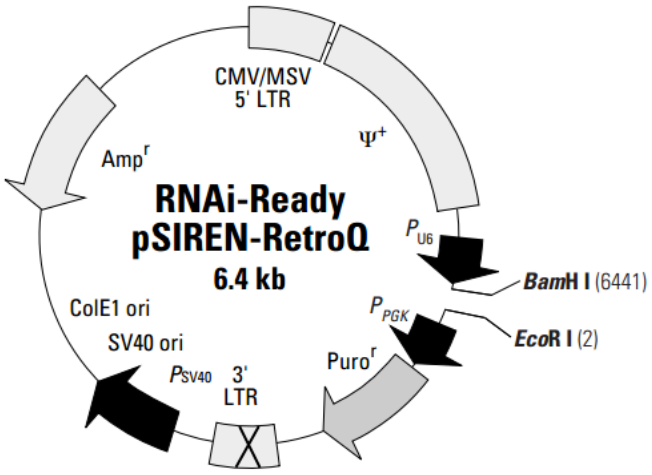

6430 6440 10 20 30 40

5'-TGTGGAAAGGACGAGGATCC[...shRNA oligo cloning site...]GAATTCTACCGGGTAGGGGAGGCGCTTTTCCCAAGGCAGT-3'

BamH I EcoR I

3'-ACACCTTTCCTGCTCCTAGG[...shRNA oligo cloning site...]CTTAAGATGGCCCATCCCCTCCGCGAAAAGGGTTCCGTCA-5'

RNAi-Ready pSIREN-RetroQ (Clontech) map and cloning site. RNAi-Ready pSIREN-RetroQ is a self-inactivating retroviral expression vector designed to express a short hairpin RNA (shRNA) using the human U6 promoter. It is used for targeted gene silencing when an oligonuceotide encoding an appropriate shRNA is ligated into the vector. This vector possesses the ampicillin resistance gene for selection in *E. Coli* and the puromycin resistance gene for the selection of stable transfectants.